Farnesoid X Receptor as a homeostat for hepatic nutrient metabolism, proliferation and intestinal inflammation:

Novel insights into mechanisms of regulation

Vittoria Massafra

Financial Support by the University Medical Center Utrecht for publication of this thesis is gratefully acknowledged.

Cover: "The chimeric FXR-Quixote knight"
by Vittoria Massafra

ISBN: 978-90-393-6713-1
Printed by: Proefschriftmaken.nl

Farnesoid X Receptor as a homeostat for hepatic nutrient metabolism, proliferation and intestinal inflammation:

Novel insights into mechanisms of regulation

De Farnesoid X Receptor als homeostaat voor metabolisme van voedingsstoffen, proliferatie en darmontsteking:

Nieuwe inzichten in de mechanismen van regulatie

(met een samenvatting in het Nederlands)

Proefschrift

ter verkrijging van de graad van doctor aan de Universiteit Utrecht op gezag van de rector magnificus, prof. dr. G.J. van der Zwaan, ingevolge het besluit van het college voor promoties in het openbaar te verdedigen op
dinsdag 24 januari 2017 des ochtends te 10.30 uur

door

Vittoria Massafra

geboren op 11 april 1987 te Martina Franca, Italië

Promotor: Prof. dr. ir. B.M.T. Burgering

Copromotor: Dr. S.W.C. van Mil

"Penso che la scienza non sia bella perchè abbiamo imparato
questo, quello e quell'altro.
La scienza è bella perchè ci dice che ci sono cose che ancora non sappiamo.
E' meraviglioso andarle a studiare passo dopo passo.
Lì, sull'orlo di quello che non sappiamo, c' è il fascino della scienza."

"I think that science is not wonderful because we learned
this, that, and the other.
Science is wonderful because it tells us that there are things which we do
not know yet, it is wonderful to go and study them step by step.
There, on the edge of the unknown, you'll find the fascination of science."

Carlo Rovelli
Theoretical physicist

Tables of contents

List of Abbreviations

ACC	acetyl-CoA carboxylase
ACSL3	long-chain-fatty-acid-CoA ligase 3
AF1	activation function domain 1
AMPK	AMP-activated protein kinase
ANXA2	annexin A2
APOB	apolipoprotein B
ARG	arginase 1
ASL	argininosuccinate lyase
ASS1	argininosuccinate synthase
BA	bile acid
BHMT	betaine-homocysteine S-methyltransferase
BSEP	bile salt export pump
CA	cholic acid
CCL25	C-C motif chemokine ligand 25
CCR9	C-C motif chemokine receptor 9
CDCA	chenodeoxycholic acid
CPS1	carbamoyl-phosphate synthase I
CREB	cAMP regulatory element-binding protein
CXCR3	C-X-C motif chemokine receptor 3
CYP7A1	cholesterol 7α-hydroxylase
DBD	DNA binding domain
DC	dendritic cell
DSS	Dextran Sodium Sulfate
ER	estrogen receptor
FA	fatty acid
FASP	Filtered Aided Sample Purification Protocol
FGF	fibroblast growth factor
FLYWCH2	FLYWCH family member 2
FXR	Farnesoid X Receptor
FXRE	FXR responsive elements
G6PC	glucose 6-phosphatase
GK	glucokinase
GLS2	glutaminase 2

GLUL	glutamine synthase
GR	glucocorticoid receptor
GSK3	glycogen synthase kinase 3
HAL	histidine ammonia-lyase
HCC	hepatocellular carcinoma
HDLBP	high hensity lipoprotein binding protein
HOXA5	homeobox A5
HOXA9	homeobox A9
IBABP	ileal bile acid-binding protein
IBD	Inflammatory Bowel Disease
LBD	ligand binding domain
LC-MS/MS	liquid chromatography–tandem mass spectrometry
LDL	low-density lipoprotein
LDLR	LDL receptor
livFXR-/-	liver-specific FXR knockout
LPK	liver pyruvate kinase
LRH1	receptor liver receptor homolog 1
LXR	liver X receptor
MHCII	major histocompatibility complex class II
MLN	mesenteric lymph node
mTORC1	mammalian Target of Rapamacin Complex
MTP	microsomal triglyceride transfer protein
NAFLD	Non-Alcoholic Fatty Liver Disease
NAGS	N-acetylglutamate synthase
NASH	Non-Alcoholic Steatohepatitis
NCOR	nuclear corepressor
NF-κB	nuclear factor kappa-light-chain-enhancer of activated B cells
NK	natural killer (T cell)
NR	nuclear receptor
NSD1	nuclear receptor binding SET domain protein 1
NTCP	Na+-taurocholate cotransporting polypeptide
OAT	ornithine aminotransferase
OCA	obeticholic acid
OTC	ornithine transcarbamylase
PBC	Primary Biliary Cholangitis

PBMC	peripheral blood mononuclear cell
PDK4	pyruvate dehydrogenase kinase
PEPCK	phosphoenolpyruvate carboxykinase 1
PGC1α	PPARG coactivator 1α
PLTP	phospholipid transfer protein
PPAR	peroxisome proliferator-activated receptor
PRODH	proline dehydrogenase
PTM	post-translational modification
PXR	pregnane X receptor
PYGL	glycogen phosphorylase
RXR	retinoid X receptor
SCD1	stearoyl-CoA desaturase
SHP	small heterodimeric partner
SILAC	Stable Isotope Labelling by Amino acids in Cell culture
SREBP-1c	sterol regulatory element-binding protein-1c
STAT3	signal transducer and activator of transcription 3
TAG	triglyceride
TGFBI	transforming growth factor, beta-induced
TR	thyroid hormone receptor
Treg	regulatory T cell
TSS	transcription start site
UT	urea transporter
VCAM1	vascular cell adhesion protein 1
VDR	vitamin D receptor
VLDL	very-low-density lipoprotein
WT	wild type
ZNF35	zinc finger protein 35


FXR
DNA

CHAPTER 1

General introduction

Thesis outline

Metabolism, cell survival and immunity

As biochemists, we try to explain how the extraordinary features of living beings derive from thousands of biomolecules, which interact functionally, following physical and chemical principles. Metabolism is the set of life-sustaining chemical reactions within the cells of living organisms, which allow organisms to grow and reproduce, maintain their structures and respond to their environment. Regulation of metabolic pathways intersects tightly with cell survival and inflammation both in health and disease. The transduction of environmental signals into a cellular response relies on protein mediators that sense the stimulus and trigger metabolic reprogramming. An example of such protein mediators are the metabolic nuclear receptors, as they bind compounds from dietary origin or intermediates in metabolic pathways and they drive transcriptional programs involved in metabolism, proliferation and inflammation [1, 2]. One of the metabolic nuclear receptors is the Farnesoid X receptor (FXR), which will be discussed in this thesis.

The meaning of FXR as a "homeostat"

Biological organisms are constantly adapting to the environment to maintain 'homeostasis' (coined from *hómoios*, "similar" and *hístēmi*, "standing still"). In 1948, William Ross Ashby - the founder of cybernetics and general systems theory - defined 'a 'homeostat' as a 'device capable of adaptive control, equipped with a sufficiently complex repertoire of possible alternative structures, in order to maintain stability in the face of highly varied and challenging environmental perturbations' [3, 4]. Regulation of different parameters within the homeostat keeps the output signal close to a setpoint value. This is analogous to switching on and off gene expression programs aiming to maintain homeostasis in organisms. In our opinion, FXR can be viewed as a homeostat of the liver. FXR is expressed in liver, intestine, kidney and adrenal glands [5-7]. FXR binds bile acids (BAs) circulating between the liver and the intestine. Upon its activation by BAs, FXR regulates the metabolism of BAs, cholesterol, glucose, lipid and – based on data described in this thesis – also amino acid metabolism [8]. In addition, FXR regulates cell proliferation, autophagy, and inflammation. We envisage FXR as a "homeostat", because FXR senses environmental signals via binding to BAs, abundance of coregulatory proteins and is subjective to posttranslational modifications (PTMs) that depend on the availability of certain nutrients. As a response, it integrates the homeostatic control of energy metabolism, proliferation and inflammation. In the post-absorptive state, lipid, glucose, amino acid, and BA concentrations increase in the liver, as a consequence of intestinal nutrient absorption and BA recycling. FXR senses these environmental changes and drives transcriptional programs that inhibit BA synthesis, and redistribute the energy substrates, thereby acting as a gatekeeper of metabolic homeostasis. A similar homeostatic role is played by FXR in controlling inflammation. Inflammation is a protective response of the organism to injury or infection, but in some cases it may turn into a disadvantageous chronic inflammation. FXR is capable of retroactively limiting the inflammatory response [9-11].

The scope of this thesis

The aim of this thesis is to investigate the molecular mechanisms of FXR function in the regulation of metabolism and inflammation in the liver and intestine.

In **Chapter 2**, we review the function of FXR as a regulator of hepatic nutrient metabolism. We integrate the new findings reported in **Chapter 3** on the role of FXR in amino acid metabolism, with the existing literature on FXR function. We conclude that FXR embraces the fate of all the three main classes of nutrients: lipids, glucose and amino acids and acts as a homeostat of energy metabolism in the liver. The physiological function of FXR is explored across the dimensions of space (hepatic FXR signaling versus FGF19 signaling coming from the intestine) and time (in the different phases of nutrition: postprandial, post-absorptive, and fasting states). In addition, the regulation of autophagy and cell proliferation is explained in the perspective of FXR as an integrator of nutrient homeostasis. Chapter 2 also touches upon the clinical benefits of targeting FXR for the treatment of liver diseases and provides an introduction for the experimental chapters 3, 4, 5, and 6 of this thesis.

In **Chapter 3** we provide experimental evidence for a novel physiological function of FXR, namely as a regulator of amino acid metabolism. We describe how FXR activation promotes amino acid degradation, ureagenesis and glutamine synthesis, using quantitative proteomics applied to mouse liver extracts. We thereby expand the understanding of the spectrum of metabolic effects underlying FXR-dependent amelioration of liver diseases.

The function of FXR is further examined in **Chapter 4**, in which we deployed *in vivo* quantitative proteomics to gain a comprehensive understanding of the FGF19 signalling cascade. FGF19 is an FXR target gene, encoding for a postprandial enterokine, signalling to the liver. Despite being a promising therapeutic target in metabolic syndrome and cholestatic diseases, FGF19 is associated with proliferation and hepatocellular carcinoma, raising concerns about safety. Therefore, we aimed to unravel proteome-wide targets of FGF19-signaling, implicated in metabolism and proliferation. In addition, we analysed whether it is likely that therapeutic applications can be developed that uncouple FGF19-mediated metabolic benefit from its mitogenic effects.

In **Chapter 5** we shift the focus to the anti-inflammatory function of FXR in the intestine and the spleen. We addressed which immunological mechanisms underlie FXR-mediated amelioration of colitis in a mouse model of inflammatory bowel disease. For that purpose, we FACS-sorted immune cell populations in mesenteric lymph nodes and spleen of mice in which colitis had been induced. We show that FXR activation by obeticholic acid (OCA) has systemic anti-inflammatory effects, which are associated with changes in the chemotactic environment at the site of inflammation in the colon.

Gaining more insights into the complexity of FXR signalling is imperative for the rational design of a new generation of FXR drugs, selectively activating or repressing sub-

groups of FXR target genes while not interfering with other target genes, thereby reducing side effects. A better understanding of the differential cofactors bound by FXR and the respective consequences on transcriptional regulation is needed. In **Chapter 6**, we have developed a SILAC-based proteomics approach to identify novel coregulatory proteins for FXR.

The themes 'FXR biology' and 'mass spectrometry-based proteomics' are the unifying threads that run through this thesis, which has been written in the perspective to use biological knowledge for progress in medical care. The discussion in **Chapter 7** is intended to take stock of the current knowledge on the role of FXR in physiology and guide throughout the opportunities and the challenges to translate biochemistry and biology knowledge on FXR into clinical applications.

REFERENCES

1. Francis GA, Fayard E, Picard F, et al. Nuclear receptors and the control of metabolism. Annu Rev Physiol 2003;65:261-311.
2. Sonoda J, Pei L, Evans RM. Nuclear receptors: decoding metabolic disease. FEBS Lett 2008;582:2-9.
3. Cariani PA. The homeostat as embodiment of adaptive control. INT J GEN SYST 2009;38:139-154.
4. Ashby WR. The homeostat. Electronic engineering 1948;20:380.
5. Makishima M, Okamoto AY, Repa JJ, et al. Identification of a nuclear receptor for bile acids. Science 1999;284:1362-5.
6. Parks DJ, Blanchard SG, Bledsoe RK, et al. Bile acids: natural ligands for an orphan nuclear receptor. Science 1999;284:1365-8.
7. Wang H, Chen J, Hollister K, et al. Endogenous bile acids are ligands for the nuclear receptor FXR/BAR. Mol Cell 1999;3:543-53.
8. Massafra V, van Mil SWC. FXR as a homeostat for hepatic nutrient metabolism. Unpublished 2016.
9. Gadaleta RM, van Erpecum KJ, Oldenburg B, et al. Farnesoid X receptor activation inhibits inflammation and preserves the intestinal barrier in inflammatory bowel disease. Gut 2011;60:463-72.
10. Massafra V, Ijssennagger N, Plantinga M, et al. Splenic dendritic cell involvement in FXR-mediated amelioration of DSS colitis. Biochim Biophys Acta 2016;1862:166-73.
11. Wang YD, Chen WD, Wang M, et al. Farnesoid X receptor antagonizes nuclear factor kappaB in hepatic inflammatory response. Hepatology 2008;48:1632-43.


fat


FXR
DNA

CHAPTER 2

FXR: a “homeostat” for hepatic nutrient metabolism

Vittoria Massafra, Saskia van Mil

Submitted review

ABSTRACT

The Farnesoid X receptor is a nuclear receptor activated by bile acids (BAs), which are amphipathic molecules that serve as fat solubilizers in the intestine in postprandial conditions and as signalling hormones regulating energy metabolic pathways. Upon BA activation, FXR provides feedback signals on BA synthesis and transport in the liver. Next to its role in BA homeostasis, FXR is an important regulator of lipid, glucose and amino acid metabolism. Therefore, FXR acts as a homeostat of all three main classes of nutrients, fats, sugars and proteins. In this review, we therefore re-analyze the function of FXR in the perspective of nutritional metabolism, and discuss the role of FXR in liver energy homeostasis in postprandial, postabsorptive and fasting/starvation states.

Sensors of food availability integrate the signalling pathways that govern cell survival and growth. We discuss that FXR, by regulating nutritional metabolism, represses autophagy in conditions of nutrient abundance, and controls the metabolic needs of proliferative cells. In addition, FXR regulates inflammation via direct effects and via its impact on nutrient metabolism. In conclusion, FXR is an attractive target for novel therapeutic strategies for liver diseases, because it functions at the crossroads between metabolic and inflammatory pathways.

INTRODUCTION

Nuclear receptors (NRs) regulate several important aspects of mammalian physiology, including development, reproduction and metabolism. They act as sensors of whole body environment and adapt to changes in the environment by regulating gene transcription. NRs bind specific DNA elements in the regulatory regions of genes, hormone response elements (HREs), via a highly conserved DNA binding domain (DBD). HREs are typically composed of two 6-base pair half-sites that may be arranged as direct, inverted, or everted repeats. Specificity for a given receptor is determined by the nucleotide sequence of the half-sites, the orientation and spacing of those half-sites, and the nucleotide sequence flanking the half-sites [1, 2]. NRs are activated upon binding specific ligands via the ligand-binding domain (LBD), which consists of 12 helices that form a hydrophobic pocket. Ligand binding induces a conformational change in the receptor, allowing dissociation of corepressors and subsequent recruitment of coactivators. These coregulators are needed to mediate the NR-dependent change in gene regulation, and act typically via modification of the chromatin and interaction with the basal transcription machinery [3, 4]. NR ligands are small lipophilic molecules that can easily cross biological membranes and regulate large transcriptional programs. Also partial agonists and antagonist are being developed which induce a "dissociated" biological response, regulating transcription of only selective genes, to avoid side effects [5-7]. NRs are seen as ideal drug targets.

In this review, we focus on the farnesoid X receptor (FXR), the nuclear receptor that is activated by endogenous bile acids (BAs). FXR belongs to a subgroup of NRs commonly regarded as the metabolic nuclear receptors, which sense physio- and pathological metabolic states, and adapt to these changes by regulating transcription of genes involved in cholesterol, fatty acid (FA) and glucose homeostasis. Next to FXR, the subgroup of metabolic nuclear receptors includes the peroxisome proliferator-activated receptors (PPARs), liver X receptors (LXRα/β), liver receptor homolog-1 (LRH-1), pregnane X receptor/steroid and xenobiotic receptor (PXR/SXR), and the constitutive androstane receptor (CAR) [8-10].

Two FXR genes have been identified: FXRα and FXRβ. FXRβ has been shown to be activated by lanosterol in rodents, rabbits, and dogs, but constitutes a pseudogene in humans and primates [11]. The FXRα gene encodes four biologically active variants (FXRα1, α2, α3, α4), resulting from differential promoter usage (α1, α2 vs α3, α4) and alternative splicing (α1, α3 vs α2, α4) [12, 13]. In mice, all four isoforms are abundantly expressed in liver, whereas α3/α4 are much higher expressed than α1/α2 in ileum and kidney. In adrenal glands, α1/α2 are the predominant isoforms [13]. Relative expression of FXR isoforms may be species-specific, as in human liver α1/α2 are predominant compared to α3/α4 [12]. FXR isoforms seem to regulate differential transcriptional programs and their expression has been shown to be dynamically regulated by bioenergetic cues, such as fasting and exercise [14]. In addition, relative expression of α1 and α2 is altered in hepatocellular carcinoma (HCC), and is associated with a marked reduction of Bsep, indicating that the relative abundance of FXR isoforms may differ critically in health and disease [15]. FXR function is also modulated by posttranslational modifications (PTMs), such as

phosphorylation [16], acetylation [17], sumoylation [18, 19] and O-GlcNAcylation [20].
FXR function has been investigated under pathophysiological conditions, by observing the phenotype of whole body FXR knockout mice and the response to pharmacological activation of FXR in disease models. From these studies one can deduce clues about its role in normal physiology, however, caution should be taken since there is only a handful of studies that investigated the function of FXR under normal conditions, as a regulator of postprandial and post-absorptive nutrient metabolism.
In this review, we discuss the role of FXR in dietary nutrient handling (Figure 1). We review the current state-of-the-art on FXR regulation of BA metabolism, and hepatic metabolism of nutrients, including glucose, lipids and – as recently discovered – amino acids. An integrative perspective is given on the role of FXR actions across all phases of nutrition: 1. postprandial phase, 2. post-absorptive phase, 3. fasting phase and 4. starvation. The transition from feeding to fasting/starvation needs key metabolic changes to meet energetic demands, and the metabolic nuclear receptors play key roles in the regulation of gene transcriptional programs to adapt to these energy demands throughout all phases of nutrition [21]. The postprandial state ensures the storage of metabolic substrates as glycogen, triglycerides (TAGs) and proteins. Later in the post-absorptive state, glucose availability is ensured by glycogen breakdown (glycogenolysis). When the glycogen stores are depleted, the fasting phase starts and the liver switches to hydrolysis of TAGs as energy source and starts to produce glucose via gluconeogenesis. If food deprivation continues, the starved organism relies on depletion of lipids and body protein degradation for ATP generation. Here we focus on the role of FXR in mediating the response to dietary nutrition and conclude that FXR functions as a body "homeostat", meaning - by a definition given by W. Ross Ashby in 1948 - a device that maintains stability in the face of highly varied and challenging environmental perturbations. FXR senses the feeding environment via binding to BAs and via PTMs and subsequently controls the storage and breakdown of nutrients and their subproducts in line with energy homeostatic needs. We also highlight the implications of FXR metabolic functions on autophagy (occurring in response to nutrient shortage) and proliferation (requiring sufficient nutrient availability). Finally, we discuss the role of FXR in inflammation and address the clinical relevance of targeting FXR, being at the crossroads of metabolic and inflammatory pathways.

BILE ACID METABOLISM AND NUTRITION

The activation of FXR by bile acids that return to the liver in postabsorptive phase

Originally shown to be activated by farnesol [22], an intermediate of the mevalonate pathway, FXR was later identified as the receptor for BAs [23-25]. BAs are synthetized in the liver from cholesterol via the classical (CYP7A1-mediated) or the acidic (CYP27A1-mediated) pathways. BAs are subsequently conjugated to glycine or taurine, secreted into the bile canaliculi via BSEP (ABCB11) and stored in the gallbladder. Meal ingestion and the subsequent cholecystokinin production in the stomach results in gall bladder contraction and secretion of bile into the intestine. Here, BAs solubilize dietary fats and vita-

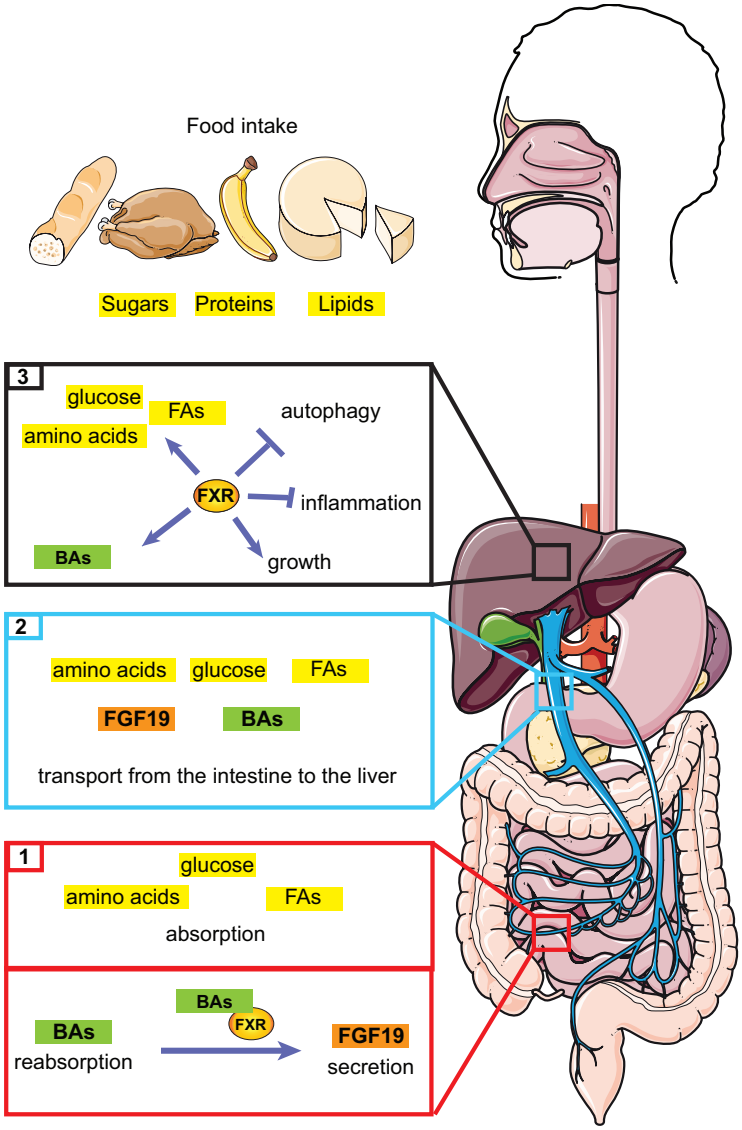

Figure 1. FXR: from BA to nutrient metabolism. Schematic representation of the interconnection between FXR activity and fate of BAs, nutrients and the enterokine FGF19, in intestine (1), portal circulation (2) and liver (3). First, amino acids, glucose and FAs of dietary origin are absorbed in the intestine. Also BAs are reabsorbed in the enterocytes, where they activate intestinal FXR, with subsequent induction of FGF19 transcription. BA, nutrients and FGF19 are subsequently transported from the intestine to the liver via the portal circulation. In the liver, FXR integrates the homeostatic control of BAs, lipids, glucose and amino acids. FXR represses autophagy in conditions of nutrient abundance, and controls the metabolic needs of growing cells. In addition, FXR regulates inflammation via direct effects and via its impact on nutrient metabolism.

mins, enabling their absorption. Most BAs are actively reabsorbed in the terminal ileum by the enterocyte apical transporter Asbt (Slc10a2) [26], transferred from the apical to basolateral membrane by the ileal BA binding protein (Ibabp) [27] and pumped into blood by the organic solute transporter heterodimer Ostα and Ostβ (Slc51a/b) [28-30]. BAs escaping from ileal reabsorption (~ 5 %) are modified by the gut microbiota into secondary BAs and either passively reabsorbed by the colonocytes or lost in the feces [31]. Reabsorbed primary and secondary BAs are then transported back to the liver via the portal venous system and taken up by hepatocytes via NTCP (SLC10A1), specifically involved in conjugated BA transport [32, 33], or by the organic anion transporting polypeptide transporters (OATPs/SLCOs) [34, 35]. In hepatocytes, BAs are re-conjugated and re-secreted into the bile canaliculus together with newly synthesized BAs that compensate for fecal loss [36].

Since the last two decades, BAs are not only regarded as emulsifiers of dietary fats and vitamins, but also as signalling molecules via interactions with receptors. Three members of the nuclear receptor family have been identified as BA sensors, FXR, PXR and VDR.

FXR is regarded as the primary BA receptor, regulating transcription of key genes involved in BA synthesis and transport. Activation of intestinal FXR by BAs leads to secretion of fibroblast growth factor 15 (FGF15; FGF19 in humans) from the enterocyte into the portal circulation. FGF15/19 binds to the basolateral FGFR4/b-Klotho receptor complex in hepatocytes, resulting in inhibition of the Cyp7a1 mediated BA synthesis [37]. Activation of hepatic FXR also inhibits BA synthesis, by downregulating the BA synthesis enzymes Cyp7a1 and Cyp8b1 via Shp and Mafg [38-40]. Additionally, hepatic FXR promotes BA efflux to the canalicular lumen through upregulation of Bsep (Abcb11) [41] and Mdr3 (Abcb4) [42] and BA efflux to the portal vein by inducing expression of Osta/b [43-45]. Moreover, active hepatic FXR sensitizes hepatocytes for intestinal FGF15/19 signalling by increasing β-Klotho levels [46]. Intestinal and hepatic FXR work therefore in a concerted manner as gatekeepers of BA homeostasis, by reducing BA synthesis and promoting BA outflow when liver BA concentrations rise following intestinal BA re-absorption. FXR has a high affinity to the conjugated BA chenodeoxycholic acid (CDCA) and binds with lesser affinity to the secondary BAs and cholic acid (CA) [23, 24]. BAs reach the highest concentration in blood in the postprandial state, due to their reabsorption in the ileum after a meal. Therefore, in normal physiology, FXR-mediated transcriptional regulation occurs in the post-absorptive phase [47].

The vitamin D receptor (VDR) and the pregnane X receptor (PXR) are mainly involved in the adaptive response to prevent BA hepatotoxicity and are activated by the secondary BA lithocholic acid (LCA) [48, 49]. And although CAR is not a BA sensor pur sang, bile salts and bilirubin induce nuclear translocation of CAR, thereby indirectly activating the transcriptional programs of this NR [50, 51]. PXR, VDR and CAR are involved in the detoxification of bile salts and xenobiotics. Next to these NRs, BAs also signal via the G-protein coupled receptor TGR5, which has high affinity to LCA and DCA [52]. TGR5 is widely distributed in the body and its activation triggers a wide range of effects, such as suppression of macrophage activation and an increase in energy expenditure [52, 53]. Overall, these observations suggest that different species of BAs may induce differential met-

abolic outcomes through specific signalling receptors.
In the next paragraphs we will summarize the evidence that FXR functions at the crossroads between BA and nutrient metabolism, by regulating not only BA homeostasis in the liver, but also the hepatic fate of nutrients: lipids, glucose and amino acids.

ROLE OF FXR IN LIPID METABOLISM

Hepatic lipid metabolism

Upon meal digestion, dietary triacylglycerols (TAGs) are hydrolysed into diacylglycerols (DAGs) and free FAs by gastric lipases. In the duodenum TAGs are emulsified by BAs and further degraded to glycerol and free FAs by pancreatic lipases [54]. Once absorbed by the intestinal mucosa, glycerol and FAs are reassembled into TAGs, packed into chylomicrons, secreted into the gut lymphatic system and transported to the systemic circulation [55]. Chylomicrons provide tissues with fats via lipolysis and chylomicron remnants eventually arrive in the liver and release the left-over non-esterified FAs via lipolysis and LDLR-mediated endocytosis [56, 57]. In the postprandial state, FAs are generated through *de novo* lipogenesis from glycolytic and amino acid subproducts in the liver [58]. Dietary and newly synthetized FAs are either oxidized for energy purposes or incorporated in triacylglycerol, phospholipids, and cholesterol esters. Subsequently, these complex lipids are stored in lipid droplets in hepatocytes, incorporated into membranes, and secreted into the circulation as very-low-density lipoprotein (VLDL) particles to supply the body with energy substrates [59]. When insulin decreases in the post-absorptive phase, lipid anabolism declines, and is gradually replaced by catabolic processes during fasting and emptying of the lipid droplets. If nutrient deprivation continues, the starved organism depletes its lipid storage in adipose tissue by TAG hydrolysis [21].
Lipogenesis in the fed state is controlled by multiple transcription factors. Here we shortly discuss the most important regulators SREBP, ChREBP and LXRα, which sense the availability of FAs, glucose and cholesterol, respectively, and activate transcriptional programs promoting lipogenesis [59, 60]. Insulin indirectly activates Srepb1c, via inhibition of the interaction between INSIG2 and SCAP, the latter being the chaperone for Srepb1c localization to the Golgi apparatus. [61]. In the Golgi, Srebp1c is cleaved by the proteases S1P/S2P, and translocates to the nucleus, where it induces transcription of several FA and TAG synthesis genes [62, 63].
ChREBP is also a transcription factor that controls lipogenesis. In the postprandial state, high glucose conditions result in increased glucose-6-phosphate (G6P), xylulose-5-phosphate (X5P), and fructose-2,6-bisphospate (F2,6bisP), which induce ChREBP activation. ChREBP in turn activates ATP citrate lyase (ACL), acetyl-CoA carboxylase (ACC), FA synthase (FAS), and stearoyl-CoA desaturase 1 (SCD1) [64]. Fasting signals, such as glucagon, prevent ChREBP activation [65, 66].
Finally, LXRα is activated by intermediates of the cholesterol pathway such as oxysterols in the postprandial and post-absorptive phase [67, 68]. LXRα promotes lipogenic gene transcription both directly by inducing expression of FAS, ACC and SCD1, and indirectly through induction of SREBP1c expression [69].

Next to lipogenesis, also VLDL secretion is tightly regulated in postprandial state. VLDL assembly in hepatocytes occurs in two steps. First, TAGs are added to the nascent apolipoprotein B (ApoB) by microsomal triglyceride transfer protein (MTP) in the ER to form a lipid-poor pre-VLDL particle [70, 71]. Then, the pre-VLDL is enriched with additional TAGs in the Golgi independent of MTP, but dependent on the incorporation of ApoCIII [72]. Finally, the mature VLDL particle is secreted into the circulation. Insulin release induces a suppression of VLDL production, and this coincides with elevated plasma lipid levels due to increased chylomicron concentrations in the postprandial phase, ensuring homeostasis of lipid levels. Conversely, a drop in insulin levels during fasting results in increased VLDL secretion. Insulin controls VLDL secretion by preventing Foxo1-mediated transactivation of MTP promoter activity and promotion of ApoB secretion [73, 74]. Concomitantly, insulin promotes clearance of circulating ApoB particles by the liver via the low-density lipoprotein receptor (LDLR) [75, 76]. Also other transcription factors, such as Foxa2, HNF4α and PPARα [77-79], and the parasympathetic nervous system [80] have been implicated in the regulation of VLDL secretion, however, the exact mechanisms have not been elucidated.
Thus, the fate of lipids reaching the liver after a meal is tightly regulated in order to adapt to the energy demands.

The role of FXR in hepatic lipid metabolism

The first evidence that FXR regulates lipid metabolism came from the comparison between wildtype and FXR knockout mice. FXR-/- mice display several defects in lipid homeostasis, including elevated hepatic cholesterol and TAGs, increased ApoB containing lipoproteins and a proatherogenic serum lipoprotein profile (high LDL) that is exacerbated by increased dietary cholesterol [40]. In line with this, treatment with CDCA, an endogenous BA with high affinity for FXR, resulted in a reduction of TAG levels in serum of hypertriglyceridemic and gallstone patients [81, 82]. Conversely, treatment of dyslipidemic patients with BA sequestrants (i.e. cholestyramine) increased the levels of triglyceride and VLDL [83]. Hypotriglyceridemic effects of FXR activation were observed in wild type, diabetic, and bile salt deficient mice, but not in FXR-/- mice [84, 85].
The TAG-decreasing action of FXR agonists is in part due to FXR-mediated increase in TAG clearance. Indeed FXR promotes triglyceride clearance, via induction of hepatic ApoC-II and repression of the lipoprotein lipase (LPL) inhibitors ApoC-III and ANGPTL3 [86-88]. FXR binds *in vitro* to distal enhancer elements upstream of the ApoC-II promoter. ApoC-II regulation by FXR is supported by increased ApoC-II expression upon CDCA in HepG2 and upon 1% CA diet in wild type, but not in FXR-/- mice [86]. Conversely, negative regulation of ApoC-III expression by FXR has been shown in both primary hepatocytes and HepG2 upon CDCA treatment. FXR binds to a negative FXRE upstream of ApoC-III promoter, and causes the displacement of HNF4α, which is a major regulator of ApoC-III [87].
Next to stimulation of lipolysis, FXR contributes to lower blood triglyceride concentrations via the inhibition of FA and TAG biosynthesis. C57BL/6J and diabetic KK-A^y mice fed a diet supplemented with cholic acid (CA), showed decreased hepatic expression of

genes encoding enzymes involved in FA and TAG biosynthesis, such as acyl-CoA synthetase (AceCS), malic enzyme (ME) and SCD1. At molecular level, FXR induces expression of SHP, which in turn inhibits LXR-induced activation of SREBP1c, thus resulting in inhibition of these hepatic lipogenic genes [88] (Figure 2). Concurrently, FXR-/- mice display a marked induction of lipogenic genes, such as SREBP1c, SCD1 and FAS [89], further substantiating FXR anti-lipogenic action.

Another intrahepatic effect of FXR activation is increased FA oxidation. CA diet increases the expression of FA oxidation genes medium-chain acyl-CoA dehydrogenase (MCAD), and long-chain acyl-CoA dehydrogenase (LCAD) in wild type C57BL/6J mice [88]. These gene expression changes are probably due to FXR-mediated induction of PPARα expression, which is known to promote hepatic FA oxidation [90]. Interestingly, a study by Xu et al. reports that induction of expression of liver carboxylesterase 1 (Ces1) is essential for systemic and hepatic lowering of TAGs induced by FXR agonists in C57BL/6 mice [91]. The authors propose that FXR directly activates Ces1 expression, which favours the release of FFAs, thereby activating PPARα, and a subsequent increase in FA oxidation. Of note, in proliferating hepatocyte cells, FXR upregulates pyruvate dehydrogenase kinase (PDK4), which promotes utilization of fat rather than glucose as an energy source [92]; however the functional meaning of this regulation in normal liver physiology is unclear.

Also VLDL secretion is regulated by FXR (Figure 2). CDCA reduced VLDL production in hamsters fed a fructose-supplemented diet and patients with hypertriglyceridemia [93, 94]. In HepG2 cells, it was established that FXR mediates the inhibition of VLDL secretion by CDCA, via the SHP-mediated suppression of HNF4α activity [95]. HNF4α is a master regulator of MTP and ApoB expression, important for VLDL secretion, as described above. According to a recent study, FXR reduces VLDL secretion in part via repression of phospholipase A2 G12B (PLA2G12B) expression [96]. The authors show that overexpression of SHP or stimulation with CDCA represses PLA2G12B promoter, however it has not been assessed whether the suppression of VLDL production by FXR activation is critically mediated by PLA2G12B.

Next to TAG metabolism, apolipoprotein metabolism is also intrinsically linked to cholesterol metabolism. FXR inhibits BA synthesis from cholesterol and induces BA hepatic outflow. On the other hand, FXR promotes reverse cholesterol transport through multiple mechanisms. Activation of FXR by CDCA promotes the activity of phospholipid transfer protein (PLTP), thus promoting the transfer of phospholipids and cholesterol from LDL to HDL [97, 98]. Moreover, expression of scavenger receptor BI (SRBI) increases upon CA diet in mice and decreases in FXR-/- mice compared to wild type, suggesting that FXR promotes hepatic uptake of HDL [99]. Finally, FXR induces ApoF expression, resulting in increased Cholesteryl Ester Transfer Protein (CETP) activity in HepG2 [100]. CETP promotes the exchange of cholesterol and TAGs between apolipoproteins and it is thought to provide an indirect way to deliver HDL cholesteryl esters to the liver [101]. Taken together, these observations depict a scenario in which FXR promotes the return of cholesterol from peripheral tissues to the liver for biliary disposal and consequent faecal elimination.

FXR activation in the ileum also drives lipid homeostasis adaptation (Figure 2). Intestinal FXR induces the expression of FGF19, the aforementioned enterokine signalling to the liver to reduce BA synthesis [102, 103]. Administration of recombinant human FGF19 or transgenic expression of the human FGF19 gene in obese/diabetic mice resulted in an increase in energy expenditure and a decrease in adipose tissue stores [104]. Concurrently, FGF19 transgenic mice showed reduced expression of acetyl CoA carboxylase (Acc2), which negatively regulates the entry of FAs into mitochondria for FA oxidation [104, 105]. FGF19 also inhibits the insulin-mediated stimulation of FA synthesis in primary hepatocytes, by reducing the expression of Srebp1c [106, 107]. Based on these observations, FGF19 action probably provides a means to counterbalance insulin anabolic signals during the transition from postprandial to post-absorptive state.
In conclusion, FXR impacts on lipid metabolism via inhibition of TAG biosynthesis and induction of FA oxidation and VLDL secretion, as inferred from pathophysiological states (Fxr knockout, diabetes, hypertriglyceridemia and cholestasis models). In the next paragraph, we will review the few papers in which the role of FXR in normal lipid physiology has been investigated.

FXR regulation of lipid metabolism in the post-absorptive state.
Following BA intestinal reabsorption, hepatic FXR is activated due to the arrival of BAs from the portal circulation. Fasting-refeeding experiments in wild type and FXR-/- mice support hepatic FXR modulation of lipid metabolism in the post-absorptive state. When fasted for 24 hours and refed for 6 hours, FXR-/- mice have higher hepatic expression of the glycolytic gene Lpk, and the lipogenic genes, acetyl-CoA carboxylase 1 (Acc1) and Fas and higher concentration of plasma TAGs than the wild type mice, indicating that FXR depletion results in impaired counter regulation of lipid synthesis from glucose in post-absorptive state [108]. Besides, VLDL production is higher in the refed FXR-/- than in wild type mice, suggesting that FXR counterbalances also VLDL secretion in post-absorptive state [108]. Based on these observations, hepatic FXR signalling, in concert with FGF19 signalling, may represent a gatekeeping system to prevent excessive lipid accumulation in the fed liver and in the blood.
The FXR-mediated inhibition of lipogenesis is maybe prolonged to the fasting state. During fasting, expression of FXRα3/4 isoforms is selectively increased [109]. In addition, PPARG coactivator 1α (PGC1α), one of the key regulators of metabolism during fasting, increases FXR transcriptional activity. Fasting decreases TAGs in wild type, but not in FXR-/- mice, supporting that in conditions of nutrient deprivation FXR acts to limit lipogenesis (Figure 2).
Post-translational modifications (PTMs) refine regulation of FXR function in lipid metabolism, by allowing FXR to promptly sense the energy status during the feeding-fasting transition. Sugars, amino acids and fats are all catabolized to Acetyl-CoA as the precursor for the energy currency ATP and for lipid synthesis. Acetyl-CoA concentration is therefore high in the hepatic nucleo-cytosolic compartment in the postprandial and post-absorptive phase. In contrast, the majority of the Acetyl-CoA pool is predominantly in the mitochondria during fasting, in order to foster ATP synthesis and ketogenesis

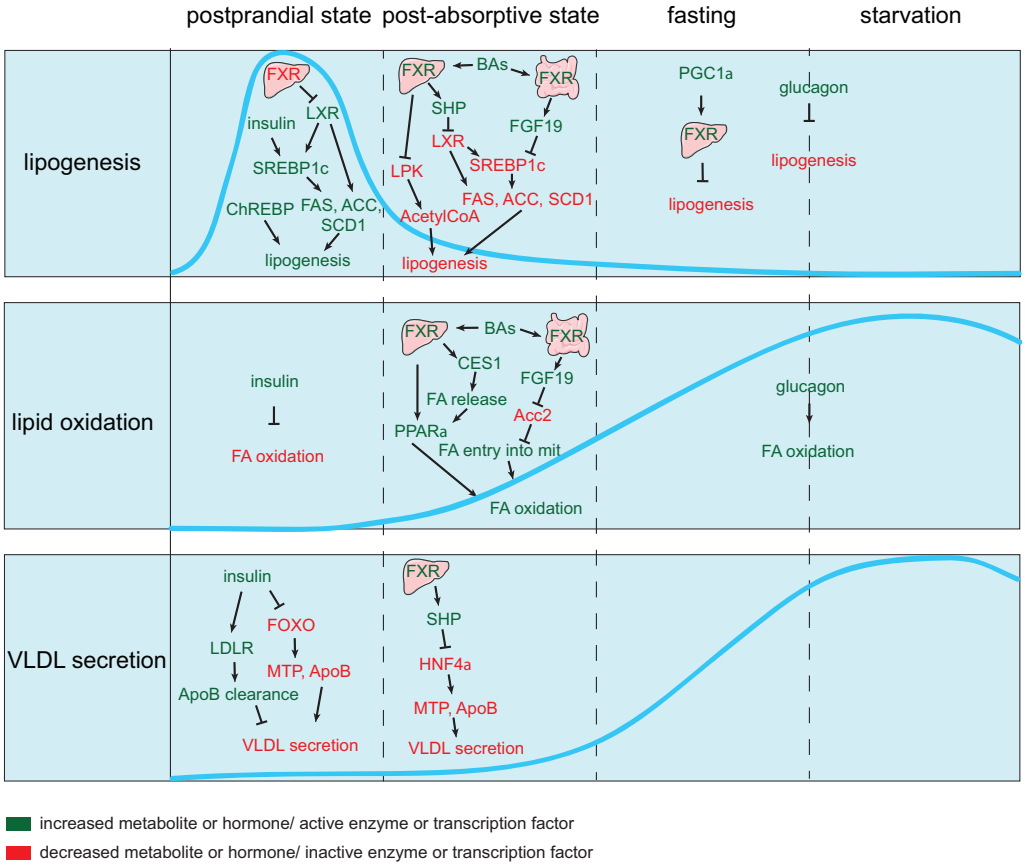

Figure 2. FXR participates to the dynamic network regulating lipid metabolism across nutrition phases. Dynamic view of hormonal, enzymatic and transcriptional regulation of lipid metabolism in postprandial, post-absorptive, fasting and starvation states. During the postprandial phase, lipogenesis peaks due to activation of insulin, LXR, SREBP1c and ChREBP signalling, whereas lipid oxidation and VLDL secretion are inhibited by insulin signalling. In the post-absorptive state, intestinal and hepatic FXR repress lipogenesis and promote FA oxidation. Hepatic FXR also inhibits VLDL secretion via HNF4α inhibition. Glucagon inhibits lipogenesis and increases FA oxidation during fasting/starvation, and FXR presumably inhibits lipogenesis, following activation by PGC1α.

[110]. Next to its use as metabolic precursor and ATP generator, Acetyl-CoA is used for protein acetylation. The acetylation state of transcription factors such as FOXOs, CREB, SREBPs, FOXA, C/EBPs and ChREBP is dynamically regulated dependent on the energy status [111]. Also FXR has been shown to be acetylated on lysine 217 and 157 and its acetylation status seems to be increased in mice fasted overnight and refed for an hour [17]. The acetylase p300 and the deacetylase Sirt1 are critical for the dynamic regulation of FXR acetylation status. Knock down of p300 alters CDCA-dependent modulation of genes involved in lipoprotein metabolism in HepG2 cells, however the dependence on FXR was not established [112]. On the other hand, adenoviral knock down of Sirt1 in mice resulted in increased FXR acetylation, and increased expression of lipogenic genes Fas and Srebp1c in the liver [17], in contrast to FXR ligand repression of lipogenic gene expression.

Expression of an acetyl mimic mutant FXR K217Q in lean mice induces the lipogenic genes Fas, Acc1, Srebp1c, Scd1, and diacylglycerol O-acyltransferase 1 (Dgat1) in the liver, whereas overexpression of the acetyl defective mutant FXR K217R in obese mice reduced liver TAGs compared to overexpression of wild type FXR [19]. Nutrient dependency in regulation of FXR acetylation is supported by detection of higher acetylation levels of FXR in obese mice than in lean mice [19]. Of note, deacetylation of FXR might be needed for FXR-mediated inhibition of lipogenesis, as supported by the findings that nuclear factor erythroid-2-related factor 2 (Nrf2) reduces p300-dependent acetylation of FXR *in vitro* and that activation of Nrf2 represses LXRα-dependent induction of lipogenesis *in vivo* [113]. Based on these observations, we hypothesize that in the postprandial state, when there is an excess of nucleo-cytosolic acetyl-CoA, FXR function is transiently reduced by acetylation to allow for occurrence of lipogenesis in response to insulin signalling. Later in post-absorptive state, the drop in acetyl-CoA and FXR acetylation may restore the function of FXR in repression of lipogenesis. (Figure 3).

Another FXR PTM regulated by the cell energetic status is phosphorylation. During fasting, AMPK is activated and blocks anabolic reactions, while promoting catabolic pathways [114]. Phosphorylation of FXR on serine 250 by AMPK decreases FXR transcriptional activity [115], however the implications on FXR regulation of lipid metabolism have not been investigated.

Overall, FXR functions as a "homeostat" for lipid metabolism in the liver, by sensing the nutrient availability via binding to BAs and via PTMs (e.g. high levels of acetyl-CoA give rise to induced protein acetylation) and regulating metabolic gene programs to control hepatic and systemic lipid concentrations in line with energy demands.

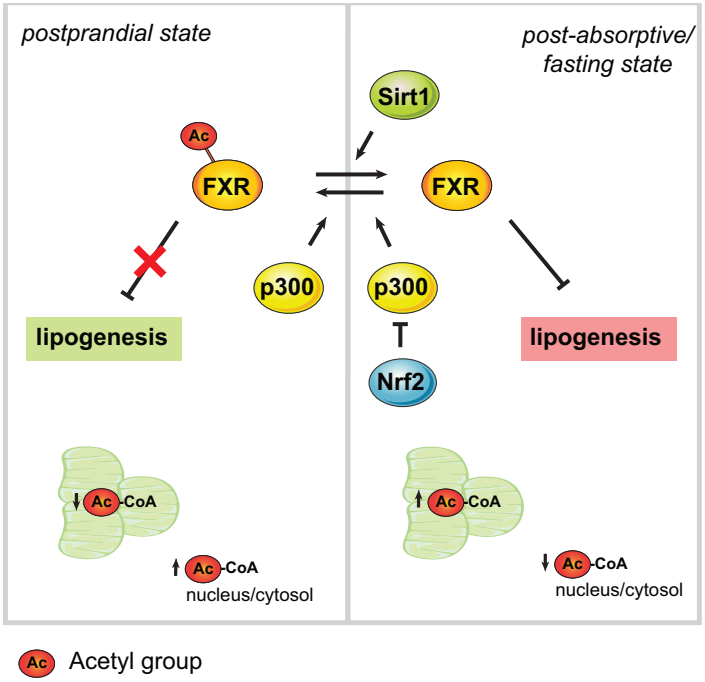

Figure 3. Hypothetic model for the dynamic acetylation status of FXR across nutrition phases. In the postprandial state, high acetyl-CoA concentrations in the hepatic nucleocytosolic compartment favour p300-dependent acetylation of FXR, which results in reduced FXR activity. In the post-absorptive and fasting states, however, p300-dependent acetylation of FXR is reduced, due to the decreased nucleo-cytosolic acetylCoA concentration and inhibition of p300 by Nrf2. In these nutrition phases, FXR is deacetylated by Sirt1 and acts as a suppressor of lipogenesis.

THE ROLE OF FXR IN GLUCOSE METABOLISM

The regulatory networks of glucose homeostasis

Carbohydrates in forms of polysaccharides are broken down by the enzymatic hydrolysis of salivary and pancreatic amylases in the mouth and in the small intestine, respectively. The resulting monosaccharides, such as glucose, galactose and fructose are absorbed by the gut brush border via active transport or facilitated diffusion before entering the bloodstream [116, 117]. Glucose enters the hepatocytes via the glucose transporter GLUT2 and is phosphorylated by glucokinase (GK) to form glucose-6-phosphate (G6P). G6P is subsequently condensed into glycogen via the glycogen synthesis pathway, is used to generate NADPH for biosynthetic processes via the pentose phosphate pathway, or is converted into pyruvate by glycolysis. Pyruvate is used in the mitochondria for ATP production or converted into FAs through lipogenesis. Up to 5% of hepatic glucose in the postprandial phase is shunted into the hexosamine biosynthetic pathway, ensuring the glycosylation of lipids and proteins. Because of the excess in glucose/glycogen, gluconeogenesis is concomitantly suppressed [118, 119]. Progression towards the post-absorptive state implies shifting to a glycogenolitic metabolism, while gluconeogenic processes occur at high rate during fasting and starvation [21].

An intricate network of transcription factors responsive to hormones and nutrients coordinate the regulation of glucose metabolism in a dynamic manner during the feeding-fasting transition (Figure 4). A primary regulator of glucose metabolism in postprandial state is insulin. In response to high blood glucose after a meal, insulin secreted by pancreatic β-cells induces GK in the liver, thereby retaining glucose in a phosphorylated state in hepatocytes [120]. A regulatory transcriptional complex consisting of HIF-1, HNF-4α, and p300 mediates GK activation in response to insulin [121, 122]. The metabolic nuclear receptor LXRα is also involved in induction of GK expression in response to insulin [123]. In addition, insulin directly enhances glycogen synthesis by inactivating GSK3, which normally phosphorylates and thereby inactivates glycogen synthase. Furthermore, insulin represses glycogenolysis by acetylation and inactivation of glycogen phosphorylase (PYGL) [59]. Finally, insulin action suppresses gluconeogenesis, via activation of PKB/AKT, which in turn phosphorylates and inactivates the pro-gluconeogenic transcription factor FOXO1, responsible for activation of transcription of phosphoenolpyruvate carboxykinase 1 (PEPCK) and Glucose 6-phosphatases (G6PC) [124].

Another key hepatic sensor of glucose metabolites in postprandial state is ChREBP. ChREBP activity is increased by acetylation [125] and O-GlcNacylation [126], two PTMs that use glucose metabolites as substrates. ChREBP binds ChORE elements to induce expression of glycolytic and lipogenic genes [64, 127]. In addition, ChREBP suppresses Sirt1, thereby presumably reducing PGC1α-dependent gluconeogenesis in the postprandial state [128, 129]. The nuclear receptor liver receptor homolog 1 (LRH1) appears to be an upstream regulator of the glucose-sensing system of the liver, since it induces GK-dependent G6P synthesis, thereby controlling the availability of the glucose metabolites needed to activate ChREBP [129, 130]. Also the oxysterol sensor LXR promotes ChREBP expression and activity [131], suggesting the existence of a shared regulatory network coordinating glucose and lipid metabolism in postprandial state.

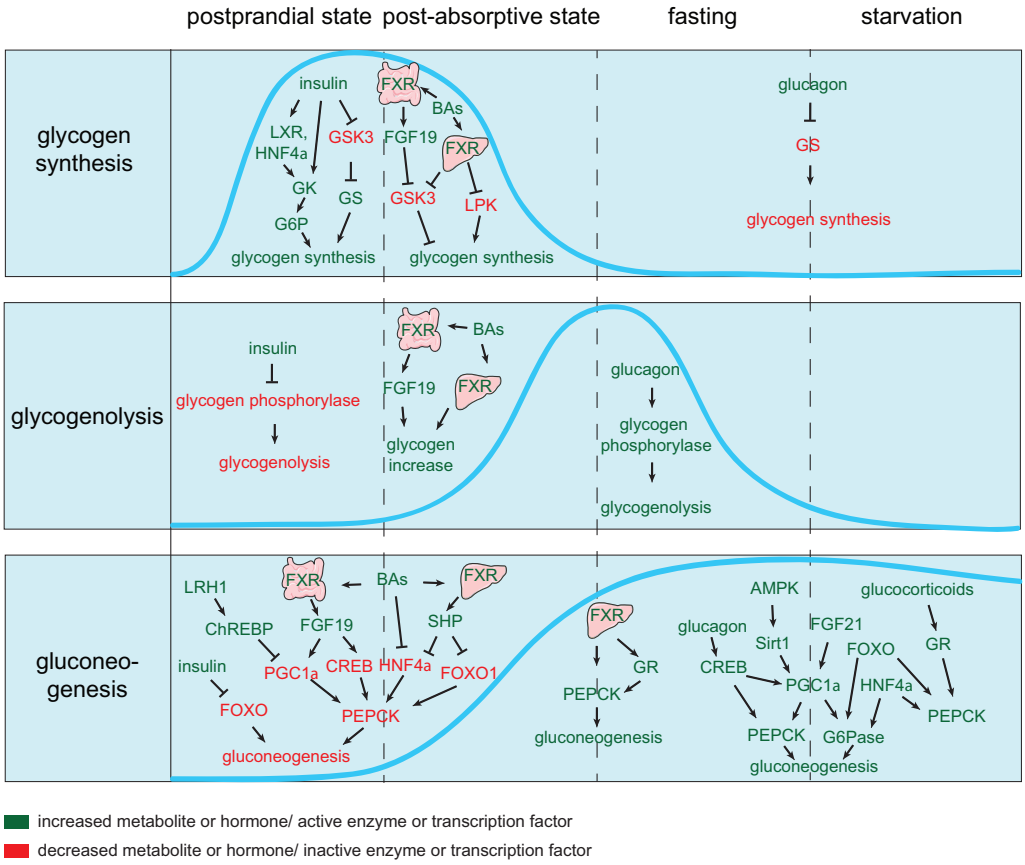

Figure 4. FXR regulation of glucose metabolism in different phases of nutrition. Dynamic view of regulation of glucose metabolism in postprandial, post-absorptive, fasting and starvation states. In the postprandial state, insulin coordinates the inhibition of glycogen synthesis (via GK activation and GSK3 inhibition), the inhibition of glycogen synthesis (via inhibition of glycogen phosphorylase) and gluconeogenesis (via inhibition of FOXO). In the late postprandial/post-absorptive state, BAs maintain a pro-glycogenic and anti-gluconeogenic signalling via the integrated activity of intestinal and hepatic FXR. Glycogen synthesis is induced both via FGF19 by GSK3 inhibition and via hepatic FXR by LPK and GSK3 inhibition, whereas repression of gluconeogenesis is mediated by PGC1α and CREB (in the FGF19 cascade) and by HNF4α and FOXO1 (in the hepatic FXR cascade). During fasting, FXR presumably participates to the intricate regulatory network that stimulates the gluconeogenic gene PEPCK. (Further details are described in the text).

When the organism endures food deprivation, gluconeogenesis is induced by glucagon, glucocorticoids and energy cofactors through the concerted action of multiple transcriptional regulators. During fasting, activation of glucocorticoid receptor (GR) by glucocorticoids increases expression and stability of PEPCK to induce gluconeogenesis [132]. In addition, in situations of low energy status, increased NAD^+ amounts due to AMP-activated protein kinase (AMPK) activation enhance Sirt1 activity and lead to the deacetylation of the transcriptional coactivator PGC1α, thereby increasing mitochondrial biogenesis and function. Differently, in conditions of caloric excess, PGC1α is acetylated by histone acetyltransferase GCN5 and thus inactivated [133, 134]. PGC1α regulates hepatic

gluconeogenesis [135] by interacting with HNF4α and FOXO1 to promote transcription of amongst others PEPCK and G6PC [124]. Also cyclic AMP response element binding (CREB) protein can directly induce PEPCK in response to glucagon and potentiate pro-gluconeogenic transcriptional programs under prolonged fasting, by inducing PGC1α expression [136]. An important hepatokine upstream of PGC1α- induction of gluconeogenesis is FGF21. During starvation PPARα activation by FA induces hepatic expression of FGF21, which in turn prompts PGC1α to stimulate gluconeogenesis [137, 138]. Noteworthy, C/EBPα enhances availability of amino acids as gluconeogenic substrates during fasting and starvation [139].

In summary, glucose homeostasis is under control of a complex network of transcription factors throughout the different nutritional phases. These factors are able to sense energy status and coordinate regulation of glucose metabolism.

The role of FXR in glucose metabolism

FXR-/- mice show increased serum glucose and impaired glucose and insulin intolerance, supporting a role for FXR in glucose homeostasis [84, 89]. Moreover, a CA supplemented diet and administration of synthetic FXR agonist GW4064 reduced serum glucose in wild type mice after a fasting period [84, 89, 140]. The relevance of FXR in BA hypoglycemic action is further substantiated by a decrease in glucose levels in mice in which constitutively active FXR is overexpressed in the liver [84].

Hypoglycemic effects of FXR activation rely on repression of gluconeogenesis and induction of glycogen synthesis. CA supplemented in the diet decreased expression of gluconeogenic genes PEPCK, G6PAse, and PGC1α. This regulation is lost in FXR-/- and SHP-/- mice [89], suggesting that downregulation of gluconeogenic genes depends on FXR activation of the nuclear repressor SHP. An independent study confirms that CA diet reduced the expression of PEPCK, G6Pase and FBP1 in wild type mice and ascribes this effect to the SHP-dependent repression of HNF4α and FOXO1, since SHP overexpression counteracts the HNF4α- and FOXO1-dependent induction of gluconeogenic gene promoter activity in HepG2 cells [141]. On the contrary, in primary rat hepatocytes and hepatoma cell lines GW4064 and CDCA resulted in increased PEPCK expression [140]. The reasons for such discrepancy are not completely clear. It has been observed that CDCA may inhibit PEPCK transcription in an FXR-independent manner, since PEPCK promoter activity is decreased by CDCA, but not by GW4064 in HepG2 cells expressing a PEPCK promoter reporter [142]. As suggested by the authors, differences in species and the existence of FXR-independent effects of BAs on glucose homeostasis should be taken into account when investigating FXR regulation of gluconeogenic genes.

Effects of FXR activation on glycogen synthesis have been assessed in diabetic mice by Zhang et al., who reported increased hepatic glycogen synthesis and glycogen content in db/db mice upon GW4064 administration [84]. The authors show that incorporation of glucose into glycogen increased in murine primary hepatocytes upon GW4064 treatment. In addition, GW4064 induces phosphorylation of GSK3β, IRS-1, IRS-2 and AKT, suggesting that FXR activation may increase glycogen synthesis in liver cells, by improving insulin sensitivity. Another mechanism underlying FXR-mediated induction of gly-

cogen synthesis is the inhibition of glucose oxidation. At high glucose concentrations, FXR activation decreases the transcription of liver pyruvate kinase (LPK), by causing the release of ChREBP from the ChORE sequences [143]. Suppression of LPK results in shunting glucose metabolites towards glycogen synthesis [108].
Interestingly, glucose impacts on FXR function by increasing FXR stability and transcriptional activity [20]. At high glucose concentrations, the abundance of metabolites into hexosamine biosynthetic pathway (HBP) promotes FXR O-GlcNAcylation, which increases its stability. *In vivo* fasting-refeeding experiments show that FXR indeed undergoes O-GlcNAcylation under fed conditions.
In conclusion, FXR belongs to the network of transcriptional regulators coordinating glucose metabolism, although some controversy exist on FXR dependent and independent effects of BAs. Strict experimental control of fasting/feeding conditions is needed to understand how FXR impacts on glucose homeostasis under normal physiology conditions, as will be further discussed in the next section.

FXR regulation of glucose metabolism in different phases of nutrition

Both intestinal and hepatic FXR contribute to glucose homeostasis after ingestion of a meal, similarly to the above discussed case of lipid homeostasis (Figure 4). The contribution of intestinal FXR involves induction of FGF19/15 gene expression with subsequent increased FGF19/15 flux from the intestine to the liver. The physiological importance of the FXR-FGF19 axis in post-absorptive glucose metabolism is underscored by the onset of hyperglycemia in FGF19 and FGFR4 knockout mice in response to a fasting-refeeding challenge [144]. FGF19 inhibits gluconeogenesis, since mice treated with FGF15/19 display reduced hepatic expression of PGC1α, G6Pase and PEPCK and reduced gluconeogenic flux, as measured by NMR [145]. Gain and loss of function studies in mice suggest that PGC1α mediates the FGF19 effects on PEPCK and G6Pase. In addition, FGF19 suppresses hepatic CREB activity [145], which impacts on gluconeogenesis, as described earlier. FGF19 regulates not only gluconeogenesis, but also glycogen synthesis. Indeed, the amount of liver glycogen is decreased in FGF19 knockout mice fed ad libitum. Effects of FGF19 on glycogen storage seems to be insulin-independent, as FGF19 activates a different signalling cascade compared to insulin [144]. Interestingly, plasma levels of FGF15/19 peak 1 hour after feeding in mice and 2-3 hours after a meal in humans, both well after the decrease in insulin levels [145]. In summary, FGF19 signalling inhibits gluconeogenesis and promotes liver glycogen accumulation in late postprandial and the post-absorptive phase, thereby prolonging some of the insulin-mediated effects on glucose metabolism.
As discussed in the former paragraph, hepatic FXR reduces gluconeogenesis via PEPCK and G6Pase and induces glycogen synthesis via GSK3β. This metabolic response mimics the outcomes of FGF19 signalling to the liver after a meal, however the physiological relevance of this metabolic regulation is not clear. Interestingly, Lpk, Fas, and Acc1 expression were increased in FXR-/- mice fasted for 24 hours and refed for 6 hours, indicating that when FXR is depleted glucose metabolites flow towards acetyl-CoA and lipid rather than glycogen generation [108]. Indeed, liver glycogen content was lower in the refed

FXR-/- mice, confirming the role of FXR in glycogen synthesis. At high glucose concentrations, activation of FXR by GW4064 inhibits Lpk expression in primary rat hepatocytes, suggesting that FXR may inhibit glycogen synthesis by blocking Lpk activity. FXR regulation of gluconeogenesis after a meal was also investigated in this study. Hepatic expression of Pepck and of the pro-glucogenic factors Pgc1α, Foxo1 and Hnf4α is lower in the refed FXR-/- mice, challenging the view that FXR inhibits gluconeogenesis. Concurrent with the reduction in gluconeogenic factors, refed FXR-/- mice have lower plasma glucose and insulin, but compensatory mechanisms cannot be ruled out. All in all, FXR has been shown to regulate glucose homeostasis in the late postprandial and post-absorptive state, controlling the gluconeogenesis rate after the decline in insulin signalling.

The effect of FXR favouring gluconeogenesis seems to persist during fasting. After 15 hours of food withdrawal, FXR-/- mice have lower blood glucose, lower hepatic Pepck expression and an impaired gluconeogenic capacity in response to a pyruvate challenge compared to wild type mice [146]. This may indicate that FXR induces gluconeogenesis in fasted state, as confirmed by increased blood glucose and PEPCK expression upon OCA treatment in fasted wild type mice. Conversely, OCA caused a reduction of PEPCK in fed mice, indicating that FXR regulates glucose metabolism differentially during the transition from fed to fasted state. In the fasted state, FXR may be required for glucocorticoid-induced stimulation of gluconeogenesis, since FXR-/- mice have an attenuated induction of PEPCK and G6Pase upon dexamethasone treatment compared to wild type mice [146]. Nevertheless, the importance of the role of FXR during fasting is not well understood, since it is expected that FXR activation is low due to BA storage in the gallbladder and the concomitant decrease in BA levels in hepatocytes. On the other hand, an isoform specific increase in FXR expression in the fasted state [14, 109] may compensate for the reduced availability of ligands. Moreover, FXR activity may be induced by other factors during fasting. In this regard, the key pro-gluconeogenic factor PGC1α has been described to activate FXR during fasting [109].

Posttranslational status of FXR might contribute to regulation of glucose homeostasis across the nutrition phases. Persistent FXR acetylation in nutrient excessive conditions is associated with glucose intolerance, as lean mice expressing an acetyl mimic FXR mutant showed a decrease in glucose tolerance [19]. In addition, expression of gluconeogenic genes Pepck and G6PC is decreased by knock down of acetylase p300 [112], however, knock down of the deacetylase Sirt1 did not yield significant changes [17]; thus the role of acetylation in modulating FXR regulation of glucose metabolism is controversial. No effects on glucose homeostasis of FXR O-GlcNAcylation, as occurring in fed state in response to glucose itself, have been described [20].

In summary, BAs signal via intestinal FXR/FGF19 and hepatic FXR to facilitate the energy switch occurring at the fasting-feeding transition, thereby partly prolonging insulin actions. Reabsorbed nutrients reaching the liver together with BAs may provide the substrates and the metabolic environment fine tuning FXR function, via PTMs and metabolic cofactors.

THE ROLE OF FXR IN AMINO ACID METABOLISM

Regulation of amino acid metabolism

Dietary proteins begin to be digested in the stomach, where the acidic environment favours protein denaturation. Denatured proteins are accessible as substrates for proteolysis by pepsin, which is active in the highly acidic environment of the stomach. Protein degradation into oligopeptides and amino acids continues in the lumen of the intestine by proteolytic enzymes secreted from the pancreas. Single amino acids, as well as di- and tripeptides, are transported from the intestinal lumen into the enterocytes and subsequently released into the blood for absorption by other tissues. Amino acids reaching the liver in the postprandial state can be incorporated into proteins or catabolized to generate energy, glucose, or fatty acids [118, 147]. In the transition from the fed to the fasted state, when amino acid substrates decline, protein synthesis and amino acid catabolism are downregulated. However, starvation triggers amino acid degradation of body proteins for generation of glucose and ATP [21].

mTORC1 regulates protein synthesis and is a signal integrator of nutrients, growth factors, energy and stress. Amino acids activate the Rag GTPases, which recruit mTORC1 on the surface of endosomes and allow it to bind to Rheb, an essential activator of mTORC1. As a result of mTORC1 activation, the rate of protein synthesis increases [148]. For an adult in physiological nitrogen balance the amount of amino acids that is catabolized almost equals the dietary intake of proteins, as the amount needed for protein synthesis is nihil compared to the intake [149].

An important step in amino acid catabolism is the removal of the α-amino group by aminotransferases (transaminases) to generate glutamate, using pyridoxal phosphate as a cofactor. Subsequently, glutamate is deaminated to NH_4^+ (ammonium) and α-ketoglutarate. The latter provides the carbon skeleton for intermediates of TCA cycle, used to produce ATP or generate precursors for FA synthesis and gluconeogenesis. Alternatively, glutamate is either carried into the mitochondria (together with NH_4^+) for excretion as urea, or converted into glutamine, as non-toxic blood carrier of nitrogen in the body [147]. Urea excretion and glutamine synthesis are essential pathways for the detoxification of ammonium in mammals and are spatially restricted in the liver, which can be described as metabolic zonation. Periportal hepatocytes are exposed to high amino acid and ammonium concentrations coming from the portal circulation and therefore rely on ureagenesis a as low affinity, but highly efficient means of ammonium disposal. On the other hand, pericentral hepatocytes serve as high affinity scavengers, which prevent nitrogen from reaching the systemic circulation in the toxic form of ammonium, by converting it into glutamine [150]. Amino acids cannot be stored in the liver, which makes ureagenesis a crucial escape route for toxic ammonium generated by amino acid catabolism in conditions of excess in dietary protein intake or of prolonged fasting. The urea cycle relies on the mitochondrial enzymes carbamoyl-phosphate synthase I (CPS1), ornithine transcarbamylase (OTC), and the cytoplasmic enzymes argininosuccinate synthase (ASS1), argininosuccinate lyase (ASL), and arginase (ARG1). Urea cycle progression requires synthesis of N-acetylglutamate (NAG) by NAG synthase (NAGS) and allosteric binding of NAG to CPS1 [151]. Other than allosteric cofactors, regu-

lation of urea cycle enzymes involves substrate availability, hormonal and transcriptional regulation, and PTMs [152, 153].

During fasting and starvation, glucagon and glucocorticoids enhance the urea cycle by transcriptional regulation of ASS1 and ASL expression, stabilization of mRNA of CPS1 and ARG1, and protein stabilization of OTC [154]. Hormonal control of ureagenesis in response to fasting may be mediated by multiple transcription factors, which have been described to regulate amino acid metabolism [155, 156]. Glucocorticoids bind the glucocorticoid receptor (GR), and increase the expression of ARG1, consistent with accumulation of arginine and a reduction in urea/ornithine in mouse models of GR loss of function [157]. Also the transcription factor C/EBP critically mediates the hormonal control of ureagenesis, because regulation of Cps1 and Arg1 mRNA expression in response to dexamethasone and/or glucagon is severely impaired in primary-cultured hepatocytes derived from C/EBP-/- mice [158]. C/EBP null mice have hyperammonemia, associated with reduced protein expression of CPS1, OTC, ASS1, ASL and ARG1 compared to wild type mice, substantiating the positive regulation of ureagenesis by C/EBP [139]. Induction of C/EBP upon fasting requires the general control nondepressible-2 (GCN2), a key sensor of amino acid deprivation and modulator of the fasting response in the liver [159]. Fasting associates with increased hepatic expression of other transcription factors, such as HNF4α and PPARα, which have also been implicated in the regulation of amino acid metabolism [160]. HNF4α induces ureagenesis via induction of OTC expression, as supported by the observed hyperammonemia and decrease in plasma urea in liver-specific HNF4α knock out mice. The regulation of OTC expression by HNF4α is consistent with the presence of HNF4α response elements in the promoter of OTC [161]. PGC1α also promotes ureagenesis in mouse periportal hepatocytes in response to glucagon, presumably via induction of expression of SIRT3 and SIRT5, which are responsible for deacetylation and activation of OTC and CPS1 [162]. In addition, ureagenesis is decreased in PGC1α null mice. In conclusion, hormonal and transcriptional regulation has been described to induce amino acid catabolism during the fasting and starvation phases (Figure 5). This is likely to occur to supply the body with energy substrates, when there is a shortage in glucose and fatty acid substrates. Urea is produced to dispose of the toxic nitrogen component.

Not much is known about the physiological regulation of amino acid metabolism in the postprandial and post-absorptive state. Insulin has been shown to reverse the glucocorticoid/glucagon-dependent increase in Cps1 synthesis [163, 164]. Notably, a high protein diet and fasting may induce activation of ureagenesis via sirtuins, since Sirt5 null mice display an impaired Cps1 activity compared to wt mice both upon fasting and high protein diet [165]. *In silico* and *in vitro* studies support that Sp1, CREB, HNF-1, and NF-Y, which are known to be responsive to hormones and diet, regulate NAGS transcription [166], however, the relevance of these regulators has not been studied *in vivo.*

FXR and amino acid metabolism: a new regulatory axis in the post-absorptive state?

Recent studies have extended the regulatory action of FXR to the third category of basic

nutrients: amino acids. Both intestinal and hepatic FXR contribute to amino acid homeostasis after ingestion of a meal (Figure 5), similarly to the above-discussed cases of glucose and lipid homeostasis. The FXR-FGF19 axis seems to promote protein synthesis in postprandial state, since FGF19 administration in mice increased the rate of protein synthesis. This was established by measuring the production of ^{2}H alanine per hour in mice injected with $^{2}H_{2}O$ and either vehicle or FGF19 [144]. Mechanistically, it was established that FGF19 may signal via RAS–ERK–p90RSK pathway to induce phosphorylation of eukaryotic initiation factors eIF4B and eIF4E, thereby promoting the initiation of translation, and to induce phosphorylation of ribosomal protein S6, thereby improving the efficiency of protein synthesis by inducing cap-dependent translation [144].
Also genome wide analysis have pointed towards a role for FXR in amino acid metabolism, since genome-wide FXR binding studies identified amino acid metabolism amongst the top enriched pathways harbouring FXR binding in or around the respective genes [167,

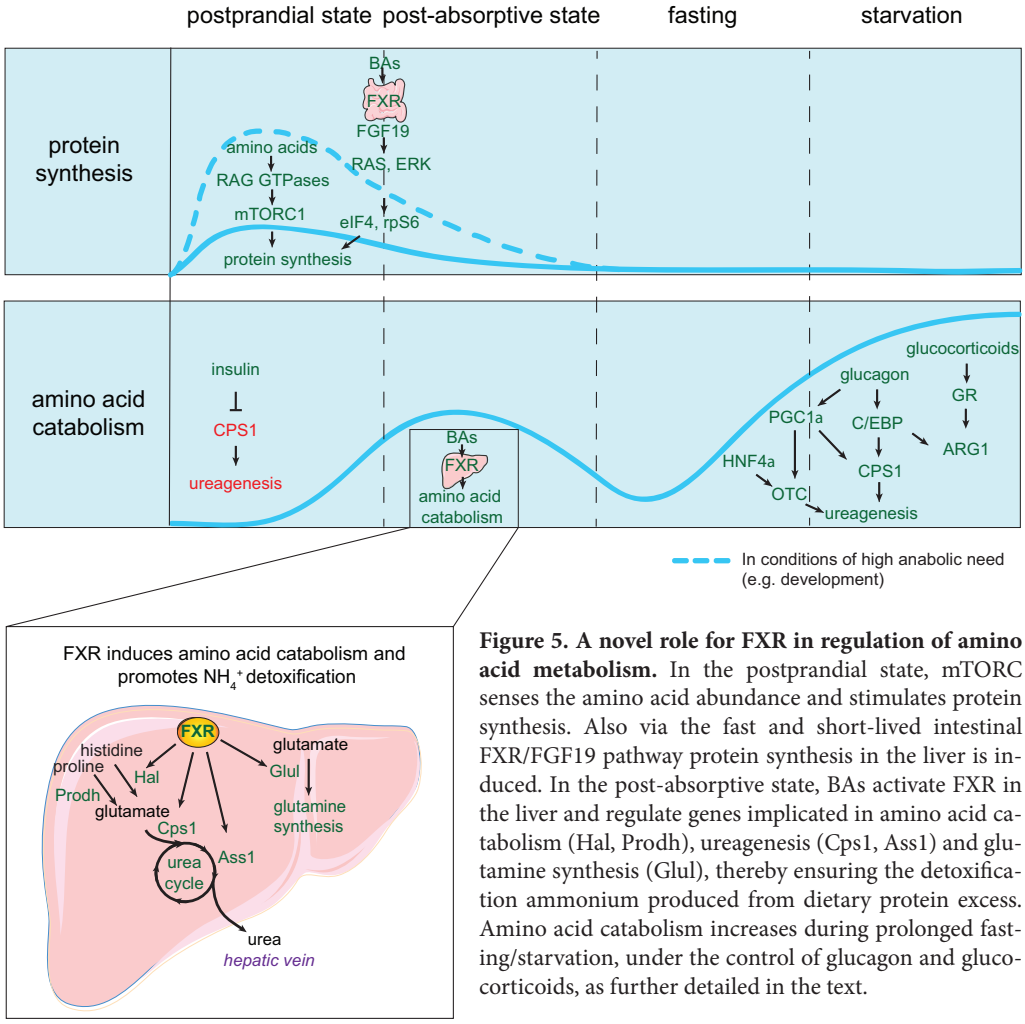

Figure 5. A novel role for FXR in regulation of amino acid metabolism. In the postprandial state, mTORC senses the amino acid abundance and stimulates protein synthesis. Also via the fast and short-lived intestinal FXR/FGF19 pathway protein synthesis in the liver is induced. In the post-absorptive state, BAs activate FXR in the liver and regulate genes implicated in amino acid catabolism (Hal, Prodh), ureagenesis (Cps1, Ass1) and glutamine synthesis (Glul), thereby ensuring the detoxification ammonium produced from dietary protein excess. Amino acid catabolism increases during prolonged fasting/starvation, under the control of glucagon and glucocorticoids, as further detailed in the text.

[168]. In addition, Gardmo et al. [169] showed increased protein expression of the transaminase Got1, the deaminase Glud1, and the urea cycle genes Ass1, Arg1, Cps1 and Oat in mice administered an FXR agonist for 3 days. However, the effects of FXR activity on amino acid catabolism had never been investigated.

In a recent study from our group, we show that FXR promotes amino acid catabolism and ammonium clearance [170]. We used an *in vivo* SILAC-based approach to accurately quantify liver proteome-wide changes in mouse livers in response to the semisynthetic FXR ligand OCA and to FXR deletion. FXR activation induced protein expression of Hal and Prodh, key enzymes for histidine and proline degradation, respectively. In addition, FXR activation induced expression of proteins implicated in both ureagenesis (Ass1, Asl, and Arg1) and glutamine synthesis (Glul), whereas FXR deletion downregulated the expression of Cps1, regarded as the rate limiting enzyme in the urea cycle. FXR binds to regulatory regions in proximity of the respective genes and activates the expression of these genes in primary hepatocytes, suggesting that FXR directly regulates their transcription. We show that FXR activation promoted ammonium clearance *in vivo,* by injecting mice with a labelled ammonium tracer and measuring newly formed labelled urea. OCA increased the conversion of a labelled ammonium tracer into urea in mice fasted for 6 hours and refed with a high protein diet, concurrent with an increased hepatic expression of Cps1, Ass1 and Gls2, implicated in ureagenesis. In contrast, FXR deletion resulted in hepatic accumulation of glutamate and aspartate, precursor metabolites for the urea cycle, further substantiating the role of FXR in regulating amino acid homeostasis.

We hypothesize therefore that FXR regulates amino acid metabolism in postprandial state in a dual manner. Firstly, as an early response, intestinal FXR directs amino acids to the synthesis of proteins via the fast and short-lived FGF19 signalling cascade. Subsequently, sustained activation of hepatic FXR due to BAs returning to the liver in the post-absorptive state drives direct transcriptional regulation of genes important in amino acid catabolism and ammonium detoxification. Based on these data, FXR has an important role in adapting to dietary protein excess, thereby detoxifying the ammonium generated in the reactions of amino acid degradation. And because FXR regulates the fate of all 3 dietary building blocks, amino acids, glucose and fatty acids, FXR can be regarded as a post-absorptive homeostat of dietary intake.

BEYOND FXR REGULATION OF NUTRIENT METABOLISM: IMPLICATIONS ON CELL BIOLOGY AND IMMUNOMETABOLISM

FXR in autophagy and proliferation: the relay between nutrient status and cell fate

Nutrient availability is intimately linked to a wide range of biological processes in the cell, including autophagy and cell growth. The investigation of transcriptional networks orchestrating these nutrient-sensing processes has led to the elucidation of novel functions of FXR. In conditions of nutrient shortage such as starvation, autophagy supplies energy to the cell, by ensuring the transport of intracellular substrates to lysosomes for degradation and recycling. According to two independent studies [171, 172], FXR is a repres-

sor of autophagy in the liver, concurrent with its function and activation in postprandial/post-absorptive state. Notably, Seok et al. show that FXR activation by GW4064 decreases expression of autophagy genes and the amount of autophagy vesicles, even in fasted mice. In addition, the decrease in autophagy markers upon feeding is absent in FXR-/- mice, supporting the role of FXR as physiological suppressor of autophagy in the fed state. Mechanistically, FXR activation disrupts the functional interaction between the autophagy activator CREB and its coactivator CRCT2, thereby trans-repressing autophagy genes [172]. Another study [171] reports crosstalk of FXR with the fasting regulator PPARα as a crucial interlocking mechanism for regulation of autophagy. These two nutrient sensing nuclear receptors compete for binding to shared sites in autophagy gene promoters, with opposite transcriptional outputs: FXR suppresses autophagy, whereas PPARα reverses this suppression. The physiological relevance *in vivo* of this coordinated regulation is supported by the observation that autophagy protein markers and autophagy vesicles increased in mouse liver upon PPARα activation even in the fed state, and were absent in PPARα null mice. Likewise, FXR activation decreased autophagy protein markers and autophagy vesicles, even in fasted state, whereas these effects were blunted in FXR null mice. Although it is not clear whether FXR crosstalk with either CREB or PPARα are complementary or occurring in response to different cues, these studies point at the relevance of FXR in fine tuning autophagy, as part of its transcriptional program in response to nutrients.

Nutrition is indispensable for cell survival and proliferation. Sensors of nutrient abundance and energy status such as mTORC play a central role in the promotion of cell proliferation, by inducing lipid and protein anabolism and inhibiting autophagy. Intriguingly, FXR has also been implicated in cell proliferation. Hepatocytes divide once every 200-300 days under healthy conditions, however their proliferation is triggered by partial liver resection or upon a tumorigenic challenge [173]. Liver regeneration in FXR knockout mice is impaired in the early stages after partial hepatectomy (PH), and 0.2% CA supplemented diet increased liver regeneration after PH, suggesting that activation of FXR by BAs contributes to hepatocyte proliferation [174]. Mechanistically, FXR may promote liver regeneration by inducing FoxM1b, which is a critical inducer of cell cycle progression, as supported by the induction of FoxM1b after PH in CA-fed wild type, but not FXR knockout mice [174].

In addition, FGF15 was shown to be an essential mediator of liver regeneration, as indicated by delayed liver growth in FGF15-/- mice after PH, and decreased expression of cell cycle regulatory genes cyclins and FoxM1b in both FGF15 knockout and FGFR4 knockdown mice [175, 176]. However, FXR-FGF15/19 signalling is not merely an inducer of proliferation, but rather seems to be a guardian of the hepatostat (ratio of liver size to body weight) [177, 178]. This was elegantly shown in Fah-/- mice in which human FAH-positive hepatocytes were transplanted. In these mice, the livers grew larger in size as compared to Fah-/- mice in which mouse Fah-positive hepatocytes were transplanted. However, in Fah-/- mice co-expressing human FGF19 in the liver, the liver to body-weight ratio was normal. This was explained by the fact that human hepatocytes fail to recognize Fgf15 and are therefore unable to control liver to body weight ratio [178]. The

exact mechanisms by which FGF15/19 control the hepatostat are currently not known. In liver cancer cell lines, FXR knockdown induces cell cycle inhibitor p16/INK4a and inhibits cell proliferation [179]. Consistently, FXR agonists GW4064 and CDCA increase proliferation in several liver cancer cells [180]. Oppositely, an independent study shows that overexpression of FXR prevents cell growth and inhibits the activation of pro-proliferative mTOR/S6K signaling pathway [181]. *In vivo* studies report tumour suppressor effects associated with pharmacological activation of FXR [182-184], however the multiple hepatoprotective effects of FXR may confound the investigation of FXR regulation of cell proliferation using these models. It is therefore still debated whether FXR has anti-proliferative effects in the presence of tumorigenic cues and whether FXR activation is essential to prevent tumour formation.

Nevertheless, regulation of proliferation in regenerative or tumorigenic liver by FXR is probably explained by the integration of metabolic, energetic and growth cues. A mechanism for such integration has been recently described. FXR promotion of cell proliferation by GW4064 in HepG2 cells is accompanied by accumulation of aerobic glycolytic intermediates, such as pyruvate [180]. This suggests that FXR activation triggers a metabolic reprogramming which might be advantageous to proliferative cells. Indeed, next to an increase in lactate-producing anaerobic glycolysis (Warburg effect), proliferative cells exhibit an adaptive increase in aerobic glycolysis to facilitate funnelling of nutrients into anabolism of nucleotides, lipids, amino acids and NADPH [185, 186]. Knockdown of the pyruvate dehydrogenase kinase 4 (PDK4), a target gene of FXR, abrogates the cell proliferative effects of GW4064 and abolishes the related metabolic reprogramming, suggesting that PDK4 is essential for FXR-mediated induction of proliferation [180]. PDK4 reduces the conversion of pyruvate into AcetylCoA, and therefore the induction PDK4 expression by FXR favours a metabolic switch towards the accumulation of aerobic glycolytic intermediates as precursors for generating biomass, required by proliferative cells.

The role of FXR in autophagy and cell proliferation strongly supports the view that the metabolic status of the cell impinges on FXR transcriptional activity likely through an interaction with energy-sensitive transcriptional coregulators. In conditions of nutrient excess, FXR activation reprograms and silences the autophagy genes, to prevent unnecessary metabolite degradation. On the other hand, when nutrient availability is required for proliferation, FXR reprograms glycolytic genes in order to fulfil the metabolic needs of the cell.

FXR, nutrient metabolism and inflammation

Coordination of metabolism and immunity is an evolutionary conserved process essential for survival. Immune defence is energy-demanding, as suggested by impaired immune function in conditions of malnutrition or starvation [187]. Intriguingly, nutrient excessive conditions such as obesity also impair immune function and induce inflammation [188]. Close interactions exist between nutrient sensing and inflammatory pathways [189]. Nutrient sensing nuclear receptors, such as PPAR, LXR and FXR, repress inflammation and therefore integrate metabolism and immunity signalling pathways [190-192].

A role for FXR in repression of the immune response is supported by the induction of pro-inflammatory cytokines and the increased monocyte/macrophage infiltration observed in the livers of FXR null mice [193, 194]. FXR activation inhibits NFκB transcriptional activation of pro-inflammatory genes in hepatocytes [195]. Anti-inflammatory activity of FXR has been described for hepatocytes, smooth muscle cells, monocytes, macrophages and dendritic cells, thereby involving liver, intestine, spleen and lungs [196-201]. Mechanisms of tethering transrepression of NFkB have been shown to underlie FXR-mediated inhibition of inflammation via NFκB [202]. Gel mobility shift and ChIP assays in HepG2 cells support that FXR agonists decrease DNA binding of NFκB [195] and reduce recruitment of the NFκB subunit p65 to pro-inflammatory gene promoters [7].

The PTM status of FXR has been shown to be relevant for repression of NFκB target genes. In fact, SUMO2 modification of agonist-activated FXR at K277 selectively decreased inflammatory gene expression [19]. In addition, in hepatocytes isolated from FXR-/- mice, overexpression of the mutant FXR-K277R expression of the inflammatory genes Il1β and Tnfα was increased compared to hepatocytes in which wild type FXR was expressed. Unlike wild type FXR, the FXR-K277R mutant decreases NFκB activity in reporter assays, whereas *in vitro* sumoylation of FXR increases its interaction with NFκB. FXR sumoylation is blocked by FXR acetylation, which is interlinked to the cell nutritional status, as discussed earlier in this review. Indeed, expression of an acetyl mimic mutant FXR-K217Q in lean mice increased the expression of inflammatory genes [19]. Moreover, the increase in acetylation correlates with a decrease in sumoylation in mice developing obesity, suggesting that these PTMs fine tune FXR function during inflammation, possibly in coordination with cell nutritional status.

Direct interference on NFκB signalling is most likely not the only mechanism underlying FXR anti-inflammatory actions. The function of FXR as a regulator of nutrient metabolism certainly has also a strong immunomodulatory effect. Saturated fatty acids contribute to the release of pro-inflammatory cytokines in the liver [203]. Therefore efficient suppression of hepatic fat accumulation by FXR activation, discussed earlier in this review, is expected to counteract the onset of inflammation. This is supported by the fact that FXR activation by OCA improves both steatosis and lobular inflammation in non-alcoholic steatohepatitis (NASH) patients [204, 205]. In steatotic livers, toxicity associated with lipid accumulation drives the development of liver disease, by inducing hepatocellular death, activation of Kupffer cells and stellate cells, resulting in fibrosis [206]. Mechanistically, lipid accumulation in the liver leads to subacute hepatic inflammation through NFκB activation and downstream cytokine production [207] and through accumulation of reactive oxygen species [208, 209]. Therefore, FXR-dependent improvement of lipid accumulation is critical for repression of liver inflammation.

FXR regulation of glucose metabolism might also contribute to repression of liver inflammation. Obesity and insulin resistance are associated with increased lipolysis in adipose tissue, responsible for the FFA accumulation in the liver and induction of liver inflammation [208]. On the other hand, chronic inflammation in the liver causes insulin resistance, leading to increased hepatic glucose production, suggesting that immune and metabolic responses are mutually interlinked [210, 211]. As previously detailed in this review,

FXR activation inhibits gluconeogenesis and improves insulin sensitivity, thus likely decreasing inflammation. Finally, it remains to be elucidated whether the recently reported FXR regulation of amino acid metabolism also has an impact on liver inflammation.
Together, these data position FXR as a regulator of "metaflammation", defined as the inflammatory status triggered by nutrients and metabolic surplus. On the one hand FXR directly decreases inflammation by interfering with NFκB signalling and on the other hand indirectly by acting as a guardian of nutrient homeostasis. In this scenario FXR-actions are fine-tuned by PTMs to integrate metabolic and inflammatory signalling.

CONCLUSION AND FINAL REMARKS

In conclusion, FXR is a guardian of nutrient homeostasis, by participating to an intricate network of transcription factors which switch on and off genes in order to control energy metabolism across the phases of nutrition. FXR function is not only regulated by BAs that return to the liver after meal ingestion, but also by the PTM status of this receptor, which is dependent on the co-absorbed nutrients. FXR embraces the fate of all three basic building blocks for nutrients: lipids, glucose and amino acids and is not only important in normal physiology of nutrient metabolism, but also in autophagy, proliferation, and inflammation.
The current investigation of FXR role in liver physiology is beginning to benefit from genome-wide binding, proteomics and metabolomics approaches, but the future holds further important challenges. Natural FXR ligands and genetic whole body gene knockout models have been widely used so far to understand FXR function in the liver. However, the widespread effects of BAs indicate that selective FXR agonism is needed in order to draw conclusions about FXR dependency. In addition, the complexity of the organism poses relevant issues to the interpretation of tissue-specific gene function based on the phenotype of whole body knockout models. Therefore, tissue specific knockout models should be preferred when aiming to unravel the role of FXR in liver physiology. Furthermore, the use of inducible knockout models can rule out the contribution of adaptation and metabolic compensation arising during the development of genetic mouse models. Ultimately, strict control of the fasting/feeding conditions will be required to uncover the physiological function of FXR in postprandial, post-absorptive and fasted state.
Such studies are needed to gain detailed insights in the physiological mechanisms by which FXR regulates metabolism, in terms of isoform-specificity, PTMs and coregulatory proteins, and will drive improvements in targeting FXR for liver diseases.

ACKNOWLEDGEMENTS

Grant support: S.W.C.v.M. is supported by the Netherlands Organization for Scientific Research (NWO) Project VIDI (917.11.365), FP7 Marie Curie Actions IAPP (FXR-IBD, 611979), the Utrecht University Support Grant, Wilhelmina Children's Hospital Research Fund. We thank Alexandra Milona for critical discussion. We thank Servier Medical Art for kindly providing the pictures adapted in Figure 1.

REFERENCES

1. Glass CK. Differential recognition of target genes by nuclear receptor monomers, dimers, and heterodimers. Endocr Rev 1994;15:391-407.
2. Mangelsdorf DJ, Evans RM. The RXR heterodimers and orphan receptors. Cell 1995;83:841-50.
3. Aranda A, Pascual A. Nuclear hormone receptors and gene expression. Physiol Rev 2001;81:1269-304.
4. Steinmetz AC, Renaud JP, Moras D. Binding of ligands and activation of transcription by nuclear receptors. Annu Rev Biophys Biomol Struct 2001;30:329-59.
5. Sladek FM. Nuclear receptors as drug targets: new developments in coregulators, orphan receptors and major therapeutic areas. Expert Opin Ther Targets 2003;7:679-84.
6. Sundahl N, Bridelance J, Libert C, et al. Selective glucocorticoid receptor modulation: New directions with non-steroidal scaffolds. Pharmacol Ther 2015;152:28-41.
7. Bijsmans IT, Guercini C, Ramos Pittol JM, et al. The glucocorticoid mometasone furoate is a novel FXR ligand that decreases inflammatory but not metabolic gene expression. Sci Rep 2015;5:14086.
8. Vacca M, Degirolamo C, Mariani-Costantini R, et al. Lipid-sensing nuclear receptors in the pathophysiology and treatment of the metabolic syndrome. Wiley Interdiscip Rev Syst Biol Med 2011;3:562-87.
9. Francis GA, Fayard E, Picard F, et al. Nuclear receptors and the control of metabolism. Annu Rev Physiol 2003;65:261-311.
10. Yan J, Chen B, Lu J, et al. Deciphering the roles of the constitutive androstane receptor in energy metabolism. Acta Pharmacol Sin 2015;36:62-70.
11. Otte K, Kranz H, Kober I, et al. Identification of farnesoid X receptor beta as a novel mammalian nuclear receptor sensing lanosterol. Mol Cell Biol 2003;23:864-72.
12. Huber RM, Murphy K, Miao B, et al. Generation of multiple farnesoid-X-receptor isoforms through the use of alternative promoters. Gene 2002;290:35-43.
13. Zhang Y, Kast-Woelbern HR, Edwards PA. Natural structural variants of the nuclear receptor farnesoid X receptor affect transcriptional activation. J Biol Chem 2003;278:104-10.
14. Correia JC, Massart J, de Boer JF, et al. Bioenergetic cues shift FXR splicing towards FXRalpha2 to modulate hepatic lipolysis and fatty acid metabolism. Mol Metab 2015;4:891-902.
15. Chen Y, Song X, Valanejad L, et al. Bile salt export pump is dysregulated with altered farnesoid X receptor isoform expression in patients with hepatocellular carcinoma. Hepatology 2013;57:1530-41.
16. Gineste R, Sirvent A, Paumelle R, et al. Phosphorylation of farnesoid X receptor by protein kinase C promotes its transcriptional activity. Mol Endocrinol 2008;22:2433-47.
17. Kemper JK, Xiao Z, Ponugoti B, et al. FXR acetylation is normally dynamically regulated by p300 and SIRT1 but constitutively elevated in metabolic disease states. Cell Metab 2009;10:392-404.
18. Balasubramaniyan N, Luo Y, Sun AQ, et al. SUMOylation of the farnesoid X receptor (FXR) regulates the expression of FXR target genes. J Biol Chem 2013;288:13850-62.
19. Kim DH, Xiao Z, Kwon S, et al. A dysregulated acetyl/SUMO switch of FXR promotes hepatic inflammation in obesity. EMBO J 2015;34:184-99.
20. Berrabah W, Aumercier P, Gheeraert C, et al. Glucose sensing O-GlcNAcylation pathway regulates the nuclear bile acid receptor farnesoid X receptor (FXR). Hepatology 2014;59:2022-33.
21. Viscarra JA, Ortiz RM. Cellular mechanisms regulating fuel metabolism in mammals: role of adipose tissue and lipids during prolonged food deprivation. Metabolism 2013;62:889-97.
22. Forman BM, Goode E, Chen J, et al. Identification of a nuclear receptor that is activated by farnesol metabolites. Cell 1995;81:687-93.
23. Makishima M, Okamoto AY, Repa JJ, et al. Identification of a nuclear receptor for bile acids. Science 1999;284:1362-5.
24. Parks DJ, Blanchard SG, Bledsoe RK, et al. Bile acids: natural ligands for an orphan nuclear receptor. Science 1999;284:1365-8.

25. Wang H, Chen J, Hollister K, et al. Endogenous bile acids are ligands for the nuclear receptor FXR/BAR. Mol Cell 1999;3:543-53.
26. Dawson PA, Haywood J, Craddock AL, et al. Targeted deletion of the ileal bile acid transporter eliminates enterohepatic cycling of bile acids in mice. J Biol Chem 2003;278:33920-7.
27. Grober J, Zaghini I, Fujii H, et al. Identification of a bile acid-responsive element in the human ileal bile acid-binding protein gene. Involvement of the farnesoid X receptor/9-cis-retinoic acid receptor heterodimer. J Biol Chem 1999;274:29749-54.
28. Dawson PA, Hubbert M, Haywood J, et al. The heteromeric organic solute transporter alpha-beta, Ostalpha-Ostbeta, is an ileal basolateral bile acid transporter. J Biol Chem 2005;280:6960-8.
29. Rao A, Haywood J, Craddock AL, et al. The organic solute transporter alpha-beta, Ostalpha-Ostbeta, is essential for intestinal bile acid transport and homeostasis. Proc Natl Acad Sci U S A 2008;105:3891-6.
30. Ballatori N, Fang F, Christian WV, et al. Ostalpha-Ostbeta is required for bile acid and conjugated steroid disposition in the intestine, kidney, and liver. Am J Physiol Gastrointest Liver Physiol 2008;295:G179-G186.
31. Ridlon JM, Kang DJ, Hylemon PB. Bile salt biotransformations by human intestinal bacteria. J Lipid Res 2006;47:241-59.
32. Slijepcevic D, Kaufman C, Wichers CG, et al. Impaired uptake of conjugated bile acids and hepatitis b virus pres1-binding in na(+) -taurocholate cotransporting polypeptide knockout mice. Hepatology 2015;62:207-19.
33. Hagenbuch B, Meier PJ. Molecular cloning, chromosomal localization, and functional characterization of a human liver Na+/bile acid cotransporter. J Clin Invest 1994;93:1326-31.
34. Hagenbuch B, Meier PJ. The superfamily of organic anion transporting polypeptides. Biochim Biophys Acta 2003;1609:1-18.
35. Csanaky IL, Lu H, Zhang Y, et al. Organic anion-transporting polypeptide 1b2 (Oatp1b2) is important for the hepatic uptake of unconjugated bile acids: Studies in Oatp1b2-null mice. Hepatology 2011;53:272-81.
36. Falany CN, Johnson MR, Barnes S, et al. Glycine and taurine conjugation of bile acids by a single enzyme. Molecular cloning and expression of human liver bile acid CoA:amino acid N-acyltransferase. J Biol Chem 1994;269:19375-9.
37. Lin BC, Wang M, Blackmore C, et al. Liver-specific activities of FGF19 require Klotho beta. J Biol Chem 2007;282:27277-84.
38. de Aguiar Vallim TQ, Tarling EJ, Ahn H, et al. MAFG is a transcriptional repressor of bile acid synthesis and metabolism. Cell Metab 2015;21:298-310.
39. Kong B, Wang L, Chiang JY, et al. Mechanism of tissue-specific farnesoid X receptor in suppressing the expression of genes in bile-acid synthesis in mice. Hepatology 2012;56:1034-43.
40. Sinal CJ, Tohkin M, Miyata M, et al. Targeted disruption of the nuclear receptor FXR/BAR impairs bile acid and lipid homeostasis. Cell 2000;102:731-44.
41. Ananthanarayanan M, Balasubramanian N, Makishima M, et al. Human bile salt export pump promoter is transactivated by the farnesoid X receptor/bile acid receptor. J Biol Chem 2001;276:28857-65.
42. Liu Y, Binz J, Numerick MJ, et al. Hepatoprotection by the farnesoid X receptor agonist GW4064 in rat models of intra- and extrahepatic cholestasis. J Clin Invest 2003;112:1678-87.
43. Dawson PA, Hubbert ML, Rao A. Getting the mOST from OST: Role of organic solute transporter, OSTalpha-OSTbeta, in bile acid and steroid metabolism. Biochim Biophys Acta 2010;1801:994-1004.
44. Landrier JF, Eloranta JJ, Vavricka SR, et al. The nuclear receptor for bile acids, FXR, transactivates human organic solute transporter-alpha and -beta genes. Am J Physiol Gastrointest Liver Physiol 2006;290:G476-85.
45. Lee H, Zhang Y, Lee FY, et al. FXR regulates organic solute transporters alpha and beta in the adrenal gland, kidney, and intestine. J Lipid Res 2006;47:201-14.
46. Fu T, Kim YC, Byun S, et al. FXR Primes the Liver for Intestinal FGF15 Signaling by Transient

Induction of beta-Klotho. Mol Endocrinol 2016;30:92-103.
47. Zhou H, Hylemon PB. Bile acids are nutrient signaling hormones. Steroids 2014;86:62-8.
48. Makishima M, Lu TT, Xie W, et al. Vitamin D receptor as an intestinal bile acid sensor. Science 2002;296:1313-6.
49. Staudinger JL, Goodwin B, Jones SA, et al. The nuclear receptor PXR is a lithocholic acid sensor that protects against liver toxicity. Proc Natl Acad Sci U S A 2001;98:3369-74.
50. Huang W, Zhang J, Chua SS, et al. Induction of bilirubin clearance by the constitutive androstane receptor (CAR). Proc Natl Acad Sci U S A 2003;100:4156-61.
51. Zelko I, Sueyoshi T, Kawamoto T, et al. The peptide near the C terminus regulates receptor CAR nuclear translocation induced by xenochemicals in mouse liver. Mol Cell Biol 2001;21:2838-46.
52. Kawamata Y, Fujii R, Hosoya M, et al. A G protein-coupled receptor responsive to bile acids. J Biol Chem 2003;278:9435-40.
53. Watanabe M, Houten SM, Mataki C, et al. Bile acids induce energy expenditure by promoting intracellular thyroid hormone activation. Nature 2006;439:484-9.
54. Lowe ME. Structure and function of pancreatic lipase and colipase. Annu Rev Nutr 1997;17:141-58.
55. Mu H, Hoy CE. The digestion of dietary triacylglycerols. Prog Lipid Res 2004;43:105-33.
56. Goldberg IJ. Lipoprotein lipase and lipolysis: central roles in lipoprotein metabolism and atherogenesis. J Lipid Res 1996;37:693-707.
57. Havel RJ. Receptor and non-receptor mediated uptake of chylomicron remnants by the liver. Atherosclerosis 1998;141 Suppl 1:S1-7.
58. Czech MP, Tencerova M, Pedersen DJ, et al. Insulin signalling mechanisms for triacylglycerol storage. Diabetologia 2013;56:949-64.
59. Rui L. Energy metabolism in the liver. Compr Physiol 2014;4:177-97.
60. Wang Y, Viscarra J, Kim SJ, et al. Transcriptional regulation of hepatic lipogenesis. Nat Rev Mol Cell Biol 2015;16:678-89.
61. Yecies JL, Zhang HH, Menon S, et al. Akt stimulates hepatic SREBP1c and lipogenesis through parallel mTORC1-dependent and independent pathways. Cell Metab 2011;14:21-32.
62. Shimano H, Shimomura I, Hammer RE, et al. Elevated levels of SREBP-2 and cholesterol synthesis in livers of mice homozygous for a targeted disruption of the SREBP-1 gene. J Clin Invest 1997;100:2115-24.
63. Jeon TI, Osborne TF. SREBPs: metabolic integrators in physiology and metabolism. Trends Endocrinol Metab 2012;23:65-72.
64. Iizuka K, Bruick RK, Liang G, et al. Deficiency of carbohydrate response element-binding protein (ChREBP) reduces lipogenesis as well as glycolysis. Proc Natl Acad Sci U S A 2004;101:7281-6.
65. Denechaud PD, Bossard P, Lobaccaro JM, et al. ChREBP, but not LXRs, is required for the induction of glucose-regulated genes in mouse liver. J Clin Invest 2008;118:956-64.
66. Filhoulaud G, Guilmeau S, Dentin R, et al. Novel insights into ChREBP regulation and function. Trends Endocrinol Metab 2013;24:257-68.
67. Chen W, Chen G, Head DL, et al. Enzymatic reduction of oxysterols impairs LXR signaling in cultured cells and the livers of mice. Cell Metab 2007;5:73-9.
68. Janowski BA, Willy PJ, Devi TR, et al. An oxysterol signalling pathway mediated by the nuclear receptor LXR alpha. Nature 1996;383:728-31.
69. Joseph SB, Laffitte BA, Patel PH, et al. Direct and indirect mechanisms for regulation of fatty acid synthase gene expression by liver X receptors. J Biol Chem 2002;277:11019-25.
70. Jamil H, Chu CH, Dickson JK, Jr., et al. Evidence that microsomal triglyceride transfer protein is limiting in the production of apolipoprotein B-containing lipoproteins in hepatic cells. J Lipid Res 1998;39:1448-54.
71. Tietge UJ, Bakillah A, Maugeais C, et al. Hepatic overexpression of microsomal triglyceride transfer protein (MTP) results in increased in vivo secretion of VLDL triglycerides and apolipoprotein B. J Lipid Res 1999;40:2134-9.
72. Sundaram M, Zhong S, Bou Khalil M, et al. Functional analysis of the missense APOC3 mutation

Ala23Thr associated with human hypotriglyceridemia. J Lipid Res 2010;51:1524-34.
73. Kamagate A, Dong HH. FoxO1 integrates insulin signaling to VLDL production. Cell Cycle 2008;7:3162-70.
74. Kamagate A, Qu S, Perdomo G, et al. FoxO1 mediates insulin-dependent regulation of hepatic VLDL production in mice. J Clin Invest 2008;118:2347-64.
75. Haas ME, Attie AD, Biddinger SB. The regulation of ApoB metabolism by insulin. Trends Endocrinol Metab 2013;24:391-7.
76. Wade DP, Knight BL, Soutar AK. Regulation of low-density-lipoprotein-receptor mRNA by insulin in human hepatoma Hep G2 cells. Eur J Biochem 1989;181:727-31.
77. Ameen C, Edvardsson U, Ljungberg A, et al. Activation of peroxisome proliferator-activated receptor alpha increases the expression and activity of microsomal triglyceride transfer protein in the liver. J Biol Chem 2005;280:1224-9.
78. Sheena V, Hertz R, Nousbeck J, et al. Transcriptional regulation of human microsomal triglyceride transfer protein by hepatocyte nuclear factor-4alpha. J Lipid Res 2005;46:328-41.
79. Wolfrum C, Stoffel M. Coactivation of Foxa2 through Pgc-1beta promotes liver fatty acid oxidation and triglyceride/VLDL secretion. Cell Metab 2006;3:99-110.
80. Bruinstroop E, la Fleur SE, Ackermans MT, et al. The autonomic nervous system regulates postprandial hepatic lipid metabolism. Am J Physiol Endocrinol Metab 2013;304:E1089-96.
81. Bateson MC, Maclean D, Evans JR, et al. Chenodeoxycholic acid therapy for hypertriglyceridaemia in men. Br J Clin Pharmacol 1978;5:249-54.
82. Leiss O, von Bergmann K. Different effects of chenodeoxycholic acid and ursodeoxycholic acid on serum lipoprotein concentrations in patients with radiolucent gallstones. Scand J Gastroenterol 1982;17:587-92.
83. Crouse JR, 3rd. Hypertriglyceridemia: a contraindication to the use of bile acid binding resins. Am J Med 1987;83:243-8.
84. Zhang Y, Lee FY, Barrera G, et al. Activation of the nuclear receptor FXR improves hyperglycemia and hyperlipidemia in diabetic mice. Proc Natl Acad Sci U S A 2006;103:1006-11.
85. Kunne C, Acco A, Duijst S, et al. FXR-dependent reduction of hepatic steatosis in a bile salt deficient mouse model. Biochim Biophys Acta 2014;1842:739-46.
86. Kast HR, Nguyen CM, Sinal CJ, et al. Farnesoid X-activated receptor induces apolipoprotein C-II transcription: a molecular mechanism linking plasma triglyceride levels to bile acids. Mol Endocrinol 2001;15:1720-8.
87. Claudel T, Inoue Y, Barbier O, et al. Farnesoid X receptor agonists suppress hepatic apolipoprotein CIII expression. Gastroenterology 2003;125:544-55.
88. Watanabe M, Houten SM, Wang L, et al. Bile acids lower triglyceride levels via a pathway involving FXR, SHP, and SREBP-1c. J Clin Invest 2004;113:1408-18.
89. Ma K, Saha PK, Chan L, et al. Farnesoid X receptor is essential for normal glucose homeostasis. J Clin Invest 2006;116:1102-9.
90. Pineda Torra I, Claudel T, Duval C, et al. Bile acids induce the expression of the human peroxisome proliferator-activated receptor alpha gene via activation of the farnesoid X receptor. Mol Endocrinol 2003;17:259-72.
91. Xu J, Li Y, Chen WD, et al. Hepatic carboxylesterase 1 is essential for both normal and farnesoid X receptor-controlled lipid homeostasis. Hepatology 2014;59:1761-71.
92. Savkur RS, Bramlett KS, Michael LF, et al. Regulation of pyruvate dehydrogenase kinase expression by the farnesoid X receptor. Biochem Biophys Res Commun 2005;329:391-6.
93. Bilz S, Samuel V, Morino K, et al. Activation of the farnesoid X receptor improves lipid metabolism in combined hyperlipidemic hamsters. Am J Physiol Endocrinol Metab 2006;290:E716-22.
94. Miller NE, Nestel PJ. Triglyceride-lowering effect of chenodeoxycholic acid in patients with endogenous hypertriglyceridaemia. Lancet 1974;2:929-31.
95. Hirokane H, Nakahara M, Tachibana S, et al. Bile acid reduces the secretion of very low density lipoprotein by repressing microsomal triglyceride transfer protein gene expression mediated by hepatocyte nuclear factor-4. J Biol Chem 2004;279:45685-92.

96. Liu Q, Yang M, Fu X, et al. Activation of farnesoid X receptor promotes triglycerides lowering by suppressing phospholipase A2 G12B expression. Mol Cell Endocrinol 2016;436:93-101.
97. Mak PA, Kast-Woelbern HR, Anisfeld AM, et al. Identification of PLTP as an LXR target gene and apoE as an FXR target gene reveals overlapping targets for the two nuclear receptors. J Lipid Res 2002;43:2037-41.
98. Urizar NL, Dowhan DH, Moore DD. The farnesoid X-activated receptor mediates bile acid activation of phospholipid transfer protein gene expression. J Biol Chem 2000;275:39313-7.
99. Lambert G, Amar MJ, Guo G, et al. The farnesoid X-receptor is an essential regulator of cholesterol homeostasis. J Biol Chem 2003;278:2563-70.
100. Li L, Liu H, Peng J, et al. Farnesoid X receptor up-regulates expression of lipid transfer inhibitor protein in liver cells and mice. Biochem Biophys Res Commun 2013;441:880-5.
101. Barter PJ, Brewer HB, Jr., Chapman MJ, et al. Cholesteryl ester transfer protein: a novel target for raising HDL and inhibiting atherosclerosis. Arterioscler Thromb Vasc Biol 2003;23:160-7.
102. Holt JA, Luo G, Billin AN, et al. Definition of a novel growth factor-dependent signal cascade for the suppression of bile acid biosynthesis. Genes Dev 2003;17:1581-91.
103. Inagaki T, Choi M, Moschetta A, et al. Fibroblast growth factor 15 functions as an enterohepatic signal to regulate bile acid homeostasis. Cell Metab 2005;2:217-25.
104. Tomlinson E, Fu L, John L, et al. Transgenic mice expressing human fibroblast growth factor-19 display increased metabolic rate and decreased adiposity. Endocrinology 2002;143:1741-7.
105. Fu L, John LM, Adams SH, et al. Fibroblast growth factor 19 increases metabolic rate and reverses dietary and leptin-deficient diabetes. Endocrinology 2004;145:2594-603.
106. Bhatnagar S, Damron HA, Hillgartner FB. Fibroblast growth factor-19, a novel factor that inhibits hepatic fatty acid synthesis. J Biol Chem 2009;284:10023-33.
107. Miyata M, Sakaida Y, Matsuzawa H, et al. Fibroblast growth factor 19 treatment ameliorates disruption of hepatic lipid metabolism in farnesoid X receptor (Fxr)-null mice. Biol Pharm Bull 2011;34:1885-9.
108. Duran-Sandoval D, Cariou B, Percevault F, et al. The farnesoid X receptor modulates hepatic carbohydrate metabolism during the fasting-refeeding transition. J Biol Chem 2005;280:29971-9.
109. Zhang Y, Castellani LW, Sinal CJ, et al. Peroxisome proliferator-activated receptor-gamma coactivator 1alpha (PGC-1alpha) regulates triglyceride metabolism by activation of the nuclear receptor FXR. Genes Dev 2004;18:157-69.
110. Shi L, Tu BP. Acetyl-CoA and the regulation of metabolism: mechanisms and consequences. Curr Opin Cell Biol 2015;33:125-31.
111. Park JM, Jo SH, Kim MY, et al. Role of transcription factor acetylation in the regulation of metabolic homeostasis. Protein Cell 2015;6:804-13.
112. Fang S, Tsang S, Jones R, et al. The p300 acetylase is critical for ligand-activated farnesoid X receptor (FXR) induction of SHP. J Biol Chem 2008;283:35086-95.
113. Kay HY, Kim WD, Hwang SJ, et al. Nrf2 inhibits LXRalpha-dependent hepatic lipogenesis by competing with FXR for acetylase binding. Antioxid Redox Signal 2011;15:2135-46.
114. Hardie DG, Alessi DR. LKB1 and AMPK and the cancer-metabolism link - ten years after. BMC Biol 2013;11:36.
115. Lien F, Berthier A, Bouchaert E, et al. Metformin interferes with bile acid homeostasis through AMPK-FXR crosstalk. J Clin Invest 2014;124:1037-51.
116. Levin RJ. Digestion and absorption of carbohydrates--from molecules and membranes to humans. Am J Clin Nutr 1994;59:690S-698S.
117. Wright EM, Martin MG, Turk E. Intestinal absorption in health and disease--sugars. Best Pract Res Clin Gastroenterol 2003;17:943-56.
118. Chandel NS. Navigating Metabolism. Cold Spring Harbor, New York: Cold Spring Harbor Laboratory Press, 2015:128.
119. Moore MC, Cherrington AD, Wasserman DH. Regulation of hepatic and peripheral glucose disposal. Best Pract Res Clin Endocrinol Metab 2003;17:343-64.
120. Agius L. Glucokinase and molecular aspects of liver glycogen metabolism. Biochem J 2008;414:1-

18.
121. Roth U, Curth K, Unterman TG, et al. The transcription factors HIF-1 and HNF-4 and the coactivator p300 are involved in insulin-regulated glucokinase gene expression via the phosphatidylinositol 3-kinase/protein kinase B pathway. J Biol Chem 2004;279:2623-31.
122. Roth U, Jungermann K, Kietzmann T. Activation of glucokinase gene expression by hepatic nuclear factor 4alpha in primary hepatocytes. Biochem J 2002;365:223-8.
123. Kim TH, Kim H, Park JM, et al. Interrelationship between liver X receptor alpha, sterol regulatory element-binding protein-1c, peroxisome proliferator-activated receptor gamma, and small heterodimer partner in the transcriptional regulation of glucokinase gene expression in liver. J Biol Chem 2009;284:15071-83.
124. Puigserver P, Rhee J, Donovan J, et al. Insulin-regulated hepatic gluconeogenesis through FOXO1-PGC-1alpha interaction. Nature 2003;423:550-5.
125. Bricambert J, Miranda J, Benhamed F, et al. Salt-inducible kinase 2 links transcriptional coactivator p300 phosphorylation to the prevention of ChREBP-dependent hepatic steatosis in mice. J Clin Invest 2010;120:4316-31.
126. Guinez C, Filhoulaud G, Rayah-Benhamed F, et al. O-GlcNAcylation increases ChREBP protein content and transcriptional activity in the liver. Diabetes 2011;60:1399-413.
127. Yamashita H, Takenoshita M, Sakurai M, et al. A glucose-responsive transcription factor that regulates carbohydrate metabolism in the liver. Proc Natl Acad Sci U S A 2001;98:9116-21.
128. Noriega LG, Feige JN, Canto C, et al. CREB and ChREBP oppositely regulate SIRT1 expression in response to energy availability. EMBO Rep 2011;12:1069-76.
129. Oosterveer MH, Schoonjans K. Hepatic glucose sensing and integrative pathways in the liver. Cell Mol Life Sci 2014;71:1453-67.
130. Oosterveer MH, Mataki C, Yamamoto H, et al. LRH-1-dependent glucose sensing determines intermediary metabolism in liver. J Clin Invest 2012;122:2817-26.
131. Cha JY, Repa JJ. The liver X receptor (LXR) and hepatic lipogenesis. The carbohydrate-response element-binding protein is a target gene of LXR. J Biol Chem 2007;282:743-51.
132. Petersen DD, Koch SR, Granner DK. 3' noncoding region of phosphoenolpyruvate carboxykinase mRNA contains a glucocorticoid-responsive mRNA-stabilizing element. Proc Natl Acad Sci U S A 1989;86:7800-4.
133. Lerin C, Rodgers JT, Kalume DE, et al. GCN5 acetyltransferase complex controls glucose metabolism through transcriptional repression of PGC-1alpha. Cell Metab 2006;3:429-38.
134. Fernandez-Marcos PJ, Auwerx J. Regulation of PGC-1alpha, a nodal regulator of mitochondrial biogenesis. Am J Clin Nutr 2011;93:884S-90.
135. Yoon JC, Puigserver P, Chen G, et al. Control of hepatic gluconeogenesis through the transcriptional coactivator PGC-1. Nature 2001;413:131-8.
136. Herzig S, Long F, Jhala US, et al. CREB regulates hepatic gluconeogenesis through the coactivator PGC-1. Nature 2001;413:179-83.
137. Lundasen T, Hunt MC, Nilsson LM, et al. PPARalpha is a key regulator of hepatic FGF21. Biochem Biophys Res Commun 2007;360:437-40.
138. Potthoff MJ, Inagaki T, Satapati S, et al. FGF21 induces PGC-1alpha and regulates carbohydrate and fatty acid metabolism during the adaptive starvation response. Proc Natl Acad Sci U S A 2009;106:10853-8.
139. Kimura T, Christoffels VM, Chowdhury S, et al. Hypoglycemia-associated hyperammonemia caused by impaired expression of ornithine cycle enzyme genes in C/EBPalpha knockout mice. J Biol Chem 1998;273:27505-10.
140. Stayrook KR, Bramlett KS, Savkur RS, et al. Regulation of carbohydrate metabolism by the farnesoid X receptor. Endocrinology 2005;146:984-91.
141. Yamagata K, Daitoku H, Shimamoto Y, et al. Bile acids regulate gluconeogenic gene expression via small heterodimer partner-mediated repression of hepatocyte nuclear factor 4 and Foxo1. J Biol Chem 2004;279:23158-65.
142. De Fabiani E, Mitro N, Gilardi F, et al. Coordinated control of cholesterol catabolism to bile acids

and of gluconeogenesis via a novel mechanism of transcription regulation linked to the fasted-to-fed cycle. J Biol Chem 2003;278:39124-32.
143. Caron S, Huaman Samanez C, Dehondt H, et al. Farnesoid X receptor inhibits the transcriptional activity of carbohydrate response element binding protein in human hepatocytes. Mol Cell Biol 2013;33:2202-11.
144. Kir S, Beddow SA, Samuel VT, et al. FGF19 as a postprandial, insulin-independent activator of hepatic protein and glycogen synthesis. Science 2011;331:1621-4.
145. Potthoff MJ, Boney-Montoya J, Choi M, et al. FGF15/19 regulates hepatic glucose metabolism by inhibiting the CREB-PGC-1alpha pathway. Cell Metab 2011;13:729-38.
146. Renga B, Mencarelli A, D'Amore C, et al. Glucocorticoid receptor mediates the gluconeogenic activity of the farnesoid X receptor in the fasting condition. FASEB J 2012;26:3021-31.
147. Lehninger AL, Nelson DL, Cox MM. Lehninger principles of biochemistry. New York: W.H. Freeman, 2013.
148. Zoncu R, Efeyan A, Sabatini DM. mTOR: from growth signal integration to cancer, diabetes and ageing. Nat Rev Mol Cell Biol 2011;12:21-35.
149. Bender DA. The metabolism of "surplus" amino acids. Br J Nutr 2012;108 Suppl 2:S113-21.
150. Rodés J. Textbook of hepatology : from basic science to clinical practice. Malden, Mass.: Blackwell, 2007.
151. Diez-Fernandez C, Gallego J, Haberle J, et al. The Study of Carbamoyl Phosphate Synthetase 1 Deficiency Sheds Light on the Mechanism for Switching On/Off the Urea Cycle. J Genet Genomics 2015;42:249-60.
152. Lee BH, Scaglia F. Inborn errors of metabolism : from neonatal screening to metabolic pathways. Oxford ; New York: Oxford University Press, 2015.
153. Morris SM, Jr. Regulation of enzymes of the urea cycle and arginine metabolism. Annu Rev Nutr 2002;22:87-105.
154. Ulbright C, Snodgrass PJ. Coordinate induction of the urea cycle enzymes by glucagon and dexamethasone is accomplished by three different mechanisms. Arch Biochem Biophys 1993;301:237-43.
155. Desvergne B, Michalik L, Wahli W. Transcriptional regulation of metabolism. Physiol Rev 2006;86:465-514.
156. Takiguchi M, Mori M. Transcriptional regulation of genes for ornithine cycle enzymes. Biochem J 1995;312 (Pt 3):649-59.
157. Okun JG, Conway S, Schmidt KV, et al. Molecular regulation of urea cycle function by the liver glucocorticoid receptor. Mol Metab 2015;4:732-40.
158. Kimura T, Chowdhury S, Tanaka T, et al. CCAAT/enhancer-binding protein beta is required for activation of genes for ornithine cycle enzymes by glucocorticoids and glucagon in primary-cultured hepatocytes. FEBS Lett 2001;494:105-11.
159. Xu X, Hu J, McGrath BC, et al. GCN2 regulates the CCAAT enhancer binding protein beta and hepatic gluconeogenesis. Am J Physiol Endocrinol Metab 2013;305:E1007-17.
160. Martinez-Jimenez CP, Kyrmizi I, Cardot P, et al. Hepatocyte nuclear factor 4alpha coordinates a transcription factor network regulating hepatic fatty acid metabolism. Mol Cell Biol 2010;30:565-77.
161. Inoue Y, Hayhurst GP, Inoue J, et al. Defective ureagenesis in mice carrying a liver-specific disruption of hepatocyte nuclear factor 4alpha (HNF4alpha). HNF4alpha regulates ornithine transcarbamylase in vivo. J Biol Chem 2002;277:25257-65.
162. Li L, Zhang P, Bao Z, et al. PGC-1alpha Promotes Ureagenesis in Mouse Periportal Hepatocytes through SIRT3 and SIRT5 in Response to Glucagon. Sci Rep 2016;6:24156.
163. Kitagawa Y. Hormonal regulation of carbamoyl-phosphate synthetase I synthesis in primary cultured hepatocytes and Reuber hepatoma H-35. Defective regulation in hepatoma cells. Eur J Biochem 1987;167:19-25.
164. Kitagawa Y, Ryall J, Nguyen M, et al. Expression of carbamoyl-phosphate synthetase I mRNA in Reuber hepatoma H-35 cells. Regulation by glucocorticoid and insulin. Biochim Biophys Acta

1985;825:148-53.
165. Nakagawa T, Lomb DJ, Haigis MC, et al. SIRT5 Deacetylates carbamoyl phosphate synthetase 1 and regulates the urea cycle. Cell 2009;137:560-70.
166. Heibel SK, Lopez GY, Panglao M, et al. Transcriptional regulation of N-acetylglutamate synthase. PLoS One 2012;7:e29527.
167. Chong HK, Infante AM, Seo YK, et al. Genome-wide interrogation of hepatic FXR reveals an asymmetric IR-1 motif and synergy with LRH-1. Nucleic Acids Res 2010;38:6007-17.
168. Thomas AM, Hart SN, Kong B, et al. Genome-wide tissue-specific farnesoid X receptor binding in mouse liver and intestine. Hepatology 2010;51:1410-9.
169. Gardmo C, Tamburro A, Modica S, et al. Proteomics for the discovery of nuclear bile acid receptor FXR targets. Biochim Biophys Acta 2011;1812:836-41.
170. Massafra V, Milona A, Vos HR, et al. Farnesoid X Receptor activation promotes hepatic amino acid catabolism and ammonium clearance. Unpublished 2016.
171. Lee JM, Wagner M, Xiao R, et al. Nutrient-sensing nuclear receptors coordinate autophagy. Nature 2014;516:112-5.
172. Seok S, Fu T, Choi SE, et al. Transcriptional regulation of autophagy by an FXR-CREB axis. Nature 2014;516:108-11.
173. Vacca M, Degirolamo C, Massafra V, et al. Nuclear receptors in regenerating liver and hepatocellular carcinoma. Mol Cell Endocrinol 2013;368:108-19.
174. Huang W, Ma K, Zhang J, et al. Nuclear receptor-dependent bile acid signaling is required for normal liver regeneration. Science 2006;312:233-6.
175. Padrissa-Altes S, Bachofner M, Bogorad RL, et al. Control of hepatocyte proliferation and survival by Fgf receptors is essential for liver regeneration in mice. Gut 2015;64:1444-53.
176. Uriarte I, Fernandez-Barrena MG, Monte MJ, et al. Identification of fibroblast growth factor 15 as a novel mediator of liver regeneration and its application in the prevention of post-resection liver failure in mice. Gut 2013;62:899-910.
177. Avila MA, Moschetta A. The FXR-FGF19 Gut-Liver Axis as a Novel "Hepatostat". Gastroenterology 2015;149:537-40.
178. Naugler WE, Tarlow BD, Fedorov LM, et al. Fibroblast Growth Factor Signaling Controls Liver Size in Mice With Humanized Livers. Gastroenterology 2015;149:728-40 e15.
179. Fujino T, Takeuchi A, Maruko-Ohtake A, et al. Critical role of farnesoid X receptor for hepatocellular carcinoma cell proliferation. J Biochem 2012;152:577-86.
180. Xie Y, Wang H, Cheng X, et al. Farnesoid X receptor activation promotes cell proliferation via PDK4-controlled metabolic reprogramming. Sci Rep 2016;6:18751.
181. Huang X, Zeng Y, Wang X, et al. FXR blocks the growth of liver cancer cells through inhibiting mTOR-s6K pathway. Biochem Biophys Res Commun 2016;474:351-6.
182. Deuschle U, Schuler J, Schulz A, et al. FXR controls the tumor suppressor NDRG2 and FXR agonists reduce liver tumor growth and metastasis in an orthotopic mouse xenograft model. PLoS One 2012;7:e43044.
183. Wang X, Fu X, Van Ness C, et al. Bile Acid Receptors and Liver Cancer. Curr Pathobiol Rep 2013;1:29-35.
184. He J, Zhao K, Zheng L, et al. Upregulation of microRNA-122 by farnesoid X receptor suppresses the growth of hepatocellular carcinoma cells. Mol Cancer 2015;14:163.
185. Hsu PP, Sabatini DM. Cancer cell metabolism: Warburg and beyond. Cell 2008;134:703-7.
186. Vander Heiden MG, Cantley LC, Thompson CB. Understanding the Warburg effect: the metabolic requirements of cell proliferation. Science 2009;324:1029-33.
187. Demas GE, Chefer V, Talan MI, et al. Metabolic costs of mounting an antigen-stimulated immune response in adult and aged C57BL/6J mice. Am J Physiol 1997;273:R1631-7.
188. Marti A, Marcos A, Martinez JA. Obesity and immune function relationships. Obes Rev 2001;2:131-40.
189. Hotamisligil GS, Erbay E. Nutrient sensing and inflammation in metabolic diseases. Nat Rev Immunol 2008;8:923-34.

190. Bensinger SJ, Tontonoz P. Integration of metabolism and inflammation by lipid-activated nuclear receptors. Nature 2008;454:470-7.
191. Cave MC, Clair HB, Hardesty JE, et al. Nuclear receptors and nonalcoholic fatty liver disease. Biochim Biophys Acta 2016.
192. Venteclef N, Jakobsson T, Steffensen KR, et al. Metabolic nuclear receptor signaling and the inflammatory acute phase response. Trends Endocrinol Metab 2011;22:333-43.
193. Kim I, Morimura K, Shah Y, et al. Spontaneous hepatocarcinogenesis in farnesoid X receptor-null mice. Carcinogenesis 2007;28:940-6.
194. Liu N, Meng Z, Lou G, et al. Hepatocarcinogenesis in FXR-/- mice mimics human HCC progression that operates through HNF1alpha regulation of FXR expression. Mol Endocrinol 2012;26:775-85.
195. Wang YD, Chen WD, Wang M, et al. Farnesoid X receptor antagonizes nuclear factor kappaB in hepatic inflammatory response. Hepatology 2008;48:1632-43.
196. Adorini L, Pruzanski M, Shapiro D. Farnesoid X receptor targeting to treat nonalcoholic steatohepatitis. Drug Discov Today 2012;17:988-97.
197. Gadaleta RM, van Erpecum KJ, Oldenburg B, et al. Farnesoid X receptor activation inhibits inflammation and preserves the intestinal barrier in inflammatory bowel disease. Gut 2011;60:463-72.
198. Li YT, Swales KE, Thomas GJ, et al. Farnesoid x receptor ligands inhibit vascular smooth muscle cell inflammation and migration. Arterioscler Thromb Vasc Biol 2007;27:2606-11.
199. Massafra V, Ijssennagger N, Plantinga M, et al. Splenic dendritic cell involvement in FXR-mediated amelioration of DSS colitis. Biochim Biophys Acta 2016;1862:166-73.
200. Vavassori P, Mencarelli A, Renga B, et al. The bile acid receptor FXR is a modulator of intestinal innate immunity. J Immunol 2009;183:6251-61.
201. Shaik FB, Panati K, Narasimha VR, et al. Chenodeoxycholic acid attenuates ovalbumin-induced airway inflammation in murine model of asthma by inhibiting the T(H)2 cytokines. Biochem Biophys Res Commun 2015;463:600-5.
202. Hollman DA, Milona A, van Erpecum KJ, et al. Anti-inflammatory and metabolic actions of FXR: insights into molecular mechanisms. Biochim Biophys Acta 2012;1821:1443-52.
203. Lyons CL, Kennedy EB, Roche HM. Metabolic Inflammation-Differential Modulation by Dietary Constituents. Nutrients 2016;8.
204. Neuschwander-Tetri BA, Loomba R, Sanyal AJ, et al. Farnesoid X nuclear receptor ligand obeticholic acid for non-cirrhotic, non-alcoholic steatohepatitis (FLINT): a multicentre, randomised, placebo-controlled trial. Lancet 2015;385:956-65.
205. Mudaliar S, Henry RR, Sanyal AJ, et al. Efficacy and safety of the farnesoid X receptor agonist obeticholic acid in patients with type 2 diabetes and nonalcoholic fatty liver disease. Gastroenterology 2013;145:574-82 e1.
206. Trauner M, Arrese M, Wagner M. Fatty liver and lipotoxicity. Biochim Biophys Acta 2010;1801:299-310.
207. Cai D, Yuan M, Frantz DF, et al. Local and systemic insulin resistance resulting from hepatic activation of IKK-beta and NF-kappaB. Nat Med 2005;11:183-90.
208. Bechmann LP, Hannivoort RA, Gerken G, et al. The interaction of hepatic lipid and glucose metabolism in liver diseases. J Hepatol 2012;56:952-64.
209. Furukawa S, Fujita T, Shimabukuro M, et al. Increased oxidative stress in obesity and its impact on metabolic syndrome. J Clin Invest 2004;114:1752-61.
210. Hotamisligil GS. Inflammation and metabolic disorders. Nature 2006;444:860-7.
211. Shoelson SE, Lee J, Goldfine AB. Inflammation and insulin resistance. J Clin Invest 2006;116:1793-801.


NH_4^+


FXR
DNA

CHAPTER 3

Farnesoid X Receptor activation promotes hepatic amino acid catabolism and ammonium clearance

Vittoria Massafra, Alexandra Milona, Harmjan R. Vos, Rúben J.J. Ramos, Johan Gerrits, Ellen C.L Willemsen, José M. Ramos Pittol, Noortje Ijssennagger, Martin Houweling, Hubertus C.M.T.Prinsen, Nanda M. Verhoeven-Duif, Boudewijn M. Burgering, and Saskia W.C.van Mil

In revision for Gastroenterology

ABSTRACT

Background & Aims: The Farnesoid X Receptor (FXR) regulates bile acid synthesis, transport and catabolism. In addition, FXR regulates postprandial lipid and glucose metabolism. In the present study, quantitative liver proteomics confirmed these roles and also identified FXR as regulator of the third nutrient breakdown product: amino acids.

Methods: We quantified liver proteome-wide changes occurring in wild type and FXR knockout mice treated with vehicle or FXR agonist obeticholic acid (OCA) for 11 days. Furthermore, we investigated FXR regulation of amino acid metabolism by gene expression studies in primary hepatocytes, chromatin immunoprecipitation assays and *in vivo* tracing studies.

Results: In liver and primary hepatocytes, FXR activation resulted in upregulation of proteins involved in amino acid degradation, ureagenesis and glutamine synthesis. FXR binds to regulatory sites of these genes, providing evidence for direct transcriptional regulation. Concurrently, FXR ablation resulted in reduced expression of urea cycle proteins and accumulation of precursors of ureagenesis.

In liver-specific FXR knockout mice, plasma concentrations of newly formed urea as well as hepatic gene expression of enzymes involved in ammonium detoxification were decreased. OCA increased hepatic gene expression of these enzymes with a concurrent near significant increase in newly formed urea.

Conclusions: FXR regulates amino acid catabolism and detoxification of ammonium via ureagenesis and glutamine synthesis in the liver. Since urea cycle failure and hyperammonemia are common complications of acute and chronic liver diseases, therapeutic FXR activation may be beneficial to promote ammonium clearance in liver disease patients.

INTRODUCTION

Carbohydrates, proteins, and fats from the diet are digested in the gastro-intestinal tract, where they are broken down into their basic units, sugars (monosaccharides, e.g. glucose), amino acids, and free fatty acids, respectively. Via the portal venous circulation, these basic energy units reach the liver where they are processed.[1] In the postprandial phase, glucose is either used as energy source, condensed into glycogen or converted into fatty acids or amino acids. Free fatty acids are either oxidized to generate energy or esterified with glycerol-3-phosphate to synthesize triacylglycerol and subsequently stored in the liver or distributed to other tissues via VLDL incorporation. Amino acids are metabolized to provide energy or used to synthesize proteins, glucose, and/or other bioactive molecules.[2] Regulation of amino acid metabolism in the liver is crucial, because in times of dietary surplus, high concentrations of amino acids and ammonium reach the liver and may cause toxicity. Amino acids which are not used for protein synthesis are degraded to NH_4^+ and a carbon skeleton. Ammonium clearance is achieved by ureagenesis and glutamine synthesis in the liver.[3, 4] Carbamoylphosphate synthetase-1, Cps1, catalyses the committed step of ureagenesis and is mostly expressed in mitochondria of periportal hepatocytes, primarily exposed to intestinal protein catabolites. Glutamine synthesis relies on glutamine synthetase, Glul, expressed in cytosol of pericentral hepatocytes, where it ensures the clearance of ammonium and thereby controls tightly blood ammonium concentration.[5]

Next to their function as detergents facilitating dietary absorption of lipids and fat soluble vitamins, bile acids (BAs) have an important function in regulation of nutrient metabolism.[6] By rapidly activating nuclear receptors and other cell signaling pathways upon their postprandial return to the liver, BAs not only induce feedback inhibition of BA synthesis but also control lipid and glucose metabolism.[7]

Signalling of BAs in the postprandial phase is mediated by the Farnesoid X receptor (FXR), which is mainly expressed in intestine, liver and kidney. Intestinal FXR activation by BAs increases BA export into the portal circulation. In addition, FXR activation in the intestine increases Fgf15 synthesis and export into the portal system. Fgf15 through its membrane receptor Fgfr4 decreases hepatic BA biosynthesis, by affecting Cyp7a1 activity. Hepatic FXR activation increases BA efflux from hepatocytes through the regulation of transporters' expression (OSTα/β, BSEP and MDR3).[8]

FXR modulates triacylglycerol clearance, by promoting lipoprotein lipase activity via induction of ApoC-II and controls fatty acid and cholesterol synthesis, via repression of Srebp1c. Moreover, FXR improves insulin sensitivity and glucose clearance via down-regulation of the gluconeogenic genes Pck1 and Fbp1.[9] Metabolic function of FXR as nutrient sensor encompasses also repression of autophagy during prolonged nutrient shortage.[10, 11] Furthermore, FXR activation promotes liver regeneration and hepatocyte survival, inhibits hepatic inflammation and enhances tumor suppressor genes.[12] FXR agonists were shown to be beneficial in clinical trials for non-alcoholic steatohepatitis (NASH) and primary biliary cholangitis (PBC) and may have therapeutic potential in gallstone disease, cirrhosis, liver cancer and metabolic syndrome.[13]

In this study, we show that FXR not only regulates glucose and fatty acid metabolism, but also regulates the metabolism of the third class of basic energy units: amino acids. We quantified liver proteome-wide changes occurring *in vivo* in response to obeticholic acid (OCA) or FXR ablation and confirmed the role of FXR in BA, lipid and glucose metabolism. We show that FXR activation *in vivo* results in upregulation of proteins involved in amino acid degradation, urea cycle and glutamine synthesis, while FXR ablation associates with reduced expression of urea cycle proteins and accumulation of upstream substrates of urea cycle. FXR binds to regulatory sites of these genes and its activation increased urea production in primary hepatocytes. *In vivo* tracing studies of the conversion of isotopically labelled ammonium into urea also support a role for FXR in ureagenesis. Combining the data on FXR metabolic functions, we argue that FXR functions as a key regulator of deciding the postprandial fate of the three nutrient breakdown units: sugars, fats and amino acids.

MATERIALS AND METHODS

Animal experiments

Homozygous FXR-floxed mice (C57BL/6 FXR fl/fl, kind gift from K. Schoonjans, Ecole Polytechnique Federale de Lausanne, Switzerland,[14]) were crossed with Meox2-cre mice and Alb-Cre mice (Jackson Laboratory, Bar Harbor, ME, U.S.) to generate whole body FXR null mice (FXR-/-), and liver-specific FXR-null mice (liver FXR-/-) containing the same floxed allele for the ultimate comparison, respectively. FXR-floxed littermates without cre alleles were used as wild type (Wt) controls. Genotyping of FXR-floxed mice was assessed as described previously.[14] FXR expression was assessed in liver, kidney, ileum and adrenal glands of Meox2-cre mice (FXR-/-) and Alb-cre mice (livFXR-/-) (Supplementary Figure 1). Mice were fed a purified diet (AIN-93M, Research Diet, New Brunswick, NJ, U.S.) ad libitum and housed in a temperature and light-controlled room. C57BL/6 male mice either Wt or FXR-/- were gavaged with either OCA (10mg/kg body weight, kindly provided by Luciano Adorini, Intercept Pharmaceuticals, San Diego, CA, U.S.) or Vehicle (1% methyl cellulose) for 11 days. In the evening prior to the sacrifice, mice received an extra gavage of OCA/Veh. Mice were fasted for 4 hours prior to sacrifice.

In an independent experiment, C57BL/6 male mice were gavaged with either OCA or vehicle for 3 days. On day 3, mice were fasted for 6 hours. One group of mice were gavaged with $^{15}NH_4Cl$ dissolved in water (20mg/kb body weight; Cambridge Isotope Laboratories, Tewksbury, MA, U.S.) directly after fasting. Another group of mice were refed with a high protein diet (ssniff EF R/M High Protein, E15209; ssniff Spezialdiäten GmbH, Soest, Germany) for 2 hours before they were gavaged the tracer. Mice were killed and livers and plasma were harvested 90 minutes after $^{15}NH_4Cl$ administration. Alb-cre mice (livFXR-/-) and their Wt FXR fl/fl controls were subjected to the same protocol of refeeding with high protein diet and $^{15}NH_4Cl$ administration. All experiments were approved by the ethics committee of the University Medical Center Utrecht.

See **Supplementary Methods** for descriptions of the SILAC-based proteomics, primary hepatocyte culturing, urea and amino acid mass spectrometry analyses.

Western blotting

Liver tissue extracts were generated and protein concentration was assessed (BCA assay kit, Thermo Scientific). Western blots were probed with antibodies against Cps1 (Origene, Rockville, MD, U.S.), Ass1 (Abcam, Cambridge, UK), Glul (BD Biosciences, Franklin Lakes, NJ, U.S), Arg1 (Cell Signalling, Danvers, MA, U.S.), Prodh (Abcam), and Hal (Abcam). α-Tubulin (Sigma), and α-actin (Abcam) antibodies were used as loading controls.

Chromatin immunoprecipitation and ChIP-seq analysis

Snap-frozen liver tissue was crosslinked with formaldehyde and processed for chromatin immunoprecipitation as described previously.[15] Primer sequences used for ChIP-qPCR are reported in Supplementary Table 1. IR1 motifs[16] were searched in peak regions proximal to target genes using the HOMER suite software. We analysed ChIP-seq datasets generated in our laboratory (Gene Expression Omnibus, GSE73624,[15]) and by others[17] to assess the binding profile of FXR in liver.

Gene expression analyses

RNA was isolated from primary hepatocytes using TRIzol reagent (Invitrogen). cDNA was generated from 1 μg of total RNA using SuperScript II Reverse Transcriptase (Invitrogen). qRT-PCR analysis was performed using SYBR green PCR master mix (Roche, Basel, Switzerland) and analysed on a MyIQ real time PCR cycler (BioRad, Hercules, California, U.S.). Primer sequences are listed in Supplementary Table 2.

Statistics

Significance of pathway enrichment was determined by Ingenuity software, setting $p < 0.05$. Amino acid concentration in mouse liver tissue is expressed as mean ± SEM. Gene expression, amino acid and urea concentration in primary hepatocytes are expressed as mean ± SD. Statistical significance was determined by Student T-test using Graphpad (version 6.02) software. Two-sided p values ($p < 0.05$) were considered significant.

RESULTS

Liver proteomic analyses of wild type and FXR-/- mice treated with obeticholic acid.

To determine the effects of FXR activation and ablation in the liver, we quantified protein expression changes in liver extracts from wild type (Wt) and FXR-/- mice treated with vehicle (Veh) or OCA. Liver protein extracts (containing 'light' lysine) were mixed 1:1 with a spike-in protein extract from $^{13}C_6$-lysine metabolically labelled mouse liver (containing 'heavy' lysine) and analysed by LC-MS/MS (Figure 1A). Spike-in efficiency, indicating the quality of the heavy signal as internal standard, was assessed as frequency of proteins in the vehicle-treated mice ranked based on their log2 heavy/light normalized ratio (Figure 1B). Most proteins had a heavy/light ratio close to 1, indicating a substantial equality in protein composition of the liver from the mice in the experiment and the 'heavy' liver tissue, thereby supporting the suitability of the heavy labelled liver as

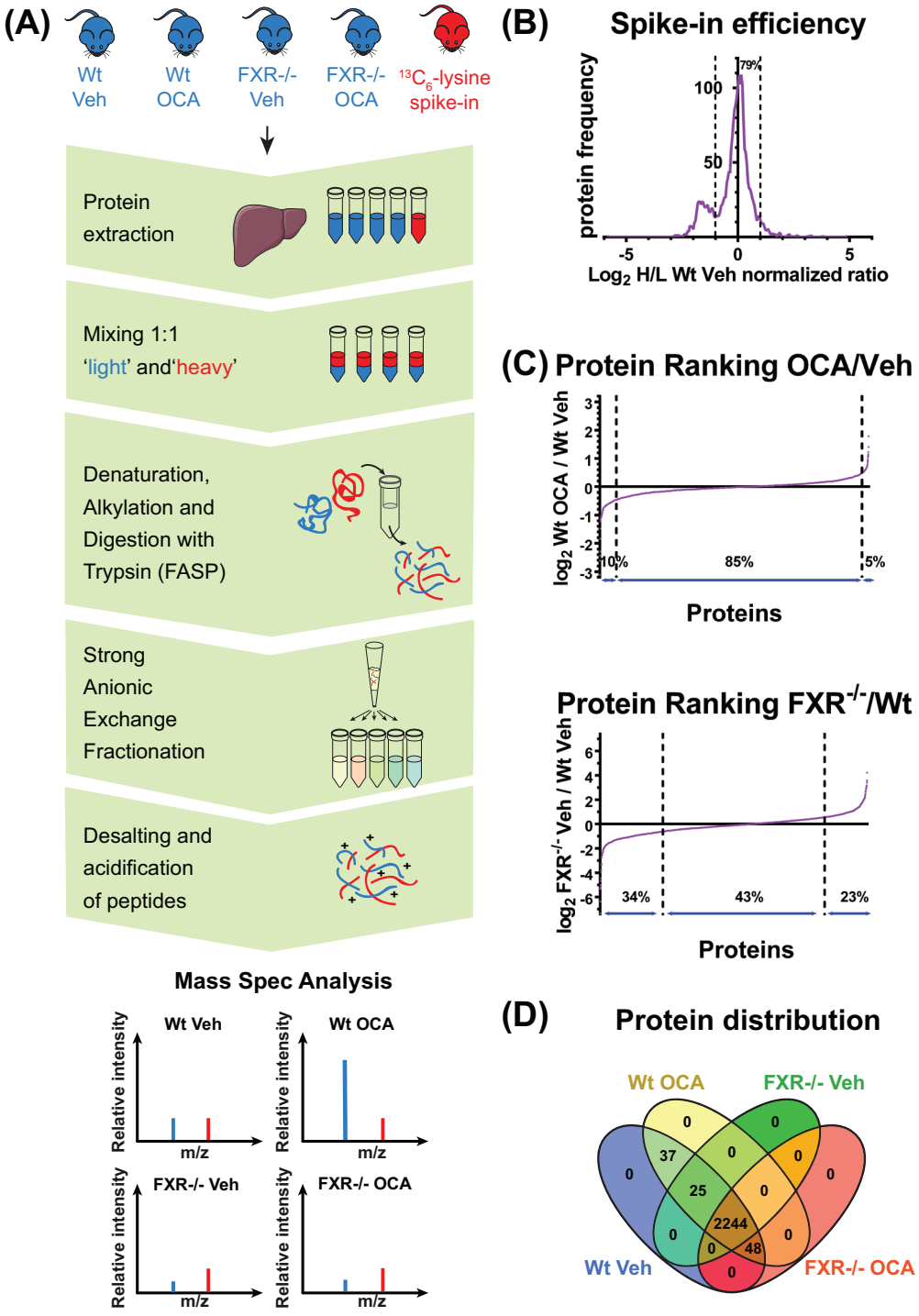
(A)
Wt Veh
Wt OCA
FXR-/- Veh
FXR-/- OCA
13C6-lysine spike-in
Protein extraction
Mixing 1:1 'light' and'heavy'
Denaturation, Alkylation and Digestion with Trypsin (FASP)
Strong Anionic Exchange Fractionation
Desalting and acidification of peptides
Mass Spec Analysis
Wt Veh
Wt OCA
FXR-/- Veh
FXR-/- OCA
Relative intensity
m/z
(B)
Spike-in efficiency
protein frequency
79%
100
50
-5
0
5
Log2 H/L Wt Veh normalized ratio
(C)
Protein Ranking OCA/Veh
log2 Wt OCA / Wt Veh
10%
85%
5%
Proteins
Protein Ranking FXR-/-/Wt
log2 FXR-/- Veh / Wt Veh
34%
43%
23%
Proteins
(D)
Protein distribution
Wt OCA
FXR-/- Veh
Wt Veh
FXR-/- OCA
0
37
25
2244
48

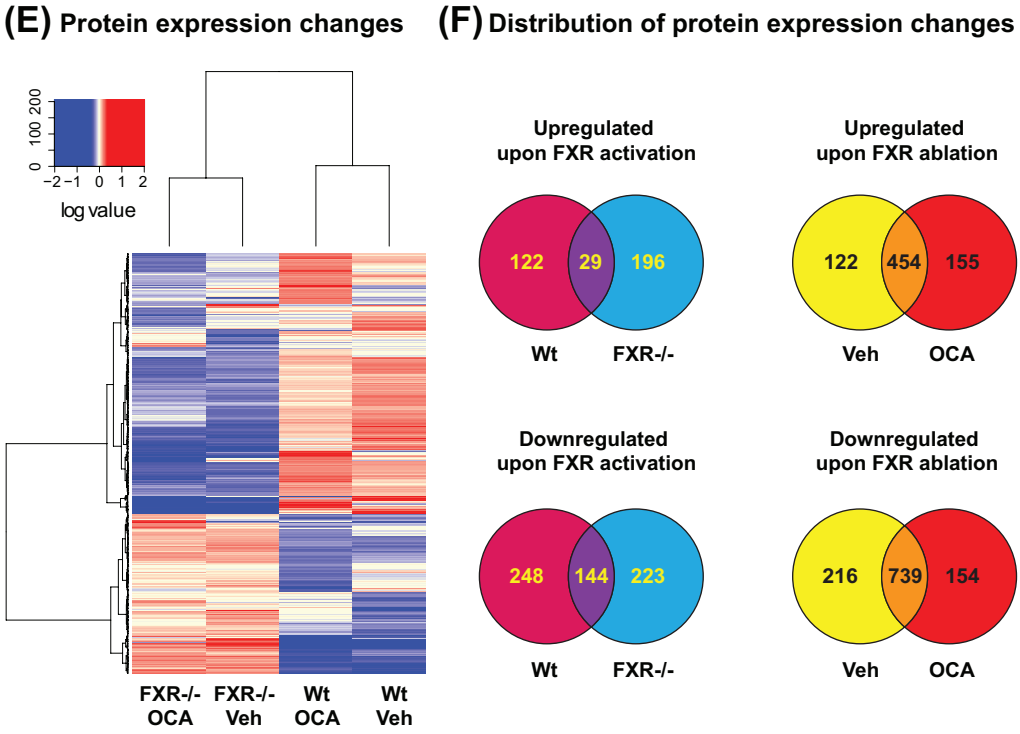

Figure 1. Proteomic analysis in liver tissue derived from Wt and FXR-/- mice treated with or without OCA. (A) Experimental outline to determine the proteome of mouse liver extracts by LC-MS/MS. (B) Frequency plot of proteins identified in Veh-treated Wt mice based on their total log2 heavy/light normalized ratio. The plot is representative of a Wt untreated condition among all livers analysed to show the basal efficiency of the heavy spike-in added to the light samples. Percentage of proteins with a log2 heavy/light normalized ratio included in interval (-1,+1) is shown. (C) Protein ranking based on changes of the log2 light/heavy normalized ratio induced by FXR activation (upper panel) and ablation (lower panel). Percentages of proteins, of which expression was decreased (≤ -1.3 fold), unchanged or increased (≥1.3 fold) are indicated. (D) Venn diagram summarizing the distribution of quantified proteins in each of the 4 experimental groups (Wt Veh, Wt OCA, FXR-/- Veh, FXR-/- OCA). (E) Comparative heatmap analysis of the effect of FXR activation and ablation on mouse liver proteome. Proteins were clustered from the top to the bottom based on similar expression profile in the four experimental groups (Wt Veh, Wt OCA, FXR-/- Veh, FXR-/- OCA). (F) Venn diagram showing the number of proteins regulated by OCA in Wt mice and in FXR -/- mice (left panels) and the number of proteins regulated upon FXR ablation in Veh and OCA-treated mice (right panels). Only fold changes ≥ 1.3 were considered.

internal standard for the light samples.

Our proteomic analysis identified 4514 proteins, of which 3070 were identified with two or more unique peptides, were not reverse hits, decoy hits or standard contaminants. 2354 proteins were quantified with a log2 light/heavy normalized ratio. FXR activation by OCA resulted in upregulation of 5% of proteins and downregulation of 10% of proteins quantified, whereas FXR ablation resulted in a more profound impact on the proteome (23% proteins were upregulated, 34% were downregulated, Figure 1C).

2244 proteins were quantified in each experimental condition (Wt Veh, Wt OCA, FXR-/- Veh, FXR-/- OCA), enabling comparative analyses of protein expression (Figure 1D).

Hierarchical clustering of quantified proteins based on their light/heavy normalized ratios revealed two general clustered regions which include proteins with decreased or increased expression in FXR-/- compared to Wt mice (Figure 1E). Within each of these clusters, subsets of proteins could be identified, which were upregulated or downregulated upon OCA only in the Wt, only in the FXR-/- or in both genotypes. 370 proteins were regulated in a FXR-dependent manner after treatment with OCA: 122 proteins were upregulated in the Wt, but not in the FXR-/- mice, whereas 248 proteins were downregulated by OCA in the Wt, but not in the FXR-/- mice. Genetic FXR ablation had a stronger impact on liver proteome: 454 proteins were upregulated, and 739 downregulated both in Veh and OCA-treated mice (Figure 1F).

Regulation of BA metabolism by FXR is supported by liver proteomic analyses .

To validate the quality of our proteome dataset, we analysed protein changes in BA metabolism pathways. Protein expression of the BA transporter Bsep (Abcb11) increased in Wt mice treated with OCA and decreased in FXR-/- compared to Wt mice (Figure 2A-B), in line with FXR dependent-increase in efflux of BAs from the liver to the canalicular lumen.[8, 18] Oppositely, the BA synthesis enzyme Cyp8b1 decreased in Wt mice treated with OCA and increased in FXR-/- mice (Figure 2A-B), in line with previous reports.[19] In Figure 2C (and Supplementary Table 3), a schematic overview is given of protein expression changes induced by FXR activation/ablation with regard to BA metabolism. Similar to Cyp8b1, expression of Cyp7a1 was upregulated by FXR ablation, however, since Cyp7a1 could not be quantified in Wt mice (possibly because the expression was very low upon OCA treatment), a ratio between OCA and Veh treated mice could not be determined. Expression of the rate limiting enzyme of the taurine metabolism Csad decreased 1.6 fold upon FXR activation and increased 9.3 fold upon FXR ablation, supporting the role of FXR in regulating taurine availability and BA conjugation, in line with a previous report.[20]

Protein expression of Slc10a1 (Ntcp), which guides the portal uptake of conjugated BAs, was severely reduced in FXR-/-, which does not concur with the equal mRNA levels of Ntcp reported in Wt and FXR-/- mice[21], but is concurrent with data showing that Ntcp protein expression is reduced in conditions of hepatic BA retention (like in cholestasis or in FXR-/- mice).[22] Finally, expression of Abcc3 (Mrp3), which promotes systemic efflux of conjugated BAs, was upregulated upon OCA treatment (2.0 fold), consistent with FXR induction of basolateral transporters promoting systemic secretion of BAs.[23]

In summary, our proteomic analyses recapitulate the role of FXR in downregulation of BA synthesis, regulation of BA conjugation and upregulation of BA efflux into the canalicular lumen and in the systemic circulation.

A novel role for FXR in regulation of the third class of basic energy units: amino acids.

Having validated our dataset, we next used our proteomic data to gain insights into novel biological functions of FXR. We performed pathway and ontology analyses on all

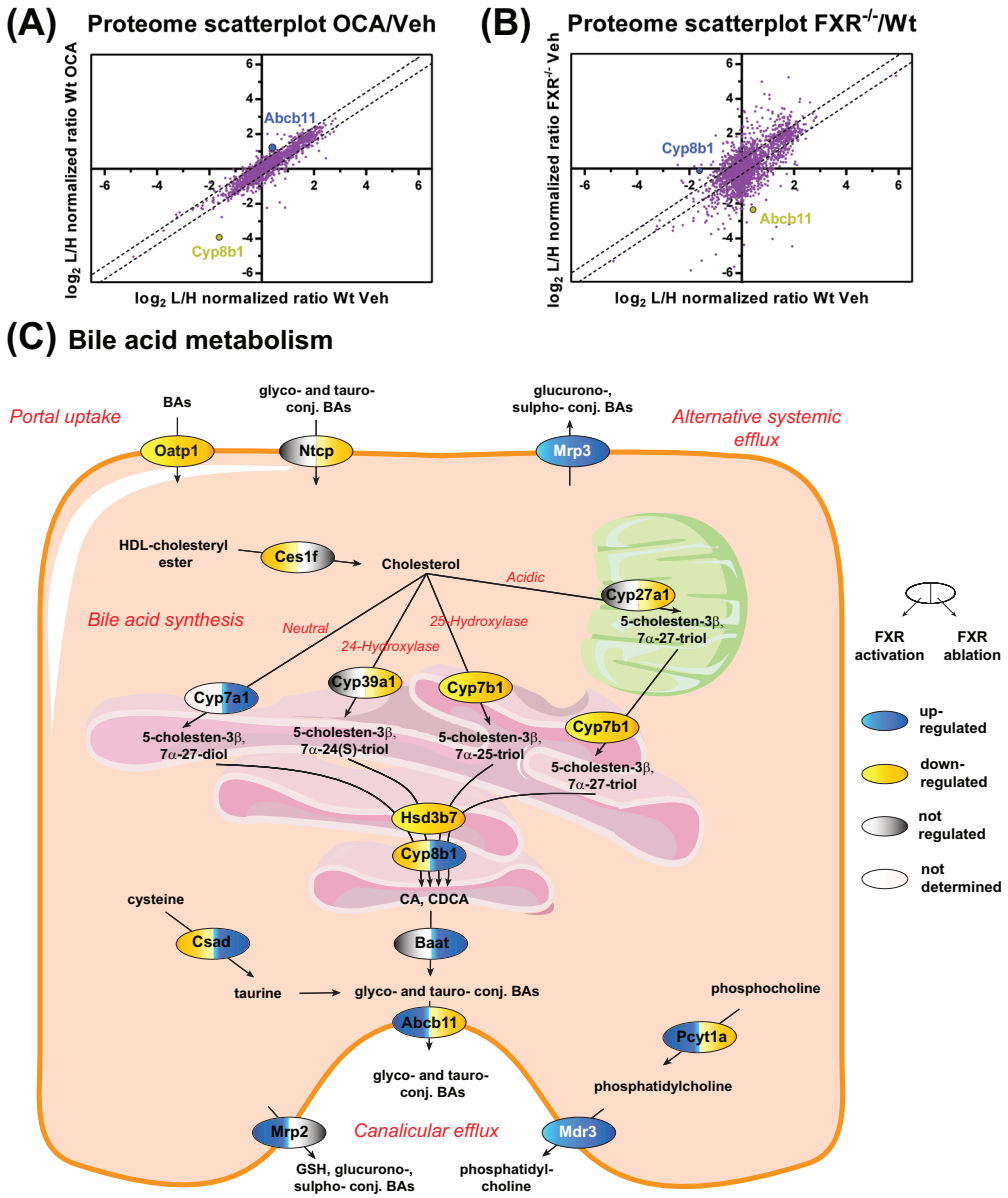

Figure 2. Proteome-wide changes in bile acid metabolism. (A-B) Protein scatterplots depicting proteome-wide changes upon FXR activation (A) and ablation (B) in liver. Abcb11 (Bsep) and Cyp8b1 are highlighted as representative proteins related to BA metabolism known to be up- or downregulated by FXR activation, respectively. (C) Schematic representation of protein expression changes (≥1.4 fold), of relevance for BA metabolism (B). Upregulated (blue), downregulated (yellow) or unchanged (grey) proteins upon OCA treatment (left half box) or FXR ablation (right half box). Non-quantified changes are indicated in white.

differentially expressed proteins (Figure 3A, and Supplementary Figure 2). Similar metabolic pathways were found to be regulated by FXR activation and ablation. As expected, FXR/RXR activation and activation of other nuclear receptors functionally related to FXR were among the most significantly changed pathways upon FXR activation/ablation (black bars). Likewise, FXR activation/ablation impacts on BA, cholesterol and steroid metabolism (yellow bars) and on metabolism of fatty acids, glucose and glutathione metabolism (grey, blue and purple bars, respectively), as has been previously shown.[7, 24,

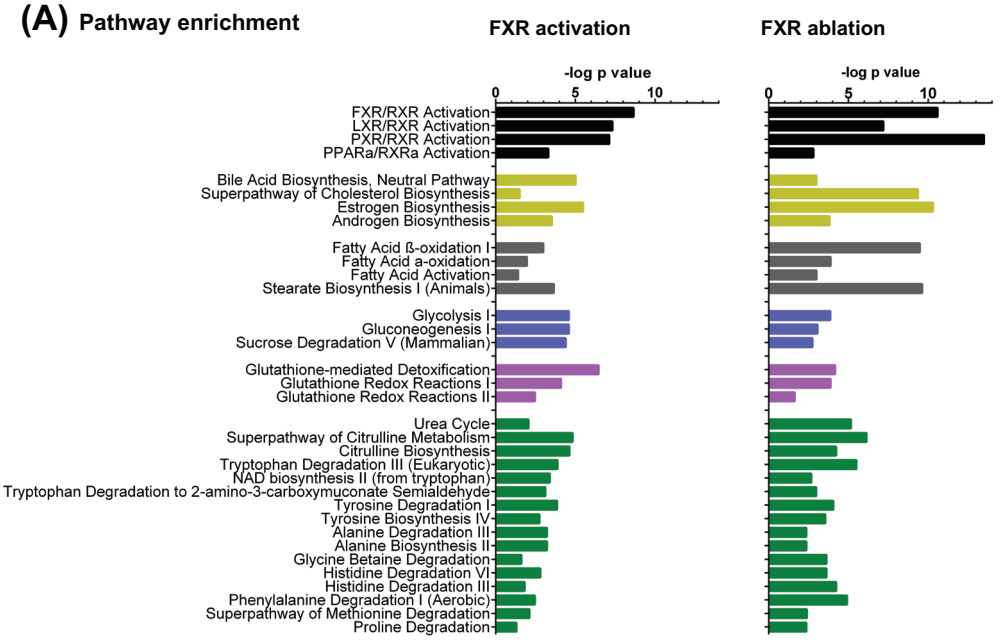

Figure 3A. FXR activation regulates amino acid metabolism. (A) Canonical pathway analysis (using Ingenuity Pathway analysis software) of protein expression changes with fold change ≥1.3 upon FXR activation and ablation. Pathways are clustered with similar colours based on their overall function.

[25] Strikingly, FXR activation and ablation significantly changed protein expression concerning amino acid metabolism, including urea cycle, citrulline, tryptophan, tyrosine, alanine, glycine, histidine, phenylalanine, methionine, glutamine, glutamate, and proline metabolism (green bars). This pathway enrichment analysis suggests that FXR regulation of nutrient metabolism applies to dietary basic units of lipids, and carbohydrates, but also extends to catabolic products of the third main energy source: proteins.

In Figure 3B, we schematically depicted the changes in protein expression in amino acid catabolism pathways upon FXR activation and FXR ablation (See also Supplementary Table 4). FXR activation increased the expression of multiple enzymes in the pathway of conversion of histidine to glutamate (Hal, Uroc1, Amdhd1, Ftcd) and of proline to glutamate (Prodh). FXR activation also increased expression of enzymes relevant for tryptophan (Tdo2, Kynu), methionine (Mat1a, Ahcy, Cth), phenylalanine (Pah), 5-hydroxy-

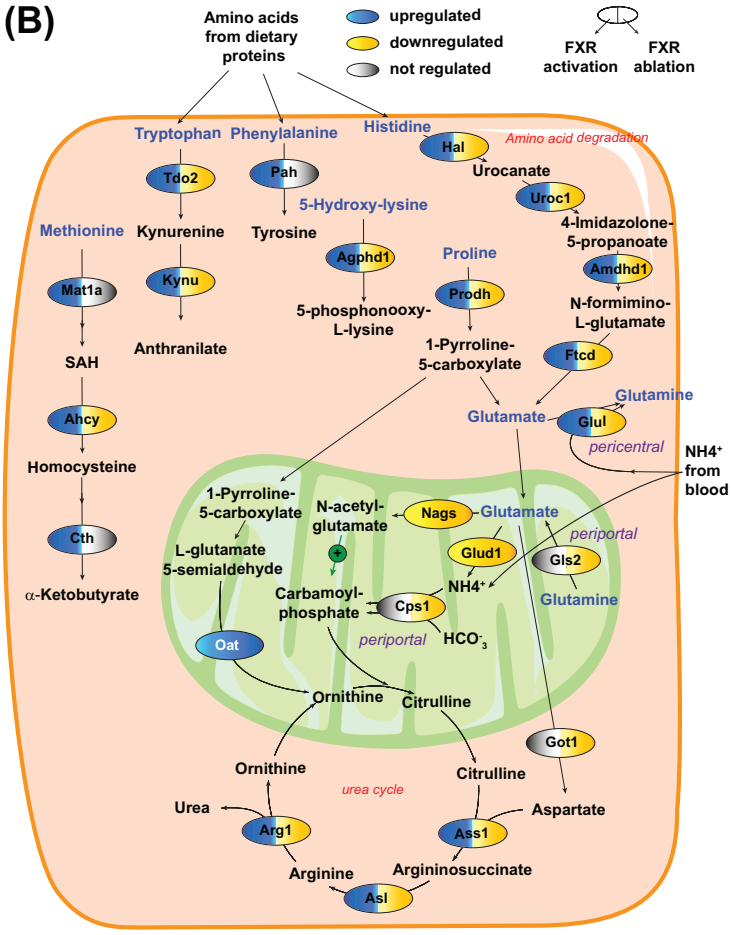

Figure 3B. Schematic representation of protein expression changes (≥1.4 fold), related to amino acid metabolism. Upregulated (blue), downregulated (yellow) or unchanged (grey) proteins upon OCA treatment (left half box) or FXR ablation (right half box).

lysine (Agphd1) degradation. On the other hand, FXR ablation resulted in downregulation of most of the above mentioned proteins related to amino acid degradation. Together, these results suggest that FXR mediates the induction of hepatic amino acid catabolism.

In postprandial state, clearance of hepatic ammonium generated from intestinal catabolism and hepatic amino acid catabolism requires the conversion into urea or glutamine.[3, 4] Expression of enzymes of urea cycle Ass1, Asl, and Arg1 were upregulated by FXR activation and downregulated by FXR ablation. Cps1 and Nags –key enzymes of urea cycle – and Gls2 and Glud1, which provide mitochondrial glutamate and ammonium to urea cycle respectively, were unchanged or downregulated upon FXR activation, but were strongly reduced in expression in FXR-/- mice.

We also observed FXR-dependent regulation of Glul, which was upregulated by OCA (1.5 fold) and downregulated upon FXR ablation (2.2 fold). Glul is important for alternative disposal of ammonium via conversion of glutamate to glutamine, especially in periportal hepatocytes[3], suggesting a role of FXR in ammonium detoxification via glutamine synthesis as well.

By immunoblot analyses, we confirmed that expression of Cps1, Ass1 and Arg1, Glul, Hal and Prodh were indeed reduced upon FXR ablation and increased or unchanged upon FXR activation, although the effect of FXR ablation was more pronounced (Figure 3C), concurrent with the proteomic data. The changes in protein expression induced by

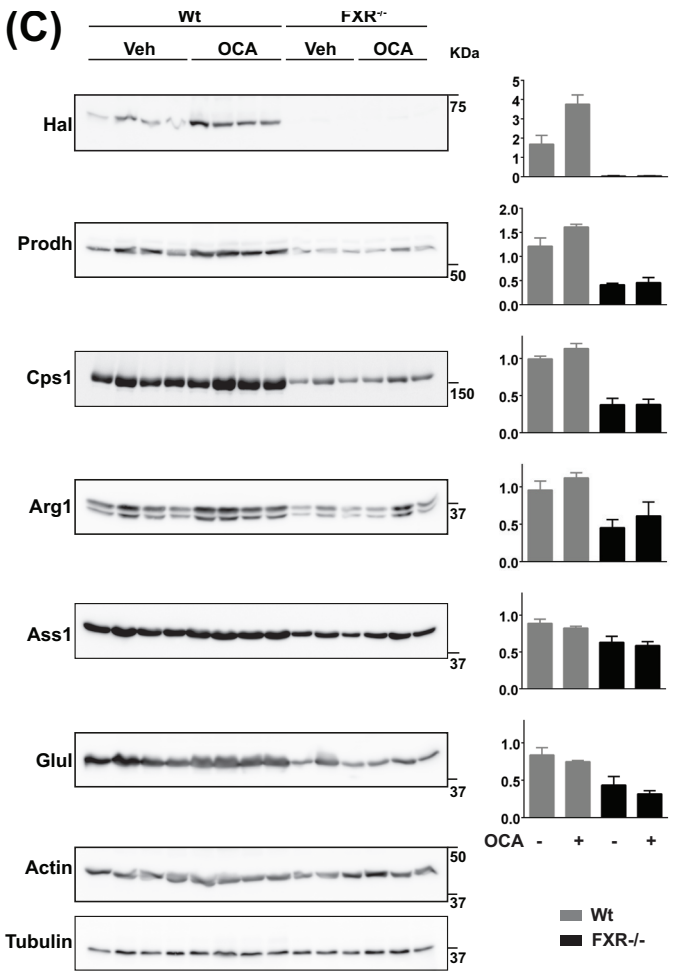

Figure 3C. Western Blot analysis of proteins involved in amino acid catabolism (Hal, Prodh), urea cycle (Cps1, Ass1, Arg1) and glutamine synthesis (Glul) in liver extracts harvested from Wt or FXR-/- mice treated either with Veh or OCA. Actin and tubulin were used as loading controls. Protein extracts from 4 Wt mice and from 3 FXR-/- mice were included in the analysis. Quantification is shown relative to tubulin and actin.

OCA are rather small or undetected, but the sensitivity of the immunoblot assay does not allow to pick small changes in protein expression. In addition, the small changes in protein expression may be due to the dynamic regulation of protein expression, i.e. we may be too early or too late after OCA stimulation to appreciate the largest fold difference compared to unstimulated mice. To validate the role of FXR in amino acid catabolism and ureagenesis, we have analysed FXR transcriptional regulation of these enzymes and amino acid and urea production in primary hepatocytes and liver-specific FXR knockouts in subsequent experiments.

FXR binds to gene regulatory sites of enzymes in the urea cycle and amino acid catabolism pathways.

To investigate whether FXR regulates the transcription of genes involved in amino acid metabolism, we analysed genome-wide FXR binding profiles in mouse liver in a ChIP-sequencing dataset generated in our lab[15], and by Thomas et al.[17] FXR peaks were identified within 10 kb from the TSS of the genes *Glul*, *Ass1*, *Asl*, *Hal* and *Prodh* and within 45 kb from the transcription start site (TSS) of *Cps1* (Figure 4A, and Supplementary Table 1). We searched for IR1 sites, the preferential binding motif for FXR[16], in the selected peaks (Supplementary Table 1) and to validate FXR binding to these sites, we performed ChIP-qPCR using primers designed around the identified IR1 motifs. We confirmed

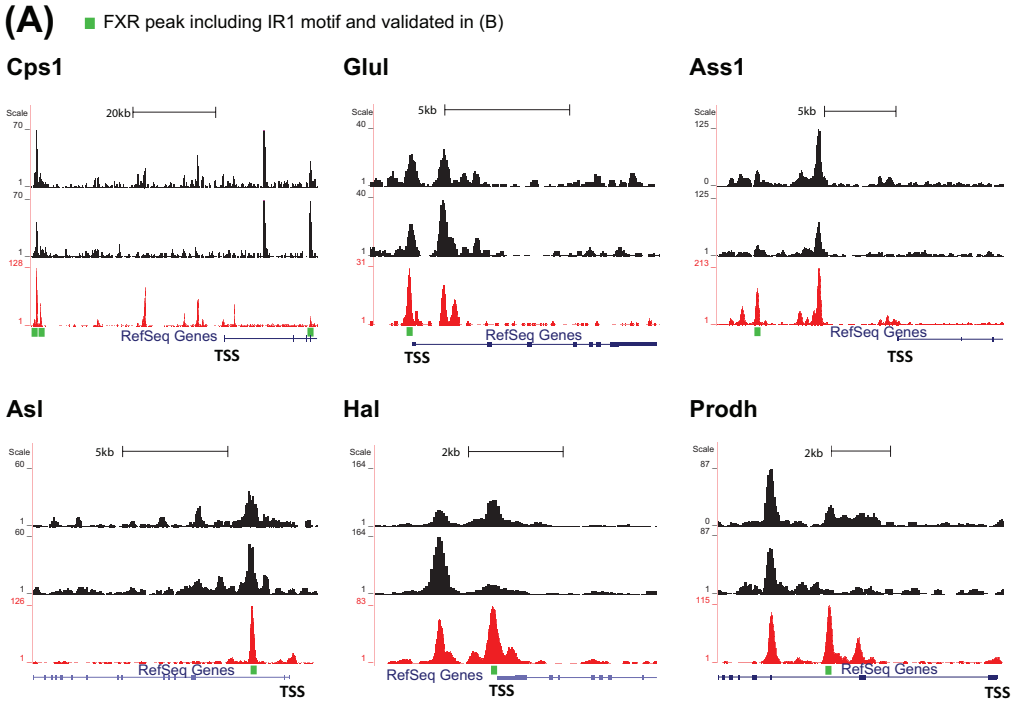

Figure 4. FXR binds to gene regulatory sites of genes encoding enzymes involved in amino acid catabolism, urea cycle and glutamine synthesis. (A) FXR ChIP-seq tracks from liver of 2 Wt mice are depicted in black [15]. The red track refers to a ChIP-seq experiment in mouse liver [17]. FXR enrichment at genomic regions proximal to Cps1, Glul, Ass1, Asl, Hal and Prodh is shown. Green boxes indicate the peaks including the IR1 motif in which FXR binding was validated by ChIP-qPCR. (B) Validation of candidate peaks by ChIP-qPCR in liver extracts from Wt mice. Globin and Fabp6 regions were used as negative controls and Slc51b (Ostβ), Nr0b2 (Shp) and Abcb11 (Bsep) were used as positive controls for FXR occupancy in the liver. Data are shown as mean ± SD, n=2, *p<0.05 by a Students t-test.

FXR binding to two peaks upstream of the TSS and a peak in an intronic region of *Cps1*, and to a peak in the promoter of *Hal* and *Glul*, in an intronic region of *Asl* and *Prodh* and upstream of the TSS of *Ass1* (Figure 4B). *Globin* and *Fabp6* (FXR target gene in intestine, not in liver) promoters were used as negative control regions, whereas *Slc51b* (Ostβ), *Nr0b2* (Shp) and *Abcb11* promoters were used as positive controls for FXR binding. These data provide evidence for a role of FXR as direct transcriptional regulator of enzymes involved in urea cycle, glutamine synthesis and histidine and proline catabolism.

FXR ablation results in accumulation of urea cycle precursors in the liver. Next, we investigated whether FXR-mediated regulation of amino acid metabolism in-

duced changes in amino acid concentrations in liver extracts (Figure 5 and Supplementary Table 5). Precursors for the urea cycle -glutamate, glutamine and aspartate- were increased in mouse livers of FXR-/- compared to Wt mice, whereas urea cycle intermediates citrulline and ornithine were decreased, indicative of a stagnation of the urea cycle in the liver (Figure 5A-B). Histidine increased in FXR-/- compared to Wt mice, in line with reduced expression of histidine degrading enzymes, such as Hal (Figure 5B). No significant changes in amino acid concentrations were detected upon OCA treatment in Wt mice. FXR depletion in mice is expected to result in hyperammonemia and a decrease in plasma urea concentration. Actually, FXR-/- mice, but not liver FXR-/- mice showed an increase in plasma urea concentrations compared to Wt mice (Figure 5C). These results have to be interpreted considering that plasma urea concentration is the final result of intestinal protein breakdown, liver urea production, degradation of urea by ureases of gastrointestinal bacteria and renal excretion of urea into urine[26], and may therefore not reflect amino acid catabolism and urea production by the liver. Therefore, in the next series of experiments, we have relied on primary hepatocyte sandwich cultures and short-term OCA treatments as well as *in vivo* tracing experiments in liver-specific knockout mice to ascertain whether FXR directly regulates amino acid catabolism and urea production.

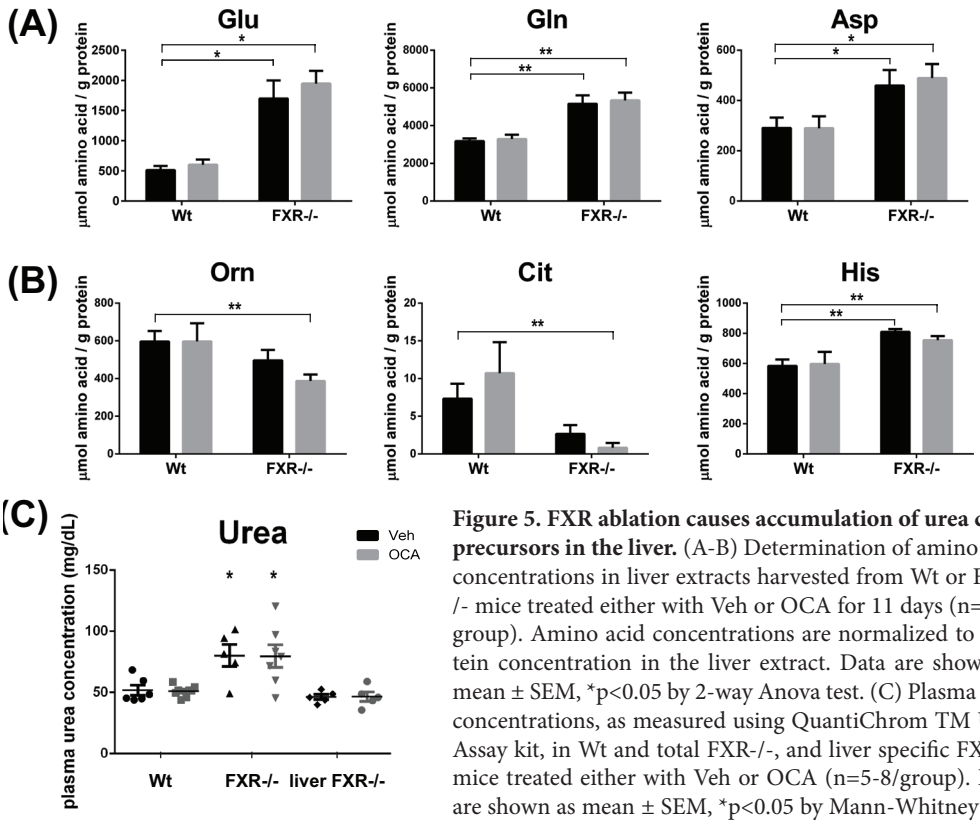

Figure 5. FXR ablation causes accumulation of urea cycle precursors in the liver. (A-B) Determination of amino acid concentrations in liver extracts harvested from Wt or FXR-/- mice treated either with Veh or OCA for 11 days (n=5-7/group). Amino acid concentrations are normalized to protein concentration in the liver extract. Data are shown as mean ± SEM, *p<0.05 by 2-way Anova test. (C) Plasma urea concentrations, as measured using QuantiChrom TM Urea Assay kit, in Wt and total FXR-/-, and liver specific FXR-/- mice treated either with Veh or OCA (n=5-8/group). Data are shown as mean ± SEM, *p<0.05 by Mann-Whitney test, compared to the respective treatment in Wt mice.

FXR activation increases gene expression of glutamine synthetase and urea cycle-related genes and enhances urea production in primary rat hepatocytes. To investigate whether FXR directly regulates transcription of genes involved in amino acid metabolism, we stimulated sandwich cultures of primary rat hepatocytes with OCA for 0, 1, 4 or 17 hours (Figure 6A). Efficient activation of FXR by OCA treatment was evaluated by increased mRNA expression of the FXR target gene *Shp* and decreased mRNA expression of *Cyp7a1*, which is known to be repressed by Shp (Figure 6B). We confirmed that *Glul*, *Ass1*, *Asl* and *Prodh* are increased upon FXR activation by OCA, albeit with different expression kinetics (Figure 6B). Expression of Cps1 and Hal increased slightly, but not significantly (Figure 6B). The OCA-dependent increase in expression of urea cycle genes concurred with a significant increase in the amount of urea produced in the medium in one hour, after 20 hours of OCA stimulation (Figure 6C). Taken together, these data indicate that FXR directly increases expression of genes involved in glutamine synthesis, urea cycle and proline catabolism and causes a concurrent increase in urea production.

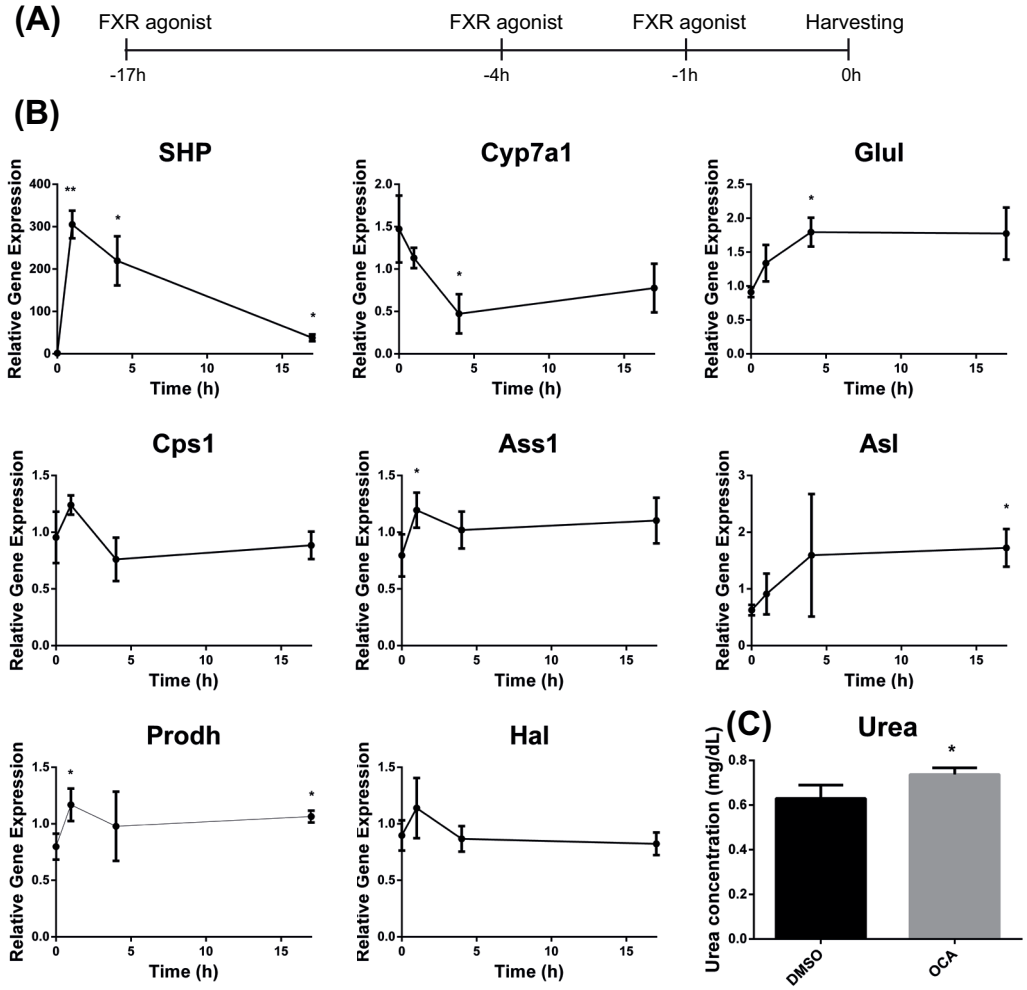

Figure 6A-C (previous page). FXR activation promotes glutamine synthesis and urea production in sandwich cultures of primary rat hepatocytes. (A) Experimental outline of primary rat hepatocytes incubated with DMSO or 1μM OCA in panels B-C. (B) Relative gene expression of Shp, Cyp7a1, Glul, Cps1, Ass1, Asl, Prodh and Hal was assessed by qRT-PCR. Expression at each time point is normalized to its respective DMSO control. Gene expression data were normalized to 36b4 (Rplp0). Significant changes compared to t=0 are indicated with *. (C) Urea concentrations in medium of sandwich cultures of primary hepatocytes treated with DMSO or OCA for 20 hours. 1h before harvesting, the medium was changed to 10 mM Hepes in HBSS, to measure urea release. All data are shown as mean ± SD, n=3, *p<0.05 by a Students t-test.

FXR activation promotes glutamine synthesis and urea production upon ammonium excess.

In order to validate whether FXR promotes expression of genes involved in glutamine synthesis and urea cycle to ensure detoxification of ammonium in excess after feeding, we exposed primary rat hepatocytes to FXR agonists for 6 hours and in the last hour before harvesting we exposed the cells to excess of NH_4Cl, ornithine and glutamine (Figure 6D). *Shp* mRNA increased upon treatment with OCA or with the synthetic FXR agonist GW4064, as expected (Figure 6E). Expression of *Cps1* increased 2 fold after OCA or GW4064 treatment when excess ammonium was present (Figure 6E), suggesting that FXR-mediated induction *Cps1* is dependent on the ammonium concentration, since we did not observe Cps1 induction in the absence of ammonium (Figure 6B). Expression of *Glul* was also induced by OCA and GW4064, implying that the investigated effects can be ascribed to FXR-mediated mechanisms, rather than FXR-independent BA functions. In agreement induced expression of genes involved in the urea cycle, urea production increased upon exposure to OCA or GW4064 (Figure 6F).

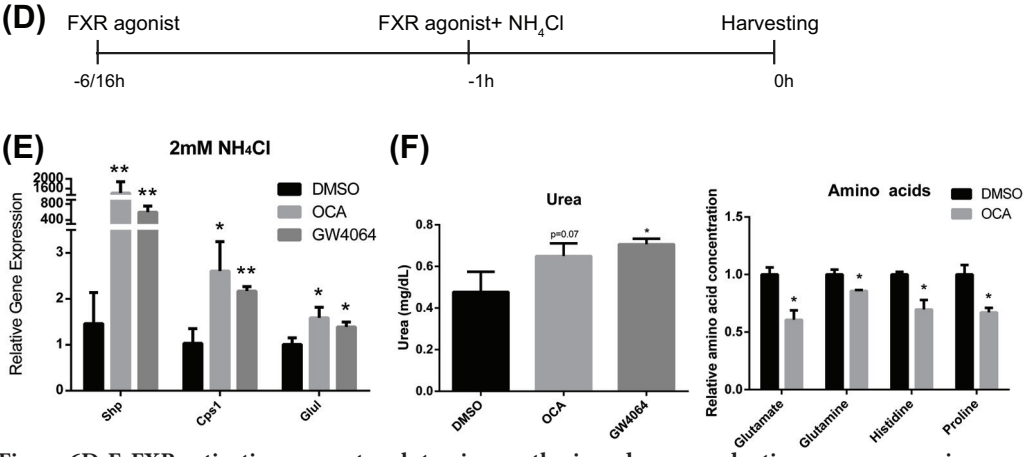

Figure 6D-F. FXR activation promotes glutamine synthesis and urea production upon ammonium excess. D) Experimental outline of treated primary rat hepatocytes. Primary hepatocytes were incubated with DMSO, 1μM OCA or GW4064 for 6h. 1h before harvesting, the medium was changed to 2 mM NH_4Cl, 0.4 mM glutamine, 0.6 mM ornithine, 10mM Hepes in HBSS. (E) Relative gene expression of Shp, Glul, and Cps1 was investigated by qRT-PCR (mean ± SD, n=3, significant changes compared to DMSO are indicated with *). (F) Urea concentrations in medium of primary hepatocytes (left panel). Amino acid concentrations in medium of primary hepatocytes incubated for 16 hours with OCA or DMSO (right panel). 1h before harvesting, the medium was changed to 2 mM NH_4Cl, 0.4 mM glutamine, 0.6 mM ornithine, 10mM Hepes in HBSS. All data are shown as mean ± SD, n=3, *p<0.05 by a Students t-test.

To further characterize the effects of OCA on amino acid metabolism, we measured amino acid concentrations in medium of primary hepatocytes incubated for 16 hours with OCA or DMSO and in the last hour before harvesting with NH_4Cl, glutamine and ornithine. The concentration of glutamate decreased upon OCA treatment (Figure 6F, and Supplementary Table 6), in line with FXR promoting the catabolism of key amino acids shuttling ammonium groups into the urea cycle. Despite the increase in Glul expression, glutamine concentration did not increase upon OCA treatment, likely as a result of decreased substrate, glutamate. Also the concentration of histidine and proline decreased upon OCA treatment, in line with the FXR-mediated induction of the protein expression of Hal and Prodh, responsible for the degradation of histidine and proline. Together, our results indicate that FXR activation ensures the nitrogen homeostasis in hepatocytes, by facilitating detoxification of the ammonium groups from excess dietary amino acids, by increasing ureagenesis and glutamine synthesis.

FXR regulates ureagenesis *in vivo*.

Finally, we set out to measure newly formed urea from a gavaged $^{15}NH_4Cl$ tracer in mice. Mice were fasted for 6 hours and half of the group was refed with high protein diet for 2h (Figure 7A). Based on the experiment performed by Youdkhoff et al. [27], we measured plasma ^{15}N-urea 90 minutes after $^{15}NH_4Cl$ administration. Under these conditions, ^{15}N-urea in refed mice nearly significantly increased upon OCA treatment (p=0.09) (Figure 7B). This was not seen in fasted mice. The concentration of ^{14}N-urea did not change upon OCA in plasma from either fasted or refed mice, presumably as a consequence of the compensatory increase in renal excretion. Concomitantly, OCA treatment resulted in significant increases in *Bsep*, *Glul* and *Gls2,* and nearly significant increase in *Ass1* expression. (Figure 7C). Administration of $^{15}NH_4Cl$ to liver specific FXR-/- and their Wt FXR fl/fl controls (Figure 7D) after fasting and refeeding a high protein diet significantly reduced ^{15}N-urea plasma concentration in liver-specific FXR-/- mice, compared to the Wt FXR fl/fl controls (Figure 7E), while the concentration of unlabelled ^{14}N-urea was unchanged (data not shown). Concurrent with an impaired formation of newly generated urea, liver specific FXR-/- mice display higher plasma concentrations of the precursor amino acids for ureagenesis glutamine and glutamate than their respective controls. Finally, liver-specific FXR deletion reduced the expression of FXR target *Bsep* and of the genes *Glul*, *Gls2*, *Ass1*, *Nags* and *Prodh* (Figure 7F). These tracer experiments show that FXR regulates amino acid catabolism in the liver *in vivo*.

DISCUSSION

Nitrogen homeostasis after feeding involves the degradation of amino acids taken up from the diet which are not required for net protein or neurotransmitter synthesis.[28] These surplus amino acids are degraded to ammonium (NH_4^+) and a carbon skeleton. The carbon skeleton can be used for the production of glucose or fatty acids. Nitrogen derived from the catabolism of these surplus amino acids cannot be physiologically stored and depends on ureagenesis and glutamine synthesis for appropriate disposal or temporary storage.[3] A major determinant of the rate of ureagenesis is substrate availabil-

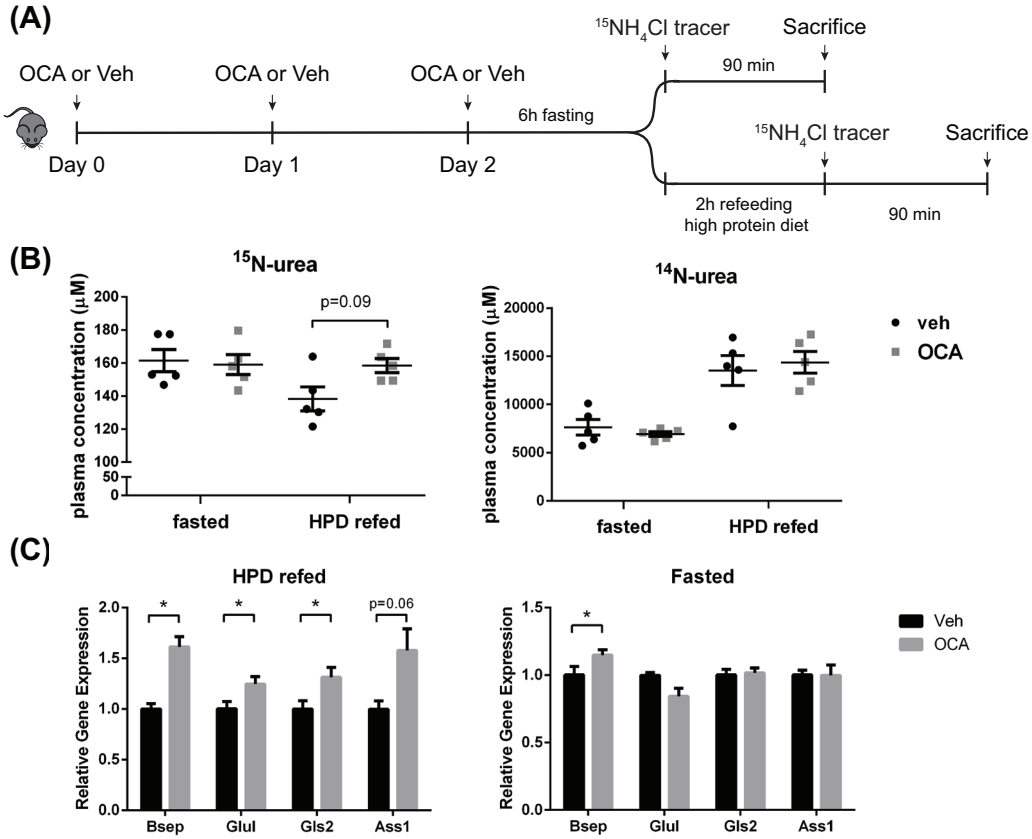

ity. In addition, glucagon, insulin and glucocorticoids have been shown to modulate the activity of enzymes in the urea cycle.[5] Noteworthy, transcriptional control of urea cycle genes has also been reported. HNF4α increases expression of ornithine carbamoyl transferase, *Otc.* PPARα and C/EBPα have been shown to oppositely regulate expression of the urea cycle genes *Cps1, Otc, Ass1, Asl and Arg1*.[29] However, the complex interplay of transcription factors in coordinating ureagenesis is far from being completely understood.

FXR is a nutrient-sensing nuclear receptor activated by BAs in the intestine and in the liver; it is an important regulator of glucose and fat metabolism.[30] We have combined an *in vivo* SILAC-based method with FASP-SAX to determine the proteome-wide expression changes in mouse liver in response to FXR activation by OCA. To our knowledge, this is the first time that such an approach is used to validate and extend established functions of FXR as well as to investigate unexplored FXR functions. We showed that FXR activation downregulates BA synthesis, modulates BA conjugation and upregulates BA efflux into the canalicular lumen and in the systemic circulation, in line with what it is reported in literature.[7] Overall, FXR ablation had a stronger effect on the liver proteome than OCA treatment, as shown in Figure 1. FXR ablation resulted in suppression of Cyp7b1, Cyp27a1, Ntcp, and Oatp1 expression and upregulation of Abcc3, which are

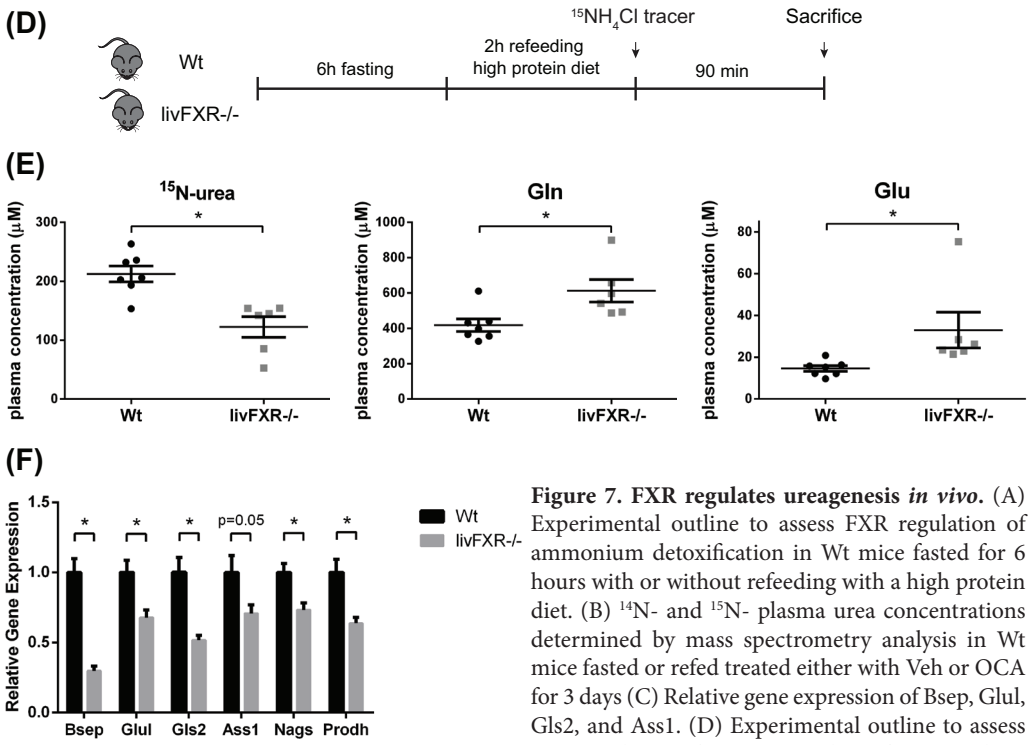

Figure 7. FXR regulates ureagenesis *in vivo*. (A) Experimental outline to assess FXR regulation of ammonium detoxification in Wt mice fasted for 6 hours with or without refeeding with a high protein diet. (B) ^{14}N- and ^{15}N- plasma urea concentrations determined by mass spectrometry analysis in Wt mice fasted or refed treated either with Veh or OCA for 3 days (C) Relative gene expression of Bsep, Glul, Gls2, and Ass1. (D) Experimental outline to assess FXR regulation of ammonium detoxification in liver specific FXR-/- and their respective Wt controls (FXR fl/fl) fasted for 6 hours and refed with a high protein diet. (E) ^{15}N plasma urea, glutamine and glutamate concentrations (F) Relative gene expression of Bsep, Glul, Gls2, Ass1, Nags and Prodh. Gene expression data were normalized to cyclophilin. Data are shown as mean ± SEM, (n=5-7/group). *p<0.05 by Mann-Whitney test.

likely to be consequences of increased BA hepatic retention in FXR-/- mice leading to a reduction in BA synthesis and BA uptake and an increase in BA efflux to compensate for the BA retention in the liver. We concluded that the proteomic dataset proved to be a valid tool to investigate additional FXR functions.

In agreement with a previous report[31], our quantitative proteome analyses support a role for FXR in ureagenesis. However, our data implicate that the role of FXR in amino acid metabolism extends to regulation of general dietary amino acid breakdown and nitrogen disposal via glutamine synthesis and ureagenesis. Indeed, protein expression of enzymes degrading histidine (Hal, Uroc1, Amdhd1, Ftcd), was induced upon OCA treatment in Wt mice, and suppressed in FXR-/- mice. The concentrations of histidine in liver extracts of FXR-/- mice were increased, concurrent with decreased expression of enzymes involved in its catabolism. OCA treatment in primary hepatocytes decreased the histidine concentration in the medium, and because FXR induced the expression of Hal and binds to an IR1 motif in the proximity of the TSS of Hal, we conclude that this is due to direct FXR-transcriptional regulation of Hal. Similarly, FXR binding to the promoter of Prodh was confirmed and proline concentration was decreased, while Prodh expression was increased upon OCA treatment in primary hepatocytes, indicat-

ing that also proline catabolism is directly regulated by FXR.
Furthermore, OCA induced the enzymes in the urea cycle Ass1, Asl and Arg1, whereas FXR ablation caused suppression of urea cycle enzymes (Nags, Cps1, Ass1, Asl, Arg1). In contrast to Renga *et al.*, we do not find evidence for a direct role of FXR in the regulation of Nags (Supplementary Figure 3), which converts glutamate to N-acetylglutamate, the latter being an essential allosteric activator of Cps1. We currently do not understand this discrepancy, but it may depend on the culture conditions of the primary hepatocytes. Lastly, FXR activation by OCA induced the expression of Glul, which converts glutamate into glutamine in pericentral hepatocytes, an alternative way to dispose of excess nitrogen.[4] Our quantitative proteomic data are in agreement with mass spectrometry identification of proteins detected by 2D-DIGE by Gardmo *et al.*, listing that FXR activation similarly leads to induced expression of Glud1, Got2, Ass1, Arg1, Cps1 and Oat.[32]

Genetic FXR ablation promotes hepatic steatosis, hyperlipidaemia, impaired glucose tolerance and hepatic BA accumulation.[14, 21, 33] Here we show that FXR-/- mice accumulate glutamine, glutamate, and aspartate in the liver (Figure 5), which represent the key amino acids for shuttling ammonium groups into the urea cycle. If liver ureagenesis would reflect plasma urea concentrations, it is expected that urea production would be decreased in FXR-/- mice. Actually, FXR-/- mice, but not liver FXR-/- mice, accumulate urea in the plasma (Figure 5G). The amount of urea in plasma is controlled also by renal excretion, which requires glomerular filtration, urea concentration in the urine by urea transporter UT-B (Slc14a1) and urea reabsorption in the blood by UT-A (Slc14a2).[26, 34, 35] Intriguingly, FXR is expressed in kidney and our analysis of microarray datasets available online[36] revealed that UT-B is significantly upregulated (3.5 fold) in kidney cells treated with GW4064, while UT-A is unchanged. From these data, it could be speculated that FXR promotes renal urea excretion. This might explain the difference in plasma urea concentrations in total and liver FXR-/- mice. Renal FXR may work in concert with hepatic FXR to ensure the clearance of excess ammonium. Inter-organ compensation complicates the detection of oscillations in total plasma urea in response to drugs, however, OCA-treatment induced a nearly significant increase in plasma ^{15}N-urea, newly formed from the gavaged $^{15}NH_4Cl$ tracer. In line with this observation, liver specific FXR deletion reduces plasma ^{15}N-urea.
We show that FXR activation promotes urea production in primary hepatocytes, especially in presence of ammonium excess (Figure 6). In this model system, we can directly measure the impact of FXR activation on hepatic ureagenesis and related enzymes. Indeed, FXR activation increased the expression of *Glul*, *Ass1*, *Asl* and *Cps1* expression. We further show that FXR binds to the IR1 motifs in proximity of the transcription start sites of *Cps1*, *Glul*, *Ass1* and *Asl,* indicating that FXR directly regulates transcription of urea cycle and glutamine synthesis genes. OCA increased while liver specific FXR deletion decreased hepatic gene expression of the Ass1, Glul, and Gls2, implicated in ammonium detoxification, also in mice refed with a high protein diet, further substantiating the relevance of this regulation *in vivo*.
mTORC1 is a protein complex that functions as a sensor for essential amino acids and controls protein synthesis by activation of the translation initiation complex.[28, 37, 38] The

activity of the mTORC1 complex is regulated by insulin, growth factors, and amino acids. We hypothesize that FXR may counterbalance mTORC1 activity by inducing amino acid catabolism if proteins are in surplus.
In conclusion, our study identifies FXR as transcriptional regulator of amino acid catabolism and detoxification of ammonium via ureagenesis and glutamine synthesis in the liver. Since urea cycle failure and hyperammonemia are common complications of acute and chronic liver diseases[39, 40], FXR activation could represent a new therapeutic strategy to promote ammonium clearance in liver disease patients.

ACKNOWLEDGEMENTS

Grant support: S.W.C.v.M. is supported by the Netherlands Organization for Scientific Research (NWO) Project VIDI (917.11.365), FP7 Marie Curie Actions IAPP (FXR-IBD, 611979), the Utrecht University Support Grant, Wilhelmina Children's Hospital Research Fund. H.R.V. is supported by Proteins At Work (NWO).

REFERENCES

1. Kohlmeier M. Nutrient Metabolism. Food Science and Technology, 2003.
2. Rui L. Energy metabolism in the liver. Compr Physiol 2014;4:177-97.
3. Adeva MM, Souto G, Blanco N, et al. Ammonium metabolism in humans. Metabolism 2012;61:1495-511.
4. Rodés J. Textbook of hepatology : from basic science to clinical practice. Malden, Mass.: Blackwell, 2007.
5. Morris SM, Jr. Regulation of enzymes of the urea cycle and arginine metabolism. Annu Rev Nutr 2002;22:87-105.
6. Zhou H, Hylemon PB. Bile acids are nutrient signaling hormones. Steroids 2014;86:62-8.
7. Lefebvre P, Cariou B, Lien F, et al. Role of bile acids and bile acid receptors in metabolic regulation. Physiol Rev 2009;89:147-91.
8. Mazuy C, Helleboid A, Staels B, et al. Nuclear bile acid signaling through the farnesoid X receptor. Cell Mol Life Sci 2015;72:1631-50.
9. Gadaleta RM, Cariello M, Sabba C, et al. Tissue-specific actions of FXR in metabolism and cancer. Biochim Biophys Acta 2015;1851:30-9.
10. Lee JM, Wagner M, Xiao R, et al. Nutrient-sensing nuclear receptors coordinate autophagy. Nature 2014;516:112-5.
11. Seok S, Fu T, Choi SE, et al. Transcriptional regulation of autophagy by an FXR-CREB axis. Nature 2014;516:108-11.
12. Huang X, Zhao W, Huang W. FXR and liver carcinogenesis. Acta Pharmacol Sin 2015;36:37-43.
13. Neuschwander-Tetri BA. Farnesoid x receptor agonists: what they are and how they might be used in treating liver disease. Curr Gastroenterol Rep 2012;14:55-62.
14. Milona A, Owen BM, van Mil S, et al. The normal mechanisms of pregnancy-induced liver growth are not maintained in mice lacking the bile acid sensor Fxr. Am J Physiol Gastrointest Liver Physiol 2010;298:G151-8.
15. Ijssennagger N, Janssen AW, Milona A, et al. Gene expression profiling in human precision cut liver slices upon treatment with the FXR agonist obeticholic acid. J Hepatol 2016.
16. Chong HK, Infante AM, Seo YK, et al. Genome-wide interrogation of hepatic FXR reveals an asymmetric IR-1 motif and synergy with LRH-1. Nucleic Acids Res 2010;38:6007-17.
17. Thomas AM, Hart SN, Kong B, et al. Genome-wide tissue-specific farnesoid X receptor binding in mouse liver and intestine. Hepatology 2010;51:1410-9.

18. Suchy FJ, Ananthanarayanan M. Bile salt excretory pump: biology and pathobiology. J Pediatr Gastroenterol Nutr 2006;43 Suppl 1:S10-6.
19. Kong B, Wang L, Chiang JY, et al. Mechanism of tissue-specific farnesoid X receptor in suppressing the expression of genes in bile-acid synthesis in mice. Hepatology 2012;56:1034-43.
20. Kerr TA, Matsumoto Y, Matsumoto H, et al. Cysteine sulfinic acid decarboxylase regulation: A role for farnesoid X receptor and small heterodimer partner in murine hepatic taurine metabolism. Hepatol Res 2014;44:E218-28.
21. Sinal CJ, Tohkin M, Miyata M, et al. Targeted disruption of the nuclear receptor FXR/BAR impairs bile acid and lipid homeostasis. Cell 2000;102:731-44.
22. Geier A, Wagner M, Dietrich CG, et al. Principles of hepatic organic anion transporter regulation during cholestasis, inflammation and liver regeneration. Biochim Biophys Acta 2007;1773:283-308.
23. Modica S, Gadaleta RM, Moschetta A. Deciphering the nuclear bile acid receptor FXR paradigm. Nucl Recept Signal 2010;8:e005.
24. Jin J, Sun X, Zhao Z, et al. Activation of the farnesoid X receptor attenuates triptolide-induced liver toxicity. Phytomedicine 2015;22:894-901.
25. Livero FA, Stolf AM, Dreifuss AA, et al. The FXR agonist 6ECDCA reduces hepatic steatosis and oxidative stress induced by ethanol and low-protein diet in mice. Chem Biol Interact 2014;217:19-27.
26. Weiner ID, Mitch WE, Sands JM. Urea and Ammonia Metabolism and the Control of Renal Nitrogen Excretion. Clin J Am Soc Nephrol 2015;10:1444-58.
27. Yudkoff M, Daikhin Y, Ye X, et al. In vivo measurement of ureagenesis with stable isotopes. J Inherit Metab Dis 1998;21 Suppl 1:21-9.
28. Bender DA. The metabolism of "surplus" amino acids. Br J Nutr 2012;108 Suppl 2:S113-21.
29. Desvergne B, Michalik L, Wahli W. Transcriptional regulation of metabolism. Physiol Rev 2006;86:465-514.
30. Teodoro JS, Rolo AP, Palmeira CM. Hepatic FXR: key regulator of whole-body energy metabolism. Trends Endocrinol Metab 2011;22:458-66.
31. Renga B, Mencarelli A, Cipriani S, et al. The nuclear receptor FXR regulates hepatic transport and metabolism of glutamine and glutamate. Biochim Biophys Acta 2011;1812:1522-31.
32. Gardmo C, Tamburro A, Modica S, et al. Proteomics for the discovery of nuclear bile acid receptor FXR targets. Biochim Biophys Acta 2011;1812:836-41.
33. Ma K, Saha PK, Chan L, et al. Farnesoid X receptor is essential for normal glucose homeostasis. J Clin Invest 2006;116:1102-9.
34. Yang B. Urea transporters. New York: Springer, 2014.
35. Yang B, Bankir L, Gillespie A, et al. Urea-selective concentrating defect in transgenic mice lacking urea transporter UT-B. J Biol Chem 2002;277:10633-7.
36. Gui T, Gai Z. Genome-wide profiling to analyze the effects of FXR activation on mouse renal proximal tubular cells. Genom Data 2015;6:31-2.
37. Chandel NS. Navigating Metabolism. Cold Spring Harbor, New York: Cold Spring Harbor Laboratory Press, 2015:128.
38. Zoncu R, Efeyan A, Sabatini DM. mTOR: from growth signal integration to cancer, diabetes and ageing. Nat Rev Mol Cell Biol 2011;12:21-35.
39. Blei AT, Cordoba J, Practice Parameters Committee of the American College of G. Hepatic Encephalopathy. Am J Gastroenterol 2001;96:1968-76.
40. Nicaise C, Prozzi D, Viaene E, et al. Control of acute, chronic, and constitutive hyperammonemia by wild-type and genetically engineered Lactobacillus plantarum in rodents. Hepatology 2008;48:1184-92.

SUPPLEMEMTARY FIGURES

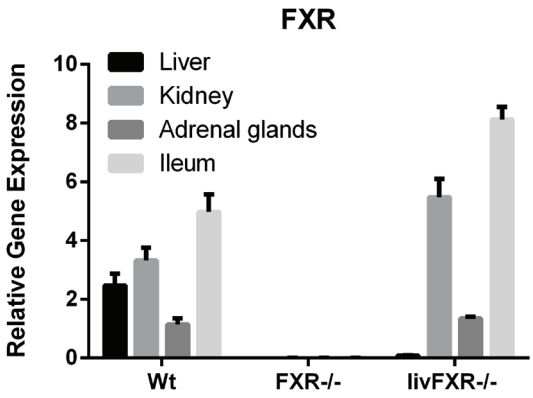

Supplementary Figure 1. Validation of FXR depletion in FXR-/- and liver FXR-/- mice. Determination of FXR expression in liver and kidney tissue of Wt, FXR-/- and liver specific FXR-/- mice by RT-qPCR. Expression is relative to cyclophilin. Data are represented as mean ± SEM.

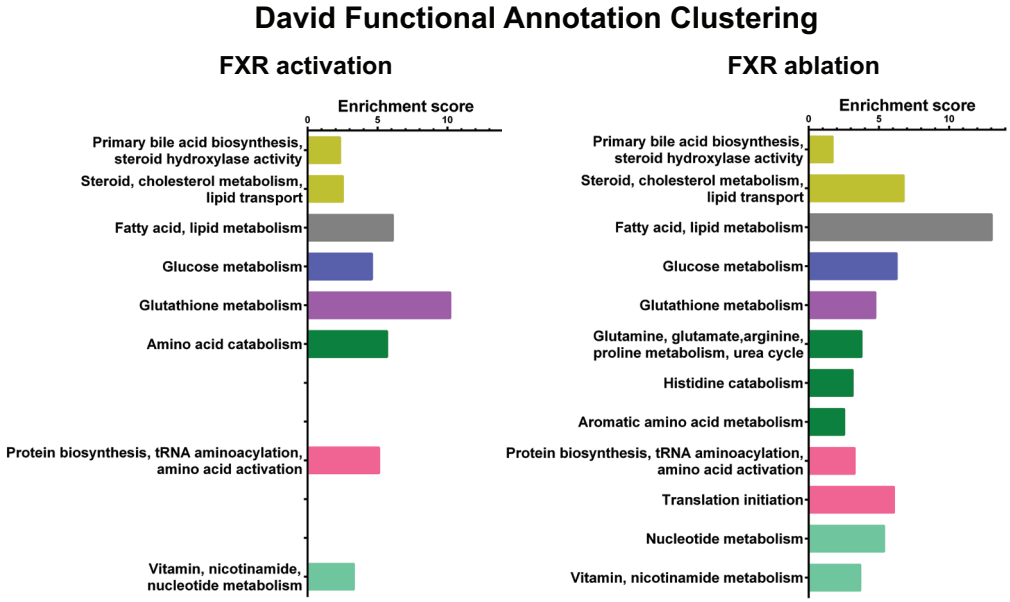

Supplementary Figure 2. Liver proteomic analysis reveals regulation of nutrient metabolism by FXR activation/ablation. David Gene Ontology cluster analysis of metabolic processes enriched upon FXR activation/ablation. Differential protein changes were included in the analysis when ≥1.3 folds.

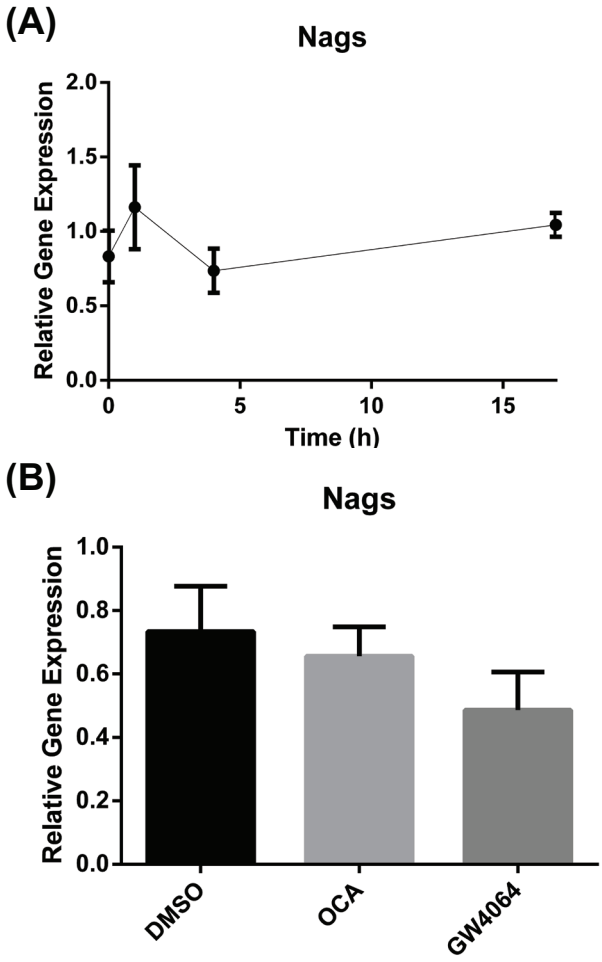

Supplementary Figure 3. Nags expression does not change upon FXR activation. (A-B) Relative gene expression of Nags was investigated by qRT-PCR in primary hepatocytes incubated with DMSO or 1μM OCA for 0, 1, 4 or 17 hours (A) and with DMSO or OCA or GW4064 for 6 hours and in the last hour before harvesting with 2 mM NH4Cl, 0.4 mM glutamine, 0.6 mM ornithine, 10mM Hepes in HBSS (mean ± SD, n=3, no significant changes).

SUPPLEMENTARY TABLES

Supplementary table 1. Regulatory sites determined by ChIP-qPCR for FXR in liver extracts.

Gene	Nr peak analyzed	Genomic location of the peak (Chr:Start-End)	Peak distance from TSS (bp)	IR-1 motif in the peak (AGGTCANTGACCTN)	ChIP-qPCR primers (5'->3')
Cps1	1	chr1:67124225-67124829	-45073	AGAGCCAATGACCC	FW gttgtttcagattagcaatgttgac RV cacatttgatttgcacagtgg
	2	chr1:67125141-67125712	-44174	AAGGCCATTGACTC	FW atgttcaactcaaagatggctct RV aggcctttggaacaaataagg
	3	chr1:67190203-67191017	+21010	GGGTCAATGGCTGC	FW ggctggctaccaagagtctg RV cctatctgacttctcacctttcc
Glul	1	chr1:155746632-155747475	-5	CGGCCAATGGCCTC	FW cacagttcctcggccaat RV ggtacttttattgacagcttgtgc
Ass1	1	chr2:31315817-31316207	-9777	AGGGCAGAGACCGC	FW gggctctaccgcttgactg RV gcaggatgtagacgctctgg
Asl	1	chr5:130497223-130499011	-2084	GGGTCCTTGACCTC	FW tgagttacgacggcctgat RV aaagtccagcccttgttcct
Hal	1	chr10:92950852-92952224	-99	GGGTCAGAGAACTA	FW agtgggctcagctacccata RV gtgttcctttggcctttctg
Prodh	1	chr16:18083266-18084303	+5499	AGGCCACTGGCCCT	FW ggctcctccccaggtaacta RV agtggcctcacatgactgc

Supplementary table 2. qRT-PCR primers.

Rat

Gene	Sequence (5'->3')
36B4	FW cgggaaggctgtggtgctgatg RV tcggtgaggtcctccttggtgaac
Shp	FW ggagtctttctggagccttg RV cacatctgggttgaagagga
Cyp7a1	FW atctcaagcaaacaccattcc RV ttgatgatgctgtctagtacc
Glul	FW tcaagtataaccggaagcccg RV gaaagggtggccgtctgtt
Cps1	FW atgctctgggtgggttagg RV aggatctggttggtcatagca
Ass1	FW ggagaaccgcttcattgg RV tgagcgtggtaaaggatggt
Asl	FW aagccatccgaagctgtttg RV cttgtccccgcctcctgt
Hal	FW tgaaggcgatgtaatgtctcc RV cccatccaaggcaatgtact
Prodh	FW gagcgcaaagaaatggagtc RV gggtggacctgatactgcttc
Nags	FW cagattcggctcatcgtgga RV tgccacagcccttgttactg

Mouse

Gene	Sequence (5'->3')
Cyclophilin	FW ggagatggcacaggaggaa RV gcccgtagtgcttcagctt
Bsep	FW aagctacatctgccttagacacagaa RV caatacaggtccgaccctctct
Glul	FW ccgcctcgctctcctgacc RV cgggtcttgcagcgcagtc
Gls2	FW ccgtggtgaacctgctattt RV tgcgggaatcatagtccttc
Ass1	FW acacctcctgcatcctcgt RV gctcacatcctcaatgaacacct
Nags	FW cttcggagagacctgcaaac RV ccgaaccagaagaagatcca
Prodh	FW gcaccacgagcagttgttc RV ctttgttgtgccggatcagag
FXR	FW acagctaatgaggacgacag RV gatttcctgaggcattctctg

Supplementary table 3. FXR$^{-/-}$ /Wt fold change in liver expression of BA metabolism-related proteins.

Protein	FOLD change Wt OCA/Wt Veh	FOLD change FXR-/- Veh/Wt Veh
Bile acid synthesis		
Cyp8b1	-7.91	2.42
Cyp7a1	ND	5.04
Cyp7b1	-2.96	-14.88
Hsd3b7	-1.43	-2.00
Cyp27a1	-1.11	-2.35
Ces1f	-1.98	-1.12
Cyp39a1	-1.13	-2.46
Bile acid conjugation/taurine synthesis		
Baat	-1.21	1.87
Csad	-1.55	9.29
Bile acid/ phosphatidylcholine transport		
Abcb11/Bsep	2.15	-5.31
Abcb4/Mdr3	1.68	1.39
Abcc2/Mrp2	1.50	-1.19
Pcyt1a	2.36	-1.62
Slc10a1/Ntcp	1.04	-4.12
Slco1a1/Oatp1	-1.49	-3.13

Supplementary Table 4. FXR$^{-/-}$ /Wt fold change in liver expression of amino acid metabolism-related proteins.

Protein	FOLD change Wt OCA/Wt Veh	FOLD change FXR-/- Veh/Wt Veh
Histidine degradation		
Hal	2.33	-2.16
Uroc1	1.83	-1.58
Amdhd1	1.86	-2.93
Ftcd	2.26	-1.75
Proline degradation		
Prodh	1.49	-2.30
Tryptophan degradation		
Tdo2	2.56	-2.25
Kynu	1.47	-1.36
Methionine degradation		
Mat1a	1.56	1.07
Ahcy	1.50	-2.02
Cth	2.16	-1.04
Phenylalanine degradation		
Pah	1.47	-1.23
Lysine degradation		
Agphd1	1.48	-1.78
Urea cycle		
Ass1	2.31	-1.74
Asl	1.36	-1.53
Arg1	1.36	-1.53
Cps1	-1.24	-2.05
Nags	-1.39	-3.67
Urea cycle-related		
Oat	2.43	3.01
Got1	1.30	-2.14
Gls2	1.12	-5.82
Glud1	-1.43	-1.50
Glutamine synthesis		
Glul	1.52	-2.22

Supplementary Table 5. FXR-/- /Wt fold change in concentration of amino acids in liver extracts.

Amino Acid	Fold change FXR-/- Veh /Wt Veh	p value	Fold change FXR-/- OCA /Wt Veh	p value
Glu	3.30	0.005 **	3.78	0.000 **
Pip	1.78	0.085	2.01	0.045
Gln	1.62	0.003 **	1.68	0.002 **
Asp	1.58	0.051	1.68	0.025 *
His	1.39	0.001 **	1.29	0.005 **
Pro	1.05	0.694	-1.03	0.770
Arg	1.05	0.292	1.05	0.453
Ser	1.00	0.993	-1.18	0.370
Trp	-1.01	0.933	-1.15	0.211
Thr	-1.07	0.615	-1.26	0.069
Ile	-1.13	0.466	-1.13	0.398
Val	-1.14	0.455	-1.28	0.135
Phe	-1.14	0.286	-1.34	0.011 *
Lys	-1.14	0.255	-1.22	0.047
Ala	-1.20	0.109	-1.27	0.023 *
Orn	-1.20	0.243	-1.54	0.007 **
Leu	-1.21	0.270	-1.46	0.018 *
Tyr	-1.21	0.162	-1.41	0.015 *
Gly	-1.23	0.154	-1.54	0.000 **
Met	-1.33	0.115	-1.70	0.001 **
Asn	-1.38	0.112	-1.41	0.074
OH-Pro	-1.63	0.006 **	-1.59	0.006 **
Cit	-2.76	0.079	-8.93	0.005 **

Supplementary Table 6. OCA/DMSO fold change concentration of amino acids in medium of primary hepatocytes.

Amino acid	FC	p-value
Glutamic acid	-1.65	0.003**
Alanine	-1.63	0.001**
Isoleucine	-1.62	0.010*
Leucine	-1.60	0.006**
Phenylalanine	-1.58	0.012*
Valine	-1.58	0.002**
Tyrosine	-1.56	0.055
Arginine	-1.55	0.100
Proline	-1.49	0.009*
Histidine	-1.43	0.018*
Methionine	-1.43	0.019*
Threonine	-1.40	0.043*
Lysine	-1.38	0.038*
Serine	-1.29	0.016*
Aspartic acid	-1.26	0.243
Tryptophan	-1.19	0.038*
Glutamine	-1.16	0.027*
Ornithine	1.00	0.809

Determination of amino acid concentrations in medium of primary hepatocytes treated for 16 hours with OCA or DMSO and in the last hour before harvesting with 2 mM NH_4Cl, 0.4 mM glutamine and 0.6 mM ornithine. OCA/DMSO fold change in concentrations of amino acids and related significance are shown..

SUPPLEMENTARY METHODS

Reagents

DL-Glutamic acid (2,4,4-D3, 98%), and Urea (15N2, 98%) were purchased from Cambridge Isotope Laboratories (Massachusetts, U.S.). Urea was purchased from Sigma-Aldrich (Zwijndrecht, the Netherlands). Glutamic acid and glutamine were purchased from VWR (Amsterdam, the Netherlands). UPLC-grade acetonitrile (ACN) and methanol were purchased from Biosolve (Valkenswaard, the Netherlands).

Mass spectrometry sample preparation for proteomics

Liver protein extracts were generated by homogenizing 50 mg liver tissue in PBS and subsequent lysis in Lysis Buffer (1% NP40, 150 mM NaCl, 1 mM DTT, 50 mM Tris pH 8.0, Roche Proteinase inhibitors). Next, 100 µg protein extract from Wt or FXR-/- mice ('light') were mixed 1:1 with a spike-in protein extract generated from $^{13}C_6$-lysine metabolically labelled mouse liver ('heavy') (Silantes, Munich, Germany), using the same homogenization protocol. Proteins were denatured in urea, alkylated with iodoacetamide (Sigma, S Louis, MO, U.S.) and digested with 1 µg of trypsin (Promega, Fitchburg, WI, U.S.) using a Filtered Aided Sample Purification Protocol (FASP,[1]). After trypsinization, peptides were fractionated based on their pH using Strong Anionic Exchange Chromatography and finally desalted and acidified on a C-18 cartridge (3M, St. Paul, MN, U.S.). C18-stagetips were activated with methanol, washed with buffer containing 0.5% formic acid in 80% ACN (buffer B) and then with 0.5% formic acid (buffer A). After loading of the digested sample, stagetips were washed with buffer A and peptides were eluted with buffer B, dried in a SpeedVac, and dissolved in buffer A.

SILAC-based proteomics and data analysis

Peptides were separated on a 30 cm column (75 µm ID fused silica capillary with emitter tip, New Objective, Woburn, MA, U.S.) packed with 3 µm aquapur gold C-18 material (Dr Maisch, Ammerbuch-Entringen, Germany) using a 4-hour gradient (buffer A to buffer B), and delivered by an easy-nHPLC (Thermo Scientific, Waltham, MA, U.S.). Peptides were electro-sprayed directly into a LTQ-Verlos-Orbitrap (Thermo Scientific) and analysed in data-dependent mode with the resolution of the full scan set at 60000, after which the top 10 peaks were selected for CID fragmentation in the Iontrap with a target setting of 5000 ions.

Raw files were analyzed with Maxquant software version 1.5.1.0.[2] For identification, the mouse Uniprot 2012 database was searched with peptide and protein false discovery rates set to 1%. The SILAC quantification algorithm was used in combination with the 'match between runs' tool (option set at two minutes), the IBAQ and the LFQ algorithms.[3, 4] Proteins identified with two or more unique peptides were filtered for reverse hits, decoy hits and standard contaminants using Perseus software 1.3.0.4[5]. Normalized ratios were used to quantify protein expression and further processed for comparative analysis of differential expression among the experimental conditions. Heatmap visualization of expression profile of all quantified proteins was generated using R Studio (0.99.879). The mass spectrometry proteomics data have been deposited to the Proteo-

meXchange Consortium via the PRIDE[6] partner repository with the dataset identifier PXD005427. Analysed data are presented in the Supplementary data file (that will be available online, with publication). Pathway and ontology analyses were performed by Ingenuity Pathway analysis (Qiagen, Venlo, The Netherlands) and David Gene Ontology tools.

Primary hepatocyte culture

Hepatocytes were isolated from male Wistar rats (160–180 g) based on a two-step collagenase perfusion method.[7] Hepatocytes were counted using Countess™ (Invitrogen, Waltham, MA, U.S.) and cell viability was determined using Trypan blue. Freshly-isolated hepatocytes with a viability of at least 85% were plated on collagen-coated plates. Sandwich cultures of primary hepatocytes were prepared by covering attached hepatocytes with collagen.[8] After 48h, hepatocytes were incubated with 1 μM OCA, 1μM GW4064 or DMSO. To evaluate gene expression changes in presence of ammonium excess and to determine urea production, we incubated hepatocytes with HBSS containing 10 mM HEPES, 2 mM NH_4Cl, 0.4 mM L-glutamine, and 0.6 mM ornithine for 1 h at 37 °C in a humidified atmosphere with 5% CO_2. Urea concentration in the medium was measured using QuantiChrom ™ Urea Assay kit (Bioassay Systems, Hayward, CA, U.S.).

Analysis of amino acids by LC-tandem mass spectrometry

Frozen liver tissue was homogenized in PBS using a Tissue Lyzer II (Qiagen). Amino acid concentrations in liver extracts were determined by UPLC-MS/MS as described previously. [9] Apart from adapting the range of the calibrators and quality control (QC) samples, no further adaptations were needed for sample preparation or analysis of the amino acids. Data were normalized to protein concentration. Similarly, amino acid concentrations were determined in medium harvested from primary hepatocytes.

Analysis of labeled urea, glutamine and glutamate by LC-high resolution mass spectrometry

A volume of 40 μL plasma was mixed with 20 μL of a internal standard (IS) solution in methanol consisting of labeled amino acids and urea (see table 1 for the concentrations). After adding 500 μl methanol and vortexing for 30 seconds, the sample was centrifuged 13000 rpm for 5 minutes. The supernatant was pipetted in an eppendorf tube and evaporated under a gentle flow of nitrogen at 40 °C. The extract was dissolved in 200 μl of a mixture of eluent A/B (10/90% $^{v}/_{v}$) and 10 μl was analyzed on the UHPLC system. For calibration, to 40 μl pool plasma a volume of 20 μl of standards diluted in methanol was added (see for the concentration range table 1), and the same procedure as above was followed.

Table 1.

Internal standard	IS Concentration (μM)	Standard	Concentration range (μM)
$^{2}H_3$-Glutamate	500	Glutamate	0.5 - 250
$^{15}N_2$-Urea	2257	Urea	45 - 24000

Some of the amino acids were calculated on different labeled internal standards, see table. The ^{15}N-isotopes were calculated on the ^{14}N-isotope calibration curves.

LC–HRMS conditions

For the chromatographic separation a ZIC-pHILIC column, 150 × 4.6 mm, 5 µm and guard column 20 x 2.1 mm; obtained from HiChrom (Reading UK) was used at a working temperature of 40 °C. A Thermo Scientific Ultimate 3000 UHPLC system controlled by Dionex chromatography MS Link 2.14 software (Thermo Fisher Scientific, Waltham, MA, USA) combined with a Q-Exactive HF mass spectrometer from Thermo Fisher Scientific (Bremen, Germany) was employed as the LC–HRMS platform in this study. Samples were kept at 15°C during the analyses.

The mobile phase used was 20 mM ammonium carbonate buffer (pH 9.2) as eluent A and pure acetonitril as eluent B. The elution gradient was programed at a flow of 0.3 ml/min as decreasing the percentage of B from 90% to 20% in 30 minutes followed by washing the column at 5% of B for 5 minutes and finally re-equilibrating the column at 90% of B for 10 minutes. The ESI interface was operated in a positive polarity mode at a spray voltage of 4.0 kV. The temperature of the ion transfer capillary was 320°C and sheath and auxiliary gas was 40 and 8 arbitrary units respectively. The full scan range was 55 to 400 m/z with settings of AGC target at $1e^6$ and resolution of 120,000 respectively. The S-lens RF level was set at 50. The data were recorded using Xcalibur 4.0 software (Thermo Fisher Scientific). The quantification was done in Tracefinder 4.0 (Thermo Fisher Scientific).

REFERENCES

1. Wisniewski JR, Zougman A, Mann M. Combination of FASP and StageTip-based fractionation allows in-depth analysis of the hippocampal membrane proteome. J Proteome Res 2009;8:5674-8.
2. Cox J, Mann M. MaxQuant enables high peptide identification rates, individualized p.p.b.-range mass accuracies and proteome-wide protein quantification. Nat Biotechnol 2008;26:1367-72.
3. Luber CA, Cox J, Lauterbach H, et al. Quantitative proteomics reveals subset-specific viral recognition in dendritic cells. Immunity 2010;32:279-89.
4. Schwanhausser B, Busse D, Li N, et al. Global quantification of mammalian gene expression control. Nature 2011;473:337-42.
5. Cox J, Mann M. 1D and 2D annotation enrichment: a statistical method integrating quantitative proteomics with complementary high-throughput data. BMC Bioinformatics 2012;13 Suppl 16:S12.
6. Vizcaino JA, Csordas A, del-Toro N, et al. 2016 update of the PRIDE database and its related tools. Nucleic Acids Res 2016;44:D447-56.
7. Seglen PO. Preparation of isolated rat liver cells. Methods Cell Biol 1976;13:29-83.
8. Chatterjee S, Bijsmans IT, van Mil SW, et al. Toxicity and intracellular accumulation of bile acids in sandwich-cultured rat hepatocytes: role of glycine conjugates. Toxicol In Vitro 2014;28:218-30.
9. Prinsen HC, Schiebergen-Bronkhorst BG, Roeleveld MW, et al. Rapid quantification of underivatized amino acids in plasma by hydrophilic interaction liquid chromatography (HILIC) coupled with tandem mass-spectrometry. J Inherit Metab Dis 2016;39:651-60.

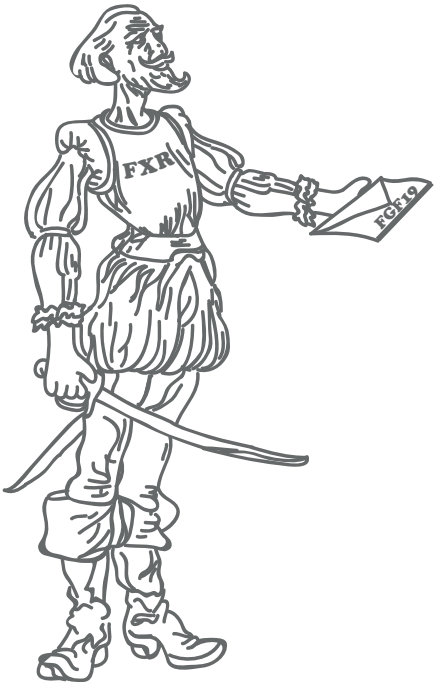
FXR
FGF19

CHAPTER 4

Quantitative liver proteomics identifies FGF19 targets that couple metabolism and proliferation

Vittoria Massafra*, Alexandra Milona*, Harmjan R. Vos,

Boudewijn M.T. Burgering, and Saskia W.C. van Mil

* These authors contributed equally to this work.

Submitted

ABSTRACT

Fibroblast growth factor 19 (FGF19) is a gut-derived peptide hormone that is produced following activation of Farnesoid X Receptor (FXR). FGF19 is secreted and signals to the liver, where it contributes to the homeostasis of bile acid (BA), lipid and carbohydrate metabolism. FGF19 is a promising therapeutic target in metabolic syndrome and cholestatic diseases, but enthusiasm for its use has been tempered by FGF19-mediated induction of proliferation and hepatocellular carcinoma. To inform future rational design of FGF19-variants, we have conducted temporal quantitative proteomic and gene expression analyses to identify FGF19-targets related to metabolism and proliferation. Mice were fasted for 16 hours, and injected with human FGF19 (1 mg/kg body weight) or vehicle. Liver protein extracts (containing 'light' lysine) were mixed 1:1 with a spike-in protein extract from $^{13}C_6$-lysine metabolically labelled mouse liver (containing 'heavy' lysine) and analysed by LC-MS/MS. Our analyses provide a resource of FGF19 target proteins in the liver. 189 proteins were upregulated (≥ 1.5 folds) and 73 proteins were downregulated (≤ -1.5 folds) by FGF19. FGF19 treatment decreased the expression of proteins involved in fatty acid (FA) synthesis, i.e. Fabp5, Scd1, and Acsl3 and increased the expression of Acox1, involved in FA oxidation. As expected, FGF19 increased the expression of proteins known to drive proliferation (i.e. Tgfbi, Vcam1, Anxa2 and Hdlbp). Importantly, many of the FGF19 targets (i.e. Pdk4, Apoa4, Fas and Stat3) have a dual function in both metabolism and cell proliferation. Therefore, our findings challenge the development of FGF19-variants that uncouple full metabolic benefit from mitogenic potential.

INTRODUCTION

Fibroblast growth factors (FGFs) are secreted signalling proteins with wide ranging functions in metabolic regulation, cell growth and differentiation, angiogenesis, embryonic development, as well as wound healing and repair [1]. Endocrine FGFs, i.e. FGF19, FGF21 and FGF23 constitute a subfamily of FGFs secreted in the circulation with roles in bile acid (BA), glucose and lipid metabolism (FGF19), metabolic adaptation during fasting (FGF21), and modulation of vitamin D and phosphate homeostasis (FGF23) [2]. FGF19 (FGF15 in rodents) is a postprandial enterokine induced by the nuclear hormone receptor Farnesoid X Receptor (FXR; NR1H4) upon activation by BAs [3]. FGF19 signals from intestine to liver via binding to FGFR4/β-klotho receptor complex to repress the gene encoding cholesterol 7α-hydroxylase (CYP7A1), which catalyses the first and rate-limiting step in the classical BA synthetic pathway [4]. In addition, FGF19 prevents lipid and glucose accumulation in the liver by inducing fatty acid oxidation and decreasing expression of acetyl coenzyme A carboxylase 2 (Acc2) involved in FA synthesis [5, 6]. Furthermore, FGF19 inhibits lipogenesis by counteracting the insulin-induced increase in sterol regulatory element-binding protein-1c (SREBP-1c) expression, a key transcriptional activator of genes involved in lipogenesis [7, 8]. FGF19 regulation of glucose metabolism involves stimulation of glycogen synthesis [9] and inhibition of gluconeogenesis via inactivation of cAMP regulatory element-binding protein (CREB) and subsequent decrease in proliferator-activated receptor g coactivator-1α (PGC-1α) [10].

The beneficial impact of FGF19 on lipid, glucose and BA homeostasis raised the possibility to pursue FGF19 as a therapeutic target for diabetes, metabolic syndrome and cholestatic liver diseases. However, the development of FGF19-based therapeutics is hampered by the mitogenic potential of FGF19 and its subsequent tumorigenic implications. FGF19-transgenic mice display increased hepatocyte proliferation at 2-4 months of age and develop hepatocellular carcinoma (HCC) at 10-12 months [11]. In concurrence with this, tumour progression in HCC patients is associated with increased FGF19 expression [12], and FGF19 gene has been shown to be a driver gene for HCC [13]. In an effort to eliminate the tumorigenic activity of FGF19 without compromising its beneficial metabolic effects, variants of FGF19 with diminished proliferative potential have been engineered, for example by eliminating the binding site to FGFR4 [14-16]. Although these results are very promising, caution should be taken since changes in metabolism have been recognized to play a driver role in oncogenesis with the ability to control both genetic and epigenetic events in cells (reviewed in [17]). It is therefore possible that the effects of FGF19 on proliferation and tumorigenesis may also be induced by its effects on metabolism.

Therefore, a comprehensive understanding of the FGF19 signalling cascade, together with mechanistic insights into the effects of FGF19 on metabolism and proliferation, are essential for the design of an FGF19-based therapeutic. Here we investigated the proteome-wide changes induced in mice upon administration of human recombinant FGF19. By using an untargeted proteomics approach, we expand the knowledge on FGF19-mediated protein expression changes and reveal that FGF19 indeed acts as a regulator of BA, lipid, glucose, amino acid metabolism and as a signalling molecule inducing expression of proliferative and tumorigenic proteins. We also show by pathway

analyses that many of the proteins regulated by FGF19 function both in metabolism and proliferation, emphasizing that FGF19-mediated effects on proliferation may not so easily be eliminated without also affecting the beneficial effects on metabolism.

MATERIALS AND METHODS

Animal experiments

Wt C5Bl/6 male mice (8 weeks) were fed standard chow until the age of 8 weeks and fasted for 16 hours prior to treatment to ensure low endogenous FGF15 signalling. Mice received a single intraperitoneal dose of human recombinant FGF19 (1 mg/kg body weight, R&D Systems, Minneapolis, U.S.) in 0.1% saline solution or vehicle. Mice were terminated after 0 min, 15 min, 1 h, 2 h, 4 hr or 12 hr and liver tissue was snap frozen for RNA and protein analyses. The study protocol was approved by the University Medical Center Utrecht Ethical Committee for Animal Experimentation.

Mass spectrometry sample preparation

Liver protein extracts were generated by homogenizing 50 mg liver tissue in PBS and subsequent lysis in lysis buffer (1% NP40, 150 mM NaCl, 1 mM DTT, 50 mM Tris pH 8.0, Roche Proteinase inhibitors). Next, 100 µg protein extract from Wt or FXR-/- mice ('light') were mixed 1:1 with a spike-in protein extract generated from $^{13}C_6$-lysine metabolically labelled mouse liver ('heavy') (Silantes, Munich, Germany). Proteins were denatured in urea, alkylated with iodoacetamide (Sigma, S Louis, MO, U.S.) and digested with 1 µg of trypsin (Promega, Fitchburg, WI, U.S.) using a Filtered Aided Sample Purification Protocol (FASP [18]). After trypsinization, peptides were fractionated based on their pH using Strong Anionic Exchange Chromatography and finally desalted and acidified on a C-18 cartridge (3M, St. Paul, MN, U.S.). C18-stagetips were activated with methanol, washed with buffer containing 0.5% formic acid in 80% ACN (buffer B) and then with 0.5% formic acid (buffer A). After loading of the digested sample, stage-tips were washed with buffer A and peptides were eluted with buffer B, dried in a SpeedVac, and dissolved in buffer A.

Mass spectrometry and data analysis

Peptides were separated in a 30 cm column (75 µm ID fused silica capillary with emitter tip (New Objective)) packed with 3 µm aquapur gold C-18 material (dr Maisch, Ammerbuch-Entringen, Germany) using a 140 minute gradient (7% to 80% ACN, 0.1% FA), and delivered by an easy-nLC 1000 (Thermo, Waltham, MA, U.S). Peptides were electro-sprayed directly into an Orbitrap Fusion Tribrid Mass Spectrometer (Thermo Scientific) and analysed in Top Speed data-dependent mode with the resolution of the full scan set at 240000 and an intensity threshold of 5000 ions. Most intense ions were isolated by the quadrupole and fragmented with a HCD collision energy of 30%. The maximum injection time of the iontrap was set to 35 milliseconds.

Raw files were analysed with the Maxquant software version 1.5.1.0. [19] For identification, the mouse Uniprot 2012 was searched with both the peptide as well as the protein false discovery rate set to 1%. The SILAC quantification algorithm was used in combination with the 'match between runs' tool (option set at two minutes), the IBAQ and the LFQ

algorithm [20]. Proteins identified were filtered for reverse hits, decoy hits and standard contaminants by using the Perseus software 1.5.1.6 [21]. The liver proteomic profile of three mice per group was determined. Light/heavy normalized ratios were used to quantify protein expression and were further processed for comparative analysis of differential expression among the experimental groups. Proteins were filtered to have more than 1 unique or razor peptide and at least two valid values per group. Pathway analysis was performed using Ingenuity Pathway Analysis Program (IPA; Ingenuity Systems, Redwood City, CA, U.S.).

Gene expression analyses

RNA was isolated from liver using TRIzol reagent (Invitrogen, Waltham, MA, U.S.). cDNA was generated from 1 μg of total RNA using SuperScript II Reverse Transcriptase (Invitrogen). qRT-PCR analysis was performed using SYBR green PCR master mix (Roche, Basel, Switzerland) and analysed on a MyIQ real time PCR cycler (BioRad, Hercules, California, U.S.). Data are presented as relative expression normalized to Gapdh gene expression. Primer sequences are listed in S1 Table.

Statistics

For the proteomic analysis a T-test was applied to determine significant differential expressed proteins between the groups (p-value <0.05). Statistical significance of pathway enrichment and upstream regulator analyses were assessed by using IPA software. Only pathways significantly enriched (setting p <0.01) are shown. For the upstream regulator analysis, p-value measures whether there is a statistically significant overlap between the dataset genes and the genes that are regulated by a transcription factor/hormone/compound, based on the published data included in Ingenuity database. It is calculated using Fisher's Exact Test, and significance was attributed to p-values < 0.01.

RESULTS

FGF19-mediated regulation of liver protein expression resolved by quantitative proteomics

In order to characterize the metabolic and proliferative effects elicited by FGF19, we quantified protein expression changes in liver extracts from wild type mice treated with FGF19 or vehicle for 12h. Prior to FGF19 injection, mice were fasted for 16 hours, in order to reduce enterohepatic BA circulation and subsequent endogenous FGF15 signalling. Liver protein extracts (containing 'light' lysine) were mixed 1:1 with a spike-in protein extract from $^{13}C_6$-lysine metabolically labelled mouse liver (containing 'heavy' lysine) and analysed by LC-MS/MS (Fig 1A). Spike-in efficiency, indicating the quality of the heavy signal as internal standard, was assessed as frequency of proteins ranked based on their log2 heavy/light normalized ratio (Fig 1B). More than 80% of proteins from the mouse liver exposed to vehicle had a heavy/light ratio close to 1, indicating a substantial equality in protein composition of the liver from our mice and the 'heavy' liver tissue commercially available, thereby supporting the suitability of the heavy labelled liver as internal standard for the light samples. In a scatterplot comparing FGF19- to vehicle-

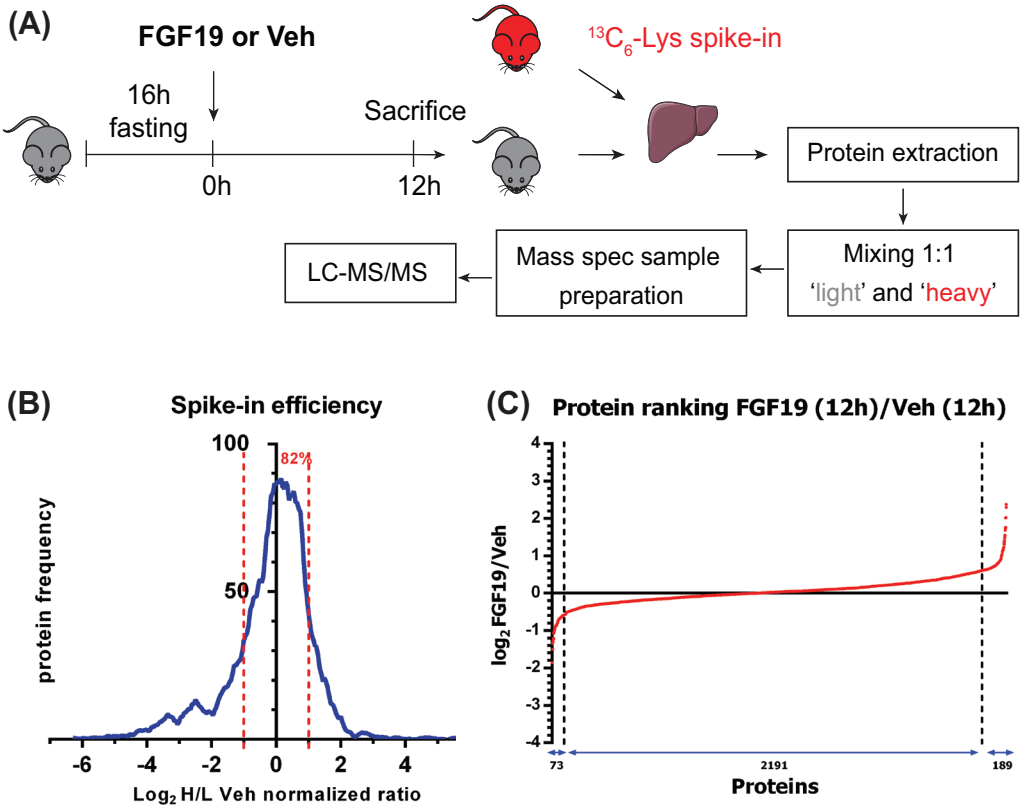

Figure 1. FGF19-mediated regulation of liver protein expression resolved by quantitative proteomics. (A) Schematic representation of the experimental outline to determine the hepatic proteomic profile of mice treated with FGF19 or Veh for 12 h. (n=3) (B) Frequency plot of proteins identified in vehicle-treated Wt mice based on their total log2 heavy/light normalized ratio. The plot is representative of mean Wt untreated condition to show the basal efficiency of the heavy spike-in added to the light samples. Percentage of proteins with a log2 heavy/light normalized ratio included in interval (-1,+1) is shown.
(C) Protein ranking based on changes of the log2 light/heavy normalized ratio induced by FGF19 when comparing FGF19 treatment for 12h to vehicle control. Number of proteins, of which expression was decreased (≤ -1.5 fold), unchanged or increased (≥1.5 fold) are indicated. (C) Volcano plot depicting the protein changes induced by FGF19 after 12h treatment.

Table 1. Proteins significantly upregulated upon FGF19 treatment
(fold change ≥1.5; n=3; p<0.05)

Gene name	Protein ID	Protein name	Fold change
Kiaa0020	Q8BKS9	Pumilio domain-containing protein KIAA0020	3.39
Hao2	Q9NYQ2	Hydroxyacid oxidase 2	2.65
Col6a3	E9PWQ3	Protein Col6a3	2.23
Nop14	Q8R3N1	Nucleolar protein 14	2.23
Tgfbi	Q3UXJ2	Transforming growth factor-beta-induced protein ig-h3	2.09
Sun2	Q8BJS4	SUN domain-containing protein 2	1.78
Abcb1	P21447	Multidrug resistance protein 1	1.77
Col14a1	B7ZNH7	Collagen alpha-1(XIV) chain	1.76
Vcam1	Q3UPN1	Vascular cell adhesion protein 1	1.76
Add3	Q9QYB5	Gamma-adducin	1.75
Nop56	Q9D6Z1	Nucleolar protein 56	1.74
Wdr75	Q3U821	WD repeat-containing protein 75	1.72
Hnrpdl	Q9Z130	Heterogeneous nuclear ribonucleoprotein D-like	1.68
Fus	Q8CFQ9	RNA-binding protein FUS	1.67
Myo1b	Q7TQD7	Unconventional myosin-Ib	1.67
Hnrnpa1	Q5EBP8	Heterogeneous nuclear ribonucleoprotein A1	1.65
Hmox1	P14901	Heme oxygenase 1	1.65
Hnrnpa2b1	F6U106	Heterogeneous nuclear ribonucleoproteins A2/B1	1.64
Ddx21	Q9JIK5	Nucleolar RNA helicase 2	1.62
Vcl	Q64727	Vinculin	1.60
Matr3	Q8K310	Matrin-3	1.59
Tnxb	O35452	Protein Tnxb	1.58
Hnrnph1	O35737	Heterogeneous nuclear ribonucleoprotein H	1.57
Snrpa	Q62189	U1 small nuclear ribonucleoprotein A	1.57
Skiv2l2	Q9CZU3	Superkiller viralicidic activity 2-like 2	1.56
Smu1	Q3UKJ7	WD40 repeat-containing protein SMU1	1.55
Slc43a1	Q8BSM7	Large neutral amino acids transporter small subunit 3	1.55
Hnrnpa3	Q8BG05	Heterogeneous nuclear ribonucleoprotein A3	1.55
Crat	P47934	Carnitine O-acetyltransferase	1.54
Slc2a9	Q3T9X0	Protein Slc2a9	1.54
Ik	Q9Z1M8	Protein Red	1.53
Susd2	Q9DBX3	Sushi domain-containing protein 2	1.52
Slc39a14	Q75N73	Zinc transporter ZIP14	1.52
Elavl1	P70372	ELAV-like protein 1	1.52
Khdrbs1	Q60749	KH domain-containing, RNA-binding, signal transduction-associated protein 1	1.50
Myof	Q69ZN7	Myoferlin	1.50

Table 2. Proteins significantly downregulated upon FGF19 treatment
(fold change ≥1.5; n=3; p<0.05)

Gene name	Protein ID	Protein name	Fold change
Fabp5	Q05816	Fatty acid-binding protein, epidermal	-3.59
Cyp7a1	Q64505	Cholesterol 7-alpha-monooxygenase	-2.53
Hist1h1a	P43275	Histone H1.1	-2.06
Ces2c	Q91WG0	Acylcarnitine hydrolase	-1.97
Scd1	Q8BNZ5	Acyl-CoA desaturase 1;Acyl-CoA desaturase 2	-1.88
Chd4	Q6PDQ2	Chromodomain-helicase-DNA-binding protein 4	-1.82
Cyp2c70	Q91W64	Cytochrome P450 2C70	-1.73
Ggcx	Q9QYC7	Vitamin K-dependent gamma-carboxylase	-1.66
F9	P16294	Coagulation factor IX	-1.61
Uqcrh	P99028	Cytochrome b-c1 complex subunit 6, mitochondrial	-1.56
Cyp7b1	Q60991	25-hydroxycholesterol 7-alpha-hydroxylase	-1.56
Hist1h1c	P15864	Histone H1.2	-1.50
Slc25a23	Q6GQS1	Calcium-binding mitochondrial carrier protein SCaMC-3	-1.50

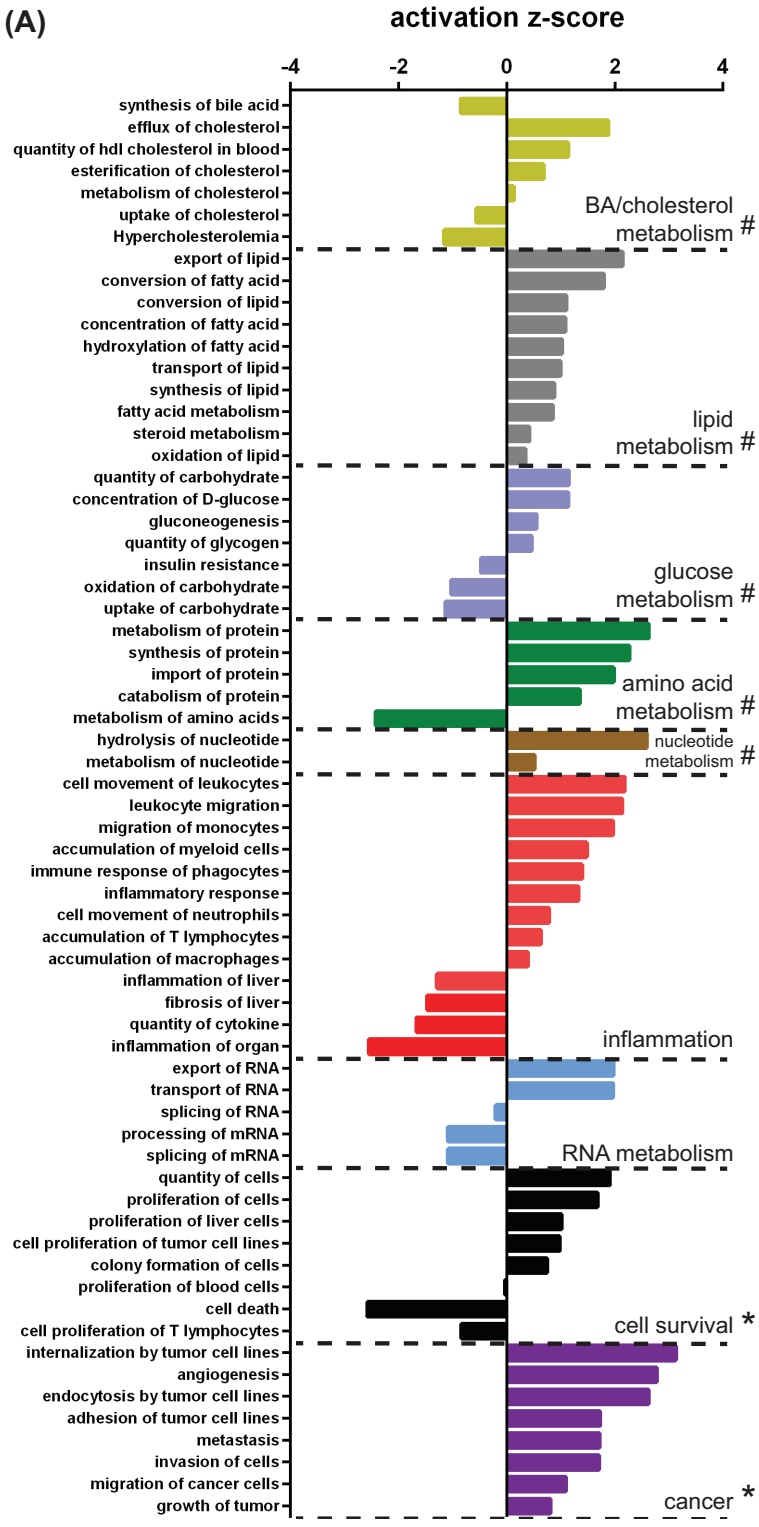
(A)
activation z-score
-4
-2
0
2
4
synthesis of bile acid
efflux of cholesterol
quantity of hdl cholesterol in blood
esterification of cholesterol
metabolism of cholesterol
uptake of cholesterol
Hypercholesterolemia
BA/cholesterol metabolism #
export of lipid
conversion of fatty acid
conversion of lipid
concentration of fatty acid
hydroxylation of fatty acid
transport of lipid
synthesis of lipid
fatty acid metabolism
steroid metabolism
oxidation of lipid
lipid metabolism #
quantity of carbohydrate
concentration of D-glucose
gluconeogenesis
quantity of glycogen
insulin resistance
oxidation of carbohydrate
uptake of carbohydrate
glucose metabolism #
metabolism of protein
synthesis of protein
import of protein
catabolism of protein
metabolism of amino acids
amino acid metabolism #
hydrolysis of nucleotide
metabolism of nucleotide
nucleotide metabolism #
cell movement of leukocytes
leukocyte migration
migration of monocytes
accumulation of myeloid cells
immune response of phagocytes
inflammatory response
cell movement of neutrophils
accumulation of T lymphocytes
accumulation of macrophages
inflammation of liver
fibrosis of liver
quantity of cytokine
inflammation of organ
inflammation
export of RNA
transport of RNA
splicing of RNA
processing of mRNA
splicing of mRNA
RNA metabolism
quantity of cells
proliferation of cells
proliferation of liver cells
cell proliferation of tumor cell lines
colony formation of cells
proliferation of blood cells
cell death
cell proliferation of T lymphocytes
cell survival *
internalization by tumor cell lines
angiogenesis
endocytosis by tumor cell lines
adhesion of tumor cell lines
metastasis
invasion of cells
migration of cancer cells
growth of tumor
cancer *

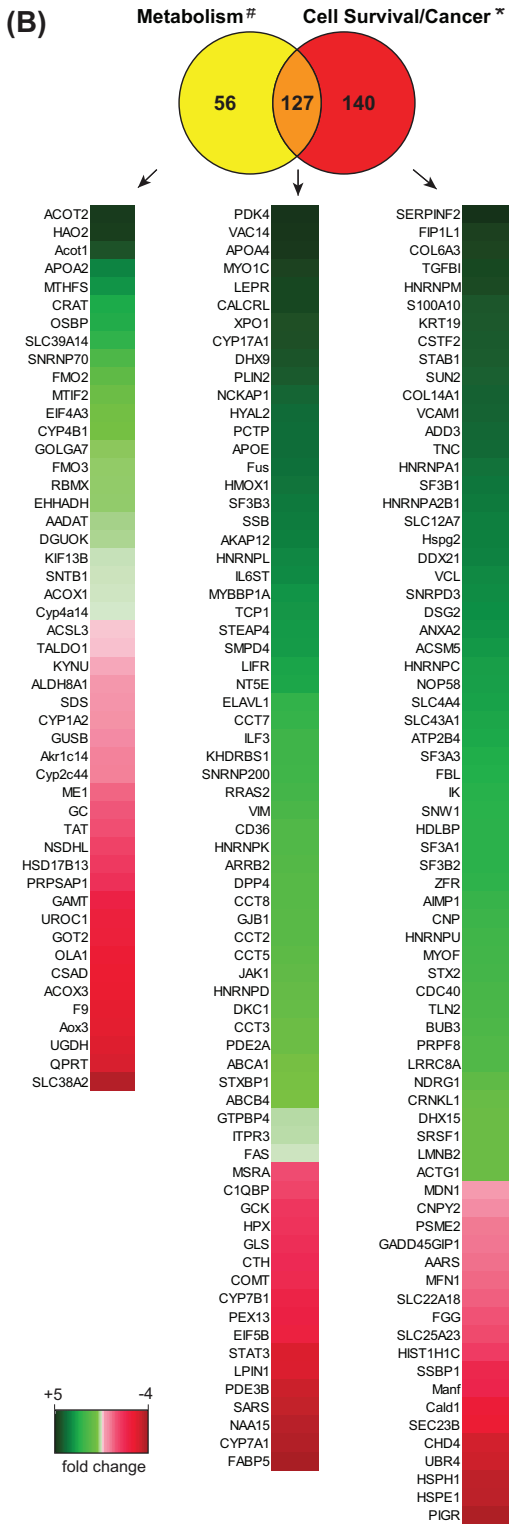

Figure 2. FGF19 modulates expression of proteins involved in metabolism and cell survival. (A) IPA of pathways enriched in mice treated with FGF19 for 12h compared to vehicle control. For the analysis, proteins with fold change ≥1.3 FGF19 over vehicle were included. Pathways related to physiology or disease that were significantly enriched (p-value < 0.01) are ranked in function of their activation z-score and grouped into functional classes. (B) Venn Diagram representation of proteins changed upon FGF19 treatment that are involved in metabolism and cell survival/cancer, inferred from the metabolic (#) and cell survival (*) pathways depicted in panel A. Fold change upon FGF19 treatment for proteins classified in metabolism, cell survival/cancer pathways or both is shown.

treated mice, light/heavy protein ratios distribute in a cloud along the diagonal with a Pearson correlation R^2=0.937 (S1 Fig).

Our proteomic analysis identified 6511 proteins, of which 5459 were identified with two or more razor or unique peptides, were not reverse hits, decoy hits or standard contaminants. All proteins were identified with a minimum false discovery rate < 0.01 (Q-value, [22]). 3 mice per group were included in the analysis and 2453 proteins had at least 2 valid values in each group. No imputation of missing values by normal distribution was performed. FGF19 treatment for 12 hours resulted in upregulation (≥ 1.5 fold) of 189 proteins and downregulation (≤ -1.5 fold) of 73 proteins compared to vehicle treatment for 12 hours (Fig 1C).

Significant expression differences upon 12h FGF19 treatment are depicted in a Volcano Plot (Fig 1D). Proteins involved in cell proliferation (e.g. transforming growth factor beta-induced protein ig-h3, Tgfbi; myoferlin), metabolism (e.g. Hao2, Crat2, Abcb1), anchoring to nuclear membrane (Sun2) and nucleolar

proteins (Nop14, Nop56) were among the most upregulated proteins 12h after FGF19 injection (Table 1). Proteins involved in BA synthesis (Cyp7a1, Cyp7b1), lipid metabolism (Fabp5, Scd1, Ces2c), oxidative phosphorylation (Slc25a23, Uqcrh) and other metabolic processes (Ggcx, Cyp2c70) were significantly downregulated (Table 2). Together, the *in vivo* proteome dataset identifies FGF19 as a regulator of metabolism and proliferation, and next to yet unknown targets, identifies Cyp7A1 amongst the highest regulated genes, as was previously reported [4].

FGF19 modulates expression of proteins involved in metabolism and cell survival

For a comprehensive understanding of FGF19 function, we performed IPA to understand which pathways were significantly enriched 12h after FGF19 treatment in comparison with the vehicle control. To have a very stringent cut-off of FGF19 targets, we did not perform imputation of missing values in each triplicate, as it is sometimes done. Consequently, the calculated number of significantly changed proteins in Fig 1 was too small for pathway analyses. We have therefore included proteins with fold change ≥ 1.3 (FGF19/vehicle) in our next analyses. FGF19 treatment yielded changes in wide ranging metabolic processes, including BA, cholesterol, lipid, glucose, amino acid, nucleotide, RNA metabolism and inflammation (Fig 2A). The pathway 'BA synthesis' was given a negative activation z-score, associated with decreased activity of this pathway, concurrent with the previously described role for FGF19 as enterohepatic negative regulator of BA synthesis [4]. The functional categories that can be summarized under 'cell survival' were enriched in the proteome dataset of the FGF19 stimulated livers, with an induction of pro-proliferative proteins and a negative activation score for proteins involved in cell death. In addition, pathways involved in tumorigenesis, such as 'invasion' and 'tumour growth' were significantly enriched and activated. Therefore, the changes observed in the liver proteomic profile of the mice receiving FGF19 confirm the role of FGF19 as a metabolic regulator, but also substantiate the concern about the tumorigenicity of FGF19 administration.

We subsequently aimed to investigate which proteins underlie FGF19-mediated regulation of metabolism and cell survival/cancer in the IPAs. Together, 183 proteins changed upon FGF19 treatment that were involved in different aspects of metabolism (e.g. Acot2, Acox1 and Acsl3) and 267 in cell survival/cancer (Col6a3. Tgfbi, Vcam1, Anxa2 and Hdlbp) (Fig 2B). However, of these proteins, 127 proteins were included in both metabolism and cell survival/cancer pathways (Fig 2B). This overlap includes Pdk4, Apoa4, Apoe, Vim, Gtpbp4, Fas (upregulated) and Stat3 (downregulated). Although the IPA algorithm is based on counting associations in published data and is therefore limited, these results suggest that separation between FGF19 proliferative and metabolic functions may be more complex than was previously anticipated.

Evaluation of changes in gene expression involved in metabolic and proliferative function of FGF19

Since FGF19 regulated the expression of the above described proteins after 12 hour

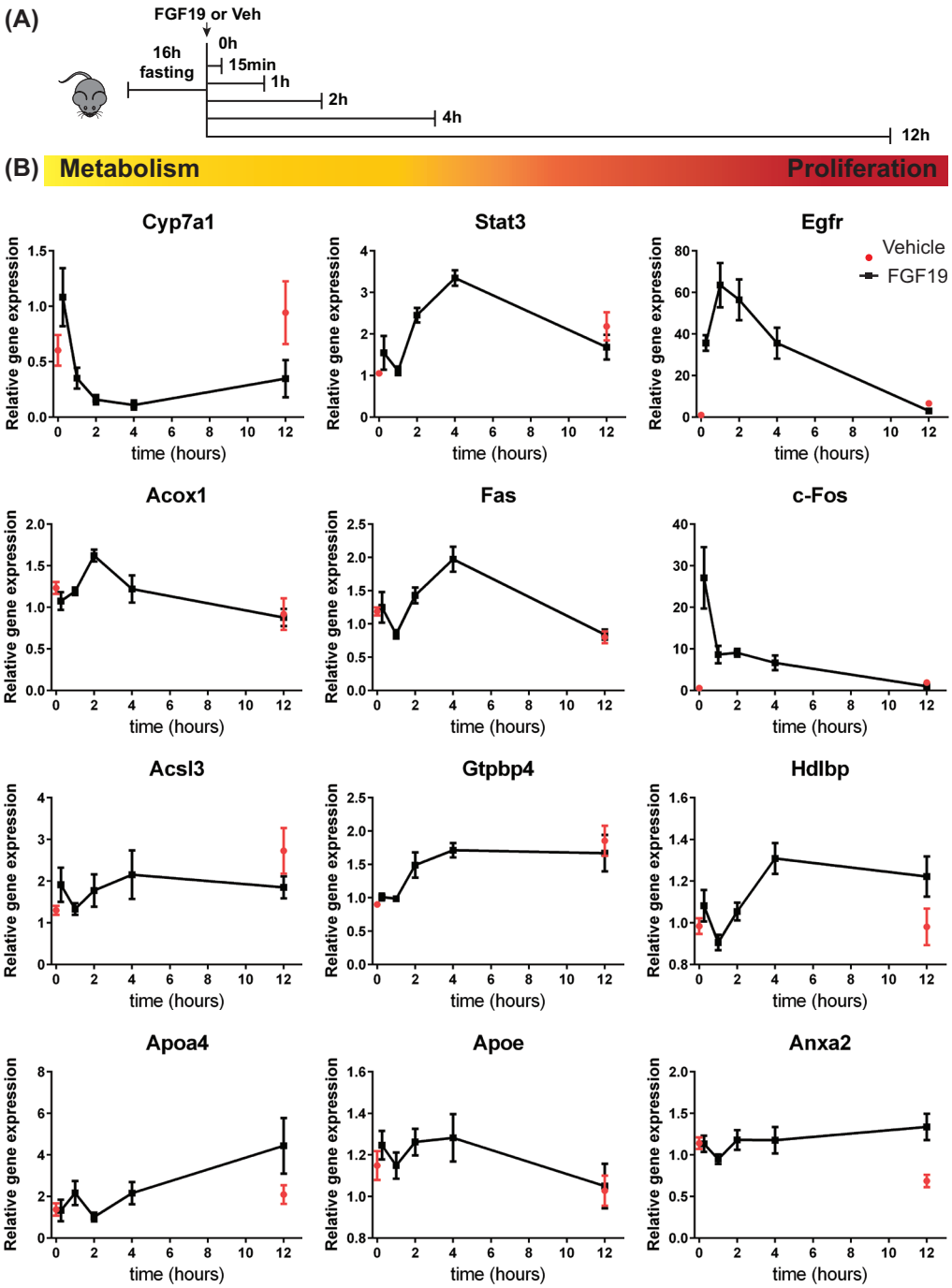

Figure 3. FGF19 stimulation affects mRNA expression of genes involved in metabolism and cell survival. (A) Schematic representation of the experimental outline to determine gene expression changes occurring upon FGF19 treatment for 0, 15 min, 1h, 2h, 4h and 12h. (B) Hepatic expression of genes involved in metabolism (Cyp7a1, Acox1, Acsl3), proliferation (Egfr, c-Fos, Hdlbp, Anxa2) or both (Stat3, Apoa4, Apoe, Fas, Gtpbp4) was determined by Real Time qPCR. (n=5-6). Data are normalized to Gapdh expression.

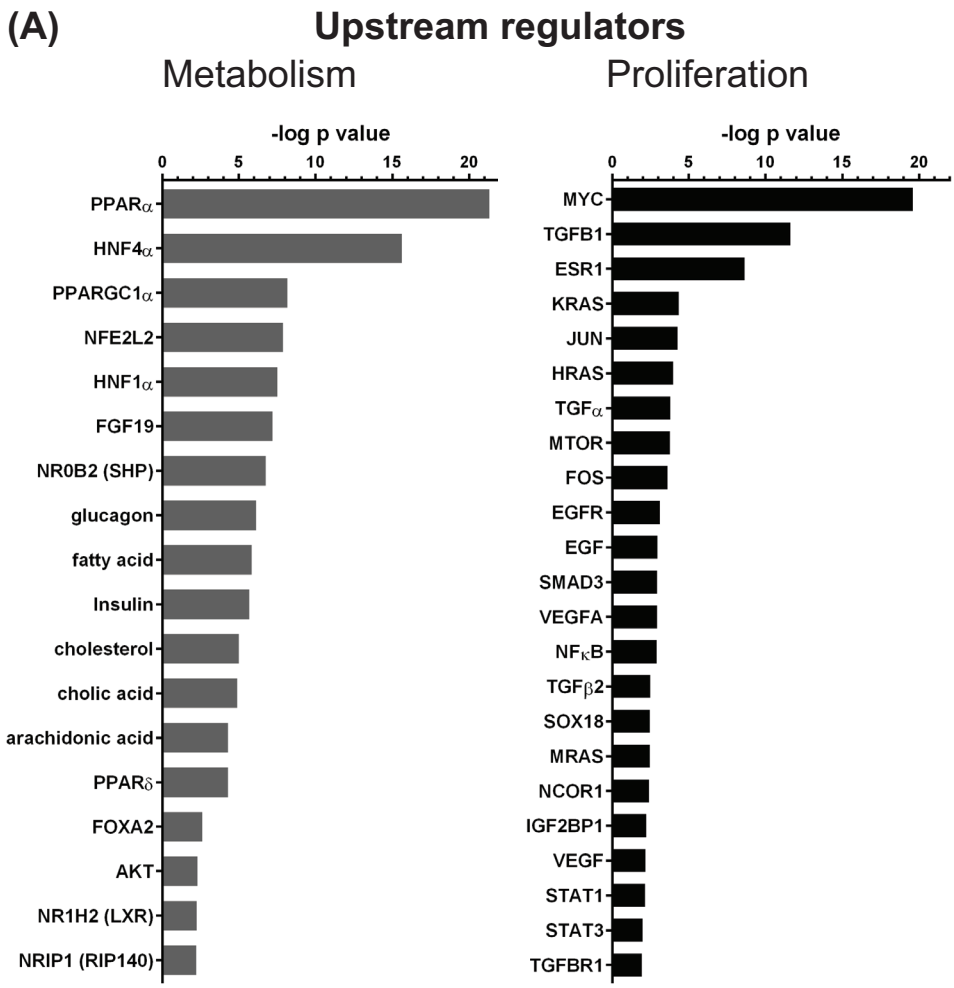

treatment, we addressed whether transcriptional regulation of metabolic and proliferative genes by FGF19 precedes the up/downregulation observed at protein level. We injected mice with FGF19 and harvested the livers at t=0, 15 min, 1h, 4h and 12h after a 16h pre-fasting period, in order to analyse FGF19 function without the confounding effect of endogenous FGF15 signalling (Fig 3A). We took along a group which received only the vehicle and was terminated after 12h, to be able to correct for differences due to prolonged starvation. Expression of the BA synthesis enzyme Cyp7a1 decreased upon FGF19 treatment, as expected (Fig 3B). The signal transducer and activator of transcription 3 (Stat3) had been previously reported to exhibit an increased phosphorylation and activation in response to FGF19, with subsequent effects both on proliferation and inhibition of FA synthesis [7, 16]. Here we show that FGF19 increases gene expression of Stat3 (Fig 3B). The mRNA expression of the proliferative markers Egfr and c-Fos (not detected at protein level in our proteome dataset) peaked within 4h after FGF19 administration, in line with a previous study [14].

(B)

TGFB target in the proteome dataset	FC upon FGF19 treatment	p-value	IPA Gene regulation by TGFB	PMID Ref
COL6A3	2.23	0.001	Up	11279127, 16457687
TGFB1	2.09	0.011	Up	18499657, 12547711, 11850808
VCAM1	1.76	0.040	Down	23113352, 9916930
HMOX1	1.65	0.023	Up	17567933, 11018038, 9721696, 8163576, 17307160
VCL	1.60	0.032	Up	16484225
VIM	1.49	0.032	Up	11967021, 22744866, 17270292, 22952236, 18499657
BSG	1.44	0.033	Up	21532623
ITGA1	1.44	0.032	Up	15604209, 23487420
GNAI2	1.43	0.034	Down	23077035
ABCA1	1.40	0.006	Up	20057170, 11742878, 16973241, 20057170
JUP	1.37	0.024	Down	11606377, 15604209, 10077641
DES	1.34	0.006	Up	20190033
PTGS1	1.33	0.024	Up	9348193, 12547711

Figure 4. FGF19 elicits expression changes in target genes of tumorigenic regulators. (A) Ingenuity upstream regulator analysis applied to protein changes observed upon FGF19 treatment for 12h. Prediction of upstream regulators is based on the overlap between the dataset proteins and the genes that are regulated by a transcription factor/hormone/compound, based on the knowledge included in Ingenuity database (overlap p-value <0.01). (B) Top list of proteins changed in our proteome dataset that are predicted as TGFB1 targets by Ingenuity upstream regulator analysis. The fold change observed in our dataset upon FGF19 treatment and the direction of gene regulation (up/down) by TGFB1 inferred from literature are reported.

We next investigated whether protein expression changes of newly identified FGF19 targets listed in Fig 2B reflect also mRNA expression regulation. Indeed, FA oxidation enzyme Acox1 mRNA expression increased and peaked 1h after FGF19 injection, whereas FA synthesis enzyme long-chain-fatty-acid-CoA ligase 3 (Acsl3) was decreased in FGF19-treated mice compared to vehicle controls (Fig 3B). Apolipoprotein Apoa4 mRNA expression increased and peaked 12h after FGF19 treatment, whereas Apoe mRNA expression was increased up to 4h after injection and was back to normal after 12h. mRNA expression of tumor necrosis factor receptor superfamily member 6 (Fas) and nucleolar GTP-binding protein 1 (Gtpbp4), implicated in both metabolism and cell survival, peaked 4h after FGF19 treatment, thus preceding the increase observed at protein level at 12h. mRNA expression of vigilin (Hdlbp), and calcium-dependent phospholipid binding protein Annexin A2 (Anxa2), both involved in cell proliferation, were increased 12h after FGF19 treatment. The change in mRNA expression of the aforementioned novel targets concur with the up/down regulation observed at protein level (Fig 2B). In contrast, Fabp5, implicated in lipid metabolism, and Tgfbi, implicated in cell survival, were not regulated at mRNA level by FGF19 (data not shown), despite their protein expression being significantly changed 12h after FGF19 injection (Tables 1-2). Therefore, these gene expression studies confirm most novel metabolic and proliferative targets of FGF19, but also indicate that not all protein expression changes observed upon 12h FGF19 treatment, are preceded by a consistent change at mRNA

level.

FGF19 elicits expression changes in target genes of tumorigenic regulators

Next, we applied the Ingenuity upstream regulator analysis to the liver proteome dataset, which allows prediction of upstream regulators associated with the detected protein expression changes. We distinguished regulators of metabolism and proliferation (Fig 4A). The analysis correctly identifies FGF19 and cholic acid (bile acid) as upstream regulators of the protein expression changes observed in our proteome dataset. In addition, the analysis identifies as upstream regulators the known FGF19 targets Egfr, c-Fos and the Stat3, the latter being activated by FGF19 and here reported to be regulated also at expression level. Furthermore, overlap with nuclear receptor signalling (PPARα, PPARδ, HNF4α, SHP, and LXR, PGC1α, and RIP140), transcription (NFE2L2, HNF1α, FOXA2) and insulin and glucagon was identified. In accordance with FGF19-dependent regulation of lipid metabolism, also arachidonic acid, fatty acid, and cholesterol were identified as possible upstream regulators.

Interestingly, Ingenuity analysis suggests that FGF19 may have a similar activation program as that triggered by growth factors (Vegf and Egf), oncogenes (Myc, Kras) and Tgfβ signalling (Tgfb1, Smad3, Tgfb2, Tgfbr1; Fig 4A, right panel). Tgfβ is considered both a tumor suppressor and pro-oncogenic factor [23]. FGF19 injection changed the expression of many proteins known to be regulated by Tgfβ, including Col6a3, Tgfbi, vascular cell adhesion protein 1 (Vcam1), heme oxygenase 1 (Hmox1), vinculin (Vcl) and vimentin (Vim) (Fig 4B). Taken together, these analyses identify similarities between FGF19 and known regulators of tumorigenesis and proliferation, indicating that FGF19 may have similar targets or mediates its effects via these regulators.

DISCUSSION

The elucidation of the molecular basis for FGF19 function is of great interest for the design of an FGF19-based therapeutic deprived of its tumorigenic potential, but retaining its beneficial effects on BA, lipid and glucose homeostasis. Investigation of the molecular mechanisms underlying FGF19 function has so far relied on targeted approaches, by addressing whether FGF19 induces the activity of key signalling proteins known to be involved in metabolism and proliferation. In the present study, we have taken an unbiased approach to determine FGF19 targets that underlie metabolic and proliferative effects. We deployed untargeted quantitative proteomics to generate a comprehensive view of FGF19 function in mouse liver. Both analysis of top regulated proteins and pathway enrichment studies in our proteome dataset support the involvement of FGF19 signalling in a wide range of processes, including BA, cholesterol, lipid, glucose, amino acid, nucleotide, and RNA metabolism, as well as cell survival and tumorigenesis. As well as decreasing the expression of BA synthesis enzyme Cyp7a1, FGF19 decreases the protein expression of Acsl3, and Scd1, implicated in FA synthesis and Fabp5, involved in FA transport. In addition, protein expression of Acox1, involved in FA oxidation and the apolipoproteins Apoe and Apoa4 are upregulated by FGF19. In almost all cases, the regulation of protein expression was preceded by a change in mRNA level.

An important mechanism for FGF19 induction of cell proliferation is the phosphorylation and subsequent activation of Stat3 [16]. Besides, FGF19 proliferative function requires the binding to FGFR4, since FGF19-induced increase in proliferative markers is attenuated in the liver of Fgfr4 knockout mice [14]. On the basis of this information, variants of FGF19 were engineered with reduced proliferative potential. The FGF19 variant M70 harbours 3 amino acid substitutions and a 5-amino acid deletion in the N-terminus [15]. As a result, M70 fails to activate the proliferative factor Stat3 and does not promote hepatocellular carcinoma formation in mice, while retaining the ability to maintain BA homeostasis and even to ameliorate BDL- and ANIT-induced cholestasis in mice [16, 24]. Another FGF19 variant (FGF19v), which does not bind and activate Fgfr4, is also devoid of proliferative effects [14]. Fgfr4 seems not be required for improvement of glucose tolerance by FGF19, therefore FGF19v may effectively control glucose homeostasis [14]. FGFR4 is essential for FGF19-dependent repression of Cyp7a1 and therefore FGF19v exhibits impaired regulation of BA metabolism [14]. These FGF19 variants deprived of tumorigenic effects are very promising from a therapeutic perspective, however, their use in clinic is challenged by the limited information available regarding FGF19 metabolic and proliferative targets. For example, although in ob/ob mice serum glucose levels were significantly decreased in mice treated with both FGF19 and M70 (24 weeks), triglycerides, cholesterol and LDL and HDL were markedly increased compared to untreated ob/ob mice [16]. This indicates that caution should be taken to interpret FGF19 actions on metabolism as beneficial under all circumstances.

It is also unclear to what extent it is mechanistically possible to discriminate FGF19 metabolic and proliferative function as changes in metabolism are known to drive tumorigenic events [17]. Our proteome analysis reveals that FGF19 upregulates the protein expression of Tgfbi, Col6a3, Vcam1, Anxa2 and Hdlbp, that are implicated in cell survival. In the case of Hdlbp and Anxa2, but not of Tgfbi, we could show that FGF19 treatment for 12 hours determined a concurrent increase in mRNA expression. Also the mRNA expression of the proliferative markers Egfr and c-Fos was upregulated by FGF19 in our experiment, as previously described [14]. Importantly, 127 of the proteins regulated by FGF19 were annotated in both metabolism and cell survival categories in the IPA analysis, e.g. Fas, Gtpbp4 and Stat3. This number is probably an underestimation of the interplay between metabolism and cell survival pathways, since this analysis relies on publicly available data. The close interlink between metabolism and proliferation is not surprising, since metabolic reprogramming is essential for cell survival. As an example, pyruvate dehydrogenase kinase 4 (Pdk4), which is upregulated by FGF19 in our experiment (Fig 2B), provides an advantage during the proliferative state of the cell by driving the accumulation of glycolytic intermediates [25].

To overcome the limits of the intimate link between metabolic and proliferative mechanisms in designing therapeutic FGF19 variants, analysis of key tumorigenic FGF19 targets with limited or no involvement in metabolism should be addressed for dissociation between metabolic and proliferative functions. Indeed, the M70-mediated adverse effects on cholesterol and triglyceride concentrations [16] are likely due to Stat3 being the transcriptional repressor of Srebp1c [7], which activates cholesterol and fatty acid biosyn-

thesis. Therefore blocking of Stat3 activity prevents proliferation, but also dysregulates cholesterol metabolism. Our study identifies Anxa2 and Tgfbi as possible tumorigenic FGF19 targets, without no apparent function in BA, cholesterol or lipid metabolism. The proliferative activity of Anxa2 has been associated with tumour progression, since increased Anxa2 expression correlates with a more invasive phenotype and induces proliferation and invasion signalling in human breast cancer cells [26-28]. Similarly, Tgfbi, which is a protein involved in cell adhesion and cell-collagen interactions [29], has also been implicated in tumorigenesis [30]. In light of these observations, it would be informative to investigate whether these proteins critically mediate FGF19-dependent tumorigenesis. And if so, whether FGF19 variants blocking the activity of these targets are devoid of tumorigenic effects and have preserved metabolic activity.

In conclusion, our untargeted liver proteome analyses show that FGF19-mediated regulation of metabolism and proliferation is complex, and involves protein expression changes relating to BAs, glucose, lipid, amino acids, together with inflammatory, proliferative and tumorigenic processes. Future studies should address the exact mechanisms by which these proteins are regulated by FGF19, to understand whether the effects on carcinogenesis can be dissociated from beneficial effects on metabolism.

ACKNOWLEDGEMENTS

Grant support: S.W.C.v.M. is supported by the Netherlands Organization for Scientific Research (NWO) Project VIDI (917.11.365), FP7 Marie Curie Actions IAPP (FXR-IBD, 611979), the Utrecht University Support Grant, Wilhelmina Children's Hospital Research Fund. H.R.V. is supported by Proteins At Work (NWO). We thank Ellen Willemsen, Noortje Ijssennagger, Ingrid Bijsmans and Margreet Vonk Noordegraaf for technical assistance and José Miguel Ramos Pittol for critical discussion.

REFERENCES

1. Beenken A, Mohammadi M. The FGF family: biology, pathophysiology and therapy. Nat Rev Drug Discov 2009;8:235-53.
2. Degirolamo C, Sabba C, Moschetta A. Therapeutic potential of the endocrine fibroblast growth factors FGF19, FGF21 and FGF23. Nat Rev Drug Discov 2016;15:51-69.
3. Holt JA, Luo G, Billin AN, et al. Definition of a novel growth factor-dependent signal cascade for the suppression of bile acid biosynthesis. Genes Dev 2003;17:1581-91.
4. Inagaki T, Choi M, Moschetta A, et al. Fibroblast growth factor 15 functions as an enterohepatic signal to regulate bile acid homeostasis. Cell Metab 2005;2:217-25.
5. Fu L, John LM, Adams SH, et al. Fibroblast growth factor 19 increases metabolic rate and reverses dietary and leptin-deficient diabetes. Endocrinology 2004;145:2594-603.
6. Tomlinson E, Fu L, John L, et al. Transgenic mice expressing human fibroblast growth factor-19 display increased metabolic rate and decreased adiposity. Endocrinology 2002;143:1741-7.
7. Bhatnagar S, Damron HA, Hillgartner FB. Fibroblast growth factor-19, a novel factor that inhibits hepatic fatty acid synthesis. J Biol Chem 2009;284:10023-33.
8. Miyata M, Sakaida Y, Matsuzawa H, et al. Fibroblast growth factor 19 treatment ameliorates disruption of hepatic lipid metabolism in farnesoid X receptor (Fxr)-null mice. Biol Pharm Bull 2011;34:1885-9.

9. Kir S, Beddow SA, Samuel VT, et al. FGF19 as a postprandial, insulin-independent activator of hepatic protein and glycogen synthesis. Science 2011;331:1621-4.
10. Potthoff MJ, Boney-Montoya J, Choi M, et al. FGF15/19 regulates hepatic glucose metabolism by inhibiting the CREB-PGC-1alpha pathway. Cell Metab 2011;13:729-38.
11. Nicholes K, Guillet S, Tomlinson E, et al. A mouse model of hepatocellular carcinoma: ectopic expression of fibroblast growth factor 19 in skeletal muscle of transgenic mice. Am J Pathol 2002;160:2295-307.
12. Miura S, Mitsuhashi N, Shimizu H, et al. Fibroblast growth factor 19 expression correlates with tumor progression and poorer prognosis of hepatocellular carcinoma. BMC Cancer 2012;12:56.
13. Sawey ET, Chanrion M, Cai C, et al. Identification of a therapeutic strategy targeting amplified FGF19 in liver cancer by Oncogenomic screening. Cancer Cell 2011;19:347-58.
14. Wu AL, Coulter S, Liddle C, et al. FGF19 regulates cell proliferation, glucose and bile acid metabolism via FGFR4-dependent and independent pathways. PLoS One 2011;6:e17868.
15. Wu X, Ge H, Lemon B, et al. Separating mitogenic and metabolic activities of fibroblast growth factor 19 (FGF19). Proc Natl Acad Sci U S A 2010;107:14158-63.
16. Zhou M, Wang X, Phung V, et al. Separating Tumorigenicity from Bile Acid Regulatory Activity for Endocrine Hormone FGF19. Cancer Res 2014;74:3306-16.
17. Hirschey MD, DeBerardinis RJ, Diehl AM, et al. Dysregulated metabolism contributes to oncogenesis. Semin Cancer Biol 2015;35 Suppl:S129-50.
18. Wisniewski JR, Zougman A, Mann M. Combination of FASP and StageTip-based fractionation allows in-depth analysis of the hippocampal membrane proteome. J Proteome Res 2009;8:5674-8.
19. Cox J, Mann M. MaxQuant enables high peptide identification rates, individualized p.p.b.-range mass accuracies and proteome-wide protein quantification. Nat Biotechnol 2008;26:1367-72.
20. Schwanhausser B, Busse D, Li N, et al. Global quantification of mammalian gene expression control. Nature 2011;473:337-42.
21. Cox J, Mann M. 1D and 2D annotation enrichment: a statistical method integrating quantitative proteomics with complementary high-throughput data. BMC Bioinformatics 2012;13 Suppl 16:S12.
22. Kall L, Storey JD, MacCoss MJ, et al. Posterior error probabilities and false discovery rates: two sides of the same coin. J Proteome Res 2008;7:40-4.
23. Jakowlew SB. Transforming growth factor-beta in cancer and metastasis. Cancer Metastasis Rev 2006;25:435-57.
24. Luo J, Ko B, Elliott M, et al. A nontumorigenic variant of FGF19 treats cholestatic liver diseases. Sci Transl Med 2014;6:247ra100.
25. Xie Y, Wang H, Cheng X, et al. Farnesoid X receptor activation promotes cell proliferation via PDK4-controlled metabolic reprogramming. Sci Rep 2016;6:18751.
26. Sharma MR, Koltowski L, Ownbey RT, et al. Angiogenesis-associated protein annexin II in breast cancer: selective expression in invasive breast cancer and contribution to tumor invasion and progression. Exp Mol Pathol 2006;81:146-56.
27. Wu B, Zhang F, Yu M, et al. Up-regulation of Anxa2 gene promotes proliferation and invasion of breast cancer MCF-7 cells. Cell Prolif 2012;45:189-98.
28. Zhang F, Zhang L, Zhang B, et al. Anxa2 plays a critical role in enhanced invasiveness of the multidrug resistant human breast cancer cells. J Proteome Res 2009;8:5041-7.
29. Skonier J, Bennett K, Rothwell V, et al. beta ig-h3: a transforming growth factor-beta-responsive gene encoding a secreted protein that inhibits cell attachment in vitro and suppresses the growth of CHO cells in nude mice. DNA Cell Biol 1994;13:571-84.
30. Han B, Cai H, Chen Y, et al. The role of TGFBI (betaig-H3) in gastrointestinal tract tumorigenesis. Mol Cancer 2015;14:64.

SUPPLEMENTARY FIGURE AND TABLE

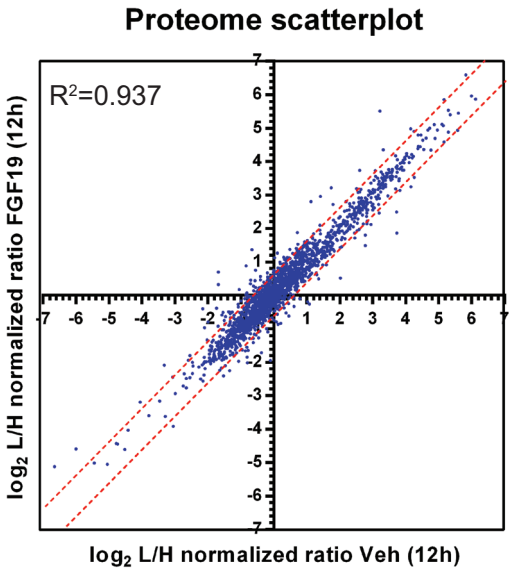

Figure S1. FGF19-mediated regulation of liver protein expression resolved by quantitative proteomics. (A) Scatterplot distribution of FGF19-induced protein expression changes expressed as log2 light/heavy normalized ratios. Pearson correlation between protein expressions in FGF19-treated mice and protein expressions in Veh-treated mice is shown.

Table S1. Mouse qRT-PCR primers

Gene	Sequence (5'->3')
Gapdh	FW CAAGGTCATCCATGACAACTTTG RV GGCCATCCACAGTCTTCTGG
Egfr	FW ACAACCCTATGAGCACCTGA RV GAGTCGTTTGGCTGGGATAA
c-Fos	FW GAAGGGAACGGAATAAGATGG RV CTGTCTCCGCTTGGAGTGTA
Cyp7a1	FW ATGTCCACTTCATCACAAACTCC RV TTTCCATCACTTGGGTCTATGC
Acsl3	FW TGTCTTTCTCATGGATGCCGA RV CAGCACGGATGTGTCTCCTT
Acox1	FW CCGCCACCTTCAATCCAGAG RV CAAGTTCTCGATTTCTCGACGG
Apoa4	FW ACCCAGCTAAGCAACAATGC RV TGTCCTGGAAGAGGGTACTGA
Apoe	FW CTGACAGGATGCCTAGCCG RV CGCAGGTAATCCCAGAAGC
Hdlbp	FW GGAAAATGACCCTCCAACCTAC RV GGGTACATGAAACACCTGAGTGA
Stat3	FW CAATACCATTGACCTGCCGAT RV GAGCGACTCAAACTGCCCT
Fas	FW AAACCAGACTTCTACTGCGATTCT RV GGGTTCCATGTTCACACGA
Gtpbp4	FW GGACGAATGTGTACTATTATCAAGAGA RV GCGGGATAAATGTTGACGTACT
Anxa2	FW ATGTCTACTGTCCACGAAATCCT RV CGAAGTTGGTGTAGGGTTTGACT


flame


FXR
DNA

CHAPTER 5

Splenic dendritic cell involvement in FXR-mediated amelioration of DSS colitis

Vittoria Massafra, Noortje Ijssennagger, Maud Plantinga, Alexandra Milona, José M. Ramos Pittol, Marianne Boes, and Saskia W.C. van Mil

Biochim Biophys Acta. 2016 Feb;1862(2):166-73

ABSTRACT

Inflammatory Bowel Disease (IBD) is a multifactorial disorder involving dysregulation of the immune response and bacterial translocation through the intestinal mucosal barrier. Previously, we have shown that activation of the bile acid sensor Farnesoid X Receptor (FXR), which belongs to the family of nuclear receptors, improves experimental intestinal inflammation, decreasing expression of pro-inflammatory cytokines and protecting the intestinal barrier.

Here, we aimed to investigate the immunological mechanisms that ameliorate colitis when FXR is activated. We analyzed by FACS immune cell populations in mesenteric lymph nodes (MLN) and in the spleen to understand whether FXR activation alters the systemic immune response. We show that FXR activation by obeticholic acid (OCA) has systemic anti-inflammatory effects that include increased levels of plasma IL-10, inhibition of both DSS-colitis associated decrease in splenic dendritic cells (DCs) and increase in Tregs. Impact of OCA on DC relative abundance was seen in spleen but not MLN, possibly related to the increased FXR expression in splenic DCs compared to MLN DCs. Moreover, FXR activation modulates the chemotactic environment in the colonic site of inflammation, as Madcam1 expression is decreased, while Ccl25 is upregulated. Together, our data suggest that OCA treatment elicits an anti-inflammatory immune status including retention of DCs in the spleen, which is associated with decreased colonic inflammation. Pharmacological FXR activation is therefore an attractive new drug target for treatment of IBD.

INTRODUCTION

Inflammatory Bowel Disease (IBD) encompasses a group of disorders characterized by chronic intestinal inflammation. IBD involves dysregulation of the local mucosal immune response combined with compromised intestinal epithelial barrier function, in genetically predisposed individuals[1]. While treatment options for IBD patients are reasonably effective, they are often accompanied by significant side-effects and 40-50% of patients on currently available IBD medication fail to respond to the treatment[2, 3]. Thus, these clinical observations underscore the need for novel treatment options for IBD. Considering that progression into active disease requires the recruitment of leukocytes to the intestine, current research for IBD treatment involves the targeting of selective adhesion molecules and chemokine receptors that guide leucocyte migration[4, 5].

Farnesoid X Receptor (FXR) is a bile acid (BA)-activated transcription factor belonging to the family of nuclear receptors. FXR regulates BA glucose and lipid homeostasis and decreases tumor formation in liver and intestine[6]. Besides its metabolic functions, FXR activation also elicits anti-inflammatory and immune modulatory effects. We, and others have shown that FXR activation attenuates the severity of colitis in two separate murine models of IBD[7, 8]. In these studies, the protection against colitis involved the repression of pro-inflammatory cytokine expression and inhibition of microbicidal genes, and thus likely modification of intestinal microbiota. FXR activation was shown to modulate *in vitro* dendritic cell (DC) differentiation and TNF production by immune cells, but the nature and extent of FXR impact on immune function in colitis *in vivo* is currently unclear.

DCs are a critical immune cell subset bridging the innate and adaptive immune responses, and are implicated in the immune dysregulation associated with colitis. Adoptive transfer of bone marrow-derived DCs exacerbated dextran sodium sulphate (DSS)-induced colitis in mice, while selective genetic ablation of DCs attenuated the severity of colitis[9]. Anti-DC therapy in colitis blocked leukocyte infiltration to the inflamed colon and controlled inflammation more effectively than targeting further downstream events, highlighting the involvement of DCs at early stages of inflammation[9]. DCs are found scattered throughout tissues, where they monitor the surroundings and capture antigens. Nuclear receptors are also sensors of the local tissue environment and can relay extracellular signals into changes in gene expression. Consistently, some nuclear receptors trigger both metabolic and immunological effector functions. Nuclear receptors involved in metabolism also modulate macrophage and DC function, affecting their maturation, their ability to activate T cells and their migratory properties[10]. For example, retinoid receptors (RXR and RAR) mostly imprint a pro-inflammatory phenotype in DCs, whereas peroxisome proliferator-activated receptor (PPARγ), vitamin D receptor (VDR) and liver X receptor (LXR) have anti-inflammatory effects[10]. Yet the widespread connections between immunology and metabolism and the potential of nuclear receptor agonists in therapy for IBD are far from being fully explored.

In this study, we examined the systemic effects of FXR activation on splenic and mesenteric lymph node (MLN) immune cell populations in DSS-induced colitis. We show that FXR activation changes the relative abundance of splenic immune cell populations and

affects the chemotaxis of cells in the colon during colitis. Together, our data suggest that obeticholic acid (OCA) treatment results in retention of DCs in the spleen, which is associated with decreased colonic inflammation.

MATERIALS AND METHODS

Animals

Wild-type (WT) C57BL/6J male mice (8 weeks old) were obtained from Charles River Laboratories (Leiden, The Netherlands). Mice were fed chow diet *ad libitum* and housed in a temperature and light-controlled room. All experiments were approved by the ethics committee of the University Medical Center Utrecht.

Colitis was induced by administration of 2,5% (wt/vol) Dextran Sodium Sulfate (DSS; MW. 36000-50000 Da, MP Biochemicals, Santa Ana, California, U.S.) in drinking water for 8 days. Pharmacological activation of FXR was accomplished by treatment with obeticholic acid (OCA, 6-ethyl-chenodeoxycholic acid, kindly provided by Luciano Adorini, Intercept Pharmaceuticals Inc., San Diego, California, U.S.). OCA (10mg/kg/day) or vehicle (1% methyl cellulose) were administered by oral gavage once a day from three days prior to DSS treatment, and continued until the end of the DSS-treatment. In the evening prior to the sacrifice, mice received an extra gavage of OCA. Mice were starved for 4 hours prior to sacrifice. 10 mice per group were used for this experiment (groups: no DSS, DSS, and DSS+OCA). Body weight was assessed daily. Rectal bleeding was scored on a scale from 0 to 4, indicating no (0) to severe (4) rectal bleeding.

Intestinal permeability assay

Intestinal permeability was examined in mice after 8 days of DSS treatment, as described previously[11]. In brief, mice were gavaged with 0.6 mg/g body weight of fluorescein isothiocyanate (FITC)-conjugated dextran (Sigma, S Louis, Missouri, U.S.; molecular mass 3-5 kDa) 4 h before termination. FITC concentrations were measured in plasma (Fluorimeter Pharos FX; BioRad, Hercules, California, U.S.).

RNA extraction, cDNA synthesis and qRT-PCR analysis

Colons were harvested, washed in PBS and snap frozen. RNA was isolated using the RNeasy Micro kit (Qiagen, Venlo, The Netherlands). cDNA was generated from 1 μg of total RNA using SuperScript II Reverse Transcriptase (Invitrogen, Carlsbad, California, U.S.). qRT-PCR analysis was carried out using SYBR green PCR mastermix (Roche, Basel, Switzerland) and analyzed on a MyIQ real time PCR cycler (BioRad, Veenendaal, The Netherlands). Relative expression of colonic genes is normalized to glyceraldehyde-3-phosphate dehydrogenase, whereas expression of splenic genes is normalized to hypoxanthine phosphoribosyltransferase 1. Primer sequences are listed in Supplementary Table 1.

Isolation of spleen and Mesenteric Lymph Node (MLN) cells for flow cytometry and cell sorting

Spleen and MLNs were passed through a cell strainer to make a single-cell suspension

and then stained with fluorochrome-labeled mouse antibodies. All antibody incubations were performed at 4°C for 30 to 45 min. For detection and phenotyping of cell subsets in cell suspensions of spleen and mesenteric lymph nodes, cells were stained with monoclonal antibodies directed against CD3, MHCII, CD11c, CD19, GR-1, CD11b, CD4, CD8 and CD25 (all from Biolegend, San Diego, California, U.S.), CD69 (BD Biosciences, Franklin Lakes, New Jersey, U.S.), Foxp3 Transcription Factor Staining Buffer Set and fixable live/dead marker Aqua (eBioscience, San Diego, California, U.S.). For intranuclear staining, cells were stained using the FoxP3 staining kit (eBioscience) according to the manufacturer's protocol. Acquisition of multicolour stained samples was done on a LSRII cytometer. Cell sorting was performed on a FacsARIA II cytometer and after cell sorting, purity was checked (always >95%). Final analysis and graphical output were performed using FACS Diva™ software (BD bioscience).

Multiplex cytokine analysis

Cytokine concentrations of IFNγ, IL-2, IL-10 and IL-17A were measured in mouse plasma, using Diaclone Murine 5-plex, following the manufacturer's protocol (Diaclone, Besançon cedex, France). In brief, antibodies coupled to differentially fluorescently labeled beads were mixed in suspension with plasma samples and incubated with biotin-conjugated secondary antibody. Phycoerythrin-Streptavidin was subsequently added to the sample and detection of the cytokine-specific intensities was performed by FacsCalibur.

Immunohistochemistry and Immunofluorescence

Paraffin-embedded colon tissue sections were incubated overnight with anti-CXCR3 1:250 (Bioss, Woburn, Massachusetts, U.S.) and for 1 h with secondary antibody goat anti rabbit 1:200 (Thermo Fisher Scientific, Waltham, Massachusetts, U.S.) and counterstained with Hematoxylin. The percentage of CXCR3-positve cells was calculated as a ratio over haematoxilin positive cells as quantified by ImageJ. Colon cryosections were fixed in acetone and incubated with antibody against MHCII conjugated with APC diluted 1:100 (Biolegend) and counterstained with NucGreen Dead488, following the manufacturer's protocol (Life Technologies, Carlsbad, California, U.S.). Imaging of the sections was performed using a confocal microscope (Zeiss LSM510).

Statistical analysis

All results are expressed as mean SEM, unless stated differently. Statistical significance was determined by unpaired non parametric T-test (Mann-Whitney test) and by Kruskal-Wallis Anova test. Statistical analyses were performed using Graphpad (version 6.02) software. Two-sided p values ($p<0.05$) were considered significant.

RESULTS

FXR activation alters the composition of splenic immune cell populations

We addressed whether amelioration of colitis induced by FXR activation involves secondary lymphoid organs. We therefore induced colitis in C57Bl6 mice by administering 2.5 % DSS in the drinking water for 8 days. Three days prior to DSS treatment, we start-

ed daily OCA administration (10 mg/kg) per oral gavage until the end of the experiment, as previously described[7]. Efficient FXR activation in the colon of OCA-treated mice was evaluated by increased mRNA expression of the primary FXR target gene IBABP (Supplementary Fig. 1A). We confirmed that FXR activation decreased rectal bleeding scores, intestinal permeability and mRNA expression of the pro-inflammatory cytokine IL-1β in the colon (Supplementary Fig. 1B- D), as previously described[7].

To understand the role of immune cells in mesenteric lymph nodes and spleen in OCA-mediated amelioration of colitis, we assayed the cellular composition of the MLNs and splenocytes by flow cytometry (Supplementary Fig. 2). Colitis induction triggered a significant decrease in splenic DCs. OCA treatment fully prevented the disease-associated decrease in splenic DCs (Fig1A). OCA did not alter the ratio of CD8-positive/CD11b-positive DCs, as the abundance of both DC subsets was equally rescued by OCA during colitis (Supplementary Fig. 3A). In MLNs, which are known to drain colonic tissues, DC counts were unaffected by DSS or OCA treatment (Fig. 1A), despite the significant increase in total number of live cells in the MLNs upon DSS treatment (Supplementary Fig. 3B). The amount of granulocytes was higher in the MLNs and the spleen in the DSS-treated groups compared to the group receiving no DSS. OCA treatment further increased the amount of granulocytes only in the spleen (Fig. 1B). The fraction of FoxP3-positive regulatory T-cells (Tregs) increased in the MLNs as well as in the spleen upon the induction of colitis by DSS. OCA treatment resulted in a significant decrease in Tregs only in the spleen (Fig. 1C). No significant differences were observed between DSS and DSS+OCA groups in the relative fraction of B cells, CD4-positive and CD8-positive T lymphocytes either in spleen or MLNs (Supplementary Fig. 3C/D).

The decrease in spleen DCs upon inflammation induced by DSS colitis and its intersection by OCA treatment may be due to impaired differentiation/maturation, increased cell death, or local depletion in favor of accumulation at sites of inflammation. We first addressed the possibility that OCA treatment causes changes in differentiation/maturation of the DCs, by assessment of gene expression of MHCII encoding genes H2Ab1 and H2Eb1 and APC markers CD80 and CD86 in spleen tissue (Fig. 2B). Expression of these maturation markers decreased significantly upon DSS but mRNA levels were not restored upon OCA treatment, suggesting that OCA-treatment probably does not cause persistence of DC markers due to increase of these markers per cell. Instead, low CD80/CD86 mRNA levels caused by DSS might be explained by DC migration out of the spleen, rather than by an effect on maturation, because it is expected that DSS treatment would increase DC maturation. Further analysis of FACS data revealed an increase in CD11c/MHCII-positive DC size (Forward Scatter) and granularity (Side Scatter) upon DSS treatment (Fig 2C), which is commonly associated with increased maturation[12, 13] and negatively associated with cell death[14]. Importantly, OCA treatment restored normal size and granularity of DCs, suggesting decreased maturation compared to DSS alone. We therefore conclude that alteration of DC maturation or cell death cannot explain the reduction in splenic DCs upon DSS treatment, nor the rescue by OCA. Instead, all available evidence supports that DSS treatment causes depletion of splenic CD11c/MHCII-positive DCs, a feature that OCA can counteract.

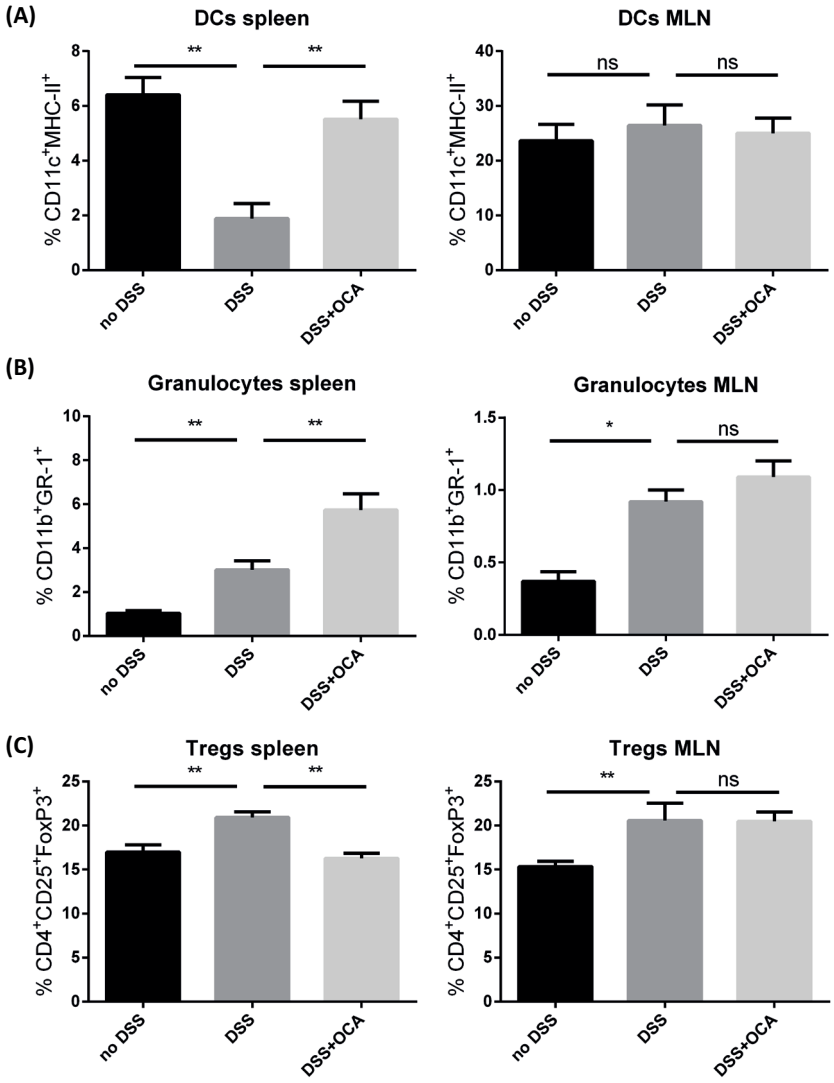

Fig. 1. FXR activation alters the composition of splenic immune cell populations. FACS analysis of DCs **(A)**, granulocytes **(B)** and Tregs **(C)** in the spleen and in the MLNs collected from mice receiving vehicle, DSS or DSS in combination with OCA. Gating on live cells and out gating T-, B-cells and granulocytes, the relative amount of DCs ($CD11c^+MHCII^+$) is depicted. Granulocytes are expressed as percentage of $CD11b^+GR\text{-}1^+$ cells. Tregs are expressed as percentage of $CD4^+CD25^+FoxP3^+$ cells. Data are represented as mean ± SEM, n=10 mice/group. Mann-Whitney T-test was performed to determine differences between groups. (* $p<0.05$, ** $p<0.01$)

FXR activation enhances systemic anti-inflammatory cytokine production

In light of the tight functional connection between the spleen and the bloodstream, we aimed at determining the systemic effects of FXR activation, by measuring cytokine production in plasma. The plasma concentration of the pro-inflammatory cytokine IL-6 was remarkably high upon DSS treatment, irrespective of OCA administration. Interestingly,

the concentration of the anti-inflammatory cytokine IL-10 was significantly increased in mice receiving OCA. No significant differences were detected in the plasma concentrations of IFNγ, IL-2 and IL-17A. (Fig. 3). In conclusion, administration of OCA resulted in higher systemic levels of the anti-inflammatory cytokine IL-10.

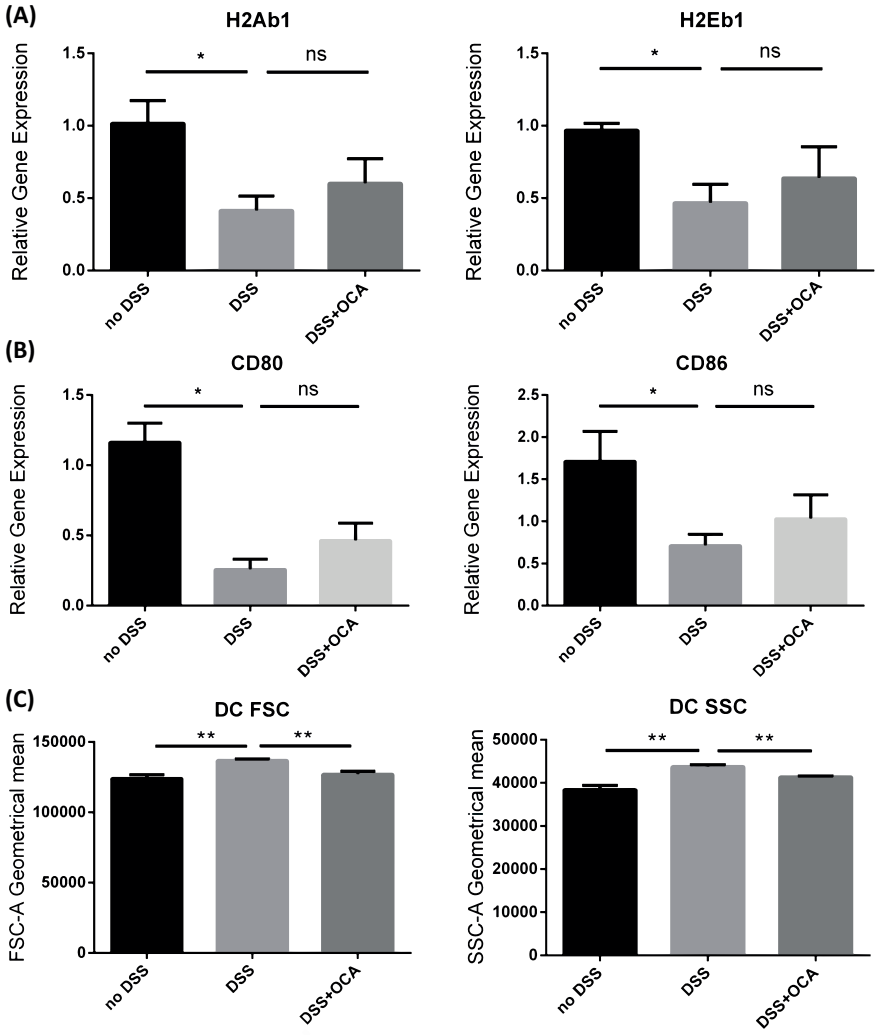

Fig. 2. OCA impacts on splenic depletion of DCs upon colitis induction. mRNA expression of MHCII encoding genes H2Ab1 and H2Eb1 **(A)** and of APC maturation markers CD80 and CD86 in spleen tissue of mice treated either with vehicle or DSS. Data are normalized to Hprt1 expression. **(B)**. **(C)** Geometrical mean of forward and side scatter signal of DCs defined as $CD11c^{+}MHCII^{+}$, derived from gating on live cells and out gating T-, B-cells and granulocytes. Data are represented as mean ± SEM. Mann-Whitney T-test was performed to determine differences between groups. (* $p<0.05$, ** $p<0.01$)

FXR is highly expressed in splenic DCs

FXR activation increased systemic levels of the anti-inflammatory cytokine IL-10, and abrogated the decrease in splenic DCs and increase in Tregs in DSS-treated mice. We

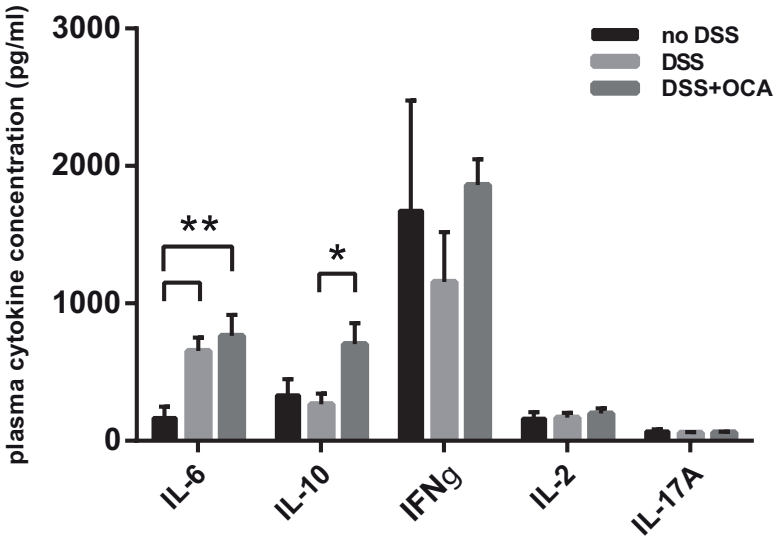

Fig. 3. FXR activation alters systemic cytokine concentration. Absolute concentration of cytokines IL-6, IL-10, IFNγ, IL-2 and IL-17A were determined in plasma of mice treated with either vehicle, DSS or DSS in combination with OCA. Data are represented as mean ± SEM, n=6 mice/group. Mann-Whitney T-test was performed to determine differences between groups. (* $p<0.05$, ** $p<0.01$)

therefore hypothesized that FXR is expressed in a subset of splenic cells. In order to investigate which immune cells express FXR, RNA was isolated from FACS-sorted subpopulations of immune cells in MLNs and spleen (Supplementary Fig. 4). FXR expression is lower in immune cells than in liver and intestinal cells (data not shown), but it is significantly higher in splenic DCs compared to lymph node DCs and splenic and MLN B, CD4-positive and CD8-positive cells (Fig. 4). Based on these data and data in Figure 1, we propose that FXR expressing splenic DCs respond to OCA treatment in DSS-treated colitis, potentially resulting in their retention in the spleen.

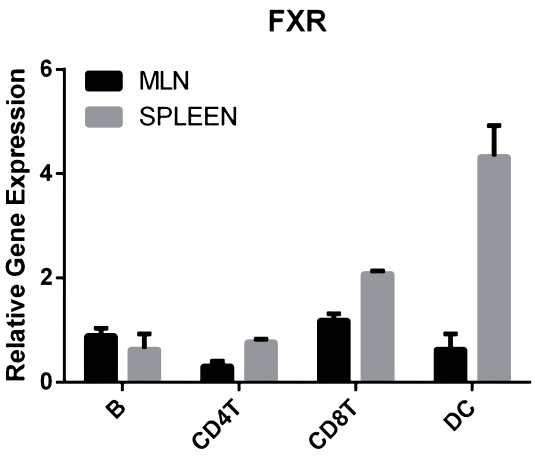

Fig. 4. FXR is expressed in splenic DCs. mRNA expression of the nuclear receptor FXR in FACS-sorted subsets of immune cells derived from either spleen or MLNs. Wild type healthy BL/6 mice were used for this purpose. RT-qPCR was performed in technical duplicate. Data are normalized to Gapdh expression. Data are represented as mean ± SD.

FXR activation modulates colonic chemotaxis events in favor of amelioration of colitis

We next addressed whether splenic DC depletion upon DSS treatment associates with an increase in migratory cells in the colon and whether OCA can counteract such immune cell infiltration. Intestinal MHCII/CD103-positive DCs express the chemokine receptor CXCR3 and migrate to the colon in response to inflammatory stimuli during a *Cryptosporidium parvum* infection[15]. In our study, the percentage of CXCR3-positive cells was significantly increased upon DSS treatment,

correlating with an increased influx of CXCR3-positive cells during colonic inflammation. OCA treatment tended to reverse the increase in CXCR3 expression in the colon (Fig. 5A/B), possibly contributing to the OCA-dependent decrease of recruitment of immune cells to the colon, including DCs. Also MHCII staining and CD11c mRNA expression were increased upon DSS treatment, and showed a trend to decrease upon OCA (Supplementary Fig. 5). To exclude that the changes in these DC markers are not due to changes in macrophage infiltration in the colon, as these markers are also expressed on macrophages, we determined gene expression of macrophage specific markers F4/80 and CD68. In support, neither of these two markers showed any enrichment upon DSS treatment or rescuing effect upon OCA (Fig. 5C/D), collectively underscoring that OCA treatment may cause a reduction in DC counts in the colon.

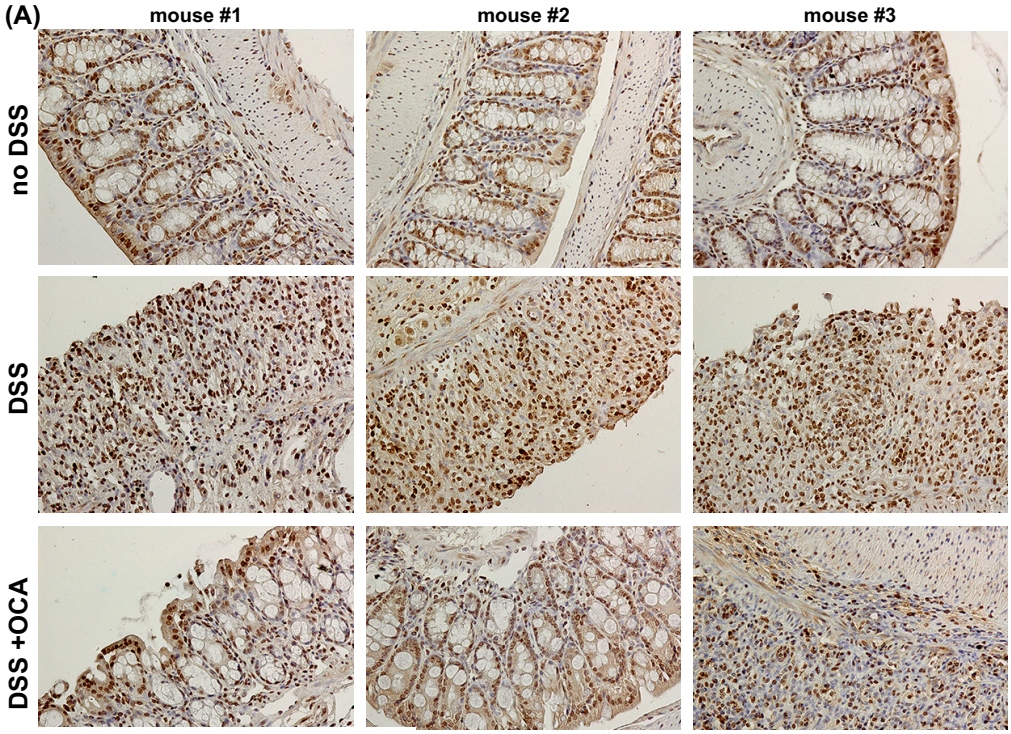

Fig. 5. FXR activation modulates colonic chemotaxis events in favor of amelioration of colitis. (A) Representative immunohistochemistry pictures of CXCR3$^+$ cells in paraffin-embedded colon sections collected from mice treated with either vehicle or DSS or DSS in combination with OCA. Sections of 3 different mice are depicted. **(B)** Relative amount of CXCR3$^+$ over hematoxylin-stained cells was determined using ImageJ; 10 independent microscope fields per section were analyzed (in 2 non consecutive sections/mouse; 10 mice/group). Data are represented as mean ± SEM. Kruskal-Wallis Anova test was performed for multiple comparison analysis.

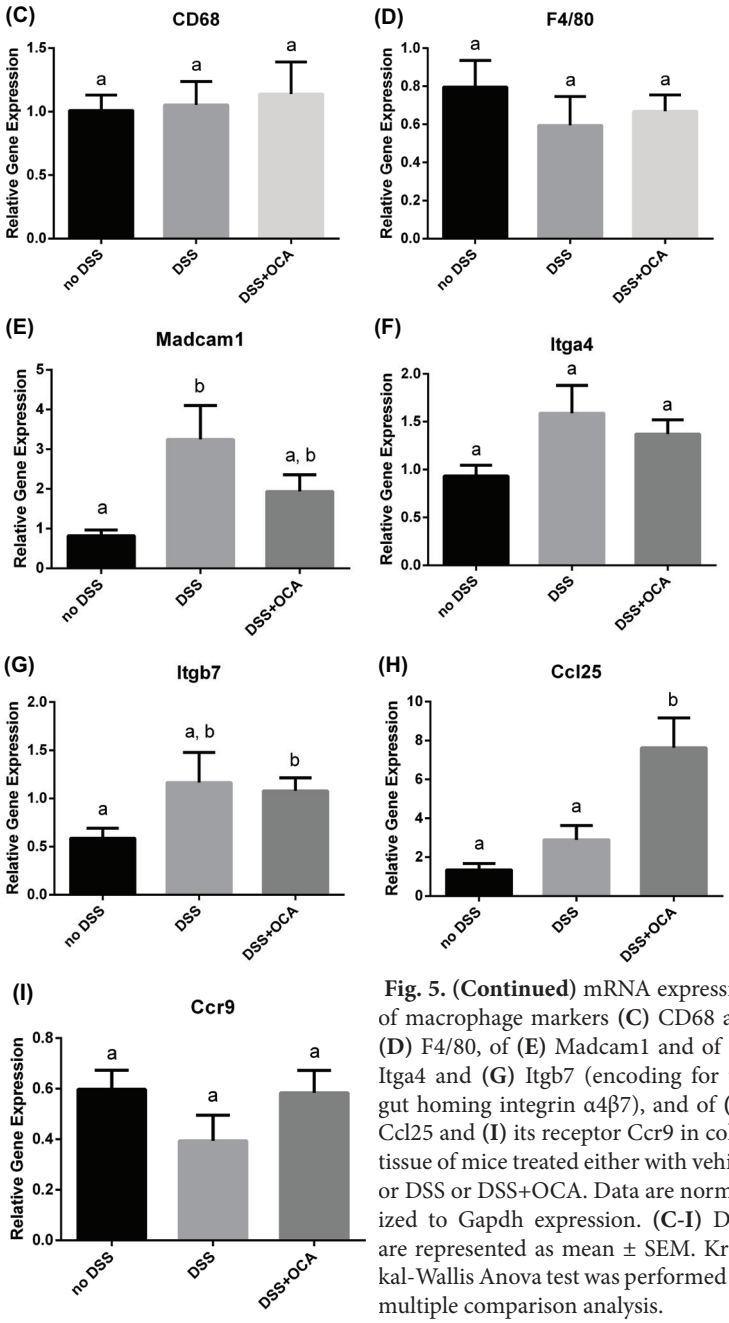

Fig. 5. (Continued) mRNA expression of macrophage markers **(C)** CD68 and **(D)** F4/80, of **(E)** Madcam1 and of **(F)** Itga4 and **(G)** Itgb7 (encoding for the gut homing integrin α4β7), and of **(H)** Ccl25 and **(I)** its receptor Ccr9 in colon tissue of mice treated either with vehicle or DSS or DSS+OCA. Data are normalized to Gapdh expression. **(C-I)** Data are represented as mean ± SEM. Kruskal-Wallis Anova test was performed for multiple comparison analysis.

To investigate further the local chemotaxis events affected by FXR activation, we determined gene expression levels of chemokine receptors and chemokine ligands in the colon (Fig. 5E-I). Madcam1 is a chemokine expressed in cytokine activated endothelial cells within the MLNs and in the lamina propria of the intestine. Colonic expression of Madcam1 increased significantly upon DSS treatment, and this increase was partially prevented by OCA treatment (Fig. 5E). The receptor for Madcam1, α4β7, an integrin expressed in T cells recruited to inflamed sites in the gut. Colonic expression of Itga4 and Itgb7 (encoding for the integrin α4β7) was not affected by OCA (Fig. 5F/G). Disruption of α4β7-Madcam axis is known to ameliorate symptoms of colitis[16]. Thus, inhibition of Madcam1 expression may contribute to OCA treatment-induced amelioration of colitis. Ccl25 is another chemokine with gut homing effects produced by small and large intestinal epithelial cells[17]. Ccl25 binds the chemokine receptor Ccr9. Tregs rely on Ccl25-Ccr9 axis for homing to intestine during ileitis[18]. Expression of Ccl25 increased upon

DSS and increased even further upon OCA treatment in DSS-treated mice, whereas changes in Ccr9 expression were modest (Fig. 5H/I). Unlike deficiency of the Madcam1-α4β7 axis which ameliorates colitis[16], disruption of Ccl25-Ccr9 axis worsens the symptoms of colitis[17]. Thus, OCA-induced improvement of colitis may depend on the increase in Ccl25 expression and the consequent recruitment of Tregs inhibiting the inflammatory process.
Together, these data suggest that FXR acts as a modulator of colonic chemotaxis of immune cells resulting in a decrease in colitis inflammatory symptoms.

DISCUSSION

IBD is thought to primarily result from a damaged mucosal barrier as a consequence of genetic factors or exogenous agents. The recurrent episodes of intestinal inflammation are promoted by the penetration of bacterial products through the damaged mucosal layer [1]. DSS-induced mouse colitis is a well-established model for studying human colitis, which encompasses a DSS-dependent damaging effect on the colonic epithelium, responsible for allowing bacterial translocation and therefore activating macrophages and neutrophils[19, 20]. However, recent studies question the role of bacterial translocation as primary event in the development of inflammation[21, 22]. Instead, DC activation is now considered a direct trigger after epithelial damage, sufficient to trigger production of chemokines and pro-inflammatory cytokines[9]. DCs are key sentinels able to sense pathogen and danger signals in the intestinal epithelium and deliver them to the lymphoid tissues, orchestrating an appropriate immune response to maintain mucosal homeostasis[9, 23]. DCs gain a functional phenotype able to enhance or attenuate the severity of DSS colitis, depending on the locally perceived stimuli[24]. Here we show that activation of the metabolic nuclear receptor FXR i) rescued depletion of splenic DCs and prevented local increases in Tregs, ii) increased the plasma concentration of IL-10, an anti-inflammatory cytokine, iii) collectively and consistently shows a trend for DC markers to be decreased in the colon, iv) decreased gene expression of intestinal homing factor for effector T cells Madcam1, and v) increased gene expression of intestinal homing factor for Tregs Ccl25 in DSS colitis (Figure 6).
MLNs host immunological changes relevant for mounting an inflammatory response in DSS colitis[25]. The relative amounts of granulocytes and Tregs were increased in the MLNs during DSS colitis (Fig. 1B/C). This is in line with a previous study[25], reporting that the percentage of CD11b/CD11c-positive phagocytes, and CD4/CD25-positive Tregs increased in MLNs upon DSS treatment. Although FXR activation improved the symptoms of colitis (Supplementary Fig. 1) in line with previous studies[7, 8], we did not observe significant immunological changes in the MLNs compared to the DSS group, suggesting that FXR mediated protection from colitis may rely on the involvement of different secondary lymphoid tissues, such as the spleen.
DSS treatment has been reported to cause splenomegaly[26, 27], and increase splenic Tregs and CD4/CD49-positive NK[25]. We report an increase in Tregs and a decrease in DCs in the spleen during DSS colitis. Tregs probably increase to restrain a dysregulated inflammatory response, and the OCA-mediated decrease in Tregs may therefore reflect the

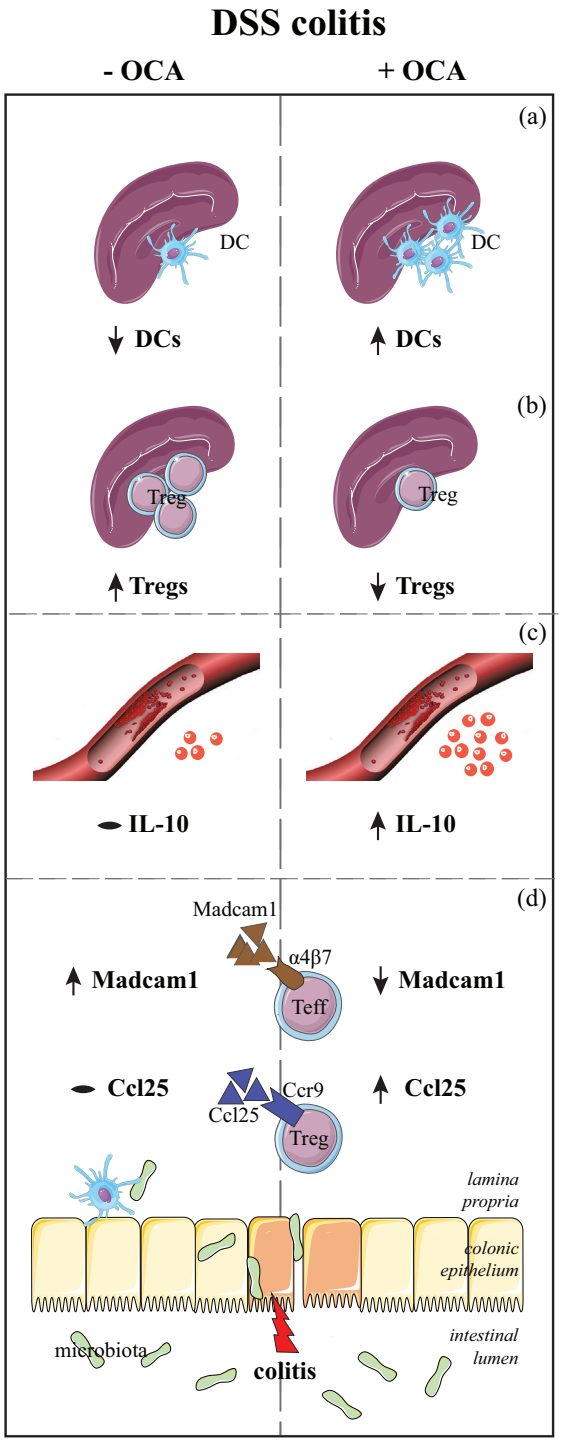

Fig. 6. Schematic representation of immunological effects of FXR activation during DSS colitis. Similar to IBD, DSS compromises the integrity of intestinal mucosal barrier, allowing bacterial translocation from the lumen to the lamina propria, where specialized antigen presenting cells react to the presence of danger signals. The inflammatory process involves the spleen where the amount of DCs reduces and Tregs increase. FXR activation reverses the effects of DSS colitis, probably via abrogation of the depletion of DCs (a) and the increase in Tregs in the spleen (b). At the systemic level, FXR activation causes an increase in anti-inflammatory cytokine IL-10 (c). In the colon, FXR activation attenuates the DSS-dependent increase of the gut homing chemokine Madcam1, which binds α4β7 on effector T cells and enhances the production of Ccl25 (d), attracting Tregs to contain the inflammation.

reduced need to limit intestinal inflammation. Analysis of DC morphology and surface-expressed activation markers suggested that DCs are likely more mature upon DSS treatment and OCA reverses this increase in maturation, suggesting that the decrease in DCs in the spleen cannot be explained by DC maturation differences. Of note, it has also been shown that the spleen stores reservoirs of monocytes readily deployable to migrate to injured tissue during acute inflammation[28, 29]. Together, the data suggest that OCA-mediated FXR activation may cause retention of monocyte DC progenitors in the spleen, which lowers their influx into the colonic inflammatory site, and thereby reduces colitis symptoms.

FXR has been shown to be expressed in immune cells derived from peripheral blood mononuclear cells (PBMCs) and immortalized immune cells[30, 31]. Here we show that FXR is highly expressed in mouse splenic DCs and we propose that it may have a role in modulation of DC function upon colitis induction. Con-

sidering that FXR activation can favor polarization of anti-inflammatory rather than of pro-inflammatory monocytes in liver inflammation[32], further studies are needed to establish whether FXR is preferentially expressed in DCs carrying a pro-inflammatory or anti-inflammatory phenotype during colitis. FXR has also been described to inhibit NF-κB transcriptional activity[7]. It could then be plausible that by FXR activation in DCs or monocyte DC progenitors, the signaling cascade that leads to migration to the colon is suppressed due to an FXR-mediated reduction in NF-kB signaling in DCs. However, our experimental setup precluded us from analysis whether OCA directly impacts on splenic immune cells or acts on the intestine, thereby indirectly altering the necessity of the splenic DCs to react to the inflammation.

Depletion of colonic DCs has proven to be beneficial for colitis, whereas adoptive transfer of DCs worsens the symptoms[9]. This indicates that DCs are critical in this model of colitis and implies that inhibition of their migration to the colon would be protective against DSS colitis features. Intriguingly, the chemokine receptor CXCR3, which is responsible for gut homing of DCs[15] was increased in mice with DSS colitis, and decreased by OCA treatment. CXCR3 is reported to be upregulated in IBD patients. In addition, ablation of CXCR3 attenuates the progression of DSS-induced colitis[33]. Taken together, these observations indicate that protection of OCA against colitis could involve colonic depletion of DCs and impaired expression of chemokine receptors. However, further cytofluorimetry-based assays of cells freshly isolated from colon are needed to validate that OCA actually impairs specific CXCR3-positive DC infiltration.

As the chemokine environment present in the colon is of utmost importance in shaping the immunological response, we determined the colonic expression of genes having gut or lymphoid tissue homing effects. α4β7-Madcam1 interaction guides effector T cells to the inflamed colon and the induction of migratory phenotype in effector T cells is dependent on DCs[34]. In our study, expression of Madcam1 increased in colitic mice and this increase was partially prevented by OCA treatment. These results provide insight into the potential effects of FXR activation on migratory properties of immune cells during colitis. Of note, targeting Madcam1 has been proven to be beneficial for colitis, as blocking Madcam1 *in vivo* reduces leukocyte extravasation and reverses both chronic and acute colitis[16, 35]. These observations support the beneficial role of FXR in counteracting gut homing signaling of immune cells fostering the inflammatory process.

The Ccr9-Ccl25 interaction is also ascribed as causal for gut homing effects, but targets different immune cells. Indeed, Tregs have been shown to be more dependent on Ccl25/Ccr9 than effector T cells for homing to the intestine[18]. Moreover, unlike α4β7-Madcam1 interaction, ablation of Ccr9-Ccl25 interaction exacerbates colitis, causes an imbalance in DC subpopulations (increase of plasmatcytoid/conventional DCs ratio) and leads to accumulation of inflammatory monocytes in the lamina propria of the colon and in the gut-associated lymphoid tissue[17]. Ccl25 levels in large intestine have been described to increase during the recovery period of DSS-treated mice, confirming a regulatory role of Ccr9-Ccl25 interactions during large intestinal inflammation[17]. In our study, expression of Ccr9 cells underwent a modest decrease upon DSS and went back to normal levels upon OCA treatment, whereas Ccl25 expression was strongly increased upon OCA

treatment. These results point to an FXR-dependent generation of strong chemotactic signals for Tregs, which can contain the inflammatory response and accelerate the recovery from colitis. It has yet to be determined whether intestinal cells expressing FXR produce Ccl25 or if FXR impacts on DC function, as bridging event for the recruitment of Tregs. Interestingly, DSS colitis increased IL-6 secretion systemically, whereas FXR activation counteracts inflammatory stimuli via systemic IL-10 increase. This is a remarkable finding, considering that IL-10 knockout mice develop colitis[36] and IL-10 administration reverses experimental colitis[37].

The extent of disease state in mice receiving DSS treatment is quite variable, depending on mouse strain[38], animal housing conditions and intestinal microbiota[39]. This probably explains why the FXR-mediated protection against DSS colitis was less pronounced than previously described[7]. Yet, the direction of changes induced by OCA treatment results in consistent beneficial effects across all measurements performed, pointing towards lowering the propagation of colonic inflammation to secondary lymphoid tissues. Our results strengthen our interest to further investigate the molecular mechanisms underlying these improvements and further encourage investigation of FXR agonists as treatment option in IBD patients.

In conclusion, our results support that FXR activation, previously shown to be beneficial for DSS colitis, impacts on the splenic immune response during colitis and can shift the balance in the colon and blood in favor of anti-inflammatory responses. Our work provides novel support to the emerging role of FXR in regulation of immune responses, broadening the well-established knowledge of its functions as metabolic sensor.

ACKNOWLEDGMENTS

Grant support: SWCvM is supported by the Netherlands Organization for Scientific Research (NWO) Project VIDI (917.11.365), FP7 Marie Curie Actions IAPP (FXR-IBD, 611979), the Utrecht University Support Grant, Wilhelmina Children's Hospital Research Fund. We thank Sameh Youssef Hassan and Ellen Willemsen for expert technical assistance and Luciano Adorini for critical reading of the manuscript.

REFERENCES

1. Podolsky DK. Inflammatory bowel disease. N Engl J Med 2002;347:417-29.
2. Farrell RJ, Kelleher D. Glucocorticoid resistance in inflammatory bowel disease. J Endocrinol 2003;178:339-46.
3. Ben-Horin S, Kopylov U, Chowers Y. Optimizing anti-TNF treatments in inflammatory bowel disease. Autoimmun Rev 2014;13:24-30.
4. Podolsky DK. Selective adhesion-molecule therapy and inflammatory bowel disease--a tale of Janus? N Engl J Med 2005;353:1965-8.
5. Wendt E, Keshav S. CCR9 antagonism: potential in the treatment of Inflammatory Bowel Disease. Clin Exp Gastroenterol 2015;8:119-30.
6. Gadaleta RM, Cariello M, Sabba C, et al. Tissue-specific actions of FXR in metabolism and cancer. Biochim Biophys Acta 2015;1851:30-9.
7. Gadaleta RM, van Erpecum KJ, Oldenburg B, et al. Farnesoid X receptor activation inhibits inflammation and preserves the intestinal barrier in inflammatory bowel disease. Gut 2011;60:463-

72.
8. Vavassori P, Mencarelli A, Renga B, et al. The bile acid receptor FXR is a modulator of intestinal innate immunity. J Immunol 2009;183:6251-61.
9. Berndt BE, Zhang M, Chen GH, et al. The role of dendritic cells in the development of acute dextran sulfate sodium colitis. J Immunol 2007;179:6255-62.
10. Kiss M, Czimmerer Z, Nagy L. The role of lipid-activated nuclear receptors in shaping macrophage and dendritic cell function: From physiology to pathology. J Allergy Clin Immunol 2013;132:264-86.
11. Cario E, Gerken G, Podolsky DK. Toll-like receptor 2 controls mucosal inflammation by regulating epithelial barrier function. Gastroenterology 2007;132:1359-74.
12. Xia CQ, Kao KJ. Effect of CXC chemokine platelet factor 4 on differentiation and function of monocyte-derived dendritic cells. Int Immunol 2003;15:1007-15.
13. Hartmann G, Weiner GJ, Krieg AM. CpG DNA: a potent signal for growth, activation, and maturation of human dendritic cells. Proc Natl Acad Sci U S A 1999;96:9305-10.
14. Darzynkiewicz Z, Bruno S, Del Bino G, et al. Features of apoptotic cells measured by flow cytometry. Cytometry 1992;13:795-808.
15. Lantier L, Lacroix-Lamande S, Potiron L, et al. Intestinal CD103+ dendritic cells are key players in the innate immune control of Cryptosporidium parvum infection in neonatal mice. PLoS Pathog 2013;9:e1003801.
16. Farkas S, Hornung M, Sattler C, et al. Blocking MAdCAM-1 in vivo reduces leukocyte extravasation and reverses chronic inflammation in experimental colitis. Int J Colorectal Dis 2006;21:71-8.
17. Wurbel MA, McIntire MG, Dwyer P, et al. CCL25/CCR9 interactions regulate large intestinal inflammation in a murine model of acute colitis. PLoS One 2011;6:e16442.
18. Wermers JD, McNamee EN, Wurbel MA, et al. The chemokine receptor CCR9 is required for the T-cell-mediated regulation of chronic ileitis in mice. Gastroenterology 2011;140:1526-35 e3.
19. Chassaing B, Aitken JD, Malleshappa M, et al. Dextran sulfate sodium (DSS)-induced colitis in mice. Curr Protoc Immunol 2014;104:Unit 15 25.
20. Okayasu I, Hatakeyama S, Yamada M, et al. A novel method in the induction of reliable experimental acute and chronic ulcerative colitis in mice. Gastroenterology 1990;98:694-702.
21. Kitajima S, Morimoto M, Sagara E, et al. Dextran sodium sulfate-induced colitis in germ-free IQI/Jic mice. Exp Anim 2001;50:387-95.
22. Fukata M, Michelsen KS, Eri R, et al. Toll-like receptor-4 is required for intestinal response to epithelial injury and limiting bacterial translocation in a murine model of acute colitis. Am J Physiol Gastrointest Liver Physiol 2005;288:G1055-65.
23. Rescigno M, Urbano M, Valzasina B, et al. Dendritic cells express tight junction proteins and penetrate gut epithelial monolayers to sample bacteria. Nat Immunol 2001;2:361-7.
24. Abe K, Nguyen KP, Fine SD, et al. Conventional dendritic cells regulate the outcome of colonic inflammation independently of T cells. Proc Natl Acad Sci U S A 2007;104:17022-7.
25. Hakansson A, Tormo-Badia N, Baridi A, et al. Immunological alteration and changes of gut microbiota after dextran sulfate sodium (DSS) administration in mice. Clin Exp Med 2015;15:107-20.
26. Zhang R, Ito S, Nishio N, et al. Dextran sulphate sodium increases splenic Gr1(+)CD11b(+) cells which accelerate recovery from colitis following intravenous transplantation. Clin Exp Immunol 2011;164:417-27.
27. Wang Y, Han G, Chen Y, et al. Protective role of tumor necrosis factor (TNF) receptors in chronic intestinal inflammation: TNFR1 ablation boosts systemic inflammatory response. Lab Invest 2013;93:1024-35.
28. Ingersoll MA, Platt AM, Potteaux S, et al. Monocyte trafficking in acute and chronic inflammation. Trends Immunol 2011;32:470-7.
29. Swirski FK, Nahrendorf M, Etzrodt M, et al. Identification of splenic reservoir monocytes and their deployment to inflammatory sites. Science 2009;325:612-6.

30. Schote AB, Turner JD, Schiltz J, et al. Nuclear receptors in human immune cells: expression and correlations. Mol Immunol 2007;44:1436-45.
31. Renga B, Migliorati M, Mencarelli A, et al. Reciprocal regulation of the bile acid-activated receptor FXR and the interferon-gamma-STAT-1 pathway in macrophages. Biochim Biophys Acta 2009;1792:564-73.
32. McMahan RH, Wang XX, Cheng LL, et al. Bile acid receptor activation modulates hepatic monocyte activity and improves nonalcoholic fatty liver disease. J Biol Chem 2013;288:11761-70.
33. Chami B, Yeung AW, van Vreden C, et al. The role of CXCR3 in DSS-induced colitis. PLoS One 2014;9:e101622.
34. Johansson-Lindbom B, Svensson M, Wurbel MA, et al. Selective generation of gut tropic T cells in gut-associated lymphoid tissue (GALT): requirement for GALT dendritic cells and adjuvant. J Exp Med 2003;198:963-9.
35. Kato S, Hokari R, Matsuzaki K, et al. Amelioration of murine experimental colitis by inhibition of mucosal addressin cell adhesion molecule-1. J Pharmacol Exp Ther 2000;295:183-9.
36. Kiesler P, Fuss IJ, Strober W. Experimental Models of Inflammatory Bowel Diseases. Cell Mol Gastroenterol Hepatol 2015;1:154-170.
37. Sasaki M, Mathis JM, Jennings MH, et al. Reversal of experimental colitis disease activity in mice following administration of an adenoviral IL-10 vector. J Inflamm (Lond) 2005;2:13.
38. Knod JL, Crawford K, Dusing M, et al. Mouse strain influences angiogenic response to dextran sodium sulfate-induced colitis. J Surg Res 2014;190:47-54.
39. Rossi O, Khan MT, Schwarzer M, et al. Faecalibacterium prausnitzii Strain HTF-F and Its Extracellular Polymeric Matrix Attenuate Clinical Parameters in DSS-Induced Colitis. PLoS One 2015;10:e0123013.

SUPPLEMENTARY FIGURES

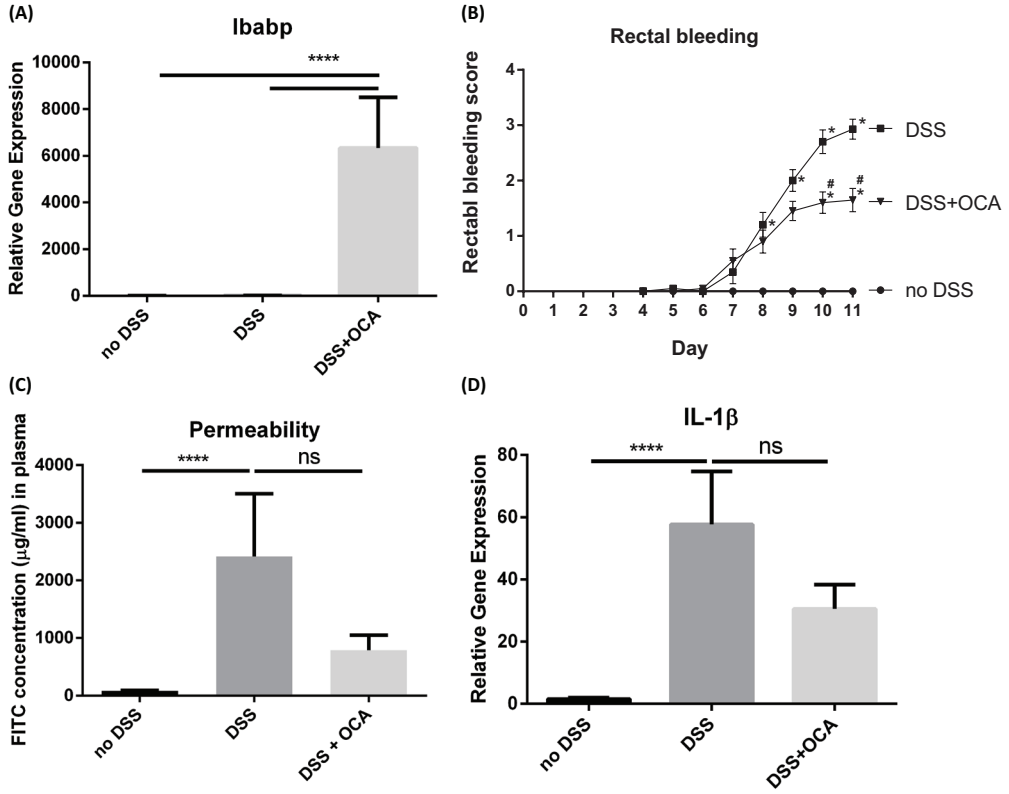

Supplementary Fig. 1. OCA improves DSS-induced colitis.
(A) mRNA expression of the FXR target gene IBABP in colonic tissue of mice treated with either vehicle or OCA after 8 days of DSS treatment. Data are represented as mean ± SEM. (n=10 mice/group). Data are normalized to Gapdh expression. Mann-Whitney T-test was performed to determine differences between groups.**(B)** Rectal bleeding score as measure for the grade of inflammation and thus for the severity of the colitis. Mann-Whitney T-test was performed to determine differences between groups. Significances are indicated with * when comparing the mice receiving DSS to the vehicle mice and with # when comparing the DSS+OCA group to the DSS group. (* or # $p<0.05$) **(C)** *In vivo* intestinal permeability measurement following 8 days either of vehicle or DSS or DSS in combination with OCA. Mann-Whitney T-test was performed to determine differences between groups. (**D)** mRNA expression of pro-inflammatory cytokine IL-1β in colonic tissue of mice treated with either vehicle or OCA after 8 days of DSS treatment. Data are normalized to Gapdh expression. Mann-Whitney T-test was performed to determine differences between groups.

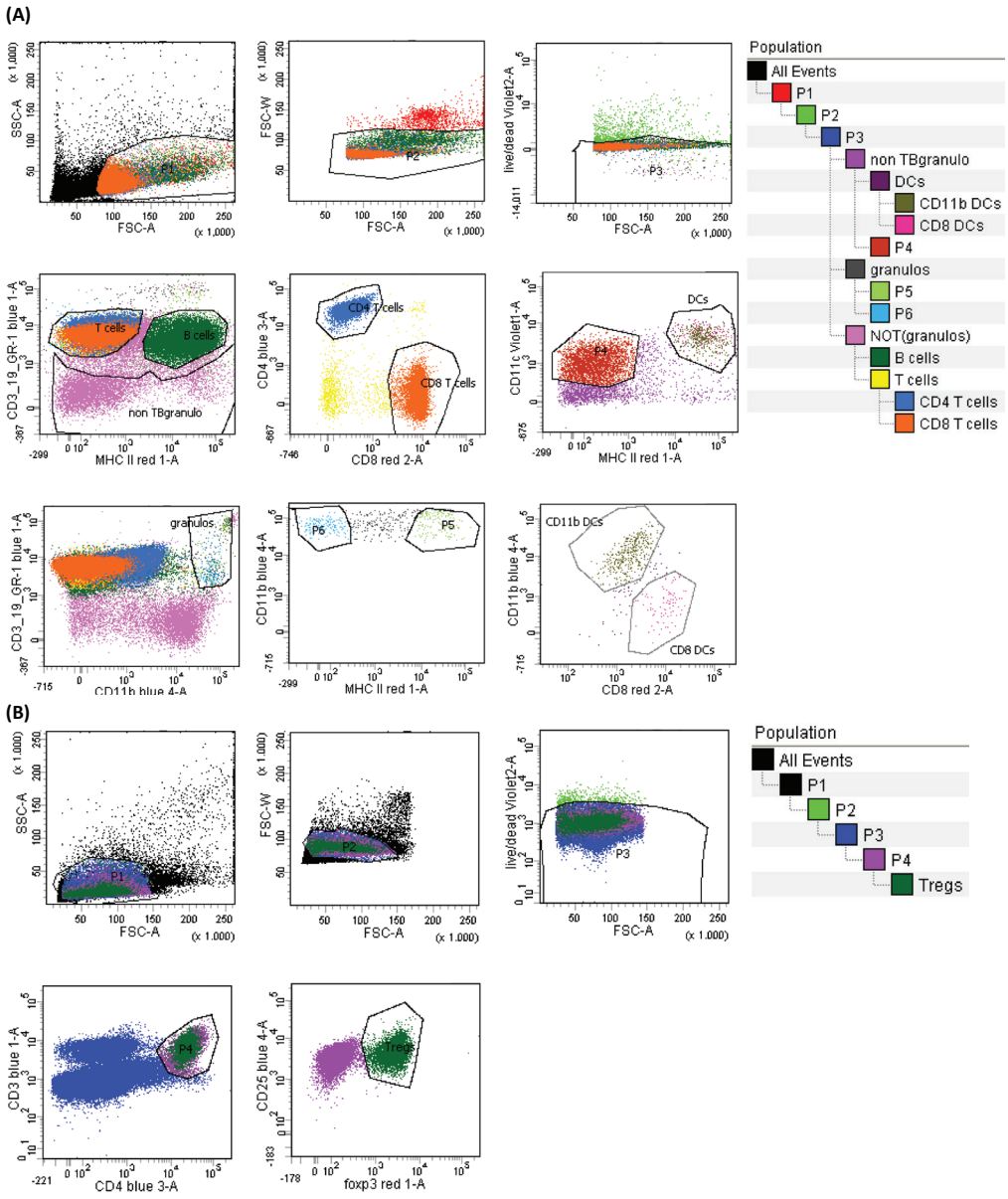

Supplementary Fig. 2. FACS analysis of immune cell populations during colitis.
Spleen and MLNs were passed through a cell strainer to make a single-cell suspension and then stained with fluorochrome-labeled mouse antibodies directed against CD3, MHCII, CD11c, CD19, GR-1, CD11b, CD4, CD8 and CD25, Foxp3. Details of the gating procedure used to define the populations of DCs, Tregs, granulocytes, B cells, CD4T and CD8T cells are depicted in **(A)** for staining of surface receptors and in **(B)** for intracellular staining.

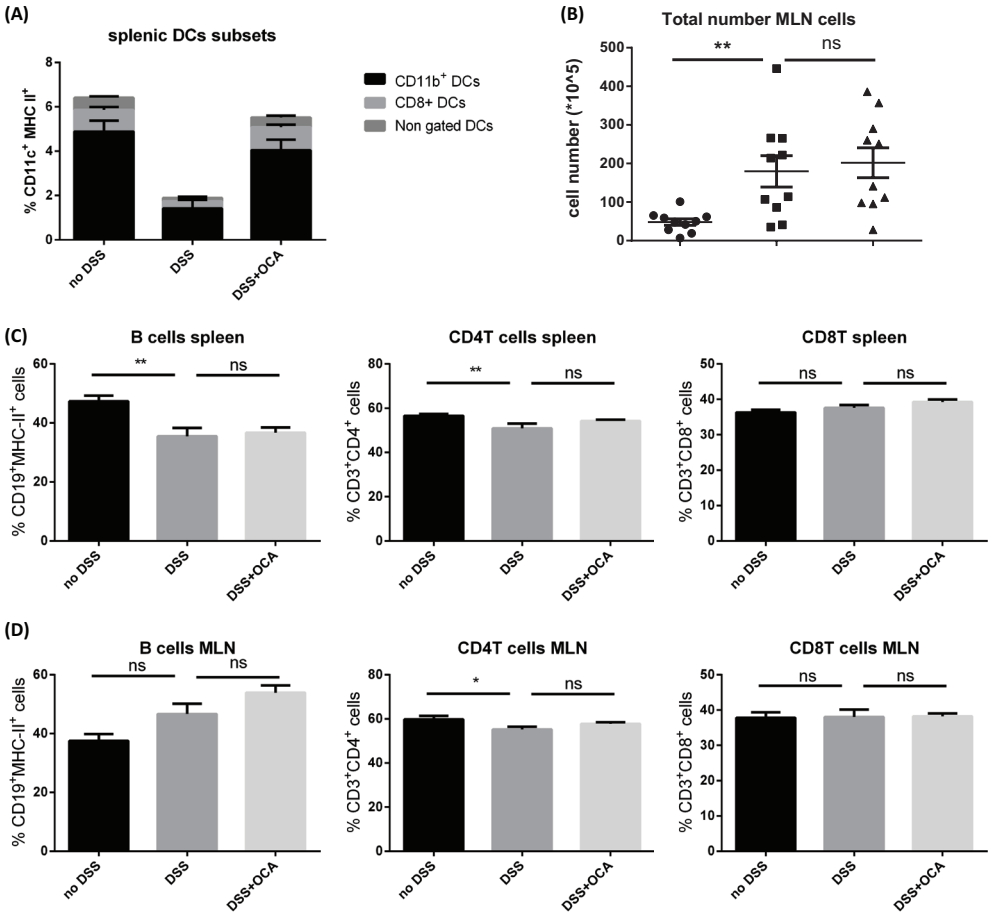

Supplementary Fig. 3. FXR activation alters the composition of splenic immune cell populations. **(A)** Composition of splenic DCs defined as $CD11c^{+}MHCII^{+}$, derived from gating on live cells and out gating T-, B-cells and granulocytes. Relative abundance of $CD11b^{+}$ and $CD8^{+}$ DCs is shown. **(B)** Determination of the total number of cells collected from MLNs. Data are represented as mean ± SEM, n=10 mice/group. Mann-Whitney T-test was performed to determine differences between groups. (**p<0.01) **(C)** FACS analysis of B cells, $CD8^{+}$ T cells and $CD4^{+}$ T cells in spleen and **(D)** MLNs. The relative amount of B cells ($CD19^{+}MHCII^{+}$), $CD8^{+}$ T cells ($CD3^{+}CD8^{+}$) and $CD4^{+}$ T cells ($CD3^{+}CD4^{+}$) was determined in mice either treated with vehicle, DSS or DSS+OCA. Data are represented as mean ± SEM, n=10 mice/group. Mann-Whitney T-test was performed to determine differences between groups. (* p<0.05, **p<0.01)

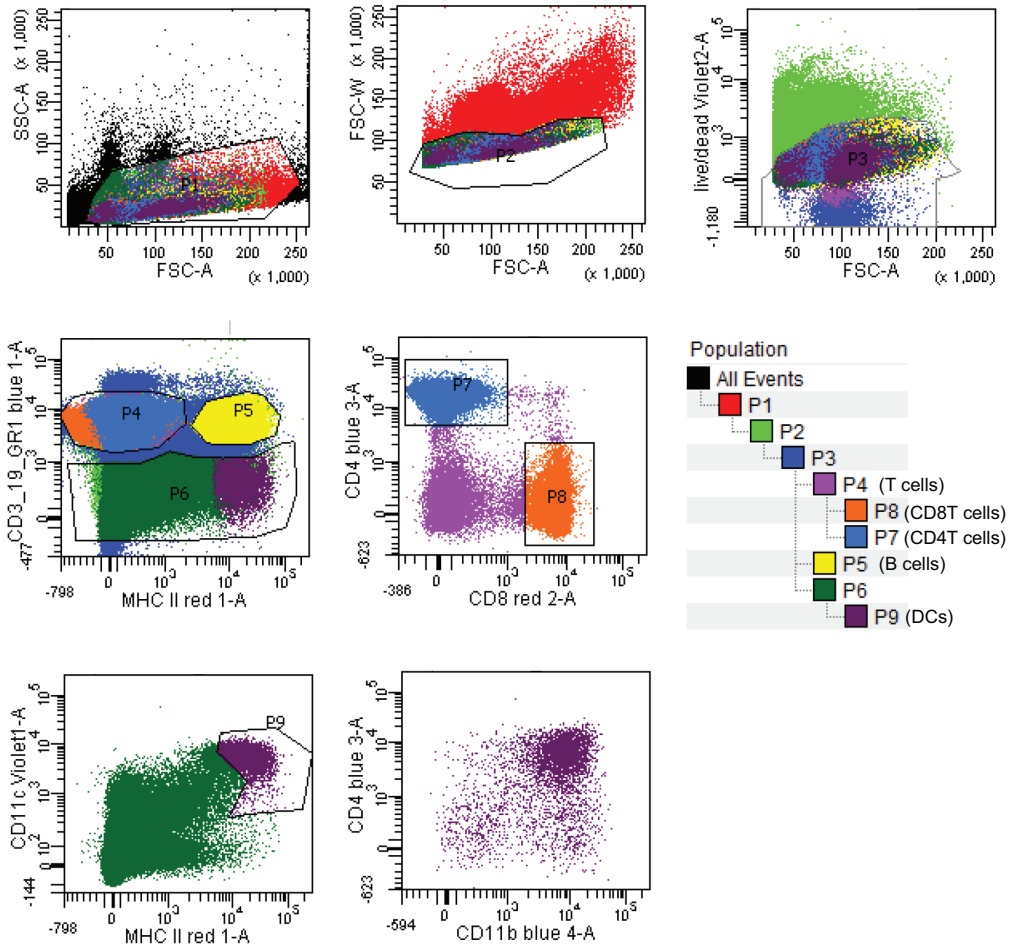

Supplementary Fig. 4. FACS sorting of immune cells for gene expression analyses.
Speen and MLN-derived cell suspentions were stained with fluorochrome-labeled antibodies against CD3, MHCII, CD11c, CD19, GR-1, CD11b, CD4, CD8 and CD25, Foxp3 and sorted by FACS in separate tubes prior to RNA extraction. Details of the gating procedure used to define the populations of DCs (P9), B cells (P5), CD4T cells (P7) and CD8T cells (P8) are depicted.

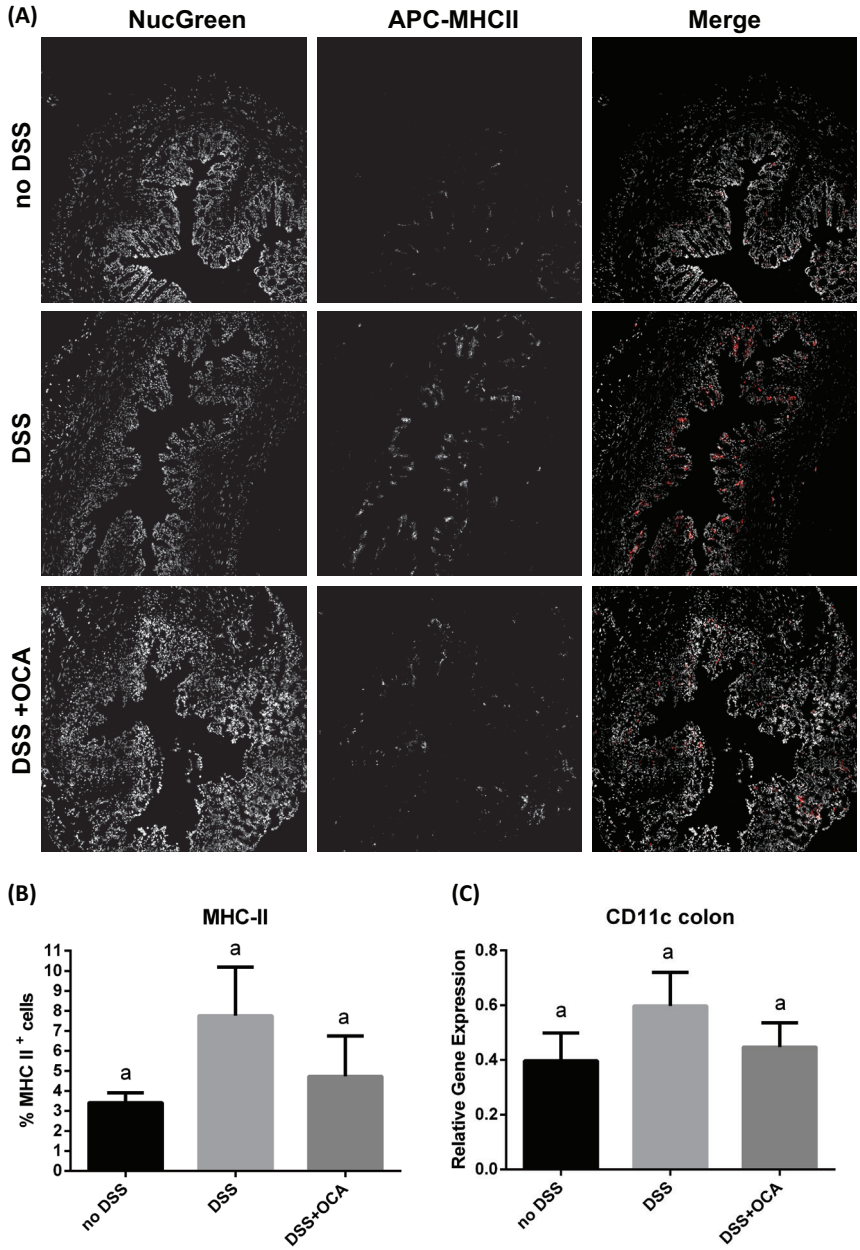

Supplementary Fig. 5. Determination of MHCII⁺ cells and CD11c expression in colon.
(A-B) Representative immunohistochemistry pictures of MHCII⁺ cells in frozen colon sections collected from mice receiving vehicle or DSS or DSS in combination with OCA. Sections were double stained with NucGreen for nuclear staining (left panels) and with an antibody against MHCII (middle panels) conjugated with the red fluorophore allophycocyanin (APC). Right panels represent a merge of both stainings from which the relative number of MHC⁺ over NucGreen-stained cells was determined using ImageJ; 2 independent microscope fields per section were analyzed in 2 non consecutive sections/mouse; 5 mice/group. **(C)** mRNA expression of the integrin CD11c in colonic tissue of mice treated with either vehicle or OCA after 8 days of DSS treatment. Data are represented as mean ± SEM. Data are normalized to Gapdh expression.

SUPPLEMENTARY TABLE

Supplementary table 1. qRT-PCR primers (5'->3')

Il1β Fw	CCTCAATGGACAGAATATCAACCAA
Il1β Rv	TCTCCTTGTACAAAGCTCATGGAG
CD11c Fw	GCAGACACTGAGTGATGCCA
CD11c Rv	TCGGAGGTCACCTAGTTGGG
Itga4 Fw	GGCACTCCTACAACCTGGAC
Itga4 Rv	GATGAGCCAGCGCTTCGAC
Itgb7 Fw	GGAAATCTACGACCGACGGG
Itgb7 Rv	TGTTGTCCTGCTTCCAGTTGA
Madcam1 Fw	GGAGATTCCAGTACTACAGAGCC
Madcam1 Rv	TGATGTTGAGCCCAGTGGAG
Ccl25 Fw	CGTGCTGTGAGATTCTACTTCC
Ccl25 Rv	CTCCTCACGCTTGTACTGTTG
Ccr9 Fw	TTCCCCTCCTGTCTCTTTCCA
Ccr9 Rv	ATAATGCAGACCAGCCTCCAG
Ibabp Fw	TTGAGAGTGAGAAGAATTACGATGAGT
Ibabp Rv	TTTCAATCACGTCTCCCTGGAA
H2Ab1 Fw	AGCCCCATCACTGTGGAGT
H2Ab1 Rv	GATGCCGCTCAACATCTTGC
H2Eb1 Fw	GCGGAGAGTTGAGCCTACG
H2Eb1 Rv	AGGCCCGTGGACACAATTC
CD80 Fw	TCGTCTTTCACAAGTGTCTTCAG
CD80 Rv	TTGCCAGTAGATTCGGTCTTC
CD86 Fw	CCTCCAAACCTCTCAATTTCAC
CD86 Rv	GGAGGGCCACAGTAACTGAA
F4/80 Fw	CTTTGGCTATGGGCTTCCAGTC
F4/80 Rv	GCAAGGAGGACAGAGTTTATCGTG
CD68 Fw	GACCTACATCAGAGCCCGAGT
CD68 Rv	CGCCATGAATGTCCACTG


FXR
DNA

CHAPTER 6

SILAC-based proteomics identifies HOXA9 and NSD1 as interactors of FXR

Vittoria Massafra, Ellen C.L. Willemsen, Harmjan R. Vos, José M. Ramos Pittol, Alexandra Milona, Boudewijn M.T. Burgering, Eric Kalkhoven, and Saskia W.C. van Mil

Manuscript in preparation

ABSTRACT

The Farnesoid X Receptor (FXR) is a bile salt nuclear receptor which regulates bile acid, lipid, glucose and amino acid metabolism in the liver and intestine. FXR also has the capacity to decrease the inflammatory response. Its transcriptional activity can be regulated through ligand binding and posttranslational modifications, and also through interactions with transcriptional cofactors and other transcription factors, but the 'FXR interactome' has not been studied extensively. In the present study, we therefore used stable isotope labelling by amino acids in cell culture (SILAC) to identify FXR interacting proteins in an unbiased manner. Besides its obligate heterodimeric partner RXR, we identified NSD1, ZNF35, HOXA9 and HOXA5 as FXR-binding proteins and validated their interaction with FXR *in vitro*. The transcription factor HOXA9 and the H3K36 methylase NSD1 decreased and increased FXR activity in reporter assays, respectively. In addition, mutagenesis of the nuclear receptor binding LXXLL motif (amino acids 1552-1556) in human NSD1 protein reduced its ability to stimulate FXR transcriptional activity. Finally, we describe that FXR induces the expression of NSD1 and BHMT, the latter being involved in the generation of methyl donor amino acids for NSD1 activity. These findings support a feed-forward mechanism in which FXR can induce expression of NSD1 (and BHMT), which in turn binds and activates FXR. Identification of novel interacting proteins, including NSD1 in the present study, may provide new insights into the metabolic and anti-inflammatory functions of this nuclear receptor.

INTRODUCTION

The Farnesoid X receptor (FXR) is a bile acid-binding transcription factor belonging to the superfamily of nuclear receptors (NRs) [1-3]. FXR functions as an enterohepatic regulator of bile acid homeostasis, nutrient metabolism, and inflammation [4]. Pharmacological modulation of FXR activity by full agonists proved to be favourable in clinical trials for primary biliary cholangitis (PBC) [5], type 2 diabetes, and non-alcoholic steatohepatitis (NASH) [6, 7] and was shown to be beneficial for gallstone disease [8, 9] and inflammatory bowel disease (IBD) [10] in mouse models. In common with other nuclear receptors, the FXR protein consists of an N-terminal activation function (AF1) domain and a DNA binding domain (DBD) that is connected to the ligand binding domain (LBD) by a flexible hinge [11, 12].

Regulation of transcription by FXR contains many layers of complexity and is thought to be mediated by different DNA binding motifs, tissue-specific isoforms, post-translational modifications (PTMs), as well as differentially recruited cofactors. The DBD of FXR binds to FXR responsive elements (FXREs) which consist of an inverted repeat of the sequence AGGTCA with a 1-base pair spacing (IR-1) [13-15], although FXR has also been shown to bind other motifs, such as the directed repeat DR-1 [16, 17] and everted repeat ER-8 [18]. Differential promoter usage and alternative splicing generate 4 different FXR isoforms (α1, α3 vs α2, α4), which regulate differential transcriptional programs [19-21]. In addition, FXR activity on the classical FXR targets BSEP and SHP is increased upon methylation of Lys206 by Set7/9 [22], whereas acetylation and sumoylation have been shown to coordinate the ability of FXR to transrepress inflammatory genes [23]. Despite recent advances in understanding the biology of FXR, the molecular mechanisms underpinning the regulation of FXR activity are largely unknown. Gaining more insights into the complexity of FXR signalling is imperative for the rational design of a new generation of FXR drugs, selectively activating or repressing subgroups of FXR target genes while not interfering with other target genes, thereby reducing side effects.

In the absence of ligands, FXR binds FXREs as a heterodimer with its obligated partner RXR, in association with co-repressor proteins, such as the nuclear corepressor (NCOR) and SMART [24, 25]. Upon bile acid (BA) binding, a conformational change of the protein complex occurs, resulting in the release of corepressors and thereby becoming permissive to the recruitment of coactivators, such as steroid receptor coactivator 1 (SRC-1) [1, 2, 26], peroxisome-proliferator-receptor (PPAR)-γ coactivator-1α (PGC1α), [27, 28], coactivator associated arginine (R) methyl transferase-1 (CARM-1) [29], and vitamin-D-receptor-interacting protein-205 (DRIP-205) [30].

Discovery of novel FXR interactors has been relying so far on targeted *in vitro* and *in cell* protein-protein interaction (PPI) studies or non-cell based screenings [31]. Here, we set out to apply an untargeted screening method to detect proteins interacting with FXR in HepG2 cells. We identified proteins co-purified with FXR by mass spectrometry, validated novel interactions by independent PPI analyses and provide evidence that some of these novel interactors regulate FXR activity.

MATERIALS AND METHODS

Generation of stable cell lines

For SILAC purposes, the FXRα2 sequence was subcloned into the pcI-113 (kind gift from Geert Kops, UMC Utrecht) and pEBB-flag vector to obtain GFP- and flag-tagged FXR fusion proteins. Tagged FXRs were subsequently subcloned into a pLenti-CMV-neo vector. For the follow-up gene expression studies of NSD1 and BHMT, GFP and GFP-FXR were cloned into a pLV-CMV-IRES-puro vector carrying a puromycin resistance cassette. Lentiviral particles were produced in HEK293T cells and used for stable overexpression of GFP-FXR and GFP in HepG2 cells.

Cell culture and SILAC labeling

HepG2 cells were cultured in DMEM 1g/L glucose containing 10% FBS, 2mM glutamine and 100 µg/mL penicillin/streptomycin at 37 °C under 5% CO_2 and 95% humidity. For the SILAC experiment, HepG2 Wt, GFP-FXR or flag-FXR were cultured in Light (K0, R0) or Heavy (K8, R10 ($^{15}N_2{}^{13}C_6$-lysine, $^{15}N_4{}^{13}C_6$-arginine, Silantes, Germany)) SILAC DMEM medium (High glucose, PPA The Cell Culture Company, Pasching, Austria) supplemented with 10% FBS (light medium) or dialyzed (3K) FBS (heavy medium) (Thermo Fisher Scientific, Waltham, MA, U.S.), 2mM glutamine, 100 µg/mL penicillin/streptomycin and natural or isotopically labelled amino acids (73 µg/mL L-lysine and 29.4 µg/mL L-arginine) for 10 doublings. Maximal incorporation of the heavy label was established by LC/MS analysis. HepG2 GFP-FXR cells (3x 15cm dishes per condition) were treated with either DMSO or 1 µM GW4064 for 24 hours.

Nuclear fractionation

Nuclear extraction was performed as described previously [32]. Briefly, cells were trypsinized and washed twice with PBS. Cells were swollen in a hypotonic buffer and then lysed by dounce homogenizing in presence of 0.15% NP40, complete proteinase inhibitor and 0.5 mM DTT. After centrifugation, the pellet consisting of nuclei was lysed by 90 min incubation in 2 volumes of nuclear lysis buffer (420 mM NaCl, 20 mM Hepes–KOH pH 7.9, 20 % (v/v) glycerol, 2 mM $MgCl_2$, 0.2 mM EDTA, 0.1% NP40, complete proteinase inhibitor and 0.5 mM DTT). After lysis, extracts were centrifuged and the supernatant containing the soluble nuclear extract was snap frozen and stored at -80°C. Protein concentrations were determined by Pierce BCA Protein Assay Kit (Thermo Fisher Scientific) and equal protein amounts of light and heavy extract were subsequently used for the GFP pull down.

GFP affinity purification and mass spectrometry sample preparation

GFP pulldown on nuclear and cytoplasmic extracts was performed as described previously [32]. Briefly, extracts were incubated with GFP-Trap_A beads (Cromoteck, Hauppauge, NY, U.S.) in lysis buffer (300 mM NaCl, 20 mM Hepes–KOH pH 7.9, 20 % (v/v) glycerol, 2 mM $MgCl_2$, 0.2 mM EDTA, 0.1% NP40, complete proteinase inhibitor (Complete, Roche Applied Science, Penzberg, Germany) and 0.5 mM DTT), with addition of 50ug/mL EtBr to prevent protein-DNA-protein interactions. Beads were washed 2 times

in lysis buffer and in PBS in presence of 0.25% NP40 and one time in PBS only. During the last wash, beads derived from light and heavy extracts were mixed 1:1. Proteins were digested on-bead and peptides were desalted and purified using a FASP protocol, as described previously [32, 33].

Mass spectrometry and data analysis

The tryptic peptides were applied to online nanoLC-MS/MS, using a 120-min gradient from 7% until 32% acetonitril followed by stepwise increases up to 95% acetonitril. Mass spectra were recorded on a LTQ-Orbitrap-Velos mass spectrometer (Thermo Fisher Scientific), selecting the 15 most intense precursor ions of every full scan for fragmentation. Raw data were analyzed by MaxQuant (version 1.2.2.5) [34] using standard settings with the additional options match between runs, LFQ and iBAQ selected. The generated list of proteins was filtered for contaminants, reverse hits, number of unique peptides (≥ 2) in Perseus (from MaxQuant package). Protein enrichment was evaluated as light/heavy log2 ratio.

Plasmids and generation of NSD1 truncation

A truncated version of mouse Nsd1 (amino acids 1-891) was generated by subcloning Nsd1 sequence from pSG5-flag-Nsd1 vector (kind gift from P. Chambon, IGBMC, Illkirch-Graffenstaden, France [35]) into the pcDNA3.1 vector. pCMV6-Myc-DDK-hNSD1, pCMV6-AC-hFLYWCH2, pCMV6-XL5-hZNF35 and pCMV6-Xl4-hHOXA5 were obtained from OriGene (Rockville, MD, U.S.). pCDNA3-hHOXA9 was kind gift from S. Bandyopadhyay ([36], Cleveland Clinic Foundation, Cleveland, OH, U.S.).

GST pull down assays

GST protein isolation and pull down assays were performed as described elsewhere [10]. Briefly, BL21 competent bacteria were transformed with expression plasmids for GST, GST-hFXRα2 or GST-hFXRα2-LBD. GST fusion proteins were expressed upon induction with 1 mM isopropyl 1-thio-β-D-galactopyranoside and purified on glutathione-sepharose beads (Amersham Biosciences, Amersham, UK), using elution buffer (20 mM glutathione, 100 mM Tris, pH 8.0, 120 mM NaCl). The full-length coding sequences of ZNF35, HOXA5, HOXA9 and the partial coding sequence of Nsd1 (amino acids 1-891) were transcribed and translated *in vitro* in reticulocyte lysate in the presence of [^{35}S] methionine (Amersham Biosciences) according to the manufacturer's protocol (TNT T7 Coupled Transcription/Translation kit, Promega, Madison, WI, U.S.). ^{35}S-Labeled proteins were incubated with GST fusion proteins in NETN buffer (20 mM Tris, pH 8.0, 100 mM NaCl, 1 mM EDTA, 0.5% NP-40) containing protease inhibitors. Samples were subsequently washed and subjected to SDS-PAGE. Coomassie brilliant blue was used to visualize GST proteins. [^{35}S]-labeled proteins were detected by autoradiography and analyzed with a Storm 820 apparatus (Molecular dynamics, Pharmacia Biotechnology, Amersham Biosciences, Diegem, Belgium).

Reporter assays

HEK293T cells were co-transfected with pGL3-SHP, pGL3-IBABP, or pGL3-BSEP, pRL-TK Renilla, and empty pCDNA3.1, pcDNA3.1-FXRα2, pCMV6-Myc-DDK-hNSD1, pSG5-flag-mNsd1 or pCDNA3-hHOXA9, together with pcDNA-RXRα, using the calcium phosphate method, as described elsewhere [37]. After 24h, cells were incubated either with DMSO or 1μM GW4064 for 24 hours. Cells were lysed and Firefly and Renilla luciferase activity were measured according to the manufacturer's instructions (Dual Luciferase Reporter Assay System, Promega, Madison, WY, U.S.), using the Centro LB 960 Luminometer (Berthold Technologies, Vilvoorde, Belgium). Protein amount of FXR (anti-FXR, Cat. Nr. sc-13063; Santa Cruz Biotechnology, Dallas, TX, U.S.), and actin (anti-actin, Cat. Nr. A5060; Sigma, Saint Louis, MO, U.S.) in the lysates used for reporter assays was assessed by immunoblotting.

Mutagenesis and *in silico* analyses

In order to generate the mutated motifs FSTAA or LGEAA in human NSD1, site-directed mutagenesis of the leucines 910-911 and 1555-1556, respectively, was carried out in pCMV6-Myc-DDK-hNSD1, according to the manufacturer's protocol (Quick change site directed mutagenesis Kit, Stratagene, La Jolla, CA, U.S.). Similarly, substitution of leucines 806-807 or 1453-1454 into alanines in mouse Nsd1 was performed in pSG5-flag-mNsd1. Primers used for the mutagenesis are listed in Supplementary table 1.
Sequence alignment of NSD1 protein across multiple species was performed using CLC Sequence viewer 7 (Qiagen, Hilden, Germany). NCBI accession numbers of the sequences included in the analysis are NP_071900.2 (H. sapiens), XP_527132.2 (P. troglodytes), AFH33588.1 (M. mulatta), XP_005619221.1 (C. lupus familiaris), XM_002689032.5 (B. taurus), NP_032765.3 (M. musclulus) and NP_001100807.1 (R. Norvegicus).

Knock down and gene expression analyses

HepG2 cells were transfected with the SMART pool ON-TARGET plus NSD1 siRNA (L-007048-00) or with ON-TARGET plus Non-targeting pool control siRNA (D-001810-10), following the manufacturer's instructions (Dharmacon, Layafette, Co, U.S.). RNA was isolated from HepG2 cells using TRIzol reagent (Invitrogen, Carlsbad, CA, U.S.). cDNA was generated from 500 ng of total RNA using SuperScript II Reverse Transcriptase (Invitrogen). qRT-PCR analysis was performed using FAST Start PCR master mix (Roche, Basel, Switzerland) and analyzed on a MyIQ real time PCR cycler (BioRad, Hercules, CA, U.S.). Primer sequences are listed in Supplementary Table 2.

Statistical analyses

For the analysis of the luciferase assays a One-way Anova test was applied to determine significant differences between groups. For the gene expression data a student T-test was applied. Statistical tests were performed, as appropriate, using GraphPad Software (La Jolla, U.S). (*p-value <0.05).

RESULTS

Identification of FXR interacting proteins by SILAC-based proteomics

We set out to identify proteins that interact with FXR in living cells, by performing SILAC-based proteomics. We cultured HepG2 overexpressing GFP-FXR in SILAC medium containing 'light' amino acids (L-lysine and L-arginine) and stimulated cells with either GW4064 or DMSO. To enable quantification of identified proteins, we cultured HepG2 wild type cells grown in SILAC medium containing 'heavy' amino acids for 10 doublings (Fig. 1A). A GFP pull down experiment was performed on the nuclear extracts, and the protein extract from light HepG2 GFP-FXR treated with or without GW4064 was mixed 1:1 to the protein extract from heavy HepG2 wild type cells. The light-heavy protein sample was trypsinized, and purified peptides were analysed by mass spectrometry. The FXR bait and its heterodimeric partner RXR were enriched in the GFP pull down (Fig. 1B), as expected. The proteins FLYWCH2, NSD1, ZNF35, HOXA9 and HOXA5 were also enriched in the GFP pull down, and therefore classify as potential novel FXR interacting proteins. The enrichment of both RXR and these proteins in the GFP pull down assay was independent of the treatment with GW4064, indicating that FXR-ligand binding does not affect the interaction to these proteins (Fig. 1B). To exclude false positive hits in our analysis, we subjected HepG2 cells that express flag-FXR - other than those expressing GFP-FXR - to the same analysis. After GFP pull down and mixing with the heavy-labelled internal standard, FLYWCH2, NSD1, ZNF35, HOXA9 and HOXA5 were pulled down in cells expressing GFP-FXR but much less in flag-FXR HepG2 cells (Fig. 1C). This indeed suggests that these proteins are detected due to binding to FXR, rather than being enriched due to FXR overexpression. Taken together, these results suggest that FLYWCH2, NSD1, ZNF35, HOXA9 and HOXA5 are putative novel FXR interactors. A full list of putative FXR interactors as determined by comparing enrichment of GFP and flag expressing cells is shown in Table 1.

Independent validation of novel FXR interacting proteins

To independently validate the interaction between FXR and the proteins identified by mass spectrometry, we analyzed the binding of recombinant purified GST-FXR or GST-FXR-LBD to *in vitro* translated, [^{35}S]-methionine-labeled Nsd1, ZNF35, HOXA9 or HOXA5. Nsd1, ZNF35, HOXA9 or HOXA5 were pulled down with GST-FXR and GST-FXR-LBD fusion proteins, but not with GST alone (Fig. 2). Addition of GW4064 did not alter the binding of FXR to these interactors, in line with the SILAC experiment. In the case of Nsd1, a truncated version of the mouse cDNA (encoding amino acids 1-891), which includes the nuclear receptor interaction domain (NID) previously reported [35], was used because of the high molecular weight of the full length NSD1 protein. The FLYWCH2 protein could not be analysed in this assay, as *in vitro* translation in the presence of [^{35}S]-methionine did not yield sufficient amounts of radioactive protein, probably due to the presence of only 2 methionine residues in FLYWCH2. The amount of GST, GST-FXR and GST-FXR-LBD proteins loaded was comparable in each case (Fig. 2, lower panels). These data therefore independently support that Nsd1 (1-891), ZNF35, HOXA9 and HOXA5 bind to FXR, irrespective of FXR activation by GW4064.

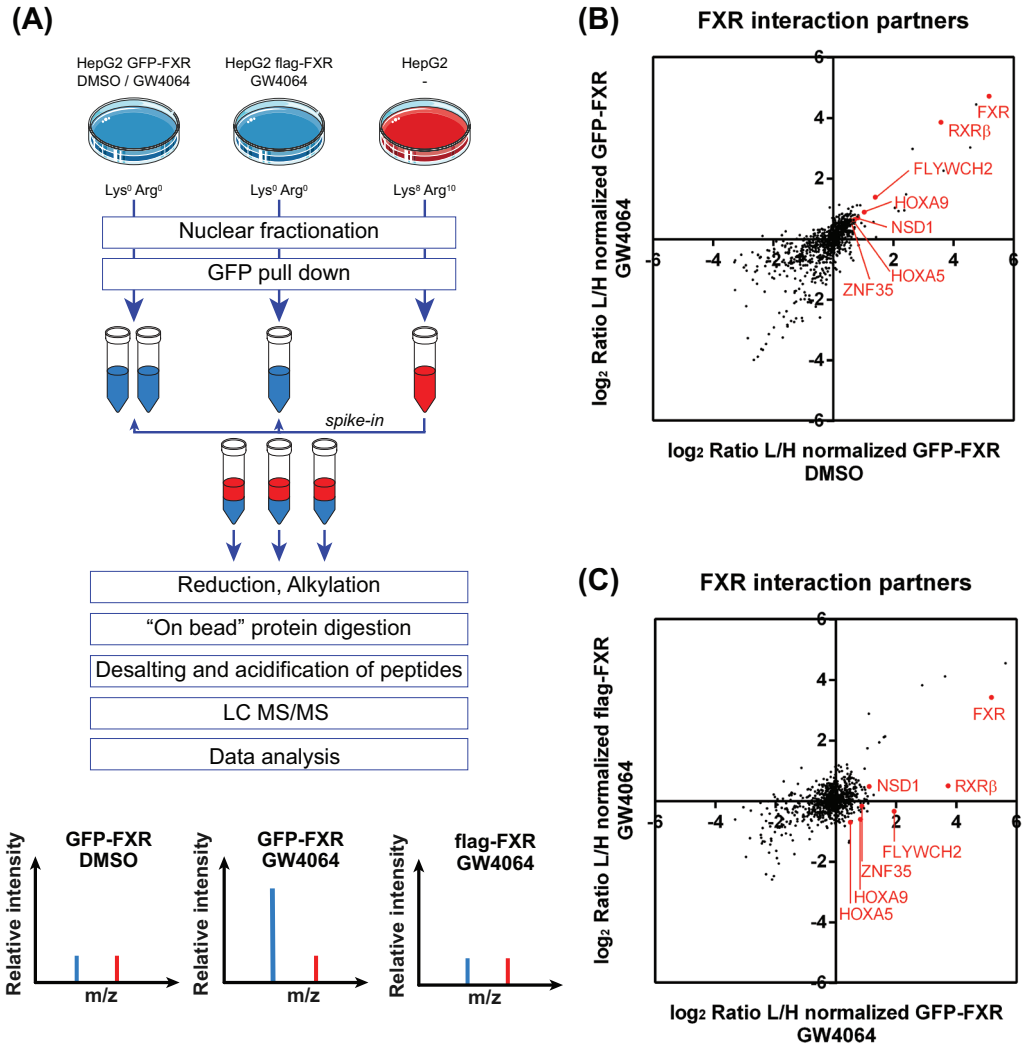

Fig. 1. Identification of FXR interacting proteins by SILAC-based proteomics. (A) Schematic representation of the experimental outline to determine FXR interactors in HepG2 GFP-FXR cultured in 'light' SILAC medium and stimulated with either DMSO or GW4064 for 24 h, while using HepG2 wild type cells grown in 'heavy' SILAC medium for 10 doublings as internal control for appropriate quantification. HepG2 cells in which flag-FXR was overexpressed, were cultured in 'light' SILAC medium and served as a control cell line to exclude false positives. (B-C) Scatterplots depicting the relative enrichment of proteins co-purified with FXR. (B) Relative enrichment of HepG2 GFP-FXR cells treated with DMSO versus GW4064. (C) Relative enrichment of HepG2 GFP-FXR versus HepG2 flag-FXR, both in presence of GW4064.

HOXA9 and NSD1 regulate FXR activity

To address the functional consequences of the binding between FXR and the interacting proteins identified above, in intact cells, we performed reporter assays in HEK293T cells. For this, FXR was expressed with or without the interacting protein, using 3 different reporter vectors harbouring the promoters of well-established direct FXR target genes:

Table 1. List of candidate FXR interactors

Gene names	Protein names	Ratio L/H normalized GFP-FXR GW4064
NR1H4 (FXR)	Bile acid receptor, farnesoid X receptor	36.0
RXRB	Retinoic acid receptor RXR-beta	13.3
FLYWCH2	FLYWCH family member 2	3.8
NSD1	Histone-lysine N-methyltransferase, H3 lysine-36 and H4 lysine-20 specific	2.2
LAS1L	Ribosomal biogenesis protein LAS1L	2.1
ZBED4	Zinc finger BED domain-containing protein 4	2.1
EXO1	Exonuclease 1	2.1
NOL9	Polynucleotide 5-hydroxyl-kinase NOL9	2.0
SMC4	Structural maintenance of chromosomes protein 4;Structural maintenance of chromosomes protein	2.0
PAX3	Paired box protein Pax-3	2.0
NUMA1	Nuclear mitotic apparatus protein 1	1.9
MAP7D3	MAP7 domain-containing protein 3	1.9
ZNF35	Zinc finger protein 35	1.8
KIF20B	Kinesin-like protein KIF20B	1.8
ZNF618	Zinc finger protein 618	1.8
TTK	Dual specificity protein kinase TTK	1.8
HSPA1B;HSPA1A	Heat shock 70 kDa protein 1A/1B	1.8
HOXA9	Homeobox protein Hox-A9	1.8
MAP1B	Microtubule-associated protein 1B;MAP1 light chain LC1	1.7
VPS37B	Vacuolar protein sorting-associated protein 37B	1.7
PAX6	Paired box protein Pax-6	1.7
SMC3	Structural maintenance of chromosomes protein 3	1.5
GEN1	Flap endonuclease GEN homolog 1	1.4
PSIP1	PC4 and SFRS1-interacting protein	1.4
YEATS4	YEATS domain-containing protein 4	1.4
BRCA1	Breast cancer type 1 susceptibility protein	1.4
SERBP1	Plasminogen activator inhibitor 1 RNA-binding protein	1.4
ARID2	AT-rich interactive domain-containing protein 2	1.4
HOXA5	Homeobox protein Hox-A5	1.4
C1orf55	UPF0667 protein C1orf55	1.4
HOXB6	Homeobox protein Hox-B6	1.4
EWSR1	RNA-binding protein EWS	1.4
KHDRBS1	KH domain-containing, RNA-binding, signal transduction-associated protein 1	1.4

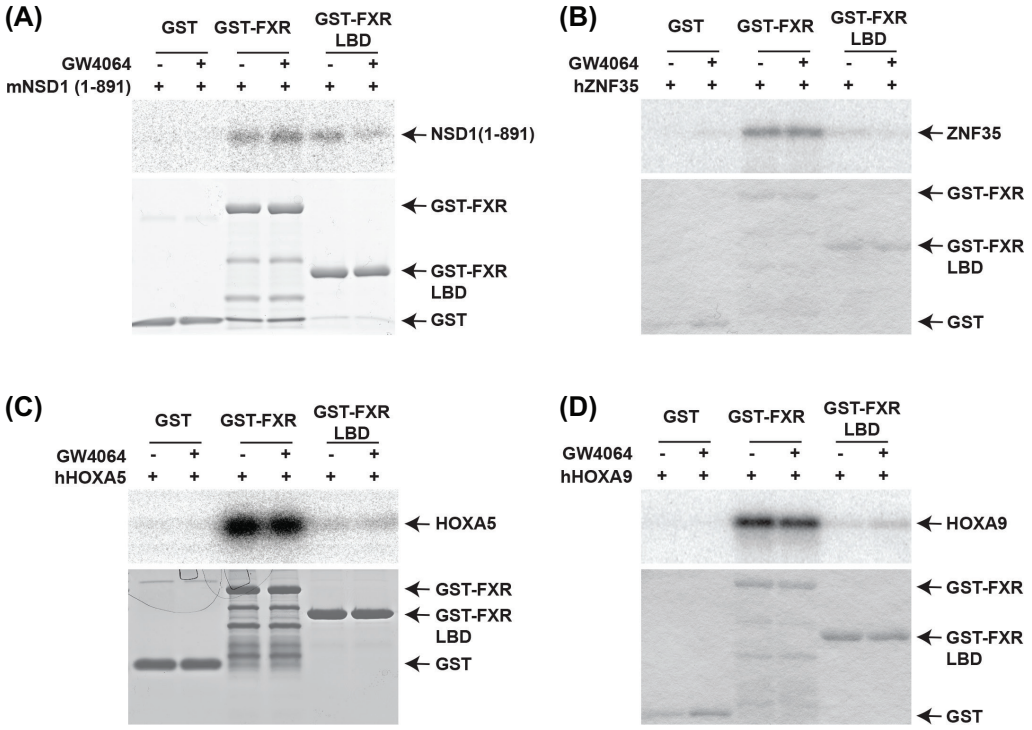

Fig. 2. Independent validation of novel FXR interacting proteins. Nsd1 (A), ZNF35 (B), HOXA5 (C) and HOXA9 (D) proteins were *in vitro* translated using [^{35}S] methionine. GST-pull down assays were performed by incubating translated proteins with GST, GST-FXR and GST-FXR-LBD bound beads. Upper panels: auto-radiograph; lower panels: Coomassie Brilliant Blue staining of GST proteins.

6

Ibabp, Bsep and Shp. As shown in Fig. 3A, the ability of FXR to activate all three reporter genes in response to GW4064 stimulation was reduced when cells were co-transfected with increasing concentrations of HOXA9 (Fig. 3A). Conversely, co-transfection of full length mouse Nsd1 enhanced FXR activity on all three target gene promoters (Fig. 3B). In agreement with these findings, overexpression of the human NSD1 protein, which shares a high degree of homology with its mouse homologue, also increased the activity of all 3 reporter genes (Fig. 3C). Hoxa5 and ZNF35, which were also identified by SILAC as potential FXR interacting proteins (Fig. 1 and 2 and Table 1), did not affect FXR activity under these experimental conditions (data not shown). Protein expression of FXR in the lysates from co-transfected cells did not change when NSD1 was co-transfected (Fig. 3D), indicating that the increase in FXR activity was not due to an NSD1-induced increase in FXR protein expression.

Nuclear receptors bind transcriptional coregulators via short α-helical LXXLL motifs [38, 39]. The NSD1 protein contains three LXXLL motifs, or variants thereof (ϕXXLL). The most N-terminal motif in the mouse Nsd1 protein (FXXLL; aa 803-808) has been characterized as a functional motif for binding to the thyroid hormone receptor (TR), retinoid acid receptor (RAR), retinoid X Receptor (RXR), and estrogen receptor (ER) [35, 40],

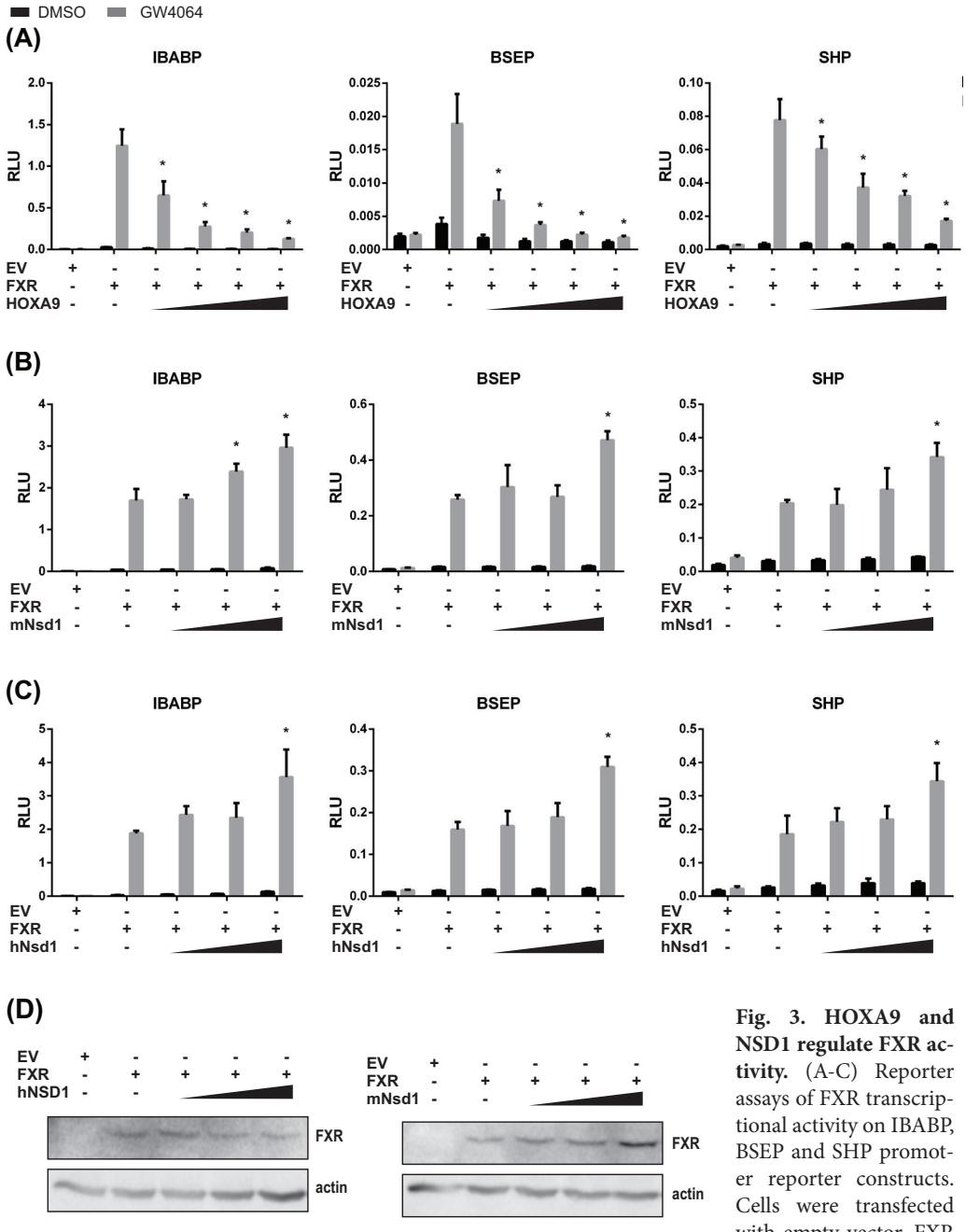

Fig. 3. HOXA9 and NSD1 regulate FXR activity. (A-C) Reporter assays of FXR transcriptional activity on IBABP, BSEP and SHP promoter reporter constructs. Cells were transfected with empty vector, FXR with or without HOXA9 (A), mouse Nsd1 (B) and human NSD1 (C), and stimulated with DMSO or 1μM GW4064 for 24h. Data are reported as mean ± SD. Statistical significance determined by 2-way Anova test is reported in comparison to cells transfected with FXR without HOXA9/NSD1 and stimulated with GW4064 (*p<0.05). (D) Representative immunoblot of FXR protein expression in lysates from cells expressing the Ibabp promoter-containing vector from panel (B) and (C).

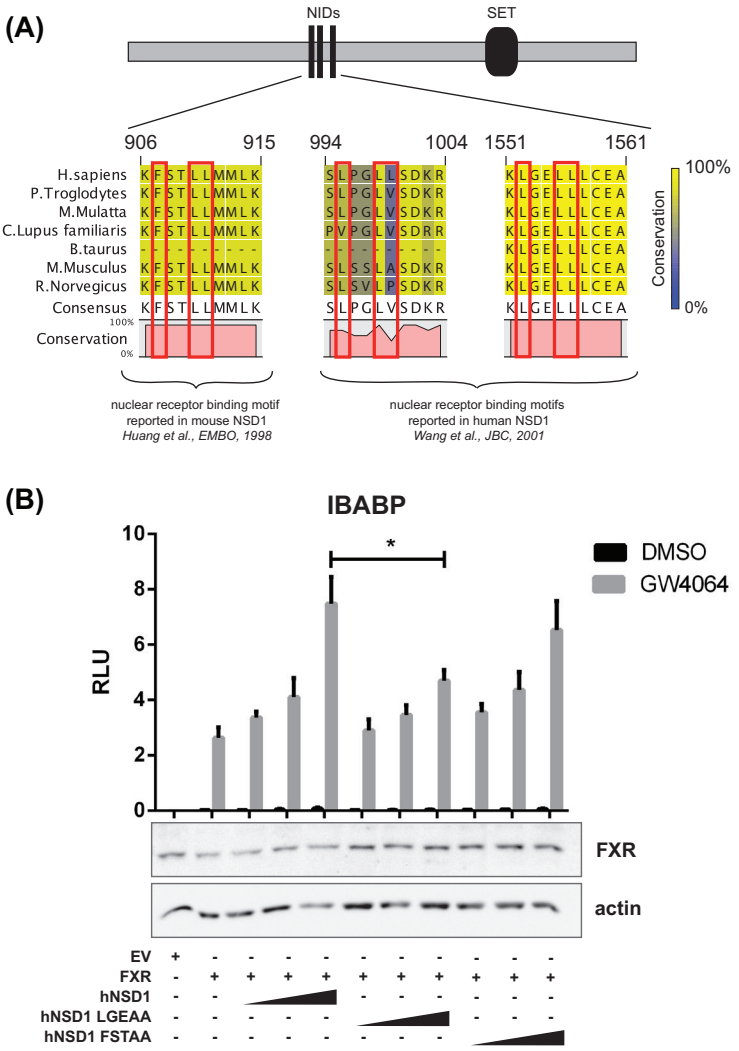

Fig. 4. Mutagenesis of LGELL motif reduces NSD1 regulation of FXR activity. (A) Amino acid sequence alignment of LXXLL motifs in NSD1 protein previously reported to bind nuclear receptors. (B) Reporter assay of FXR transcriptional activity on IBABP. Cells were transfected with empty vector, FXR alone or in combination with either wild type NSD1, NSD1-LGEAA or NSD1-FSTAA. Data are reported as mean ± SD. Statistical significance was determined by 2-way Anova test (*p<0.05). Lower panel represents protein expression of FXR and actin loading control in the respective lysates from cells treated with GW4064 used in the reporter assay.

while a region including the central and C-terminal motif in the human NSD1 protein (LXXLL; aa 726-730 and aa 1283-1287) have been shown to interact with the androgen receptor (AR) [41]. Further downstream, NSD1 contains a catalytically active SET domain (Su(var)3-9 and 'Enhancer of zeste' proteins (Fig. 4A). Our analysis of the conservation of these three motifs across multiple species reveals that the FSTLL sequence (aa 907-911, hNSD1 isoform b) and the LGELL sequence (aa 1552-1556, hNSD1 isoform b) are conserved in human, chimpanzee, Rhesus monkey, dog, cow, mouse and rat (Fig. 4A). As the amino acid context surrounding the LXXLL motif contributes to binding specificity in the interaction with certain nuclear receptors [42], we analysed the amino acid context surrounding the LXXLL motifs in NSD1 and found that this is strongly conserved across multiple species as well. The centrally located LPGLL motif (aa 995-999, hNSD1 isoform b) is not conserved between species and is unlikely to have a functional α-helical binding motif due to the presence of a proline residue.

In order to assess whether NSD1 increases FXR activity, as a result of NSD1 binding to

FXR, we mutated the FSTLL (aa 907-911) and LGELL (aa 1552-1556) sequences in human NSD1. Substitution of LGELL into LGEAA significantly decreased FXR activity induced by NSD1, whereas mutagenesis of the FSTLL sequence did not alter NSD1 effect on FXR activity (Figure 4B). Protein concentration of FXR in the lysates from co-transfected cells did not change upon NSD1 co-transfection. These preliminary data suggest that FXR binding to NSD1 occurs via the LGELL motif.

FXR activation regulates the expression of NSD1 and its cofactor generator BHMT

To investigate whether a positive or negative feedback loop may exist between FXR and NSD1, we examined NSD1 mRNA expression in HepG2-GFP-FXR cells treated with or without GW4064. We observed that GW4064 treatment increased the expression of NSD1 in GFP-FXR, but not in GFP HepG2 cells (Fig. 5A). In addition, FXR overexpression rescued the decrease in NSD1 expression achieved by NSD1 knock down (Fig. 5B), further substantiating that FXR regulates NSD1 at the mRNA level. In conclusion, an intricate bidirectional regulation seems to exist between NSD1 and FXR; NSD1 induces FXR function, and FXR activates transcription of NSD1.

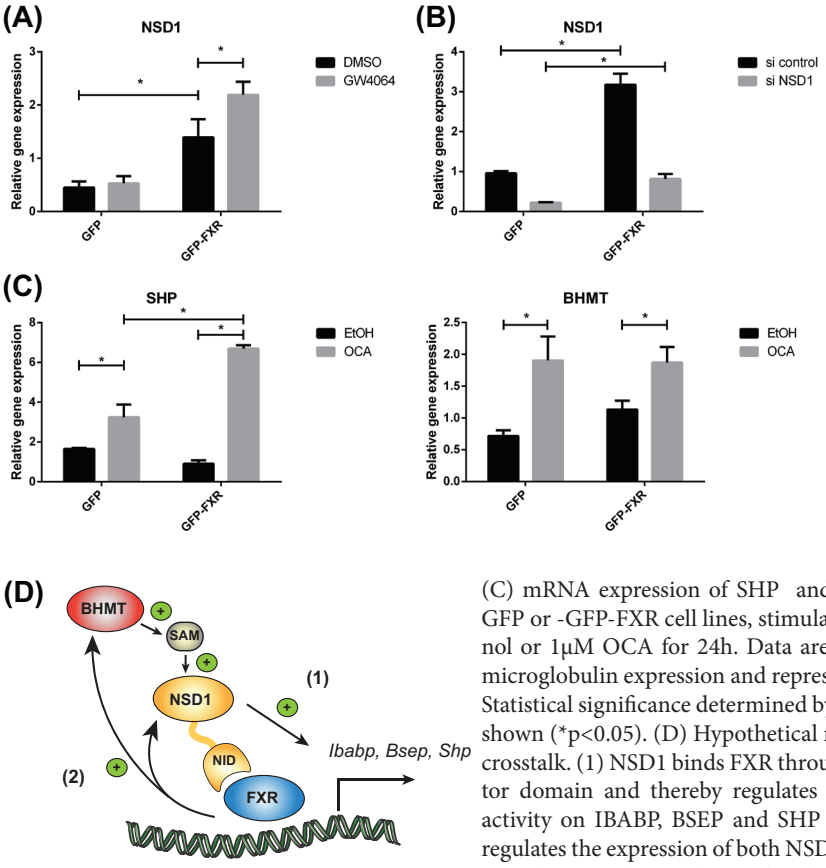

Fig. 5. FXR activation regulates the expression of NSD1 and its cofactor generator BHMT. (A) mRNA expression of NSD1 in HepG2-GFP or HepG2-GFP-FXR cell lines stimulated with either DMSO or GW4064 for 24h. (B) NSD1 mRNA expression analysis in HepG2-GFP and HepG2-GFP-FXR cells transfected with either control siRNA or NSD1 siRNA. (C) mRNA expression of SHP and BHMT in HepG2-GFP or -GFP-FXR cell lines, stimulated with either ethanol or 1μM OCA for 24h. Data are normalized to β-2-microglobulin expression and represented as mean ± SD. Statistical significance determined by 2-way Anova test is shown (*p<0.05). (D) Hypothetical model of FXR-NSD1 crosstalk. (1) NSD1 binds FXR through its nuclear receptor domain and thereby regulates FXR transcriptional activity on IBABP, BSEP and SHP promoters. (2) FXR regulates the expression of both NSD1 and BHMT, which contributes to the synthesis of S-adenosylmethionine required for NSD1 methylase activity.

NSD1 enzymatic activity methylates Lys36 of histone H3 and Lys20 of histone H4, using S-adenosyl-methionine (SAM) as a methyl donor [43]. A key enzyme in the SAM synthesis pathway in the liver is betaine-homocysteine methyltransferase (BHMT), an enzyme which recycles methionine from homocysteine [44, 45]. Intriguingly, FXR activation by ligand (obeticholic acid, OCA) increased the expression of BHMT, as well as the FXR target gene SHP in HepG2 cells (Fig. 5C). In line with these results, in a previous study in which the mouse liver proteome was studied, we observed that protein expression of Bhmt increased 2.1 fold upon FXR activation and decreased 1,5 fold upon FXR ablation [46].

Taken together, these data indicate a positive feedback model in which 1) FXR regulates the expression of the methyltransferase NSD1 as well as the BHMT enzyme that is essential for the synthesis of methyl groups, and 2) NSD1 binds to FXR through its LGELL motif and functions as a transcriptional cofactor for FXR (Figure 5D).

DISCUSSION

Its central role in various aspects of metabolism and inflammation makes FXR an attractive drug target, but the current generation of FXR agonists fails to distinguish between desired and undesired biological actions. Therefore, better insights in the molecular mechanisms underlying FXR regulation are needed for the rational design of a new generation of FXR drugs, selectively activating or repressing subsets of FXR target genes. NR coregulator complexes act as sensors that cooperate with nuclear receptors to generate specific gene expression programs [47]. Investigation of FXR coregulators has been limited so far to targeted approaches or non-cell based screenings. In the present study, we used an unbiased SILAC-based proteomic approach to detect novel FXR binding-proteins in HepG2 cells. Next to its obligate heterodimeric binding partner RXR, we identified FLYWCH2, NSD1, ZNF35, HOXA9 and HOXA5 amongst the proteins co-purified with FXR in HepG2 cells. We were able to validate the binding of FXR to ZNF35, HOXA9, HOXA5 and NSD1 (amino acids 1-891) by independent *in vitro* binding assays. Further research is needed to validate the binding to FXR of the other proteins identified by SILAC listed in Table 1. It should be noted that many other previously identified FXR coregulators were not identified in our SILAC screen, such as P300, SMRT, PRMT1 [24, 30, 48]. Possible reasons could be the limit of detection of highly dynamic PPIs in the absence of cross-linking conditions, and the low natural enrichment of certain coregulators due to cell type-, stimulus-, timing-, and target gene- specificity.

Here we showed that FXR transcriptional activity on three different promoters of well-established target genes (Bsep, Ibabp, and Shp) was modulated by HOXA9 and NSD1 in a dose-dependent manner. HOXA9 is a transcription factor which binds the methyltransferase PRMT5 in a protein complex required for induction of E-selectin and VCAM-1, two proteins that are expressed on the endothelial cell surface at sites of inflammation [36, 49]. Binding of HOXA9 to nuclear receptors has not been reported before. NSD1 is a methyltransferase for H3K36 and H4K20 histone marks and plays an essential role in early post-implantation development [43]. Unlike HOXA9, NSD1 has been previously reported to interact with NRs. Mouse Nsd1 was shown to interact with TR, RAR,

RXR, and ER, exhibiting characteristics of both a corepressor and a coactivator [35]. Another study reported that human NSD1 (also named ARA267) can bind and activate AR [41]. Our data indicate that NSD1 increases transcriptional activity of FXR, probably via binding the LGELL sequence in NSD1. Noteworthy, H3K36 methylation has been involved in both transcriptional activation and repression, splicing and DNA repair [50]. Besides, maintenance of H3K36 methylation by NSD1 at the BMP4 locus was shown to promote transcriptional initiation [51]. We therefore speculate that NSD1 may increase FXR transcriptional activity by methylating histone proteins at the promoter of FXR target genes, similarly to what has been reported for the methylase CARM1 [29]. Alternatively, FXR itself may be a substrate for NSD1-mediated methylation, reminiscent of Set7/9-mediated methylation of FXR, also resulting in increased FXR activity [29]. Future experiments are required to determine whether histones, FXR itself or other proteins in the transcription complex are the primary enzymatic target(s) of NSD1 in FXR-mediated gene regulation. Of note, NSD1 bound FXR in a ligand-independent manner, based on both SILAC and GST pull down assays. This concurs with the previous observation that NSD1 is able to bind to unliganded NRs [35]. However, the LGELL sequence seemed important for the regulation of FXR activity, which contrasts observations that the LXXLL motif is commonly mediating binding to transcriptionally active NRs [38]. We currently do not understand these seemingly conflicting results.

The finding that FXR regulates the mRNA expression of NSD1 as well as BHMT, a key enzyme for the generation of S-adenosylmethionine in the liver, hints at the existence of an elaborate feed- forward loop in the regulation of gene transcription by FXR. However, further investigations are needed to substantiate that BHMT activity is essential for regulation of FXR transcriptional activity by NSD1 and S-adenosylmethionine. Intricate regulatory circuitries are not novel in the field of NRs. The NR PPARα and its coregulator PGC1α provide a case for such a feed-forward loop, as PGC1α is able to activate PPARα transcriptional activity [52] and induces PPARα expression [53], while PPARα induces PGC1α expression [54].

In conclusion, the current search of FXR interacting proteins using a quantitative proteomic method in living liver cells identified amongst others the novel FXR-binding proteins HOXA9 and NSD1. These findings add valuable insights into the complex regulation of FXR activity, which is decreased by HOXA9 and increased by NSD1. Future studies should aim at unravelling which stimuli trigger the binding of these proteins to FXR and whether these coregulators play a role in the specificity of transcriptional programs activated by FXR in response to differential nutritional, inflammatory or other environmental factors.

ACKNOWLEDGEMENTS

Grant support: S.W.C.v.M. is supported by the Netherlands Organization for Scientific Research (NWO) Project VIDI (917.11.365), FP7 Marie Curie Actions IAPP (FXR-IBD, 611979), the Utrecht University Support Grant, Wilhelmina Children's Hospital Research Fund. H.R.V. is supported by Proteins At Work (NWO). We thank Roy Baas for-data analysis tools and critical discussion and Anne Gelderloos for literature discussion.

REFERENCES

1. Makishima M, Okamoto AY, Repa JJ, et al. Identification of a nuclear receptor for bile acids. Science 1999;284:1362-5.
2. Parks DJ, Blanchard SG, Bledsoe RK, et al. Bile acids: natural ligands for an orphan nuclear receptor. Science 1999;284:1365-8.
3. Wang H, Chen J, Hollister K, et al. Endogenous bile acids are ligands for the nuclear receptor FXR/BAR. Mol Cell 1999;3:543-53.
4. Massafra V, van Mil SWC. FXR as a "homeostat" for hepatic nutrient metabolism. Unpublished 2016.
5. Nevens F, Andreone P, Mazzella G, et al. A Placebo-Controlled Trial of Obeticholic Acid in Primary Biliary Cholangitis. N Engl J Med 2016;375:631-43.
6. Mudaliar S, Henry RR, Sanyal AJ, et al. Efficacy and safety of the farnesoid X receptor agonist obeticholic acid in patients with type 2 diabetes and nonalcoholic fatty liver disease. Gastroenterology 2013;145:574-82 e1.
7. Neuschwander-Tetri BA, Loomba R, Sanyal AJ, et al. Farnesoid X nuclear receptor ligand obeticholic acid for non-cirrhotic, non-alcoholic steatohepatitis (FLINT): a multicentre, randomised, placebo-controlled trial. Lancet 2015;385:956-65.
8. Moschetta A, Bookout AL, Mangelsdorf DJ. Prevention of cholesterol gallstone disease by FXR agonists in a mouse model. Nat Med 2004;10:1352-8.
9. Yu DD, Andrali SS, Li H, et al. Novel FXR (farnesoid X receptor) modulators: Potential therapies for cholesterol gallstone disease. Bioorg Med Chem 2016;24:3986-93.
10. Gadaleta RM, Oldenburg B, Willemsen EC, et al. Activation of bile salt nuclear receptor FXR is repressed by pro-inflammatory cytokines activating NF-kappaB signaling in the intestine. Biochim Biophys Acta 2011;1812:851-8.
11. Glass CK. Differential recognition of target genes by nuclear receptor monomers, dimers, and heterodimers. Endocr Rev 1994;15:391-407.
12. Mangelsdorf DJ, Evans RM. The RXR heterodimers and orphan receptors. Cell 1995;83:841-50.
13. Chong HK, Infante AM, Seo YK, et al. Genome-wide interrogation of hepatic FXR reveals an asymmetric IR-1 motif and synergy with LRH-1. Nucleic Acids Res 2010;38:6007-17.
14. Laffitte BA, Kast HR, Nguyen CM, et al. Identification of the DNA binding specificity and potential target genes for the farnesoid X-activated receptor. J Biol Chem 2000;275:10638-47.
15. Thomas AM, Hart SN, Kong B, et al. Genome-wide tissue-specific farnesoid X receptor binding in mouse liver and intestine. Hepatology 2010;51:1410-9.
16. Claudel T, Inoue Y, Barbier O, et al. Farnesoid X receptor agonists suppress hepatic apolipoprotein CIII expression. Gastroenterology 2003;125:544-55.
17. Lee JM, Wagner M, Xiao R, et al. Nutrient-sensing nuclear receptors coordinate autophagy. Nature 2014;516:112-5.
18. Kast HR, Goodwin B, Tarr PT, et al. Regulation of multidrug resistance-associated protein 2 (ABCC2) by the nuclear receptors pregnane X receptor, farnesoid X-activated receptor, and constitutive androstane receptor. J Biol Chem 2002;277:2908-15.
19. Boesjes M, Bloks VW, Hageman J, et al. Hepatic farnesoid X-receptor isoforms alpha2 and alpha4 differentially modulate bile salt and lipoprotein metabolism in mice. PLoS One 2014;9:e115028.
20. Huber RM, Murphy K, Miao B, et al. Generation of multiple farnesoid-X-receptor isoforms through the use of alternative promoters. Gene 2002;290:35-43.
21. Zhang Y, Kast-Woelbern HR, Edwards PA. Natural structural variants of the nuclear receptor farnesoid X receptor affect transcriptional activation. J Biol Chem 2003;278:104-10.
22. Balasubramaniyan N, Ananthanarayanan M, Suchy FJ. Direct methylation of FXR by Set7/9, a lysine methyltransferase, regulates the expression of FXR target genes. Am J Physiol Gastrointest Liver Physiol 2012;302:G937-47.
23. Kim DH, Xiao Z, Kwon S, et al. A dysregulated acetyl/SUMO switch of FXR promotes hepatic inflammation in obesity. EMBO J 2015;34:184-99.

24. Li CW, Dinh GK, Chen JD. Preferential physical and functional interaction of pregnane X receptor with the SMRTalpha isoform. Mol Pharmacol 2009;75:363-73.
25. Xu X, Xu X, Liu P, et al. Structural Basis for Small Molecule NDB (N-Benzyl-N-(3-(tert-butyl)-4-hydroxyphenyl)-2,6-dichloro-4-(dimethylamino) Benzamide) as a Selective Antagonist of Farnesoid X Receptor alpha (FXRalpha) in Stabilizing the Homodimerization of the Receptor. J Biol Chem 2015;290:19888-99.
26. Pellicciari R, Costantino G, Camaioni E, et al. Bile acid derivatives as ligands of the farnesoid X receptor. Synthesis, evaluation, and structure-activity relationship of a series of body and side chain modified analogues of chenodeoxycholic acid. J Med Chem 2004;47:4559-69.
27. Savkur RS, Thomas JS, Bramlett KS, et al. Ligand-dependent coactivation of the human bile acid receptor FXR by the peroxisome proliferator-activated receptor gamma coactivator-1alpha. J Pharmacol Exp Ther 2005;312:170-8.
28. Zhang Y, Castellani LW, Sinal CJ, et al. Peroxisome proliferator-activated receptor-gamma coactivator 1alpha (PGC-1alpha) regulates triglyceride metabolism by activation of the nuclear receptor FXR. Genes Dev 2004;18:157-69.
29. Ananthanarayanan M, Li S, Balasubramaniyan N, et al. Ligand-dependent activation of the farnesoid X-receptor directs arginine methylation of histone H3 by CARM1. J Biol Chem 2004;279:54348-57.
30. Pineda Torra I, Freedman LP, Garabedian MJ. Identification of DRIP205 as a coactivator for the Farnesoid X receptor. J Biol Chem 2004;279:36184-91.
31. Lien F, Berthier A, Bouchaert E, et al. Metformin interferes with bile acid homeostasis through AMPK-FXR crosstalk. J Clin Invest 2014;124:1037-51.
32. Baymaz HI, Spruijt CG, Vermeulen M. Identifying nuclear protein-protein interactions using GFP affinity purification and SILAC-based quantitative mass spectrometry. Methods Mol Biol 2014;1188:207-26.
33. Wisniewski JR, Zougman A, Nagaraj N, et al. Universal sample preparation method for proteome analysis. Nat Methods 2009;6:359-62.
34. Cox J, Mann M. MaxQuant enables high peptide identification rates, individualized p.p.b.-range mass accuracies and proteome-wide protein quantification. Nat Biotechnol 2008;26:1367-72.
35. Huang N, vom Baur E, Garnier JM, et al. Two distinct nuclear receptor interaction domains in NSD1, a novel SET protein that exhibits characteristics of both corepressors and coactivators. EMBO J 1998;17:3398-412.
36. Bandyopadhyay S, Ashraf MZ, Daher P, et al. HOXA9 participates in the transcriptional activation of E-selectin in endothelial cells. Mol Cell Biol 2007;27:4207-16.
37. Van Mil SW, Milona A, Dixon PH, et al. Functional variants of the central bile acid sensor FXR identified in intrahepatic cholestasis of pregnancy. Gastroenterology 2007;133:507-16.
38. Heery DM, Kalkhoven E, Hoare S, et al. A signature motif in transcriptional co-activators mediates binding to nuclear receptors. Nature 1997;387:733-6.
39. Savkur RS, Burris TP. The coactivator LXXLL nuclear receptor recognition motif. J Pept Res 2004;63:207-12.
40. Chan CM, Fulton J, Montiel-Duarte C, et al. A signature motif mediating selective interactions of BCL11A with the NR2E/F subfamily of orphan nuclear receptors. Nucleic Acids Res 2013;41:9663-79.
41. Wang X, Yeh S, Wu G, et al. Identification and characterization of a novel androgen receptor coregulator ARA267-alpha in prostate cancer cells. J Biol Chem 2001;276:40417-23.
42. McInerney EM, Rose DW, Flynn SE, et al. Determinants of coactivator LXXLL motif specificity in nuclear receptor transcriptional activation. Genes Dev 1998;12:3357-68.
43. Rayasam GV, Wendling O, Angrand PO, et al. NSD1 is essential for early post-implantation development and has a catalytically active SET domain. EMBO J 2003;22:3153-63.
44. Pajares MA, Perez-Sala D. Betaine homocysteine S-methyltransferase: just a regulator of homocysteine metabolism? Cell Mol Life Sci 2006;63:2792-803.
45. Skiba WE, Taylor MP, Wells MS, et al. Human hepatic methionine biosynthesis. Purification and

characterization of betaine:homocysteine S-methyltransferase. J Biol Chem 1982;257:14944-8.
46. Massafra V, van Mil SWC. Farnesoid X Receptor activation promotes hepatic amino acid catabolism and ammonium clearance. Under consideration in Gastroenterology 2016.
47. Rosenfeld MG, Lunyak VV, Glass CK. Sensors and signals: a coactivator/corepressor/epigenetic code for integrating signal-dependent programs of transcriptional response. Genes Dev 2006;20:1405-28.
48. Fang S, Tsang S, Jones R, et al. The p300 acetylase is critical for ligand-activated farnesoid X receptor (FXR) induction of SHP. J Biol Chem 2008;283:35086-95.
49. Bandyopadhyay S, Harris DP, Adams GN, et al. HOXA9 methylation by PRMT5 is essential for endothelial cell expression of leukocyte adhesion molecules. Mol Cell Biol 2012;32:1202-13.
50. Wagner EJ, Carpenter PB. Understanding the language of Lys36 methylation at histone H3. Nat Rev Mol Cell Biol 2012;13:115-26.
51. Lucio-Eterovic AK, Singh MM, Gardner JE, et al. Role for the nuclear receptor-binding SET domain protein 1 (NSD1) methyltransferase in coordinating lysine 36 methylation at histone 3 with RNA polymerase II function. Proc Natl Acad Sci U S A 2010;107:16952-7.
52. Vega RB, Huss JM, Kelly DP. The coactivator PGC-1 cooperates with peroxisome proliferator-activated receptor alpha in transcriptional control of nuclear genes encoding mitochondrial fatty acid oxidation enzymes. Mol Cell Biol 2000;20:1868-76.
53. Mazzucotelli A, Viguerie N, Tiraby C, et al. The transcriptional coactivator peroxisome proliferator activated receptor (PPAR)gamma coactivator-1 alpha and the nuclear receptor PPAR alpha control the expression of glycerol kinase and metabolism genes independently of PPAR gamma activation in human white adipocytes. Diabetes 2007;56:2467-75.
54. Hondares E, Rosell M, Diaz-Delfin J, et al. Peroxisome proliferator-activated receptor alpha (PPARalpha) induces PPARgamma coactivator 1alpha (PGC-1alpha) gene expression and contributes to thermogenic activation of brown fat: involvement of PRDM16. J Biol Chem 2011;286:43112-22.

SUPPLEMENTARY TABLES

Supplementary table 1. Primers for the mutagenesis of LXXLL motifs in human NSD1.

Motif	Primer sequence 5'->3'
FSTLL (aa 907-911) → FSTAA	Fw TACAAATTCAGTACAGCGGCAATGATGTTGAAAGATA Rv TATCTTTCAACATCATTGCCGCTGTACTGAATTTGTA
LGELL (aa 1552-1556) → LGEAA	Fw TGAAAAATTGGGTGAGGCGGCGTTATGTGAGGCTCAGT Rv ACTGAGCCTCACATAACGCCGCCTCACCCAATTTTTCA

Supplementary table 2. Primer for qPCR in HepG2 cells.

Gene	Primer sequence 5'->3'
hNSD1	Fw CGGTCAGAGAAGAAACGCCT Rv TTCCTCTTCACAGCGGGAAC
hBHMT	Fw TGGAGAACAGGGGCAACTATG Rv CTGACTCACTCCTCCTGCTAC

CHAPTER 7

General Discussion

THE ROLE OF FXR IN NORMAL PHYSIOLOGY: THE PAST, THE PRESENT, AND THE FUTURE

In this thesis we aimed to investigate the molecular mechanisms of FXR function in the regulation of metabolism and inflammation in the liver and intestine. Why do we study FXR biology? What is our current understanding of the role of FXR in normal physiology? And what are the future perspectives?

The past: the de-orphanization of FXR and the growing evidence of its role as a metabolic regulator

A mammalian receptor owing the structural features of hormone receptors, but lacking a known endogenous ligand (therefore 'orphan'), was isolated in complex with the retinoid X receptor (RXR) in 1995 [1]. This nuclear receptor was given the name Farnesoid X Receptor, because it was shown to be activated by farnesol derivatives, which are intermediates in the mevalonate pathway for the synthesis of cholesterol, bile acids (BAs), retinoids and steroid hormones. As described in **Chapter 2**, three studies in 1999 de-orphanized FXR, by identifying BAs as the endogenous ligands for FXR [2-4], thereby paving the way for studies into the regulation of BA homeostasis. Next to FXR, BA homeostasis turned out to be regulated also by other BA-activated receptors (VDR, PXR, TGR5). FXR downregulates Cyp7a1 expression via upregulation of SHP, thereby repressing BA synthesis [5]. In addition, FXR upregulates Abcb11/Bsep expression, thereby inducing BA efflux in the bile canaliculi [6]. Our liver proteome data in **Chapter 3** recapitulate the well-established role of FXR in regulation of BA synthesis, conjugation and liver efflux, and suggest that FXR function extends to the regulation of key proteins in taurine (Csad) and phosphatidylcholine (Pcyt1a) metabolism (Chapter 3, Figure 2C), with implications on taurine availability for BA conjugation and on bile salt secretion, respectively. The generation of FXR knockout models advanced the understanding of the role of FXR in the regulation of lipid and glucose metabolism. As reviewed in **Chapter 2**, both intestinal FXR (via the FGF19 signalling cascade) and hepatic FXR repress lipogenesis and promote fatty acid oxidation in the liver (Chapter 2, Figure 2). Besides, intestinal and hepatic FXR induce a pro-glycogenic and anti-gluconeogenic signalling (Chapter 2, Figure 4). The quantitative proteomic approaches adopted in **Chapter 3** and **4** confirm a role for FXR and FGF19 in lipid and glucose metabolism (See Chapter 3, Figure 3A and Chapter 4, Figure 2A). Since the identification of FXR and other receptors for BAs two decades ago, we now view BAs not only as detergents of dietary fats and vitamins, but also as hormones regulating the metabolism of nutrients.

The present: an extended view of FXR as a homeostat for hepatic nutrient metabolism

The current investigation of nuclear receptor biology is greatly benefiting from quantitative proteomics. As shown in **Chapter 3**, analysis of the proteome in livers from wild type mice and FXR knockout mice treated with an FXR agonist, uncovered novel, yet unexplored functions of FXR, such as its regulation of amino acid metabolism. FXR activation in mouse liver and in primary hepatocytes increased the expression of enzymes

implicated in histidine and proline degradation, ureagenesis and glutamine synthesis. In line with this, FXR ablation resulted in reduced expression of urea cycle proteins and accumulation of precursors of ureagenesis. We provided evidence that FXR acts as a transcriptional regulator of amino acid catabolism, as FXR activation regulates mRNA expression of enzymes in the urea cycle and glutamine synthesis both in primary hepatocytes and in mice refed with a high protein diet. In addition, FXR binds to gene regulatory sites of these enzymes and of proteins degrading histidine and proline. Based on these results, we conclude that FXR regulates the fate of amino acids in the post-absorptive state, by promoting degradation of the surplus in amino acids not used for protein synthesis. Moreover, FXR induces the synthesis of urea and glutamine, important for the disposal of the toxic ammonium derived from amino acid catabolism (Chapter 2, Figure 5). This new function of FXR in amino acid catabolism and ureagenesis positions FXR as a regulator of all three main classes of nutrients: fats, sugars and proteins.

The liver is exposed to nutrient fluxes and oscillates between a fasted state and an energy-replenished postprandial state. Regulation of nutrient metabolism by hormones, posttranslational modifications (PTMs) and transcription factors is therefore highly dynamic across the different nutritional phases [7]. There is only a handful of studies in which FXR function was studied under physiological conditions, as a regulator of postprandial and post-absorptive nutrient metabolism. In **Chapter 2**, we re-analyze the function of FXR in the perspective of nutritional metabolism, and discuss the role of FXR in liver energy homeostasis in postprandial, post-absorptive and fasting/starvation states. Fasting-refeeding experiments performed by Duran-Sandoval and co-workers [8] suggest the relevance of FXR counter regulation of lipid synthesis and VLDL secretion in post-absorptive state, whereas another study [9] extends FXR inhibitory action of lipogenesis even to fasting state. How FXR regulates glucose metabolism in post-absorptive phase is less clear. The inhibition of gluconeogenesis and induction of glycogen synthesis by the FXR-FGF19 axis concur with the energy needs of the postprandial/post-absorptive phase. Nevertheless, a few studies [8, 10] challenge this classical view, providing evidence for FXR favouring gluconeogenesis in the post-absorptive state and during fasting. Most likely, the FXR-FGF19 axis controls the gluconeogenesis rate in a dynamic manner across the nutritional phases. Finally, FXR regulation of liver enzymes involved in ammonium detoxification pathways seems to occur in the post-absorptive phase, based on our preliminary study in mice fasted for 6 hours and refed for 2 hours with a high protein diet (Chapter 3, Figure 8D). In light of these observations, we envisage FXR as a homeostat for hepatic nutrient metabolism, meaning that FXR acts as a gatekeeping system to prevent excessive lipid, glucose and amino acid accumulation in liver and in the circulation, by favouring the redistribution of energy substrates.

The future: the need for an integrated and dynamic view of regulatory networks and the methodological challenges

Biological considerations. Future research needs to address how the fate of nutrients in the liver is dynamically regulated and further our understanding of the intricate hormonal, enzymatic and transcriptional network in which multiple players collaborate to-

gether in an integrated and dynamic manner to ensure energy homeostasis. FXR regulates hepatic nutrient homeostasis across the phases of nutrition alongside other regulatory proteins, such as LXR, SREBP1c, FOXO, HNF4α, CREB and PGC1α (further detailed in **Chapter 2)**. The mechanisms underpinning this integrated regulation are still not clear. Posttranslational modifications (PTMs) are a key mechanism allowing transcription factors to sense the energy status. As an example, the transcription factor SREBP1c, implicated in fat synthesis, is acetylated (and thereby activated) in fed state and deacetylated (and thereby inactivated) in the fasted state [11, 12]. Similarly, the PGC1α protein is acetylated (becoming inactive) in conditions of caloric excess, whereas it is deacetylated (becoming activated) in situations of low energy status, thereby promoting gluconeogenesis and mitochondrial function, depending on energy demand [13, 14]. We discussed knowledge on dynamic acetylation of FXR and propose that this could be an additional mechanism for FXR to sense nutrient abundance (in this case the abundance of acetyl-CoA in the nucleus/cytosol) and the subsequent inhibition of *de novo* lipogenesis by FXR (Chapter 2, Figure 3). Acetylation could be a common mechanism integrating the activity of several proteins dependent on energy status of the hepatocyte. It may well be that also other PTMs/coregulators/metabolites account for integrating the regulation of hepatic nutrient metabolism.

Future methodological perspectives. Whole body genetic knockout models have been widely used so far to investigate the role of FXR in physiology. However, tissue specific knockout models would be more suitable to rule out the potential contribution of FXR deletion in other organs. For example, in **Chapter 3**, renal FXR activity potentially complicates investigations into the role of hepatic FXR in regulation of ureagenesis. In addition, inducible knockout models could help understanding the function of FXR, without the interference of metabolic adaptation arising during the whole life-long protein deletion in genetic knockout models. Of note, strict control of the fasting/feeding conditions will be required to uncover the physiological function of FXR in postprandial, post-absorptive and fasted state.

Moreover, an integrated view of regulatory networks dictates further methodological challenges, since redundancy in regulatory pathways often obscures the understanding of the function of a single deleted protein. Shifting from a 'one protein-centric' perspective towards a 'multi-protein' perspective implies the adoption of platforms suitable to perform interactome studies across multiple time-, cell type-, stimulus, and gene- specific conditions. Determination of phospho-, acetyl-, other PTM-proteome across nutritional states could add valuable insights into the landscape of modifications modulating simultaneously the multiple components of regulatory networks.

The ultimate challenge is the translation of our understanding of FXR biology to human physiology. Currently, most insights into the effects of FXR activation are derived from animal models or cell lines. It should be noted that human and rodents differ in respect to many features relevant to FXR biology, such as regulation of BA synthesis, BA composition, intestinal microbiome, and FXR target genes [15, 16]. Therefore, future efforts should focus on the development and use of model systems with human relevance, like precision cut liver slices and liver organoids [16, 17]. Optimalization and inclusion of human

model systems is crucial in order to understand whether knowledge obtained in animal models has relevance for human health.

FXR-BASED CLINICAL INTERVENTIONS: THE PAST, THE PRESENT, AND THE FUTURE

The research in this thesis has been conducted in the perspective to use biological knowledge for progress in health care. Which mechanisms underlie the therapeutic benefits of FXR activation? Which diseases can we potentially treat with FXR-drugs? What should we aim for in the future?

The past: the therapeutic benefits of FXR activation for liver diseases and diabetes

The functional role of FXR as a metabolic and anti-inflammatory regulator has inspired the use of FXR ligands for therapeutic purposes. Systemic activation of FXR by the synthetic ligand GW4064 was shown to protect against cholestasis in animal models, in line with the role of FXR in maintaining BA homeostasis [18]. The FXR-FGF19 axis is important for this protection, since selective activation of intestinal FXR was sufficient to protect mice from obstructive cholestasis, by inhibiting hepatic BA synthesis [19]. Besides, treatment with a synthetic FXR agonist prevented cholesterol gallstone disease in mice, by increasing biliary bile salt and phospholipid concentrations, therefore restoring cholesterol solubility [20]. In addition, pharmacological activation of FXR has been considered for the treatment of type 2 diabetes, because of its role in improving insulin sensitivity [21, 22]. FXR function is also important in the reversal of diabetes after bariatric surgery [23]. The regulatory role of FXR in BA, lipid and glucose homeostasis and its anti-inflammatory function have been shown to ameliorate symptoms of nonalcoholic steatohepatitis (NASH) by FXR agonists in animal models, as reviewed by Adorini et al. [24] and further discussed in **Chapter 2**. Similarly, treatment with recombinant FGF19, an intestinal FXR target, was shown to be beneficial in obesity-associated disorders such as type 2 diabetes and NASH, because FGF19 decreases hepatic triglycerides content and improves insulin sensitivity ([25, 26], and discussed in **Chapter 5**). Taken together, these pre-clinical studies encouraged to investigate the therapeutic benefit of FXR ligands in human clinical trials.

The present: the FDA-approval of FXR agonists for human liver disease and the potential extension to more disease indications

The semi-synthetic FXR ligand obeticholic acid (OCA, Ocaliva™) has recently been tested in a Phase III clinical trial [27] and approved by the FDA for the treatment of primary biliary cholangitis, a chronic disease in the liver leading to progressive cholestasis. In addition, OCA improved the histologic features of NASH in a Phase III clinical trial [28], and a Phase IV clinical trial is currently underway, highlighting that OCA is also considered for treatment of NASH in the nearby future.

In the meantime, research was undertaken to explore novel potential therapeutic applications of FXR agonists. Activation of FXR has therapeutic potential also for inflammatory bowel disease (IBD), as administration of OCA inhibited colitis symptoms in mu-

rine models of IBD [29]. Mechanistically, FXR-mediated inhibition of pro-inflammatory cytokines (via interference with the NFκB function) and preservation of the intestinal barrier may contribute to OCA-mediated amelioration of colitis. However, it has not been fully elucidated whether the overall protection can be attributed to FXR function in the enterocytes, in the immune cells or even in the liver cells. In the latter case, it could be hypothesized that hepatic FXR may participate in improving intestinal inflammation, by changing the composition of the BA pool reaching the intestine, which is important for the microbiota composition [30]. In **Chapter 5,** we aimed to investigate the immunological mechanisms that ameliorate colitis upon FXR activation. We show that FXR activation by OCA has systemic anti-inflammatory effects, since it decreased the levels of plasma IL-10, and counteracted the depletion in splenic dendritic cells (DC) and the increase in Tregs, both occurring as a consequence of colitis. We propose that OCA treatment may induce DC retention in the spleen and affect the chemotactic environment in the colon. We thereby substantiate that FXR-mediated regulation of the immune response contributes to ameliorate intestinal inflammation. Further studies will need to assess whether the therapeutic indications of FXR agonists can be extended to patients with IBD.

The future: from full agonists towards selective modulators

OCA has been shown to improve the histological features of NASH with parallel lowering of serum aminotransferase concentrations, however, concerns have been raised on its long-term clinical outcomes and safety [31]. Indeed, it is unclear whether histological improvement seen reflects long-term clinical outcomes, since the primary aim of NASH treatment is prevention of hepatic complications, such as cirrhosis and hepatocellular carcinoma. In this thesis, we described a role for FXR in in amino acid homeostasis (**Chapter 3**). It would be interesting to investigate whether FXR ligands may reduce the risk for hyperammonemia and hepatic encephalopathy, which are frequent complications of liver cirrhosis [32]. With regard to the safety concerns, OCA treatment has been shown to result in an unfavourable serum lipid profile, with an increase in total cholesterol and low-density lipoprotein cholesterol and a decline in high-density lipoprotein cholesterol [28, 33]. NASH is associated with metabolic syndrome and cardiovascular disease, and therefore worsening of dyslipidaemia by OCA may be disadvantageous. Overall, the central role of FXR in various aspects of metabolism and inflammation makes FXR an attractive drug target, but current compounds act as full agonists of FXR that may have undesired biological actions.

We believe that future research efforts should focus on the rational design of a new generation of FXR drugs, selectively activating or repressing specific FXR functions. A study from our group has provided evidence that pharmacological dissociation between metabolic and inflammatory actions of FXR is feasible [34]. These results represent a promising basis for the rational design of drugs for the treatment of IBD, because selective targeting of FXR anti-inflammatory function, without interfering with its role in metabolic homeostasis, is expected to reduce side effects. A similar rationale can be applied to the development of FGF19 variants which uncouple the full metabolic benefit from mito-

genic effects, as discussed in **Chapter 5**. The enthusiasm for FGF19-based therapeutics for the treatment of cholestasis, diabetes and metabolic syndrome is tempered by safety concerns, since FGF19 drives proliferation and the formation of hepatocellular carcinoma [35]. Dissociating the metabolic from mitogenic activity of FGF19 requires a comprehensive understanding of FGF19 signalling. The analysis of the liver proteome in mice treated with recombinant FGF19 in **Chapter 5** supports the role of FGF19 signalling in a wide range of processes, including BA, cholesterol, lipid, glucose, amino acid, nucleotide, and RNA metabolism, as well as cell survival and tumorigenesis. We show that many of the FGF19 targets (i.e. Pdk4, Apoa4, Fas and Stat3) have a dual function in both metabolism and cell proliferation (Chapter 4, figure 2B). This is not unexpected, as it is probably a consequence of the evolutionary conserved integration of metabolic and cell survival signalling pathways. This integrated regulation challenges the engineering of selective FGF19 modulators with metabolic but no proliferative activity. We also highlight that FGF19 increased protein expression of Anxa2 and Tgfbi, which have been implicated in tumorigenesis, but with no apparent function in BA, cholesterol or lipid metabolism. In light of these observations, it would be informative to investigate whether these or other proteins critically mediate FGF19-dependent tumorigenesis. And if so, whether FGF19 variants blocking the activity of these targets are devoid of tumorigenic effects and have preserved metabolic activity.

In another attempt to increase our understanding on the regulation of FXR activity to guide the future design of selective FXR modulators, we adopted a SILAC-based proteomic approach to identify FXR interacting proteins (**Chapter 6**). We show that the

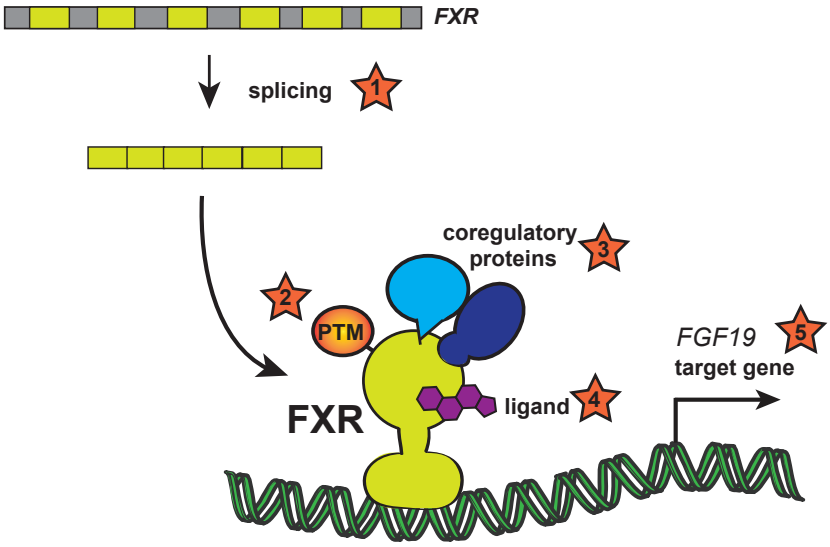

Figure 1. FXR activity is regulated at different levels; implications for the rational design of selective FXR modulators. To enable rational design of FXR therapeutics that target specific subsets of target genes, we could think to target (1) alternative splicing and promoter usage of FXR resulting in expression of different isoforms, (2) posttranslational modifications, (3) binding to coregulatory proteins, (4) 'dissociating' ligands, (5) variants of FXR target gene FGF19.

transcription factor HOXA9 and the methylase NSD1 bind to FXR and decreased or increased FXR activity, respectively. A nuclear receptor binding LXXLL motif in human NSD1 protein was shown to be important for its ability to stimulate FXR transcriptional activity. We propose a feed-forward mechanism, in which NSD1 binds and regulates FXR activity, while FXR induces gene expression of NSD1 and BHMT, the latter providing methyl donors for NSD1 methylase activity.

Selective modulation of FXR function could potentially be achieved by targeting the regulation of FXR activity at multiple levels, as depicted in Figure 1. In addition, the development of FXR ligands with tissue-specific tropism based on the pharmacokinetic behaviour could represent a potential modality of selective modulation [36]. As explained in **Chapter 2**, posttranslational modifications play an important role in differential regulation of FXR activity, depending on the nutritional status. Different cofactors can also act as sensors that cooperate with nuclear receptors to generate specific gene expression programs [37]. In addition, different FXR isoforms were also shown to regulate differential transcriptional programs in response to bioenergetic cues [38].

By increasing our understanding of the molecular mechanisms of FXR activation, rational design of a second generation of selective FXR-targeting drugs will become within reach. Metabolic syndrome, NASH and IBD are complex multifactorial diseases. The ultimate goal of developing drugs with a high benefit-risk ratio for the treatment of these diseases can be only pursued with patience, persistence and hard work.

REFERENCES

1. Forman BM, Goode E, Chen J, et al. Identification of a nuclear receptor that is activated by farnesol metabolites. Cell 1995;81:687-93.
2. Makishima M, Okamoto AY, Repa JJ, et al. Identification of a nuclear receptor for bile acids. Science 1999;284:1362-5.
3. Parks DJ, Blanchard SG, Bledsoe RK, et al. Bile acids: natural ligands for an orphan nuclear receptor. Science 1999;284:1365-8.
4. Wang H, Chen J, Hollister K, et al. Endogenous bile acids are ligands for the nuclear receptor FXR/BAR. Mol Cell 1999;3:543-53.
5. Sinal CJ, Tohkin M, Miyata M, et al. Targeted disruption of the nuclear receptor FXR/BAR impairs bile acid and lipid homeostasis. Cell 2000;102:731-44.
6. Ananthanarayanan M, Balasubramanian N, Makishima M, et al. Human bile salt export pump promoter is transactivated by the farnesoid X receptor/bile acid receptor. J Biol Chem 2001;276:28857-65.
7. Viscarra JA, Ortiz RM. Cellular mechanisms regulating fuel metabolism in mammals: role of adipose tissue and lipids during prolonged food deprivation. Metabolism 2013;62:889-97.
8. Duran-Sandoval D, Cariou B, Percevault F, et al. The farnesoid X receptor modulates hepatic carbohydrate metabolism during the fasting-refeeding transition. J Biol Chem 2005;280:29971-9.
9. Zhang Y, Castellani LW, Sinal CJ, et al. Peroxisome proliferator-activated receptor-gamma coactivator 1alpha (PGC-1alpha) regulates triglyceride metabolism by activation of the nuclear receptor FXR. Genes Dev 2004;18:157-69.
10. Renga B, Mencarelli A, D'Amore C, et al. Glucocorticoid receptor mediates the gluconeogenic activity of the farnesoid X receptor in the fasting condition. FASEB J 2012;26:3021-31.
11. Ponugoti B, Kim DH, Xiao Z, et al. SIRT1 deacetylates and inhibits SREBP-1C activity in regula-

tion of hepatic lipid metabolism. J Biol Chem 2010;285:33959-70.
12. Walker AK, Yang F, Jiang K, et al. Conserved role of SIRT1 orthologs in fasting-dependent inhibition of the lipid/cholesterol regulator SREBP. Genes Dev 2010;24:1403-17.
13. Fernandez-Marcos PJ, Auwerx J. Regulation of PGC-1alpha, a nodal regulator of mitochondrial biogenesis. Am J Clin Nutr 2011;93:884S-90.
14. Lerin C, Rodgers JT, Kalume DE, et al. GCN5 acetyltransferase complex controls glucose metabolism through transcriptional repression of PGC-1alpha. Cell Metab 2006;3:429-38.
15. Glossmann H. The Bile Acid Metabolome in Humans and Rodents. Biocrates Life Sciences 2015.
16. Ijssennagger N, Janssen AW, Milona A, et al. Gene expression profiling in human precision cut liver slices in response to the FXR agonist obeticholic acid. J Hepatol 2016;64:1158-66.
17. Huch M, Gehart H, van Boxtel R, et al. Long-term culture of genome-stable bipotent stem cells from adult human liver. Cell 2015;160:299-312.
18. Liu Y, Binz J, Numerick MJ, et al. Hepatoprotection by the farnesoid X receptor agonist GW4064 in rat models of intra- and extrahepatic cholestasis. J Clin Invest 2003;112:1678-87.
19. Modica S, Petruzzelli M, Bellafante E, et al. Selective activation of nuclear bile acid receptor FXR in the intestine protects mice against cholestasis. Gastroenterology 2012;142:355-65 e1-4.
20. Moschetta A, Bookout AL, Mangelsdorf DJ. Prevention of cholesterol gallstone disease by FXR agonists in a mouse model. Nat Med 2004;10:1352-8.
21. Cariou B, van Harmelen K, Duran-Sandoval D, et al. The farnesoid X receptor modulates adiposity and peripheral insulin sensitivity in mice. J Biol Chem 2006;281:11039-49.
22. Zhang Y, Lee FY, Barrera G, et al. Activation of the nuclear receptor FXR improves hyperglycemia and hyperlipidemia in diabetic mice. Proc Natl Acad Sci U S A 2006;103:1006-11.
23. Ryan KK, Tremaroli V, Clemmensen C, et al. FXR is a molecular target for the effects of vertical sleeve gastrectomy. Nature 2014;509:183-8.
24. Adorini L, Pruzanski M, Shapiro D. Farnesoid X receptor targeting to treat nonalcoholic steatohepatitis. Drug Discov Today 2012;17:988-97.
25. Fu L, John LM, Adams SH, et al. Fibroblast growth factor 19 increases metabolic rate and reverses dietary and leptin-deficient diabetes. Endocrinology 2004;145:2594-603.
26. Kir S, Beddow SA, Samuel VT, et al. FGF19 as a postprandial, insulin-independent activator of hepatic protein and glycogen synthesis. Science 2011;331:1621-4.
27. Nevens F, Andreone P, Mazzella G, et al. A Placebo-Controlled Trial of Obeticholic Acid in Primary Biliary Cholangitis. N Engl J Med 2016;375:631-43.
28. Neuschwander-Tetri BA, Loomba R, Sanyal AJ, et al. Farnesoid X nuclear receptor ligand obeticholic acid for non-cirrhotic, non-alcoholic steatohepatitis (FLINT): a multicentre, randomised, placebo-controlled trial. Lancet 2015;385:956-65.
29. Gadaleta RM, van Erpecum KJ, Oldenburg B, et al. Farnesoid X receptor activation inhibits inflammation and preserves the intestinal barrier in inflammatory bowel disease. Gut 2011;60:463-72.
30. Ridlon JM, Kang DJ, Hylemon PB, et al. Bile acids and the gut microbiome. Curr Opin Gastroenterol 2014;30:332-8.
31. Wong VW, Wong GL, Chan FK. Is obeticholic Acid the solution to nonalcoholic steatohepatitis? Gastroenterology 2015;148:851-2.
32. Cordoba J. Hepatic Encephalopathy: From the Pathogenesis to the New Treatments. ISRN Hepatol 2014;2014:236268.
33. Mudaliar S, Henry RR, Sanyal AJ, et al. Efficacy and safety of the farnesoid X receptor agonist obeticholic acid in patients with type 2 diabetes and nonalcoholic fatty liver disease. Gastroenterology 2013;145:574-82 e1.
34. Bijsmans IT, Guercini C, Ramos Pittol JM, et al. The glucocorticoid mometasone furoate is a novel FXR ligand that decreases inflammatory but not metabolic gene expression. Sci Rep 2015;5:14086.
35. Nicholes K, Guillet S, Tomlinson E, et al. A mouse model of hepatocellular carcinoma: ectopic expression of fibroblast growth factor 19 in skeletal muscle of transgenic mice. Am J Pathol

2002;160:2295-307.
36. Pellicciari R, Passeri D, De Franco F, et al. Discovery of 3alpha,7alpha,11beta-Trihydroxy-6alpha-ethyl-5beta-cholan-24-oic Acid (TC-100), a Novel Bile Acid as Potent and Highly Selective FXR Agonist for Enterohepatic Disorders. J Med Chem 2016.
37. Rosenfeld MG, Lunyak VV, Glass CK. Sensors and signals: a coactivator/corepressor/epigenetic code for integrating signal-dependent programs of transcriptional response. Genes Dev 2006;20:1405-28.
38. Correia JC, Massart J, de Boer JF, et al. Bioenergetic cues shift FXR splicing towards FXRalpha2 to modulate hepatic lipolysis and fatty acid metabolism. Mol Metab 2015;4:891-902.

APPENDIX

Thesis summary

Nederlandse samenvatting

Acknowledgements/Ringraziamenti

Curriculum Vitae

List of Publications

THESIS SUMMARY

Our body hosts several molecules that function as hormones to regulate metabolism in the liver. Bile acids (BAs) are molecules produced by the liver and stored in the gall bladder. After eating a meal, BAs are secreted in the intestine, where they help the digestion of fats and vitamins. Subsequently, most BAs are re-absorbed in the intestine and recycled to the liver, where they function as hormones to regulate hepatic metabolism. Meanwhile, fats, carbohydrates and proteins in the diet are digested and absorbed in the intestine and reach the liver as glucose, triacylglycerols and amino acids, respectively. The fate of BAs and nutrients in the liver is tightly connected through the function of one protein, the Farnesoid X Receptor (FXR).

BAs activate FXR in the intestine and in the liver. In response, FXR regulates transcription thereby preventing the accumulation of BAs in the liver and intestinal cells. Since BAs are toxic, this function of FXR is very important to protect from disease. In addition, FXR acts as a gatekeeper for the metabolism of nutrients. At the molecular level, FXR binds to the DNA and increases the expression of genes that inhibit the hepatic accumulation of fat and glucose. In Chapter 3, we report a novel function of FXR in hepatic nutrient metabolism. Other than regulating fat and glucose metabolism, FXR controls metabolism of the third category of nutrients: amino acids. We showed that in mouse liver tissue and isolated liver cells, FXR activation resulted in upregulation of proteins involved in amino acid degradation, ureagenesis and glutamine synthesis. FXR binds to regulatory sites of the respective genes encoding those proteins, providing evidence for direct transcriptional regulation. Importantly, plasma concentrations of newly formed urea as well as hepatic gene expression of enzymes involved in amino acid catabolism were decreased in liver-specific FXR knockout mice challenged with a high-protein diet. Ammonium toxicity is a harmful complication in patients with liver disease. The impact of our findings is therefore substantial, as it might be possible to prevent the accumulation of toxic ammonium in patients with liver disease, by activating FXR in these patients.

In view of previously published functions in combination with our findings in Chapter 3, we can envisage FXR acting as a 'homeostat' of liver metabolism, meaning a gatekeeper of metabolic homeostasis, since it senses environmental changes (fed state) and drives transcriptional programs that inhibit BA synthesis, and redistribute the energy substrates (as discussed in Chapter 2).

Metabolism relates closely to cell proliferation and inflammation, since you need to adapt your metabolic needs in order to grow or defend yourself from pathogens or injury. In the fed state, FXR activates FGF19 in the intestine. FGF19 is a hormone-like molecule that contributes to prevent BA, lipid and glucose accumulation in the liver, but is also implicated in cell survival and tumorigenesis. In Chapter 4, we studied the effect of FGF19 administration on the proteome-wide profile of the liver, in order to gain a comprehensive understanding of the FGF19 signalling cascade. We show that several FGF19 targets have a dual function in both metabolism and cell proliferation. This integrated regulation challenges the engineering of selective FGF19 modulators with metabolic but no proliferative activity. However, some other FGF19 targets implicated in pro-

liferation and tumorigenesis, have no apparent function in BA, cholesterol or lipid metabolism, thereby keeping open the opportunity to develop FGF19 variants for therapeutic purposes. Those variants would display a preserved metabolic activity that is advantageous in cholestatic liver diseases and diabetes, but would not have tumorigenic risks.

The combination of environmental factors (e.g. diet), dysregulation of immune response and damage in the intestinal epithelial barrier function, may trigger inflammatory bowel disease (IBD) in genetically predisposed individuals. FXR activation attenuates the severity of colitis in murine models of IBD. In Chapter 5, we aimed to investigate the immunological mechanisms that ameliorate colitis upon FXR activation. We show that FXR activation has systemic anti-inflammatory effects, since it decreases the levels of anti-inflammatory cytokines in plasma, and counteracts the depletion in splenic dendritic cells (DC) and the increase in Tregs, both occurring as a consequence of colitis. We propose that FXR activation may induce DC retention in the spleen and affect the chemotactic environment in the colon.

The central role of FXR in various aspects of metabolism and inflammation makes FXR an attractive drug target in cholestatic diseases, non-alcoholic steatohepatitis (NASH), IBD, and metabolic syndrome, but current compounds act as full agonists of FXR that may have undesired biological actions. Future research should focus on the rational design of a new generation of FXR drugs, selectively activating or repressing specific FXR functions. Understanding the regulation of FXR activity is pivotal to guide the future design of selective FXR modulators. In Chapter 6, we adopted a SILAC-based proteomic approach to identify proteins which bind FXR in liver cells. We report two novel FXR interactors, named HOXA9 and NSD1, that can decrease or increase FXR activity, respectively. Together with posttranslational modifications (PTMs), coregulatory proteins are eligible targets for pharmacological modulation of selective FXR functions.

In conclusion, active FXR can be compared to a knight protecting his damsels (liver and intestine) from the wind-mill shaped giants (ammonium toxicity, fat accumulation and inflammation). Strategic planning (elucidation of FXR mechanistic actions) is necessary to guide the direction of the knight's sword to defeat the enemy (targeting selective FXR actions as therapy for liver and intestinal diseases).

NEDERLANDSE SAMENVATTING

In het menselijk lichaam zijn hormonen aanwezig die verschillende processen in de lever aansturen. Een voorbeeld van deze hormonen zijn de galzouten. Galzouten worden gemaakt in de lever en opgeslagen in de galblaas. Wanneer na het eten van een maaltijd het voedsel de maag bereikt, trekt de galblaas samen en komen de galzouten in de darm terecht. In de darm zorgen galzouten voor het oplosbaar maken van vetten en vitamines uit het dieet, zodat deze kunnen worden opgenomen in het lichaam. Aan het einde van de dunne darm worden de galzouten weer in het bloed opgenomen. Ze bereiken vervolgens de lever, alwaar ze als hormonen functioneren en de verwerking van nutriënten uit het dieet bevorderen. Ondertussen worden vetten, vitamines en koolhydraten afkomstig van de maaltijd in het maag-darmkanaal verteerd tot vetzuren, glucose, en aminozuren en vervolgens opgenomen. Gelijktijdig met de galzouten bereiken deze nutriënten de lever. Het lot van de galzouten en nutriënten in de lever is gekoppeld door de functie van de farnesoid X receptor (FXR).

Galzouten activeren FXR in de lever en darm cellen (hepatocyten en enterocyten). Actief FXR reguleert transcriptie van genen die betrokken zijn bij de synthese en transport van galzouten. Dit is erg belangrijk omdat galzouten toxisch zijn en op deze manier wordt voorkomen dat leverschade ontstaat. Ook reguleert FXR het metabolisme van glucose en vetten, door te binden op specifieke plaatsen in het DNA, waardoor expressie van genen wordt gereguleerd die voorkomen dat vetzuren en glucose ophopen in de hepatocyten. In hoofdstuk 3 beschrijven we een nieuwe functie van FXR in lever metabolisme. Naast glucose- en vetmetabolisme reguleert FXR namelijk ook aminozuur metabolisme. We laten zien dat in muizenlevers en geïsoleerde hepatocyten, FXR activatie resulteert in een toename van eiwitten betrokken bij aminozuur degradatie, ureum productie en glutamine synthese. FXR bindt aan het DNA in de regulatiore sequenties van de genen die coderen voor deze eiwitten, wijzend op mogelijke directe transcriptionele regulatie door FXR. In muizen die specifiek in de lever geen FXR tot expressie brengen, zijn de concentratie nieuw gevormd ureum en genexpressie van genen betrokken bij aminozuur afbraak sterk verlaagd. Ammonium toxiciteit is een ernstige en veelvoorkomende complicatie van leverziekten in het algemeen. Mogelijk kan activatie van FXR in patiënten met leverziekten het ophopen van het toxische ammonium voorkomen. Samengevat kunnen we FXR dus zien als een “homeostaat” van levermetabolisme, door een sleutelbijdrage te leveren aan de verwerking, opslag en re-distributie van energiesubstraten afkomstig uit het dieet (bediscussieerd in Hoofdstuk 2).

Levermetabolisme is nauw verbonden met celdeling en ontsteking, omdat het metabolisme van een cel moet worden aangepast voordat celdeling of de afweer tegen pathogenen kan plaatsvinden. Na een maaltijd activeert FXR de expressie van FGF19 in de darm. FGF19 is een hormoon peptide dat in de lever de ophoping van galzouten, vetten en glucose tegengaat, maar het bevordert ook de proliferatie en overleving van cellen en tumorvorming. In hoofdstuk 4 bestuderen we het effect van FGF19 toediening op het eiwitprofiel van de lever, zodat we beter inzicht krijgen in de signaleringsroute van FGF19 in de lever. We laten zien dat FGF19 signaleert naar eiwitten die zowel een belangrijke rol hebben in metabolisme als ook in cel proliferatie. Dit bemoeilijkt de pro-

ductie van selectieve FGF19 varianten voor ziekten als diabetes en metabool syndroom, omdat cel proliferatie en tumor vorming niet wenselijk zijn. Echter, we beschrijven ook FGF19-gemedieerde eiwit veranderingen betrokken bij cel proliferatie, die geen beschreven functie hebben in lever metabolisme. Dus afhankelijk van welke eiwitten de tumor vorming aansturen, is het misschien toch mogelijk om FGF19 varianten te produceren die geen proliferatie activiteit laten zien. Hiervoor is meer onderzoek nodig.
De combinatie van omgevingsfactoren, een foutieve afweerreactie en schade aan het darmepitheel kan chronische darmziekten induceren in individuen die een genetische aanleg hiervoor hebben. In hoofdstuk 5 onderzoeken we de mechanismen waarmee FXR activatie leidt tot een vermindering van darmontsteking in muizen. We laten zien dat FXR activatie niet alleen lokaal in de darm, maar ook systemisch anti-inflammatoire effecten heeft. FXR activatie verlaagt de concentratie van verschillende anti-inflammatoire cytokines in het bloed en zorgt voor retentie van dendritische cellen in de milt, en een verlaging van Tregs. We stellen ons voor dat door de FXR-gemedieerde retentie van dendritische cellen de chemotactische omgeving in de dikke darm wordt beïnvloed en daardoor het ontstekingsproces wordt afgeremd.
De centrale rol van FXR in verschillende aspecten van levermetabolisme en ontsteking maken FXR tot een aantrekkelijk therapeutisch target eiwit voor cholestatische ziekten, niet-alcoholische steatohepatitis (NASH), chronische darmziekten (IBD) en metabool syndroom, maar de huidige moleculen die voorhanden zijn, zijn agonisten die alle FXR target genen activeren, en hebben om die reden vrijwel zeker ongewenste bijeffecten. Vervolgonderzoek zou daarom als focus moeten hebben om selectieve liganden te ontwikkelen, die een specifieke groep van FXR target genen activeren of inactiveren. Gedegen kennis omtrent de regulatie van FXR activiteit is cruciaal om de toekomstige rationele ontwikkeling van selectieve liganden te bevorderen. In hoofdstuk 6 rapporteren we HOXA9 en NSD1 als nieuwe interactoren van FXR, die respectievelijk FXR functie remmen en stimuleren. Samen met post-translationele modificaties zijn co-regulerende eiwitten potentiele farmacologische targets voor selectieve FXR functies.
Samenvattend kan FXR worden gezien als een ridder die z'n jonkvrouwen (lever en darm) beschermt tegen vijanden (ammonium toxiciteit, vet ophoping en ontsteking). Door het ontwikkelen van een strategie (het ophelderen van de moleculaire mechanismen van FXR regulatie) kan de ridder de richting van zijn zwaard bepalen om de vijand uit te schakelen (mbv selectieve FXR liganden lever en darmziekten tegengaan).

ACKNOWLEDGEMENTS / RINGRAZIAMENTI

The one person I could never thank enough is my supervisor **Saskia** van Mil. Thanks for giving me trust when we met at first and renewing daily your trust throughout my whole journey as a Ph.D student. Your guidance, support, patience and persistence were crucial for my development. You taught me many things in science and in life. I strongly appreciated your efforts to teach me how to design experiments in order to answer biological questions of clinical relevance, how to be a critical on scientific research, and how to write peer-reviewed scientific articles. I loved our intense discussions about science; thanks for your constant constructive criticism to my work. Sorry for being stubborn in some cases and thanks for being always open-minded and available to re-think together strategies and research directions. Thanks also for your help me to finalize successfully this thesis. I have been honoured to be part of your research group and I wish you being always surrounded by motivated, hard working and passionate group members and collaborators and to pursue with success your future scientific goals.

Beste **Boudewijn**, thanks for being my promoter and being often available to provide pieces of advice, reflecting an impressive scientific knowledge and a superior criticism. Thanks also for helping me to finalize my research work with Saskia in this last year.

Dear **Alex**, you have been my scientific mentor, my teacher in English, my lab-mate, my really good friend, my squash-partner, and finally my paranimf! Thanks heartily for all the time to help me, guide me and support me while being here in Utrecht and even while not here anymore. Even better now that I am at the end of this complicated journey, I can appreciate all the efforts and time you invested in me above all in the beginning of my Ph.D. Thanks for conveying to me your knowledge, your patience, your persistence and your passion for science. I wish you to achieve your most desired objectives in science and at the same time to reconcile scientific efforts with a happy and fulfilling life.

José, my other beloved paranimf! Thanks for the scientific discussions, for teaching me being twice as critical on science, for your lab help, for the laughs, for the jumps, for the smiles, for the funny scared-to-death hiccups, for the movies, for the shared food, for the candies and chocolates, for your joyful company, for always lifting the spirits of people around you and for all the other things we shared together in these last years. I wish you to reach your perfect balance in life between love for rational and intense science and healthy social craziness!

Beste **Ellen**, thanks for all your help and support. Thanks for your technical and scientific assistance throughout all the years of my Ph.D. in between two pregnancies and a house building! I appreciate your help in the beginning to get a bit more integrated in the Netherlands and get familiar and comfortable to the Dutch world. I am indebted to you for initiating me to several lab techniques as well to stroopwafels, bitterballen, boerenkool, the Dutch Carnival and many unique Dutch expressions and feelings like the "*plaatsvervangende schaamte*" ("place-replacing shame", feeling ashamed for something

someone else has done). I wish you the best for everything.

Beste **Noortje**, thanks for all your scientific feedback and collaboration. Always so kind and available. Thanks also for re-reading critically part of this thesis and giving meinsightful InDesign clues.

Danielle, molecular-minded and computer science-oriented lady! We have been sharing intense days as PhD candidates in Saskia's group, thanks for our fruitful scientific discussions, support, and for forcing me to have healthy coffee breaks! I wish you to have success in life in the things you most crave for!

Dear first BA-group and then FXR-group partner **Ingrid**, thanks for the scientific feedback, for your lab help and for being always available for advice. I wish you the success in your career that you deserve!

Beste **Eric**, thanks for all your scientific feedback throughout my whole time as a Ph.D. I considered myself greatly lucky to count on the next-door opinion of an expert of nuclear receptor biology and metabolism. I really feel I learned a lot from you in our Friday morning meetings. Success!

Beste **Stan**, thanks for your scientific feedback in the first years of my Ph.D. I have been delighted and honoured you to be in our joint 'BA scientific meetings'. You have been for me an awesome key figure as a scientific thinker and a teacher. And many thanks for not sparing to me your honest and insightful pieces of advice also after leaving the Stratenum, across meetings at the Tygat Institut, or at scientific retreats. I wish you to pursue with great success your future scientific goals.

Beste **Harmjan**, you guided and shaped the frame of my research in Saskia's group very much more that you might think! Thanks for making ready and available for me all the mass spec technology I ever needed to answer our research questions. And also thanks for all our discussions, in which many you were right! (Yes, now it is on paper! Nero su bianco!). Dear **Nanda**, thanks for your support, collaboration and for reading my thesis. **Rùben** and **Johan**, thanks for your help! You opened to me the doors of metabolite analyses, thus giving me precious tools to address my most desired scientific questions. I treasured a lot the collaboration with you all! **Martin Houweling**, thanks for your technical help and your helpful comments on our work. **Marianne Boes** and **Maud Plantinga**, thanks for all your help and support! I think that bridging multiple research fields and competences may be challenging, but is essential and can turn out to be extremely fruitful to understand integrated procceses in biology, such as metabolism and immunology. Thanks for making that possible!

Dear **Carlie de Vries** and **David Egan**, thanks for your helpful comments and support during our yearly meetings and for reading my thesis. I heartily appreciated your impartial assessment and advice to progress in science and career. Dear **Alain** de Bruin and **Madelon** Maurice, thanks for reading my thesis.

Dear office-mates and "Adipo" group members across the years **Ismayl, Arjen, Marjoleine , Myriam, Astrid, Inkie, Nicole**, and **Bob** thanks for your cheerful company, and for fruitful scientific discussions! **Bob**, thanks also for finally bringing sunglasses to let me enjoy the few rays of sun in our office! **Astrid**, good luck with your GR selective moldulators!

My dear students **Anne** Gelderloos, **Rizzo** Sutmuller, **Dave** Hennekens, **Maaike** and **Robin**, I loved your enthusiasm and motivation, that let me enjoy the experience of teaching!

Dear good friend **Roy**, we have shared 5 amazing years of Ph.D from the start till the end, between failure and success and highs and lows. Thanks for your lovely company, for all your support, for the ready-to-use bioinformatics advice first across the corridor and then in the next institute! I wish you the best for your future! **Simona**, thanks for the cheerful company. I wish you good luck with finishing your Ph.D., success with learning Dutch and the best for your career! **Maria** Koster, thanks for the time spent together. I wish you the best too!

Marten, I enjoyed our conversations about everything! Thanks for your good company across all our years of Ph.D, and for you always-participative presence at our work discussions, full of constructive and helpful comments! I wish you an excellent and joyful Ph.D defence! **David**, thanks for initiating me to the mass spec sample preparation and for your precious and unforgettable company. **Marieke**, I enjoyed your company! I send you my best wishes as a future mum and as a scientist! **Tobias, Sasha, Maaike, Marrit, Evi, Astrid,** and **Maria José**, I loved the scientific environment that you created with insightful and inspiring research. Thanks for your availability and scientific discussion! **Loes, Maaike** Meerlo**, John**, and **Lisa**, thanks for all the organized dinners, the borrels and your nice company. I wish you the best!

I also would like to thank the Vermeulen's lab ladies, **Irem**, **Nelleke,** and **Susan,** for helping me with mass spec sample preparations, for the nice dinners we had together, for your pleasant company and for imposing good music in our lab (Skyradio forever)! Thanks also to **Pascal** and **Arne** and the rest of the Vermeulen's lab.

Stiaan, thanks for the nice time spent together in the beginning of my Ph.D and for giving me the huge honour of being your paraninf! I hope once we can still keep the promise to meet in South Africa.

Livio, thanks for all your help with microscopy.

Thanks also to **Bos** and **Snippert** lab, especially **Fried** for organizing the fruitful scientific meetings and for your constructive criticism. **Willem-Jan**, thanks for scientific discussions and for your nice company and humour! **Nizar**, thanks for your funny and crazy company, I wish you the best! **Lucas**, good luck with your close defence! **Ingrid** Verlaan and **Marjolein** Vliem, thanks for your constant help and availability!

Dear prof. **Pellicciari**, **Francesca**, **Tiziana**, **Daniela**, **Andrea** Cristiani, **Antimo** and **Gianmario**, thanks for hosting me at TES Pharma. I wish you all the best!

Also thanks to Holger **Rehman**, Arjan **Brenkman,** Marc **Timmers**, **Kops lab**, **Lens lab**, **de Rooij lab** and the rest of **Bos** and **Burgering lab** for scientific discussions.

Eelco, **Banafsheh**, **Amanda**, and all the other Ph.D students of the CSND program, that I had the chance to meet, shared borrels, co-organize LSD day, Sinterklaas parties, and have interesting chats with throughout the years, I enjoyed doing all of this with you! Thanks.

Cristina, **Marianne**, **Marjoleine**, **Cheuk**, **Marcel**, **Wim** van Driel and the rest of the ICT crew, and **Lenie**, thanks for all your help, for organizing millions of unforgettable events, washing, cleaning and all the technical assistance!

Of course, I would like to address huge thanks also to my friends here in Utrecht. **Carlo**, this thesis is also thanks to you, che mi sei sempre stato vicino in questi anni. Ho adorato i momenti di svago con te, che indirettamente tanto hanno contribuito a tutto questo. Sono troppe le cose che abbiamo condiviso assieme. Non ho parole per ringraziarti di tutto e non ti auguro nulla per il futuro, fra il meglio che ti augurerei, perche' spero non ci perdiamo di vista. **Heriberto, Irene e Leonardo**, thanks for the amazing evenings and time spent together! **Casper**, thanks for your unforgettable company and help, while living next-door. And thanks for making me open-minded about Dutch food cooking!

Grazie anche ai miei amici lontani, Valentina, Francesco, Isabella, Mariafrancesca e Dalila, che né il tempo né la distanza ci separano.

E mio fratello e mio padre, sempre premurosi per me, e per me il pilastro e punto di riferimento, su cui posso sempre contare.

E infine un grazie senza fine al mio amore, Anchise, che hai sempre rispettato le mie scelte e che sai condividere con me ogni momento, rendendo vicini i momenti lontani e indimenticabili quelli vicini.

CURRICULUM VITAE

Vittoria Massafra was born on the 11th of April 1987 in Martina Franca (Taranto), in the south-east of Italy. In 2006 she completed the classic-scientific Liceo "Tito Livio" in Martina Franca, with a specialization in languages. Subsequently, she attended Biotechnology of Health and Pharmaceutics at the University of Bari. In her final Bachelor laboratory training, she studied autism-associated genetic variants in the mitochondrial aspartate/glutamate carrier AGC1 in the group of prof. Palmieri (Department of Pharmaco-Biology). In 2011 she was awarded a Master Degree with Honours in Medical Biotechnology and Molecular Medicine at the University of Bari. Her graduation research project explored the nuclear receptor transcriptome in liver regeneration and hepatic carcinogenesis under the supervision of Dr. Michele Vacca and Dr. Antonio Moschetta at the Laboratory of Lipid Metabolism and Cancer (Consorzio Mario Negri Sud, Santa Maria Imbaro, Italy). In January 2012 she started her Ph.D. at the Department of Metabolic Diseases (Center for Molecular Medicine) at the University Medical Center in Utrecht, under the supervision of Dr. Saskia van Mil and Prof. Boudewijn Burgering. The results of her research are described in this thesis.

LIST OF PUBLICATIONS

"Splenic dendritic cell involvement in FXR-mediated amelioration of DSS colitis."
Massafra V, Ijssennagger N, Plantinga M, Milona A, Ramos Pittol JM, Boes M, van Mil SW.
Biochim Biophys Acta. 2016 Feb;1862(2):166-73

"Nuclear receptors in regenerating liver and hepatocellular carcinoma."
Vacca M, Degirolamo C, **Massafra V**, Polimeno L, Mariani-Costantini R, Palasciano G, Moschetta A.
Mol Cell Endocrinol. 2013 Apr 10;368(1-2):108-19.

"Clustering nuclear receptors in liver regeneration identifies candidate modulators of hepatocyte proliferation and hepatocarcinoma."
Vacca M, D'Amore S, Graziano G, D'Orazio A, Cariello M, **Massafra V**, Salvatore L, Martelli N, Murzilli S, Lo Sasso G, Mariani-Costantini R, Moschetta A.
PLoS One. 2014 Aug 12;9(8):e104449